NICKEL HYDROMETALLURGICAL WASTE RESIDUE CHARACTERIZATION, GEOCHEMICAL REACTIVE TRANSPORT MODELING AND DISPOSAL RISK MANAGEMENT

ABIGAIL STEEL


CENTRE FOR NFLD. STUDIES
MEMORIAL UNIVERSITY
OF NEWFOUNDLAND

NICKEL HYDROMETALLURGICAL WASTE RESIDUE CHARACTERIZATION, GEOCHEMICAL REACTIVE TRANSPORT MODELING AND DISPOSAL RISK MANAGEMENT

by

©Abigail Steel

A thesis submitted to the School of Graduate Studies
in partial fulfillment of the requirements for the degree of
Doctor of Philosophy

Faculty of Engineering and Applied Science

Memorial University of Newfoundland

March, 2010

St. John's **Newfoundland** **Canada**

ABSTRACT

There has been limited experience in the use of hydrometallurgy to process nickel sulfide concentrate, thus the hydrometallurgical process residue is generally not well characterized in the open literature. This research will assist in ensuring the long-term stability of the waste and increase the understanding of its degradation and reactivity on disposal. The research pertains to the mobility of metals and sulfur compounds, their stability in minerals and phases associated with hydrometallurgical residues and the development of a risk-based methodology for selection of mine waste disposal designs. The research focuses on sulfur compounds and ore metals, such as nickel, cobalt and copper, which are target metals for the proposed hydrometallurgical processing facility in Long Harbour, Newfoundland. It will be particularly important to understand the effect of high sulfur waste material in Newfoundland's wet, temperate climate and generally slightly acidic surface water conditions. The research objectives are to characterize the mobility of metals from hydrometallurgical residue and assess residue reactivity/stability under different disposal conditions in order to determine the most favourable waste disposal procedures. Specific research objectives include: 1) characterization of the waste residues through mineralogical studies and elemental analysis; 2) assessment of acid and metal generating potential of the waste through static and kinetic tests and geochemical modeling; 3) assessment of decant water conditions in the residue impoundment through a calibrated numerical model; 4) evaluation of residue subsurface disposal conditions on a spatial and temporal basis through numerical modeling calibrated by in-situ field testing; and 5) prediction of the fate of heavy metals in the receiving environments. Finally, a risk-

based, multi-criteria decision making approach is developed to assess various mine waste disposal options and applied through a case study.

As there is very limited experience in the processing of nickel sulfide concentrate through hydrometallurgy the high sulfur, process residue is generally not well characterized. The mineralogical and sequential extraction work provided key residue mineral and microstructure information; suggested how target metals are present in the residue minerals and phases; and provided metal partitioning results which are important in understanding the residues metal leaching potential. The static and kinetic testing conducted further characterized the residues by assessing their acid generating and metal leaching capacity.

Geochemical modeling of process residues is not widely reported in the literature due in part to the complexity of the mineralogical assemblage. This work, through calibrated models, was successfully able to model the residue that led to a greater understanding of factors impacting the chemistry of groundwater and surface water and enabled the prediction of longer term subsurface conditions in the residue impoundment.

The design of a mine waste disposal site is waste and site specific and is complex. Using a risk-based decision-making to assess design options for a mine waste disposal project is novel and effective approach. This approach integrated the results from the mineralogical characterization and contaminant fate and transport modeling and included uncertainty in the human health and ecological risk analysis; then incorporated this risk analysis in a multi-criteria decision making analysis to evaluate the optimal mine waste disposal alternative.

ACKNOWLEDGEMENTS

First, this work would not have been possible without the never ending support, inspiration and love from my children; Kyla, Skye and Landon. You are a constant source of joy.

I would like to thank my supervisors, Dr. Kelly Hawboldt, Dr. Faisal Khan and Dr. Christina Bottaro of my supervisory committee for their valuable advice and encouragement during my research. I'd also like to thank Mr. Donald Stevens of Vale Inco for providing data from the demonstration site, his interest in this project and his review of publications.

I thank the Faculty of Engineering and Applied Science, Memorial University of Newfoundland, Atlantic Canada Opportunities Agency (ACOA), Natural Sciences and Engineering Research Canada (NSERC), the Canadian Memorial Engineering Foundation and the Vale Inco Atlantic Innovation Fund for their financial support.

TABLE OF CONTENTS

LIST OF TABLES

LIST OF FIGURES

PAGE

CHAPTER 1

INTRODUCTION AND OVERVIEW

The ore at Voisey's Bay, NL Canada exists mainly as a nickel sulfide, pentlandite and this nickel sulfide ore is currently being milled and concentrated at the mine site. It is noteworthy that the concentrate contains large quantities of sulfur (33 %), iron (42 %) as well as minor quantities of: lead, arsenic, chromium and zinc (VBNC, 2002). In the refining process all of these materials will be removed and will become part of the process waste. The traditional method of refining nickel is a smelter. In a smelter the deleterious metals are removed from the nickel in the form of a slag containing large quantities of iron. Sulfur is removed from the nickel and released to the air in the form of SO_2. The SO_2 partitions in the air and will produce H_2SO_4 (acid rain) therefore it must be removed through diligent air stripping methodologies.

Vale Inco is testing a novel process to refine nickel, cobalt and copper from the nickel sulfide concentrate from Voisey's Bay. As this Pressure Oxidative Leach (POL) process does not involve smelting prior to the refining there is expected to be cost savings of approximately 30 % over the traditional pyrometallurgical (smelting and refining) process (Vale Inco, 2002). After initial testing at a 1:1000 scale plant (mini-plant) at Vale Inco's research facility, a larger scale (1:100) Demonstration Plant was constructed in Argentia, Newfoundland and operated from 2006 to 2008. As of June, 2009 a full-scale hydrometallurgical plant is under construction.

In the hydrometallurgical process a significant amount of the sulfur from the ore is washed into the waste water and is neutralized then precipitated out largely in the form of

$CaSO_4 \cdot 2H_2O$. With the hydrometallurgical process there is not the problem of sulfur in the air emissions rather there may be a concern of sulfur in the waste water and residue. The wastes from the plant are derived through precipitation processes and pressure leaching and are in the form of sludges. The two main sources of sludges/residues are: 1) the solids remaining when the pulp from the pressure leaching (leach residue) is washed by Counter Current Decantation (CCD) and 2) the precipitate (filter cake) formed during the iron removal and neutralization stage. Each of these sludges has a solid and liquor portion. The solid waste from the hydrometallurgical process is approximately 55 % Neutralized Leach Residue (NLR) and 45% Neutralized Filter Cake (NGR) (VBNC, 2006). The Vale Inco hydrometallurgical process consists of nine main steps which are outlined in Appendix I along with the process flow diagram.

The amount of residue predicted to be produced from a full-scale facility would be in the order of 375,000 tonnes/yr (VINL, 2008) or 5.8 million cubic meters. At the Demonstration Plant, the solid residue and residue liquor waste is mixed with the Process Effluent Neutralization (PEN) solution and deposited into lined ponds that retain the solids and the liquids are further neutralized if necessary so that effluent meets regulatory guidelines. The proposal for the full-scale facility, to be located in Long Harbour, Newfoundland near the site of the demonstration plant, is to deposit the mixed residue (Neutralized Combined Residue (NCR)) subaqueously as a slurry in an existing lake which will be enlarged by dam construction.

As the NLR and NGR from the plant contain a large percentage of sulfur there is potential that the sulfur could oxidize to form Acid Rock Drainage (ARD) (Chapter 8)

and cause leaching of metals from the residue or bedrock. Although, the waste will be neutralized before it is sent for disposal, it will be important to perform both short and longer term tests on the residues to determine its acid generating potential at the time of disposal and with age. Preliminary Acid Base Accounting (ABA) (Sobek et al., 1978) analyses on samples provided indicate the residue may be acid generating in the long term. There are several concerns related to the residue that will be generated from the full-scale facility.

- Metals in the liquid effluent discharge;
- Surface and groundwater contamination;
- Metals and sulfur concentration in the residue;
- Acid generating potential of the residue at the time of disposal and over time; and
- Role of thiosalts in acid generation.

The three main objectives for this thesis are listed below and are addressed in the following chapters: 1) to characterize the residue through assessment of the mineralogy of the residue and through static and kinetic testing; 2) to conduct geochemical reactive modeling to predict the metal concentrations in the decant water in the residue disposal pond and the pore water through residue depth and with time; 3) to develop a methodology to ascertain the human health and ecological risk associated with different residue disposal options and then use a multi-criteria decision making process to rank the disposal options.

This thesis consists of a series of manuscripts either published, accepted or to be submitted for publication. Chapter 2 provides an overall literature review which expands

on that provided in each paper. Chapters 3 through 7 represent each of the manuscripts. The status of each publication and the contributions made to the publication are provided as a preface before each chapter. Chapter 8 consists of data collected but not in manuscript format. Chapter 9 is a discussion that links together the ideas presented in the earlier chapters and includes recommendations. Additional information is provided in the Appendices. References are provided at the end of each manuscript chapter and at the end of the main body of the thesis for Chapters1, 2, 8 and 9.

The first publication (Chapter 3) does a mineralogical characterization of the residues. It considers the main minerals and phases present in each residue, compares the demonstration plant residue to that from the mini plant and presents sequential extraction experimental data that provides information on metal availability and phases or minerals to which they are associated. The second publication (Chapter 4) provides results of kinetic testing on the residues and infers trends with time for specific analytes in the leach solution. Chapters 5 and 6 present the geochemical reactive transport numerical modeling work on the residue. Chapter 5 presents a modeled residue consisting of a mineralogical assemblage (presented in Chapter 3) which is used to predict the decant water chemistry in the Demonstration Plant residue impoundment and to compare it with site conditions. The model is calibrated using results from previously described kinetic tests. The modeled residue is examined by way of sensitivity analysis as well as kinetics of dissolution reactions. Chapter 6 uses the modeled residue to examine the geochemistry of the pore water in the residue for different disposal cases. First, subaerial disposal is examined and the model calibrated based on field results then the subaqueous

disposal case is calibrated based on Demonstration Plant data. Finally these results are used to predict geochemistry of the pore water throughout the depth of the full-scale disposal pond for both disposal scenarios and with time. The final publication (Chapter 7) proposes a methodology for risk-based decision making relating to disposal of mine waste from a processing plant or mine site. Information derived from previous numerical models is incorporated into this paper. The ecological and human health risk for different residue disposal options is examined while incorporating uncertainty in risk parameters. A multi-criteria decision making process is used to rank the disposal options. Chapter 8 provides additional unpublished kinetic and static test results on the residues.

CHAPTER 2

LITERATURE REVIEW

2.1 VINL CONCENTRATE AND NICKEL HYDROMETALLURGICAL PLANTS

In the ovoid of the Voisey's Bay ore deposit, for location refer to Fig 2.1, 70 % of the deposit is crystalline massive sulfide minerals. The massive sulfide zones are principally pyrrhotite, pentlandite, chalcopyrite and minor magnetite (VBNC, 1997). The ore mineralogy indicates nickel, copper and cobalt is largely found in conjunction with iron-sulfide compounds (VBNC, 1997).

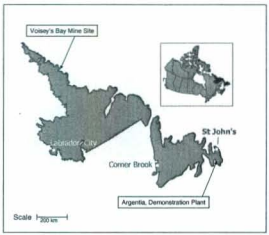

Figure 2.1: Location of Voisey's Bay Mine site.

In the milling process the ore is crushed and the non-sulfide minerals are removed, leaving the concentrate. The VINL concentrate typically contains 27.9-34.9 % sulfur, 16-20 % nickel, 0.8 % cobalt and 4.6 % copper. Quantities of other metals present include

arsenic 100-150 g/tonne, lead 120-360 g/tonne, zinc 290-1490 g/tonne and chromium 5-70 g/tonne (VBNC, 1997). The Activox process developed by Western Minerals Technology is the hydrometallurgical process used by Vale Inco at the Argentia Demonstration Plant. This Pressure Oxidative Leach (POL) process is described in Appendix I along with the process flow diagram (Fig. A.1). As previously indicated, due to the high sulfur content in the waste Vale Inco has recommended that the waste be deposited subaqueous to limit the supply of oxygen to the waste thus limiting acidic drainage. Subaqueous disposal of acidic mine tailings is well documented (Robertson, 1991; Dave et al., 1997; Li et al., 1997; Li et al., 2000; Lindvall, 2003). The disposal of a similar hydrometallurgical waste is not widely reported.

There exist several hydrometallurgical demonstration or mini-plant facilities that process nickel around the world. The patented processes include: BioNic, Intec Nickel Process, Activox and CESL Nickel process (Palmer and Johnson, 2005). There currently are no full-scale hydrometallurgical plants to process nickel sulfide concentrate. Palmer and Johnson (2005) indicated that with the success of the Tati hydrometallurgical demonstration plant (in Botswana) and approval for their 40 kilotonnes/yr nickel Activox refinery, Activox is at the forefront of the nickel sulfide technology race. The Tati full-scale hydrometallurgy refinery started construction in 2006 (Creamer's Media Miner's Weekly, 2006).

2.2 HYDROMETALLURGICAL RESIDUE CHARACTERIZATION

Although much work has been completed on pilot-plant and demonstration plant testing of the nickel hydrometallurgical process, there is limited data in the literature relating to

this process residue. Sammut and Welham, (2002) have provided perhaps the most detailed published information in recent times relating to metal sulfide hydrometallurgical residue from the Intec copper process with their work describing environmental analysis. H.G. Engineering concluded that the Intec copper process is suitable for commercial application (Sammut and Welham, 2002). The analysis conducted on demonstration plant residue included stability and characterization work. The following stability studies were conducted: TCLP (Toxicity Characteristics Leaching Procedure), modified TCLP, Specific Contaminant Concentration test and Multiple Extraction Procedure (MEP). Characterization work included: X-Ray Diffraction (XRD), Thermal Gravimetric Analysis (TGA), Differential Thermal Analyser-Fourier Transform Infrared Spectroscopy (DTA FTIR) and Raman and Mossbauer Spectroscopy plus elemental analysis. Study highlights indicate the solids residues contained 35 % hematite (crystalline), 33 % gypsum, 25 % elemental sulfur and 6 % quartz and iron oxides in the residue were primarily crystalline (>95 %) with high stability. The residues showed low leachability even under conditions exceeding those expected of in an unmanaged, uncapped landfill. Tests indicated contaminant levels were below threshold levels for the majority of EPA notifiable elements for classification of "Solid" or "Inert" waste as described by EPA (1999) and other stability tests (MEP) on mixed residue indicated after initial dissolution of gypsum, the leaching dropped off to negligible levels.

Peacey et al. (2002) indicated in their work comparing copper hydrometallurgy processes that "Based on the experiences with zinc plant leach residues that are only about 20 % of the volume of the chalcopyrite leach residues per unit of metal produced, leach residue

disposal will be a major issue and will limit hydrometallurgical processes to remoter areas." Residues generated during batch tests and mini plant tests on the concentrate from Voisey's Bay were reported on by Chen et al. (2006). The authors noted the residues generated by batch and continuous leach methods were similar however the morphologies were different. Also the residues consisted primarily of hematite and sulfur with minor amounts of goethite, and iron species. In the batch produced residue, in addition to tiny spheroids, the hematite produced larger "hollow" shell-like particles that contained residual pentlandite or sulfur cores.

2.2.1 Prediction of Metal Leaching and ARD

Methods used to predict metal leaching and ARD are laboratory, field and model based. Role of pyrite and pyrrhotite in acid generation, the rate of acid generation and function of carbonates are described in Appendix II. Standard laboratory methods (MEND, 2000) can be applied using static and kinetic testing of the material. These methods have been used on mine waste rock, mill tailings and non-mining applications. However, there is very little in the literature relating to the prediction of metal leaching and ARD from metal sulfide hydrometallurgical residues or specifically the long-term prediction of metal leaching in subaqueous and subaerial non-lined, disposal sites. Static tests are useful in predicting whether leachate will become acidic at some point in time (Parker and Robertson, 1999). Kinetic tests are valuable in comparing the rate of metal leaching and oxidation, however extending the results from laboratory scale to full-scale can lead to a high degree of uncertainty and neglects oxygen availability (Salomons, 1995).

Work has been conducted on the characterization of zinc hydrometallurgical refining process materials including the residue. The type of characterization work of interest for hydrometallurgical residue is similar to that of other potentially acid generating material. Price et al. (1997) outlines guidelines and procedures for prediction of ARD and metal leaching. Price (2005) provides an updated list of potential information required for metal leaching, ARD assessment and mitigation work. This characterization work includes: the geology, mineralogy, static tests, kinetic tests, elemental analysis, standard waste assessment characterization and site components.

2.2.2 The Role of Mineralogy

The importance of assessing the mineralogy of mine waste is unquestioned and there exists numerous techniques to investigate the minerals present and their surfaces. Jambor (1994) indicated that there exists no application to a systematic investigation of mineralogy of a tailings impoundment. This is also true for mine processing waste in general. Jambor (1994) further indicated that integrated hydrogeochemical-mineralogical studies for sulfide-rich tailings impoundments have mainly involved optical microscopy, standard XRD, Scanning Electron Microscopy (SEM) and electron-microprobe analyses. The mineralogy of mine waste including waste rock, tailings and processing waste is well described in the literature with examples provided in Chapter 3. The literature has reported the mineralogy of hydrometallurgical waste predominantly related to zinc extraction and the resulting iron bearing residue. One significant challenge with the hydrometallurgy of metals associated with iron bearing minerals is the removal of iron from the pregnant solution to a stable form. Individual iron oxide minerals have differing

properties thus it is important to identify the exact iron minerals produced. The stability of iron minerals is generally accepted as being, from least stable to most stable: jarosite, goethite and hematite. As hematite is the most stable form of iron oxide hydrometallurgical processes more recently try to form this mineral when precipitating iron out of the pregnant solution. Outlined in Table 2.1 is a selection of the literature cited on methods to control of iron during hydrometallurgy.

The challenges associated with the disposal of jarosite and goethite, iron oxide residues common to the zinc hydrometallurgical process, are well reported in the literature. Typical concerns can include: elevated concentrations of heavy metals such as: lead, zinc, cadmium, copper, mercury and arsenic which is some cases are leaching from the iron residue. Table 2.2 provides a sampling of some of the studies conducted to remediate existing jarosite or goethite disposal sites to immobilize the metals and to treat process residues.

Table 2.1: Selection of literature on iron control in hydrometallurgy

Author	Title
Muir and Jamieson (2006)	Precipitation of iron oxides from iron (II)/(III) chloride media at ambient temperatures using caustic, lime or magnesia.
Defreyne, et al. (2006)	The role of iron in the CESL Process.
Lahtinen, et al. (2006)	Hematite versus jarosite precipitation in zinc production.
Queneau and Weir (1986)	Control of iron during hydrometallurgical processing of nickelerous laterite ores.
Ritcey (1986)	Iron- an overview of its control in solvent extraction of metals.
Au-Yeung and Bolton (1986)	Iron control in processes developed at Sherritt Gordon Mines.
Scott et al. (1986)	Iron- the good with the bad- Kidd Creek zinc plant experience.
Agatzini et al. (1986)	Removal of iron from iron-nickel-cobalt solutions by precipitation and solvent extraction techniques.

The residue produced from zinc concentrate processing cannot be readily compared to that of the VINL residue, as the VINL residue is derived from a nickel sulfide concentrate with individual processing methods and conditions and the resulting residue has different mineralogy and morphology. Chapter 3 discusses test results related to VINL mineralogical assemblage and how metals are associated with the minerals and phases present. This information is important in modeling the residue and understanding its potential for acid generation and metal leaching and has not been previously available in the open literature.

Table 2.2: Selection of literature on disposal of iron oxide residues

Author	Title
Takayama et al. (2006)	Environmental aspects of the generation and disposal of iron residues at a Votoratim Zinc refinery in Brazil
Menge et al. (2006)	Closing of a goethite pond at Umicore Balen, Belgium
Foged et al. (2006)	How to substantially improve the life of a 30 ha tailings pond at a Umicore Zinc plant
Uusipaavalniemi and Kalman, (1996)	Handling of iron at the zinc plant in Kokkola
Vega-Farfan and Tamargo (1996)	Bentonites as a material for controlling contamination related to zinc hydrometallurgy
Pophanken (1996)	Constructing, operating and capping of the jarosite pond, Galing 1.
Tindall and Muir (1996)	Transformation of iron oxide in nickel laterite processing
Hage and Schuiling (1996)	An integrated jarosite and sludge treatment process
Geldart et al. (1996)	Hydrothermal processing of Kidd Creek jarosites for stabilization and metal recovery
Berg and Borve (1996)	The disposal of iron residue at Norzink and its impact of the environment
Buckle and Lorenzen (1996)	The stability and disposal of jarosite

2.2.3 Static Tests

Accurate prediction of ARD potentially offers the most cost effective means of reducing the impact of ARD on the environment (MEND 1991). All mine waste and mine processing waste is subjected to static tests and often kinetic tests to help predict drainage chemistry. The type of static tests varies depending of composition and form of the waste. In general, the static tests compare the acid generating potential of the material (the sulfides) to its acid neutralizing capacity (carbonates). Price (2005) recommends the following static tests: elemental content which includes elemental concentration in the solids and water soluble concentration, and ABA analyses. The static tests determine the potential for acid drainage and metal leaching; further kinetic testing is required when results from the static tests indicate potential adverse drainage conditions. Chapter 3 includes results from sequential extraction tests on the residues which provide valuable information relating to metal availability.

ABA Analysis

ABA is the most well-known method to test a material for its acid generating potential. It was developed in the 1960's and 1970's and now the Sobek ABA (Sobek et al., 1978) has been in use for a few decades. Table 2.3 provides an outline of variations on the Sobek ABA method. The majority of these tests have similar procedures as the Sobek ABA method. A description of ABA analysis and results on NLR and NGR samples is provided in Chapter 8.

There have been many contributions to this area of research over the years. The international static database reported by Hutt and Morin (1999) and Morin and Hutt

(1997) provides additional insight to the general relationship between ABA parameters with data from over 20,800 static-test analyses and 126 mine sites. Work has also been conducted on improving the standard ABA method and correlating it with other methods for example: Miller et al. (1997) suggested a field version of the test; Skousen et al. (1997) introduced the SobPer method to remove the problem of incomplete hydrolysis of Fe^{3+} in the standard Sobek test and authors have reported cautions in using the ABA method (Miller et al., 1991) while Lapakko (1993) compared NP values from five different techniques. Another type of short term test that could be considered is the batch leachability test. It has been described by Marcus (1997) and is similar to paste pH test. These batch tests are conducted at high solid to liquid ratios and the equilibriated sample is analyzed for metals of interest as well as pH, Total Dissolved Solids (TDS) and major ions.

Table 2.3: Methods to determine acid generating potential of a sample (MEND, 1991)

Title/ Reference	Description
Paste pH/ Sobek 1978, BC AMD Task Force, 1989	Using a 2:1 ratio of soil to distilled-deionized water mix paste of waste and determine pH. Assesses readily available acidity or alkalinity.
Sobek Standard ABA method/ EPA 600 ABA method, Sobek et al., 1978	Determines balance between acid consuming and acid generating components of the waste. Standard method, widely used and accepted.
Modified ABA method/ Lawrence, 1990	Like the above but sample is treated for 24 hours before titration.
Lawrence and Wang, 1996, 1997	Further modifications to the standard ABA test; including using 1.0N HCl and NaOH and the acid is added in 1-3 stages.
B.C. Research Initial Test/ Bruynesteyn and Hackel, 1984	If sample from ABA test is potentially acid generating this test can be conducted. A biological oxidation test used to determine the degree that the sulfur content of the sample might be oxidized.

Waste Classification Tests

Waste classification tests provide a national classification based on a set of testing protocols and guidelines as prescribed by regulatory agencies. In the United States a waste can be described as "toxic" or "hazardous" in terms of subtitle C or D of the Resource Conservation Recovery Act (RCRA). The analytical results are compared to a set of criteria and if there are exceedances the waste is described as "toxic" or "hazardous". This type of test may also be used to assess metal leaching from mine wastes.

The most common tests protocols used to conduct this classification are: EPA Method 1310, the EPA Toxicity Test, EPA Method 1311, the Toxicity Characteristic Leach Procedure (TCLP) and EPA Method 1312. Table 2.4 lists several tests used to assess metal leaching. These tests assess low concentration and high volume waste as is the case with mining waste. The first two methods use an organic acid to leach the waste; this can result in a preferred complexation of metals Marcus (1997). Smith (1997) indicated that Method 1312 comes closest to simulating an inorganic leaching system such as found at mine or mine process sites. As these methods do not utilize site conditions they can only be used for regulatory compliance purposes. Regulatory agencies often require the TCLP test.

In the case of acidic mine drainage the heavy metals are of particular concern and the concentrations in the leachate are compared to guidelines. There are eight metals of concern currently listed by U.S. EPA; arsenic, cadmium, chromium, lead, barium, selenium, mercury and silver (U.S. EPA, 1996). Further information on leaching tests is

available in Price (1997), Lapakko et al., (1995) and Norecol (1992). The results of TCLP tests on NLR and NGR are provided in Chapter 8.

Table 2.4: Selection of waste classification tests

Test Name	Reference
Extraction Procedure Toxicity Test EP Tox, US. EPA Method 1310	US EPA, 1996
Toxicity Characteristics Leaching Procedure (TCLP), US EPA Method 1311	US EPA, 1996
Ontario Leaching Extraction Procedure (LEP)	Ministry of Environment, 1985
Quebec Leaching Protocol	Ministre de L'Environnement, 1985
BC Special Waste Extraction Procedure (SWEP)	Price, 1997, Province of BC, 1992.
CGSB Leachate Extraction Procedure (CGSB)	CGSB, 1987
Synthetic Precipitation Leaching Procedure (SPLP), US. EPA Method 1312	US EPA, 1996
Multiple Extraction Procedure (MEP), US. EPA Method 1320	US EPA, 1996
Leaching Solid Waste in a Column Apparatus, ASTM D-4874	ASTM, 2006
Sequential Batch Extraction of Waste with Acidic Extraction Fluid, ASTM D-5284	ASTM, 2004

2.2.4 Kinetic Tests

The purpose of kinetic testing is to assess the influence of time on the leachate characteristics from waste materials. The test conditions vary considerably with the test type, variations include: size of sample, test cell configuration, leach solution, leach volume, air flow conditions, drainage conditions, measurement procedure and length of test. The main kinetic tests used to evaluate mine waste including waste rock and tailings (adapted from MEND, 1991) are: humidity cell test (Chapter 8), column /lysimeter test, B.C research confirmation test, shake flask experiment (Chapter 4) and Soxhlet

extraction test. Examples of kinetic tests conducted on tailings from the literature are provided in Chapter 4. The tests not described in other chapters are outlined below.

The column/lysimeter tests are larger scale than humidity cell weathering tests and are designed to permit the measurement and quality of water draining through the soil (Ritchey, 1989). The leachate volume and concentration of metals and other species in the leachate is measured over time. The B.C. Research confirmation test is similar to the waste classification tests described in the previous section. It is used to determine whether sulfide oxidizing bacteria can generate more acid than the sample can consume. This test indicates the potential for biochemical oxidation. The soxhlet extraction test provides a confirmation of static prediction test results and models geochemical weathering by determining leachability of the sample through extended sample distillation. The waste rock pile leach test and rock wall test are field tests used to assess sulfide oxidation particularly for waste rock. Both of these tests are not commonly used and are not applicable to hydrometallurgical residue material.

There is very little in the literature on kinetic testing of any hydrometallurgical process residues, particularly residue from nickel sulfide ores. As indicated previously, the hydrometallurgical residue from nickel laterite ore does not contain high concentrations of sulfur or the same iron oxide minerals as that from the Vale Inco hydrometallurgical process. Chapters 4 and 8 describe and analyze results from kinetic testing on the VINL residues. This work is important as it provides information relevant to its acid generation and metal leaching capacity which has not been available previously in the literature and is relevant to modeling the residue and defining potential disposal methodologies.

2.3 GEOCHEMICAL REACTIVE TRANSPORT MODELING

Geochemical models simulating mine drainage can include many processes including: groundwater flow, geochemical reactions, transport of chemicals, biological processes, gas transport and potentially heat transport. In this section background is provided on types of geochemical codes, then geochemical reactive transport codes and coupled codes are discussed along with solution methods and examples of software and finally the application of geochemical reactive transport modeling to the hydrometallurgical residue disposal pond is outlined.

Although modeling studies on hydrometallurgical waste are not available in the open literature, numerous studies have been completed and reported on ARD from mill tailings (Morin and Cherry, 1988; Frind and Molson, 1994Nordstrom and Alpers, 1999; Kimball et al., 2003; Mayer et al., 2003; Glynn and Brown, 1996;; Hecht et al., 2002; Salmon, 2003). Models have become much more sophisticated over the past decade, even though MEND (2000), Parker and Roberston (1999), Zhu and Anderson (2002) and others have indicated the limitations in the predictive capability of these models.

Reactive transport codes incorporate relevant transport processes and geochemical reactions as well as feedback between the processes. Steefel and VanCappellen (1998) indicated this that type of code over the empirical models has the advantage of conducting sensitivity analyses to test non-intuitive behavior. To effectively simulate sulfide-mineral oxidation and pH buffering it is necessary to incorporate kinetically controlled reactions. Mayer et al. (2003) describes inclusion of kinetic processes in the

models and calibration of models with field data. General information relating to reactive transport modeling in acid mine drainage is provided by Frind and Molson (1994).

2.3.1 Background in Geochemical Reactive Transport Models

In order to model drainage quality in the residue disposal pond it is important to understand surface water mixing, groundwater flow, contaminant transport, chemical reactions and biological processes in the flow path. VBNC (2006) has proposed a 1 m head of water be maintained above the residue in the full-scale disposal pond. The overflow from the pond will be treated at an on-site waste water treatment plant prior to release. A simple mixed flow model (batch reactor) has been used to estimate the decant water properties in the residue disposal pond. For groundwater chemistry, a one dimensional column is employed to model flow in disposal pond while two-dimensional flow is modeled in the underlying bedrock.

The background of every reactive transport model is a flow model. The flow model describes potential or velocity fields due to groundwater flow or unsaturated flow in order to calculate transport behavior. Equations in Table 2.5 (adapted from Merkel and Planar-Friedrich, 2005) approximate laminar flow in the saturated and unsaturated zone.

Table 2.5: Description of homogeneous, laminar transport processes of a mass C in the saturated and unsaturated zone

	Saturated Zone	**Unsaturated Zone**
	Hydraulic head	**Matrix Head**
Model Equation	Darcy	Richards
	$\frac{\partial C}{\partial t} = K \frac{\partial h}{\partial l} \cdot \frac{C}{\partial z}$ (2.1)	$\frac{\partial C}{\partial t} = \left[K(P_s) \frac{\partial P_m}{\partial z} \right] \cdot \frac{C}{\partial z}$ (2.2)
Permeability (K)	Constant	Function of matrix head Pm

where:

C - Contaminant concentration in solution

dh/dl – Hydraulic gradient

t - Time

z - Depth

P_m - Matrix pressure head

This assumes there are no interactions between the species dissolved in the water and the solid phase through which the water is flowing. Other important terms to include in the mass transport equation are dispersion, diffusion and retardation. Diffusion usually has a small effect on mass transport except where the solids permeability is very low. Retardation is a culmination of effects that suppress the spread of species in relation to that of groundwater. Sometimes degradation and retardation are grouped together. Degradation is any process that removes species from aqueous solution, such as: sorption, ion exchange as well as biological and radionuclide degradation.

The simplified transport equation below describes advective-dispersive-diffusive reactive transport in one dimension in saturated porous media.

$$\frac{\partial C_i}{\partial t} = D_l \frac{\partial^2 C_i}{\partial x^2} + D_l \frac{\partial^2 C_i}{\partial x^2} + D_t \frac{\partial^2 C_i}{\partial x^2} - v_t \frac{\partial C_i}{\partial x} + \sum_n^k R_i \qquad (2.3)$$

where C_i - Contaminant concentration

R_i - The addition or removal of C_i to or from groundwater due to reaction k and n represents the number of reactions affecting C_i (Bear 1972).

V_t - Groundwater velocity

x - Distance in direction of flow

D_l, D_b, D_t - Coefficients for diffusion, lateral dispersion and transverse dispersion.

The terms advection, dispersion and diffusion can only account for transport of non-reactive species in groundwater. Almost all species in groundwater react with the each other, water or solids. These reactions include: dissolution, precipitation, sorption, de-sorption, ion exchange, reactions between aqueous and gas phase, complexation, redox reactions and formation of colloids.

2.3.2 Types of Geochemical Codes

Zhu and Anderson (2002) indicated that geochemical codes can be divided according to their level of complexity. Speciation- solubility codes do not contain spatial or temporal information and model a closed system. These codes provide information on: concentration and activities of analytes in solution; saturation information of minerals present and direction towards equilibrium; and stable species distribution at equilibrium conditions. Reaction path codes calculate a sequence of equilibrium states subject to step-wise changes in mass transfer between phases of a system or changes in a reactant in a system. Mass balance and thermodynamic equilibrium are the basis of reaction path models. Processes that are modeled in this way include: titration (mixing), buffering, flush (mixed-flow reactor) and kinetic reaction path model. Inverse mass balance models use the mass balance principle with thermodynamics, and equilibrium is not considered. These mass transfer reactions consider reactions that result in mass transfer between phases. Coupled reactive mass transport codes assume contaminant fate and transport is affected both by the partitioning of contaminants between phases and the movement of

the contaminant. Coupled models solve these sets of equations together and can include heat transport. Reactive transport codes are considered most appropriate for this research and described in more detail.

Local Equilibrium Assumption

When selecting a geochemical code one must examine whether local equilibrium assumption is a valid approximation of the system. This is discussed in detail by Knapp (1989). Knapp indicates that local equilibrium assumption is a good approximation if the time to reach equilibrium from disequilibrium (*teq*) is less than the time step and the distance the fluid has moved during this period (*leq*) is less than the grid spacing of the model. The Damkohler number (*Da*) is used to represent the rate of the reaction relative to advective transport. The Peclet number (*Pe*) expresses the relative importance of advective flow versus dispersion. Large *Da* values express that reaction rate is fast relative to transport and large *Pe* values indicate that advective transport dominates. Using values of *Da* and *Pe* approximations of *teq* and *leq* can be calculated. In general, it has been found (Knapp, 1989) for environmental problems the times and distances to attain equilibrium are quite large which is a significant factor in employing thermodynamically based models.

Isotherm-based Reactive Transport Models

Most "reactive transport models" are based on empirical isotherms (Zhu and Anderson, 2002). In these models, chemical reactions are described by an isotherm relating concentration in a solid to that in groundwater as shown below.

$$R_i \frac{\partial C_i}{\partial t} = D_i \frac{\partial^2 C_i}{\partial x^2} - v \frac{\partial C_i}{\partial x} \qquad (2.4)$$

Where $R_i = 1 + \frac{\rho}{\theta}(\partial S_i / \partial C_i)$ (Fetter, 1999)

and S_i - Concentration of *i* in solid matrix

ρ/θ - Bulk density/effective porosity

Note: diffusion has been neglected in this case.

Geochemical reactions are also described with the basic sorption or desorption concept. In this case only one species is considered and its change in concentration is determined using *Ks* or *Kd* (sorption or desorption factor). This simplification does not adequately describe natural systems where there is extensive interaction between species. Due to the simplification the isotherm or sorption-based model it will not be used for this work.

Coupled Reactive Transport Codes

In coupled models, the reaction term is often solved separately by using a chemical module such as PHREEQC or MINTEQ. In the chemical module the partitioning of chemical components between solid phases and aqueous solutions is calculated based on aqueous speciation, solubility and surface complexation reactions. The chemical reactions are solved by mass-balance and mass action equations. In coupled reactive transport models two set of equations are solved together. The transport equation for coupled models can be solved by either finite difference or finite element methods. Finite difference has the potential problem of numeric dispersion which can mostly be handled by high resolution discretization.

2.3.3 Solution of Coupled Multi-Component Reactive Transport

As Merkel and Planer-Friedrich (2005) indicated two methods are used to couple physical transport and geochemical reactions:

1. the one-step approach or global implicit formulation; and
2. the operator-splitting formulation also referred to as the two-step or sequential approach.

Using the global-implicit method the physical transport and geochemical reactions equations are solved simultaneously so that there's an equation for each species. The two-step approach employs a sequential method to solve equations in two steps with or without iterations. With the global-implicit method the equilibrium expression or kinetic rate equations are substituted directly into the transport equations. This was referred to as the direct substitution approach.

An alternate approach is based on the sequential iteration approach (SIA) or the sequential non-iterative approach (SNIA). With this method the reactive-transport phenomena is divided into two steps, the physical step and the chemical step as described by Frind and Molson (1994). SNIA solves the transport equation and in a separate step obtains concentrations at the new time. SIA uses the same technique as SNIA in addition includes iteration between the two steps. Steefel and MacQuarrie (1996) provide a detailed discussion of this topic. For complex problems a multi-step approach may be used. MINTOX code (Wunderly et al., 1996) employs a three-step approach to solve acid mine drainage problems; they are: sulfide mineral oxidation and contaminant release, transport of dissolved species and geochemical equilibrium reactions.

The advantages and disadvantages of the solution approaches for reactive-transport modeling have been discussed extensively (Steefel and MacQuarrie, 1996; Saaltink et al., 2001). For saturated systems the computational effort is reduced with the two-step method (Yeh and Tripathi, 1989), except for the case of strongly attenuated chemical species with moderate transport velocity (Saaltink et al., 2001). Slow attenuation rates is common in mine waste favoring the two-step method however rapid influx of oxygen to mine waste deposits can lead to quasi steady-state conditions which favors one-step methods (Mayer et al., 1999). In addition, the sequential method is usually easier to program and more flexible with complex systems. The advantage of one-step method is the simultaneous treatment of all processes and as convergence properties may be better it is possible to take larger time steps than for the two-step method. This method leads to the development and manipulation of very large matrices.

2.3.4 Examples of Geochemical Codes

In this section a short list of geochemical codes is presented and a few details are provided of one of the codes used for this work. Merkel and Planer-Friedrich (2005) give an overview of the evolution of various hydro-geochemical models. From a literature review, the tools used most commonly in evaluation of mine drainage quality include: PHREEQC, TOUGHREACT, STEADYQL, MIGRATE and HYDROGEOCHEM with MINTRAN (and related MIN3P) used commonly in the research setting. These codes are described in more detail in Table A.1, Appendix III. Other frequently employed codes include: CHEMSAGE, MINTEQA2, WATEQ, EQ3 and SEVIEW. CHEMSAGE being employed most frequently in the analysis processes within industrial plants. MINTEQ is

geochemical equilibrium speciation software for dilute solutions which can be used with multiple solid and gas phases and has a widely used comprehensive database. WATEQ and EQ3 have been widely applied to investigate surface water chemistry. SEVIEW with transport modeling provided by AT123D is widely used to assess subsurface transport of organics and inorganics. This reaction path code does not consider interaction of chemical species or reactions with solids and is based on partitioning species to solids. These and other well reported codes used for the most part for non-mining related assessments are outlined in Table A.2, Appendix III.

To evaluate residue drainage chemistry a common tool, developed by United States Geological Survey (USGS), PHREEQC (Parkhurst and Appelo, 1999) was considered. Program options for PHREEQC are given below and examples of how speciation and geochemical reactions are incorporated into the code are briefly outlined in Appendix IV.

- Mixing of waters;
- Equilibrium with aquatic phase through dissolution-precipitation reactions;
- Model effects of temperature;
- Input data includes measured concentration of different species;
- Model advective transport with 1-D transport, dispersion and diffusion into stagnant zones;
- Define redox potential either by Eh value or redox couple;
- Model surface-controlled reactions such as surface complexation and ion exchange;

- Variation in the number of exchange sites in proportion to the mineral or kinetic reactant;
- Model reactions with multi-component gas phases as closed or open systems;
- Fixed –volume or pressure gas –phase equilibria;
- Solid solution equilibria;
- Use of PITZER equations for ionic strengths greater than 1 mol/L; and
- Kinetic reactions with user-defined conversion rate.

2.3.5 Future in Geochemical Reactive Transport Modeling

Zhu and Anderson (2002) outlined several processes in geochemistry that are not well developed in codes. For example: most models do not include time and spatial information; there is a lack of kinetic data for critical environmental and geochemical processes (equilibrium is often assumed); the application of laboratory data to field situations is not well developed; importance of surface adsorption is not well understood and there is no provision for modeling uncertainties. In this research the model includes time and spatial information, utilizes laboratory and field data, includes surface adsorption and considers aspects of modeling uncertainities.

In Chapters 5 and 6 a model of the VINL residue is developed and employed and the codes PHREEQC and MIN3P are used to predict decant water chemistry and groundwater geochemistry over depth and time in the residue disposal ponds. Although these codes have been used previously for mine tailings and waste rock they have not to the authors knowledge been employed for assessment for hydrometallurgical residues

which consist of mineralogical assemblages that include amorphous phases, altered minerals and metals attached surfaces. This novel application of the codes provides a basis from which to assess other hydrometallurgical residue deposits.

2.4 RISK-BASED DECISION MAKING

In this section, a review is provided of 1) processes and techniques associated with risk-based decision making; 2) the Canadian Council of Ministers of the Environment (CCME) ecological risk assessment (ERA) process (CCME 1996, 1997); 3) risk management in the ERA framework; and 4) summarized examples on risk assessment applied to site remediation.

2.4.1 Background

Risk analysis is the quantitative estimate of damage using engineering evaluation and mathematical techniques. It involves both the determination of the magnitude of damage along with its probability (frequency) of occurrence. Methodologies for risk assessment include: WHO (World Health Organization), International Study Group on Risk Analysis (ISGRA) and quantitative risk assessment. The WHO method encompasses: identification of hazards, assessment of hazards and accident consequence analysis. The ISGRA methodology for risk assessment is: hazard identification, consequence analysis and quantification of risk. Quantitative risk analysis includes frequency estimation in addition to the procedures outlined by ISGRA.

Through a probabilistic risk assessment (PRA) point of view, risk is defined in terms of frequency and magnitude of consequences or the failure probability (Equation 2.5). The

objective of the risk analysis is to determine a probability of possible failure consequences. Estimation of appropriate probability values are achieved by the use of reliability theory, expert judgment, stochastic simulations, and/or historical information (Asante-Duah, 1993).

Total Failure Probability=$\sum$ [Frequency (events/time) x Magnitude (consequence/event)] (2.5)

Various techniques and methodologies have been presented to assess risk, they include: Fault Tree Analysis (FTA), failure mode effect analysis (FMEA), hazard indices, check list and "what if" analysis. Each technique is described briefly. Decision/logic trees use deductive (event tree) or inductive (fault tree) reasoning to determine the occurrence of an undesirable event. Frequency of an event can be deduced knowledge of human reliability and component failure data. The FMEA identifies failure modes for components of concern and traces the effects on other components. Another useful tool is hazard indices, for example the DOW Chemical Exposure Index, which is used to identify and rank hazards. The "check list" and "what if" analysis are the most common methods used to assess risks (albeit qualitatively). A comprehensive "check list" of process components ensures proper operating conditions of a system and through "what if" analysis deviations from normal procedures are explored and effects considered. A final important concept is that of Pathway Probability (PWP). The consequence probability is defined as the product of an initiating probability and the consequence probabilities.

2.4.2 Environmental Risk Assessment Process

The CCME (1997) has set forth guidelines for a three-tiered system for an Ecological Risk Assessment (ERA) that can be used to derive environmental quality criteria or serve as a basis for making remediation decisions. The main study components (Fig. 2.2), as outlined by CCME (1997), include receptor characterization, exposure assessment, hazard assessment and risk characterization.

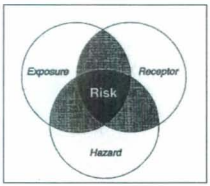

Figure 2.2: Relationship between the main study components of the CCME ERA

Suter (1993) provided an outline of the components of the human health and chemical risk assessment process adapted from U.S. EPA (1989a). The CCME ERA uses receptor characterization while U.S. EPA human health risk assessment employs toxicity assessment. The receptor assessment is a detailed part of the ERA as there are several areas of concern: loss of habitat, reduction in population size, changes in community structure and changes in ecosystem structure and function. A brief description of the main study components of the CCME ERA follows (CCME, 1997).

Receptor characterization in the ERA, using the CCME procedure, includes: characterization of habitat and characterization of receptors (including species,

population, community and ecosystems). For human health risk assessment usually there are four categories of receptors: children under 5 years, children 5-12 years, adult and site worker; and exposure is based on Chronic Daily Intake (CDI).

The exposure assessment in the ERA comprises: selection of target chemicals, contaminant release, transport and fate, exposure pathway analysis (aquatic, terrestrial exposure) and uncertainty analysis. Identification of target chemicals includes the Potential Contaminants of Concern (PCOC's) properties (such as toxicity, persistence, bioaccumulation) and concentration. Contaminant release, transport modeling and fate are assessed through: identification of source and important release mechanisms; outline likely transport pathways and fates; and finally quantitative estimates of release (preferably through direct measurement), distribution and concentration of contaminants in each environmental media (CCME, 1997).

The fate and transport modeling, validated through field measurements will provide information for input into an exposure model. For every Valued Ecosystem Component (VEC) identified in through ecological risk assessment there are various plausible exposure pathways. The pathways can include direct contact, water ingestion, soil or sediment ingestion or via food web, in addition indirect contact and applicable Bioconcentration Factors (BCF) and Bioaccumulation Factors (BAF) should be considered (CCME, 1997).

Human health exposure assessment associated with contaminated sites involves a number of issues. Primary pathways include: inhalation and/or dermal exposure; soil, water and/or crops ingestion while secondary pathways include: ingestion of mother's milk,

fish, poultry, egg, meat, dairy and/or crops. The receptor exposures are well documented (U.S. EPA, 1989a, 1989b).

In the hazard assessment for human health risk assessment chemicals are categorized as carcinogenic or non-carcinogenic. The appropriate values of threshold limits and cancer slope factors are determined through the hazard assessment as described in Chapter 7. Mathematical models (such as tolerance distribution models, mechanistic models and time to occurrence models) are used to extrapolate doses to the sub-experiments dose range (Asante- Duah, 1993).

In the ecological risk assessment it is important to assess endpoints that can accomplish goals and are relevant to the hazard, can be operationally defined and can be assessed (Suter, 1993). CCME (1997) indicates that assessment endpoints for an ERA are generally at the community level, for example "no more than a 10 % reduction in game fish population". The methodology of using ERA endpoints for an assessment conducted on the VINL disposal pond could include: conduct laboratory toxicity measurements of COC's on a number of species, complete field toxicity assessments on some species and fish populations; predict the effect of contaminant exposure on population through population-level models and determine standardized limits based on findings. Details of risk estimation calculations are provided through a case study in Chapter 7.

2.4.3 Risk Management and Risk Assessment Framework

Waste management involves balancing competing objectives of minimizing hazards and minimizing waste management costs within the constraints of the project. Generally, the

risk the higher the costs involved and vice versa. There is an optimum combination of hazard level and cost for a set risk level.

Part of the risk management program is to compare risks, benefits and costs for various strategies. A few methods used are: 1) apply weighting factors to each factor related each alternative decision. Typical factors could include: level of risk, cost and level of experience with technology for each alternative, 2) compare the costs of alternative methods to achieve a set goal of risk reduction, 3) optimize the risk-cost-benefit analysis. In this case, risks, costs and benefits are measured and uncertainties and potential tradeoffs are identified, and 4) utilize risk-time or cost-time curves in the selection between remediation alternatives. Lui (2004) is an example where risk time curves were employed. The benefit of these curves is the immediate indication of periods of elevated societal risk.

In the ERA framework, risk information is developed to assist in making decisions relative to remediation of contaminated sites and minimization of risks to humans and the environment. The estimated risk is evaluated against acceptance criteria and used to design a risk mitigation strategy. During the development of a remedial action plan the level of cleanup is determined. It is usually a site specific level that remediation will have to satisfy. Conversely, the action level is the level that when exceeded presents significant risk of adverse impact to the receptors. Clean-up decisions can be developed by deriving through modeling acceptable soil concentrations based on the chemical intake/dose that represents an acceptable level of risk. A site-specific clean-up level

considers: the degree and type of risk, intended use of site, exposure pathway, site characteristics, and variability in exposure scenarios.

U.S. EPA (1987) and others proposed methods to compute cleanup levels that account for attenuation or dilution. Specific approaches used to evaluate the risks associated with remedial options include: ranking priorities by Hazard Index (HI) and Carcinogenic Risk (Q) values; categorizing site or options for disposal based on levels of Q; developing remediation objectives by back-modeling acceptable soil concentrations based on existing site responses; establishing remediation criteria using benchmark concentrations values adjusted by safety factor; applying a safety factor to all Q values to get estimates of acceptable concentrations for exposed species.

2.4.4 Incorporating Uncertainty

To evaluate uncertainty associated with the risk assessment in this research, methods are derived to deal with the uncertainty and the most critical components of the risk assessment are prioritized. Probabilistic analysis presents a systematic method to consider uncertainty and their effects on a given decision. Chapter 7 outlines specifics on evaluating uncertainty for this research. Tools that can be used to assess uncertainty include: Monte Carlo simulation, sensitivity analysis and model calibration with monitoring data. Suter (1993) indicates that the steps involved in a Monte Carlo simulation include: define the statistical distributions of input variables, randomly sample from these distributions, perform repeated model simulations using randomly selected set of input variables and analyse the results. The result is a probability distribution of risk or an exposure, and the curve describes the uncertainty around the

calculated risk. Burnmaster and Anderson (1994) have highlighted principles of good practice for Monte Carlo techniques in ERA.

2.4.5 Risk Assessment Applied to Site Remediation and Residue Disposal

There has been considerable use of risk assessment as a decision making tool for remediation options. In order to illustrate how risk assessment has been used in the site remediation process four examples mentioned in Chapter 7 are described here in more detail.

On the topic of disposal of materials Proctor et al. (2002) considered the human health and ecological risk posed by steel slag in the environment. The study examined the potential human health risks associated with environmental applications (such as fill, roadbase and landscaping) of iron and steel making slag. Characterization data was compared to "screening" benchmarks to determine constituents of interest. A stochastic analysis was conducted to assess variability and uncertainty in the inhalation and risk estimates. The work found no significant hazards to human health from slag applications however; ecological risk may be significant in and around small water bodies due to predicted pH and aluminum levels.

Maxwell et al. (2003) used a risk-based approach to account for the differences in risk to individuals arising from variability in individual physiology and water use and the uncertainty associated with estimating chemical carcinogens, and uncertainties and variability in contaminant concentration in groundwater. This methodology was applied to a superfund site with a hypothetical contamination scenario. Initially, the human exposure and health risk was calculated when contaminated groundwater was pumped

from the site. In the second scenario, a pump-and-treat system was installed to remediate the site. This paper illustrated the importance in understanding the link between hydrogeologic regime, contaminant source, municipal receptors and remediation wells. Two different pumping rates were studied and their change in exposure and risk to different individuals was predicted and represented through cost-benefit curves which included uncertainty.

Liu et al. (2004) used a risk assessment approach to assist in the management of petroleum contaminated sites in western Canada. The project framework included a multi-phase, multi-component transport model and an ELCR (Excess Lifetime Cancer Risk) - based human health risk assessment. Six remedial alternatives were proposed and divided into hybrid exsitu and insitu approaches and integrated insitu approaches. Site monitoring reported high TPH (total petroleum hydrocarbons) and BTEX concentrations in the soil and free phase hydrocarbons (20-450 mm thick) in the groundwater. The integrated approach included: i) development of an effective modeling system for simulating fate of contaminants in soil and groundwater, ii) use of a model to predict BTEX concentrations at different temporal and spatial units under remediation scenarios, iii) assessment of environmental risks given different land use, remediation scenarios and evaluation criteria and iv) identification of desired remediation alternatives through: analysis of site conditions; technology suitability; experimental remediation studies; and interpretation of simulation and risk assessment results. The authors used a multiphase flow, multi-component transport model based on finite element method. The model was calibrated and verified using monitoring data. The model output included

three scenarios and various modeled times. The scenarios were: no remediation, remediation with 60 % efficiency and remediation with 90 % efficiency. For the study site ingestion of groundwater was considered the principal exposure pathway for the human health risk assessment. The ELCR was determined through the general equation for determining the CDI and the slope factor for the particular compound (in this case benzene). A criterion level of $1x10^{-5}$ for excess lifetime cancer risk due to benzene was used to trigger remedial action. A decision for remedial action was based on considerations and tradeoff analysis of: contaminant volatility, soil permeability, cost, remediation efficiency and clean-up time. The results were useful in assessing human health effects when on-site water is used for drinking water supply.

A final example of the use risk assessment in decision analysis is described by Ibrahim et al. (2003). This paper discusses some of the limitations of cost-benefit analysis particularly in the definition of risk and cost of risk through the presentation of an integrated approach for management of contaminated groundwater resources using health risk assessment and economic analysis. The proposed multi-criteria decision analysis framework integrates probabilistic health risk assessment in a comprehensive, cost-based multi-criteria decision analysis framework. The focus of the methodology is to develop decision criteria to provide the decision maker with insight on remedial alternatives. Three methods are explored for alternative ranking: a structured explicit decision analysis, a heuristic approach based on order of importance of decision criteria and a fuzzy logic approach. The authors indicate this structured decision analysis could be applied consistently across many different and complex remediation settings.

The focus of this work is the methodology of employing a risk-based approach to select a mine waste disposal pond design for a particular site as described in Chapter 7 through a case study. The procedure will incorporate aspects of a detailed environmental risk assessment which includes ecological and human health risk assessment and could be applied to the VINL hydrometallurgical residue and its disposal or another mine waste and other locations. The research emphasis is developing the methodology which includes managing uncertainty in the model and providing the risk assessment framework and applying a multi-criteria decision making approach. Previous authors often have not addressed uncertainty associated risk assessment and environmental risk related to waste disposal is commonly assessed once contamination is detected not during the design process. Using a risk-based decision making methodology which incorporates uncertainty at the design stage of mine waste management project is novel application in risk assessment.

CHAPTER 3

ASSESSMENT OF MINERALS AND IRON-BEARING PHASES PRESENT IN HYDROMETALLURGICAL RESIDUES FROM A NICKEL SULFIDE CONCENTRATE AND AVAILABILITY OF RESIDUE ASSOCIATED METALS

A. Steel, K. Hawboldt[a], F. Khan[a]

[a] *Faculty of Engineering and Applied Science, Memorial University of Newfoundland, St. John's, Newfoundland, Canada.*

ABSTRACT: *Hydrometallurgical facilities refining nickel sulfide ores produce waste residues in the form of sludges which contain concentrations of metals as well as iron and sulfur- bearing minerals and phases. The geochemical and mineralogical character of hydrometallurgical residues is important for the management of this type of industrial waste. Scanning Electron Microscope (SEM) and X-Ray Diffraction (XRD) analysis indicate that the minerals produced in the process are principally gypsum and the iron oxides, hematite and magnetite, iron hydroxides and residual sulfur and sulfides in the form of FeS, chalcopyrite, pyrrhotite and pentlandite. The iron oxide particles in the leach residue exhibit an atypical framboidal structure that is relevant to its metal leaching properties. The mineralogy and microstructure of mini plant residue is compared to that of the demonstration plant residue through the SEM and XRD. Sequential extractions are used to determine the association between different phases/minerals and select metals in each residue.*

A version of this paper has been published in the international journal *Hydrometallurgy.*

The lead author is Abigail Steel and the co-authors are Dr. Kelly Hawboldt and Dr. Faisal Khan. Ms. Steel's contribution to this paper is as follows:

- Wrote the paper
- Performed all laboratory testing and analysis (except ICPMS analysis)
- Calibrated and verified the experimental techniques

- Conducted interpretation of experimental results
- Performed all literature searches required for background information.

Dr. Hawboldt and Dr. Khan provided technical guidance and editing of the manuscript. The figure and table numbers and reference formats have been altered to match the formatting guidelines set out by Memorial University. The Editor-in-Chief for *International Journal of Hydrometallurgy* is aware that this manuscript will be published in this thesis and has given permission.

3.1 INTRODUCTION

Vale Inco Newfoundland and Labrador Limited (VINL) has tested a novel hydrometallurgical process to refine its nickel, cobalt and copper from the nickel sulfide concentrate derived from Voisey's Bay mine site, in Labrador, Canada. A demonstration plant operated from 2005 through 2008 with construction of a full-scale plant starting in 2009.

The nickel hydrometallurgical process eliminates SO_2 emissions, and transfers the sulfur and minor concentrations of metals, such as nickel, copper and cobalt, into wastewater and process residue. There has been limited experience in the use of hydrometallurgy to process nickel sulfide concentrate, thus characterization information on the process residue has not been widely reported. The ore from the ovoid at Voisey's Bay consists 70 % pyrrhotite, 15 % pentlandite, 10 % chalcopyrite and 5 % ilmenite (VBNC, 1997). In the disseminated to semi-massive zone 40 % plagioclase or olivine are present along with other accessory minerals. Typical VINL feed concentrate analysis is provided in Table 3.1. In the VINL hydrometallurgical process, the concentrate is subjected to a chlorine pre-leach followed by pressure oxidative leach with hydrochloric acid at 150°C (D. Stevens, pers. comm. Sept. 23, 2009).

As the residue contains a high percentage of sulfur and sulfur-bearing compounds as well as a small percentage of non-processed sulfide minerals there is potential that the sulfur oxidizes to produce acid and cause leaching of residue metals. This work outlines mineralogical characterization and sequential extraction experiments completed on the hydrometallurgical residues from the demonstration plant and mini-plant which are 1:100

and 1:1000, respectively of the full-scale plant under construction. Understanding how metals and sulfur are partitioned with iron-bearing phases and minerals present in the residue and the relative availability of the metals will aid in predicting the operation of the full-scale plant residue disposal system and the residue stabilization requirements in the long-term.

Table 3.1: Composition of Typical Feed Concentrate (VBNC, 1997)

Element	Nickel Concentrate	Element	Nickel Concentrate
Sulfur	27.9-34.9 %	Magnesium	220-20,000 g/t
Aluminum	30- 10,100 g/t	Manganese	40-250 g/t
Arsenic	100-150 g/t	Sodium	100-2262 g/t
Calcium	5330-15,600 g/t	Nickel	120,000-152,000 g/t
Cadmium	Less than 5 g/t	Phosphorus	Less than 20 g/t
Cobalt	5530-6770 g/t	Lead	120-360 g/t
Chromium	5-70 g/t	Selenium	Less than 100 g/t
Copper	15,800-28,000 g/t	Zinc	290-770 g/t
Iron	350,000-460,000 g/t		

Hydrometallurgical residue samples were taken from test campaigns conducted at the demonstration plant in Argentia, Newfoundland. The demonstration plant operated under continuous concentrate feed and variable operation conditions while the mini-plant operated under both batch and continuous feed operation. The residues from the plant are derived through either precipitation processes or pressure leaching and are in the form of sludges. There are two main sources of sludges/residues. The solids remaining when the pulp from the concentrate pressure leaching is washed by Counter Current Decantation (CCD) and neutralized with a lime slurry (Neutralized Leach Residue; NLR) and the precipitate (Neutralized Gypsum Residue; NGR) formed from the pregnant solution

during the iron removal and neutralization stage through addition of lime or limestone and air. The Neutralized Combined Residue (NCR) sent for disposal at the full-scale plant will consist of a mixture of approximately 55 % NLR and 45 % NGR; with a pulp density of approximately 40 % adjusted through addition of wastewater (VINL, 2006).

3.1.1 Acid Generation from Iron Sulfide Minerals

The oxidation of the iron sulfide mineral, pyrite, by oxygen or ferric iron on exposure to dissolved oxygen follows a chain of chemical reactions (Evangelou, 1998) that has been well documented in the literature and is well understood in comparison to that of pyrrhotite which is the predominant iron sulfide mineral present in the VINL concentrate (Nicholson and Sharer, 1990; Belzile et al., 2004). The oxidation of pyrrhotite by oxygen, as described by Nicholson and Sharer (1990), produces ferrous iron and hydrogen ions (Equation 3.1) and the ferrous iron can be further oxidized to produce $Fe(OH)_{3(s)}$ (Equation 3.2). Under anaerobic conditions oxidation of pyrrhotite by ferric iron is favored.

$$Fe_{1-x}S_{(s)} + (2-\frac{x}{2})O_2 + xH_2O \rightarrow (1-x)Fe^{2+} + SO_4^{2-} + 2xH^+ \qquad (3.1)$$

$$Fe^{2+} + \frac{1}{4}O_2 + \frac{5}{2}H_2O \rightarrow Fe(OH)_{3(s)} + 2H^+ \qquad (3.2)$$

Marcasite or pyrite, another potential mineral present in the VINL NLR, has been formed during pyrrhotite oxidation as described by Burns and Fisher (1990) using reaction (3.3).

$$2Fe_{1-x}S + \left(\frac{1}{2}-x\right)O_2 + (2-4x)H^+ \rightarrow FeS_2 + (1-2x)Fe^{2+} + (1-2x)H_2O \qquad (3.3)$$

3.1.2 The Role of Mineralogy

Characterization work for potentially acid generating material includes: the geology, mineralogy, static tests, kinetic tests, elemental analysis, standard waste assessment characterization and site components (Price et al., 1997; Price, 2005). In this paper, information pertaining to the mineralogy and microstructure of the residues is provided and then, details on the stability of minerals and associated trace metals in the residues is described.

The mineralogy of iron-bearing residue derived from copper and zinc hydrometallurgical extraction processes has been widely reported (Chen and Cabri, 1986; Romero and Rincon, 1997; Mohapatra et al., 2002). One challenge with hydrometallurgical extraction of metals associated with iron bearing minerals is the removal of iron from the pregnant solution to a stable form (Scott et al., 1986; Lahtinen and Lehtinen, 2006). Environmental concerns related to the disposal of jarosite and goethite, iron oxide residues common to the zinc hydrometallurgical process, are well reported in the literature (Vega-Farfan and Tamargo, 1996; Berg and Borve, 1996; Takugama et al., 2006). They can include: elevated concentrations of heavy metals such as: lead, zinc, cadmium, copper, mercury and arsenic which is some cases are leaching from the iron residue.

There exist numerous techniques to investigate the minerals present and their surfaces. Jambor (1994) indicated that integrated hydrogeochemical-mineralogical studies for sulfide-rich tailings impoundments have mainly involved optical microscopy, standard X-ray diffraction (XRD) methods, scanning electron microscopy (SEM) and electron-

microprobe analyses. The mineralogy of the hydrometallurgical residues is unlike that of tailings as the minerals have been formed under different conditions (temperature, pressure and time periods). This means they may have slightly different structure as well as properties than naturally formed minerals (Claassen et al., 2002). Mineralogical characterization work on mine waste, tailings or laboratory formed samples has been described by Bruckard and Woodstock (2004), Jambor and Blowes (1991), Alpers et al. (1994), Jambor (1994) and Janzen and Nicholson (1997) and others.

Sammut and Welham, (2002) provides detailed published information relating to hydrometallurgical residue from the Intec copper process. Their mineralogical characterization was conducted through XRD, Thermal Gravimetric Analysis (TGA), Differential Thermal Analyser-Fourier Transform Infrared Spectroscopy (DTA FTIR) and Raman and Mossbauer Spectroscopy plus elemental analysis.

Chen et al. (2006) reports on the residues generated during batch tests and mini plant tests on concentrate from Voisey's Bay. The authors note the residues consist primarily of hematite and sulfur with minor amounts of goethite, and the iron species generated by batch and continuous leach methods were similar however the morphologies different.

In this study, the minerals present are determined through elemental analysis, SEM and XRD analysis. XRD was used to determine the primary minerals because the analysis of the bulk sample did not readily permit the identification of low levels of constituents in the sample mass. The SEM was used to assist in the identification and quantification of the both the minerals and elements present and their microstructure. Both methods are

used to compare residues generated during the VINL mini-plant stage and the demonstration plant operation.

3.2 MATERIALS AND METHODS

3.2.1 Mineralogy of Vale Inco Hydrometallurgical Residues

The FEI Quanta 400 SEM with JKMRC Mineral Liberation Analyzer (MLA) and Rigaku Ru-200 12kW automated XRD were used to indicate elemental content and form of iron-bearing phases and potential minerals in the residues. The SEM was used to give spot analysis of elemental content of individual particles through the spectrums generated. In this case many of the similar type of particles were analyzed prior to selecting a representative spectrum. Area spectrums were also produced to provide estimates of the average elemental content of the mounted samples. In each case several area spectrums were conducted in order ensure reproducibility.

The NCR and NLR samples were analyzed with the MLA software of the SEM to determine the percent distribution of mineral groups/phases in the sample. First, the main mineral groups/phases for each type of particle are identified by spot assessment of sample particles with variations in elemental composition. After many such assessments a select number of spectrums are chosen to represent particles present in the mounted sample. These spectrums are put into the MLA database, and the MLA software is run to determine the quantity and distribution of each mineral group or phase in the sample.

In this paper, the terms "phases" or "iron-bearing phases" are used to refer amorphous or poorly crystalline minerals present in the residues. The principal residue minerals,

present in crystalline or amorphous form, are gypsum, iron hydroxide, and iron oxide with residual sulfur and sulfides in the forms of FeS, chalcopyrite, pyrrhotite and pentlandite. All but the metal sulfides (chalcopyrite, pentlandite and pyrrhotite) are secondary minerals produced by the leaching and/or precipitation processes. FeS is an iron sulfide phase identified by the SEM consisting largely of iron and sulfur with little oxygen. This amorphous pyrite or mackinawite may be similar to the FeS precipitate described by Berner (1967) and framboidal pyrite whose possible formation is provided in Wilkin and Barnes (1998).

3.2.2 Trace Metal Partitioning in Residue Minerals

Sequential extractions were conducted on the NGR, NLR and NCR in order to assess to which mineral/phases metals are associated. The method selected was a five-step extraction used for the speciation of particulate trace metals (Tessier et al., 1979). Filgueiras et al. (2002) provides a comprehensive review of sequential extraction schemes for metal fractionation of environmental samples. Elemental analysis of the residues is provided in Table 3.2.

In each step of the extraction there is dissolution of different minerals/phases freeing any attached metals at the same time. It is assumed that reagents are able to selectively extract a specific mineral/phase without affecting other minerals/phases. The extraction solutions and target minerals/phases which are dissolved for each step are provided in the Table 3.3. Refer to Tessier et al. (1979) for details of the sequential process steps including time, temperature and rinsing procedure. The dissolution of minerals for each

step is more explicitly described by the method of release rather than exact minerals. Step 1 metals are released by a solution of excess cations. Step 2 metals are precipitated or co-precipitated and are released by a mild acid. Step 3 metals are absorbed or co-precipitated and are released by reduction. Step 4 metals are complexed or absorbed and are released through oxidation. Step 5 metals are only available through strong acid digestion. The dry weight of the sample used for sequential extraction was 5.0000 g. The use of sequential extractions on hydrometallurgical residue has not been widely reported but the author believes it aids in understanding the release of residue associated metals and their partitioning amongst phases and minerals.

Table 3.2: Concentration of Main Elements/Compounds of Interest

Element/Compound	Filter Cake Solids (%) n=1-4	Leach Residue Solids (%) n=1-4
SO_4	54-57	5-6
S_{total}	18-20	27-32
Ca	19-22	0.15-2.0
Fe	3-5	45-49
Ni	0.2 -0.40	0.3-1.1
Cu	0.05-0.22	0.3-0.6
Co	0.001-0.005	<0.001-0.02
Na	0.02-0.04	<0.05-0.09
Mg	0.005	0.01-0.04
Si	0.05-0.2	0.08-0.19
Pb	<0.006-0.01	0.008-0.011
Mn	0.004-0.02	0.002-0.008
Cd	<0.0001	0.0001-0.005
Cr	0.0005-0.005	<0.001-0.017
Se	<0.01	0.007-0.01
Al	0.1-0.2	0.04

Notes: n: number of samples analyzed

Table 3.3: Sequential Extraction Solutions and Associated Mineral Categories

Extraction Step	Extraction Solution	Dissolved Mineral Categories (residue examples)
1	Magnesium Chloride	Exchangeable
2	1M NAOAC adjusted to pH 5 with HOAC	Carbonates (calcite and gypsum)
3	0.04M NH_2OH·HCl with 25% (v/v) HOAC	Fe-Mn Oxides (goethite and ferrihydrite)
4	0.02M HNO_3 with 30% (v/V) H_2O_2 (at pH 2) heat 3.2M NH_4OAC with 20% (v/v) HNO_3	Organic Matter and Sulfur (FeS, S, iron sulfides)
5	HF with 8N HNO_3 twice, then 8N HNO_3 twice, then 12N HCl	Residual (hematite)

3.3 EXPERIMENTAL RESULTS AND DISCUSSION

3.3.1 Neutralized Gypsum Residue (NGR)

The wet mount SEM image (Fig. 3.1a) shows dispersed needle-shaped (maximum size ~300 μm) gypsum particles and smaller, sub-rounded iron hydroxide particles of the demonstration plant NGR. The SEM dry-mount image (Fig. 3.1b) is of the mini-plant NGR. The largest mini-plant gypsum particles are at least three times larger than those from the demonstration plant, probably due to longer mixing times. In addition, a significant percent of smaller gypsum particles are present in both micrographs as well as a small quantity of iron hydroxides (~5% by mass Fe). The XRD spectrums (Fig. 3.2) show good agreement between the mini and demonstration plant filter cake samples suggesting the residues have similar mineral composition. It is noteworthy that the mini-plant sample appears to have more intenser gypsum (Gyp) peaks as evident at approximately 11.6 and 23.4 2-Theta, corresponding to a higher percentage of gypsum.

Several iron hydroxides are potential matches for the non-gypsum peaks including ferrihydrite (Fer) and goethite (Goe). XRD analysis also indicates presence of minor quantities of nickel and copper compounds.

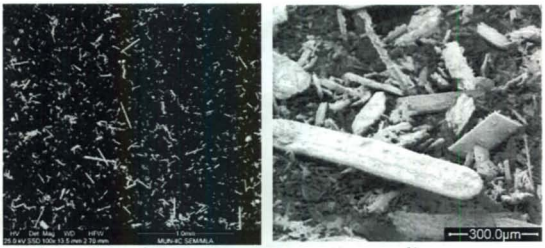

a) b)

Figure 3.1: SEM wet-mount image of demonstration plant filter cake (25X) (a), SEM dry-mount image of mini-plant filter cake (100X) (b)

During the iron removal step in hydrometallurgy, there are advantages and disadvantages to iron precipitation as jarosite, goethite, hematite or magnetite (Dutrizac, 1980). Due to the small percentage of iron hydroxides and the small particle size it was difficult to determine the specific iron hydroxide present through XRD analysis as was the findings by Sammut and Welham (2002). It has been recognized that most hydrometallurgical residues contain ferrihydrite as well as goethite (Jambor and Dutrizac, 1998; Loan et al. 2002a, 2002b). Ferrihydrite can readily absorb a wide range of dissolved species (Zinck and Dutrizac, 1998). The adsorption or co-precipitation of metals on iron hydroxides is also well documented (Webster et al., 1994; McGregor et al., 1998; Corwin et al. 1999) and could account for a portion of the metals found in the NGR. Thus the NGR probably

contains iron hydroxides in the form of goethite as well as ferrihydrite and metals are adsorbed on the ferrihydrite and possibly the goethite. Chen et al. (2006) confirmed the presence of goethite in residue derived from the VINL concentrate during continuous leaching tests.

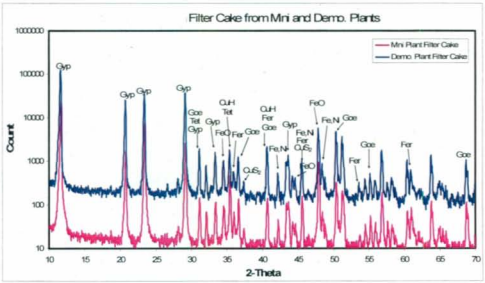

Figure 3.2: XRD results on filter cake samples from mini and demonstration plant
(note: Mini. Plant spectrum is displaced by a factor of 10 for readability.)

3.3.2 Neutralized Leach Residue (NLR)

SEM examination of a polished demonstration plant sample, Fig. 3.3a, identified the presence of un-reacted, highly reflective sulfide ore mineral particles such as: pyrite, pyrrhotite and pentlandite along with the iron oxide particles. Other larger particles evident through SEM analysis in the mini-plant leach residue are plagioclase, albite or amphibole. The un-processed sulfide ore particles and gangue minerals in the some of the SEM images are similar to that studied by Chen et al. (2006). The Chen et al. (2006) results were obtained by varying periods of continuous leaching of the VINL concentrate.

After iron oxides, sulfur is the prevalent compound present in the NLR. Fig. 3.3b shows the epoxy-mounted NLR with elemental sulfur particle.

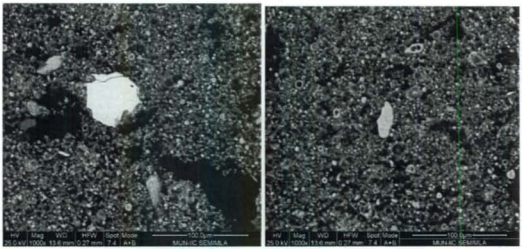

a) b)

Figure 3.3: SEM image of epoxy-mounted demonstration plant leach residue sample showing pentlandite (250X) (a), SEM image of epoxy-mounted demonstration plant leach residue sample showing sulfur (250X) (b)

a) b)

Figure 3.4: SEM image of wet-mounted demonstration plant leach residue sample showing iron-oxide spheres (2300X) (a), SEM image of epoxy-mounted demonstration plant leach residue sample showing hollow iron-oxide spheres (3600X)(b)

One of the interesting aspects of NLR is the spherical amorphous iron oxide particles, shown in Fig. 3.4a, of the wet-mounted demonstration plant residue. This image illustrates the framboidal nature of the particles which are 1-10 microns in diameter. Similar to that described in the Intec Copper Process (Sammut and Welham, 2002; Claassen et al., 2002). The epoxy-mounted sample, Fig. 3.4b, reveals the apparently hollow larger sectioned particle also identified by Dutrizac and Chen (2001). Chen et al. (2006) suggested that sulfur or residual pentlandite was present inside the larger "hollow" shell-like iron oxide particles produced by their batch method experiments. Evidence of this phenomenon in the NLR was not confirmed through the work conducted in this study. The larger grains are comprised of iron and oxygen with varying amounts of sulfur, calcium and trace of silicon and aluminum.

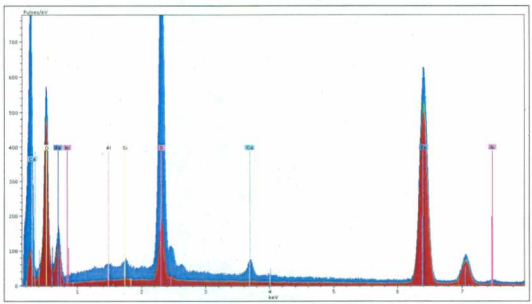

Figure 3.5: SEM spectrum iron oxide spheres in NLR

Examination of the SEM spectrums (Fig. 3.5) of a number of individual iron oxide spheres indicates the percentage of sulfur varies significantly from particle to particle (5 % - 25 %) as does the percentage of calcium. Some particles are largely comprised of iron and sulfur (FeS) or iron and oxygen (potentially Fe_2O_3) while others have a lower sulfur content and higher calcium content. There is also a variation between particles in the percentage of oxygen. Berner (1967) described FeS formed in the laboratory and suggested that the originally precipitated FeS may be oxidized first to greigite before being further oxidized to pyrite.

An area, or whole sample, SEM spectrum (Fig. 3.6) of a NLR sample shows a sample composition which includes iron, sulfur, calcium, oxygen, magnesium, aluminum, silicon, nickel and copper. The chloride and carbon also shown in the spectrum are likely from the carbon coating and epoxy material. The magnesium, aluminum and silicone

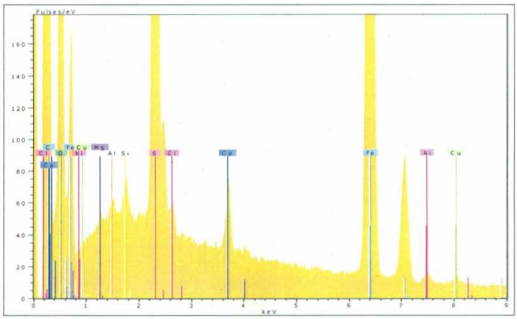

Figure 3.6: SEM area spectrum of demonstration plant in NLR

could be associated with plagioclase, albite or amphibole type minerals that are present in minor quantities in the concentrate. The copper and nickel are either associated with the unreacted concentrate or adhered to the iron oxide particles.

A processed MLA image on the NLR sample (Fig. 3.7) reveals the percentages of 17 different mineral/phase groups previously identified by spot analysis and forming the sample MLA database. The iron oxides (FeO_S_high and FeO_S_high_Ca) with high sulfur content make up approximately 67 % of the material, while the ore primary sulfides (probably un-processed concentrate) are 8 %. Sample composition of pure sulfur is about 2 % and the FeS (labeled as altered FeS_2) approximately 12 %.

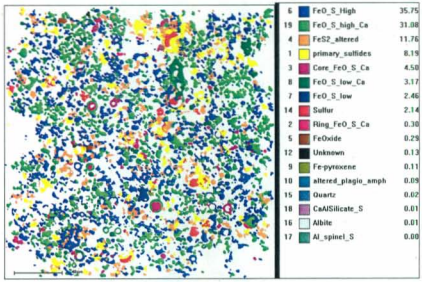

Figure 3.7: SEM MLA image of NLR with mineral compositions (325X)

The iron oxides were separated into those with high (FeO_S_high) and low (FeO_S_low) sulfur content; then further divided into those with appreciable amounts of calcium (FeO_S_high_Ca and FeO_S_low_Ca). When a mass balance was conducted between

the percentages of minerals and thus elements determined from Fig. 3.7 and that of ICPMS analysis on the NGR and NLR (Table 3.3) there was a large amount of sulfur and a smaller amount of calcium unaccounted for by estimated quantities and minerals for the NLR and a smaller amount of sulfur for the NGR. It is likely that a portion of the sulfur is adhered to the iron oxides and present as metal sulfides while the calcium is derived from residue neutralization. Table 3.4 summarizes the revised estimated percentages of the minerals/phases present in the residues after taking into account SEM/MLA results.

Table 3.4: Estimated Percentages of Residue Minerals Based on SEM/MLA Work

Filter Cake (NGR)			**Leach Residue (NLR)**			
Compounds/ minerals[b]	Chemical Formula	Percent[a] (%)	Compounds/ minerals[b]	Chemical Formula	Percent[a] (%)	Revised Percent (%)
Gypsum	$CaSO_4 \cdot 2H_2O$	93	Hematite	Fe_2O_3	67	55
Ferrihydrite	$Fe(OH)_3$ or $5Fe_2O_3 \cdot 9H_2O$	3.5	Magnetite	Fe_3O_4	10	13
Goethite	FeO(OH)	3.5	FeS	Fe S	12	10
Nickel & other metal hydroxides		Minor amounts	Sulfur	S	2	2
Ni, Cu, Co adhered to iron hydroxides		Minor amounts	Pyrrhotite	$Fe_{(1-x)}$ S	2	2
			Pentlandite	$(Fe,Ni)_9 S_8$	2	1.5
			Chalcopyrite	Cu,FeS_2	2	1
			Calcite		Not known	6
			Sulfur associated with Fe_2O_3		-	10
			Plagioclase	ie. $CaAl_2 Si_2 O_8$	Minor amounts	Minor amounts
			Ni, Cu, Co adhered to iron oxides		Minor amounts	Minor amounts

Notes: [a] Amounts are estimated from SEM/MLA work
[b] Some minerals may be present in crystalline or amorphous

The XRD spectrum (Fig. 3.8) shows a close comparison between the mini-plant NLR to that of the demonstration plant suggesting the same minerals are present in similar percentages, that applies to both the main minerals and the metal sulfates and hydroxides. The significant difference in the two spectrums is the presence of gypsum (Gyp) in the mini-plant residue. The other minerals/phases present include: hematite (Hem), magnetite (Mag), sulfur (S) and FeS (Mar). Mineral stabilities indicate that the formation of hematite (Fe_2O_3) is favored over other iron oxide minerals, at higher temperatures and lower pH values (Chen and Cabri, 1986; Cornell and Schwertmann, 2003) such as the Vale Inco process. The value of interpreting the XRD spectrum for the NLR may be limited as it does not readily identify amorphous forms of minerals such as FeS; athough marcasite and pyrite (FeS_2) were identified. A detailed examination of the composition of the FeS particles was challenging due to their small size and their nature could vary with sampling from different campaigns.

The presence of very minor quantities of metal sulfates (such as pointvinite) detected by XRD analysis in either the NLR or NGR was also reported by Romero and Rincon (1997) while considering goethite residue mineralogy from the zinc hydrometallurgy process. In addition, evidence of precipitated metal hydroxides, as detected by XRD in both residues, has previously been identified in hydrometallurgy waste. Dzombak and Morel (1990) indicated metal hydroxides precipitate at concentrations less than 10^{-6} mol/L with the sequence (Fe^{3+}, Pb, Cu, Zn, Fe^{2+}, Cd) increasing with pH; furthermore the same pH dependent sequence exists for metal adsorption on hydrated ferric oxide surfaces.

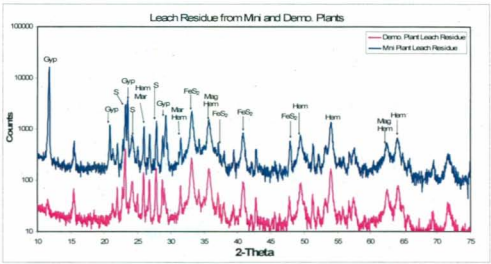

Figure 3.8: XRD spectrum of mini and demonstration plant NLR
(note: Demo. Plant spectrum is displaced by a factor of 10 for readability.)

3.3.3 Trace Metal Partitioning in Residue Phases

Results from sequential extractions are provided as concentrations of specified metals for each Step of the extraction (details of Steps are shown in Table 3.3). Concentrations for the following elements were compiled for each residue: calcium, iron, manganese, cobalt, nickel, copper, selenium, zinc, chromium and lead. The results for nickel, zinc, selenium and iron are summarized in Fig. 3.9a) through 3.9d) to illustrate the trends described below.

In general, metals associated with the NGR are more available than those attached to the NLR where the majority of metals are bound to the extraction residual suggesting they are less available for leaching. Also the metals usually exhibited highest concentrations in the NLR, lower in the NCR and lowest in the NGR. After the last step of the extraction the NGR dissolved completely while NLR and NCR did not. Iron remained in

the residual in the NCR and NLR indicating it is very stable and in a different form from that in the NGR where it was removed at Step 3. XRD analysis suggests hematite is the stable predominant iron bearing mineral in the NLR and its associated metals are resistant to dissolution by strong acids as found by Domenech et al. (2002).

Several of the metals followed similar extraction patterns; although their overall concentrations differed. NLR had the highest total concentration for cobalt and nickel (Fig. 3.9a) and the largest percentage (~70 %) of these metals left in the residual or associated with Fe_2O_3 with the remainder associated with other phases/minerals. For the NGR, the cobalt and nickel were mostly associated with the phases in extraction Step 3 in the case of the NGR likely iron hydroxides. Copper, in both the NLR and NCR, shows the same trend; approximately half the copper is associated with the hematite (in the residual) and half in the sulfurs (Step 4). The zinc and lead in the residue is slightly more available than the copper (Fig. 3.9b). About half of the zinc and more than half of the lead is associated with phases removed by Steps 1 through 4 of the extraction with Step 3 phases containing 20-40 % of these metals. About 10 % of zinc will partition with the exchangeable (Step 1) phases/minerals and 20 % with sulfur phases. The selenium is more available than other trace metals studied, with the majority of the selenium being associated with carbonate (Step 2) phases for the NCR and NLR and exchangeable (Step 1) phases/minerals for the NGR (Fig. 3.9c). Iron and chromium (53) in the NLR do not dissociate readily during extraction leaving the majority of these metals in the extraction residual (Fig. 3.9d).

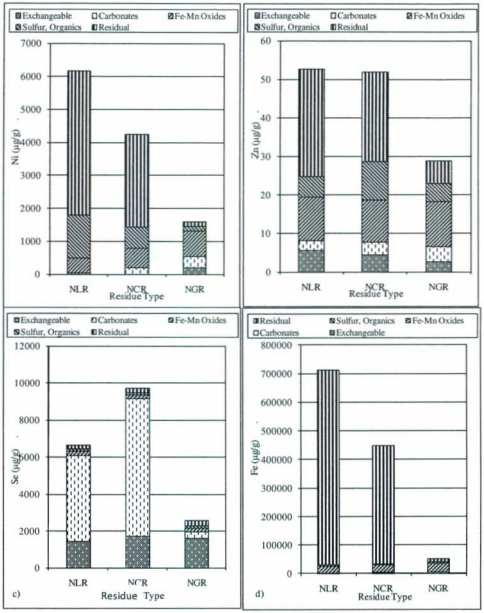

Figure 3.9: a) nickel extraction, b) zinc extraction, c) selenium extraction and d) iron extraction.

3.4 CONCLUSIONS

The SEM and XRD analyses were able to reveal mineralogical characteristics of the hydrometallurgical residue valuable in understanding how it will weather on disposal. NLR exists mainly as very small framboidal, spherical particles comprised largely of iron with varying and significant quantities of oxygen, calcium and sulfur. A total of 16 different phases were identified in the NLR by SEM analysis. They include: Fe-S phases, pure sulfur and several Fe-O phases. XRD analysis, which does not reflect the amorphous nature of some NLR minerals, indicated that the main minerals present were hematite, sulfur and pyrite. The SEM work on the NGR clearly showed two types of particles, gypsum and a small percentage of an iron-bearing mineral. The XRD analysis confirmed the strong presence of gypsum, potential iron hydroxides minerals as well as nickel bearing hydroxides. The SEM and XRD work indicated that both the mini-plant and demonstration plant residues were similar in micro-structure and composition with variations in gypsum percentages generally indicating that the mini-plant residue is representative of the larger scale plant residue and could potentially be used in residue weathering and treatment/management studies.

The results of the five-step sequential extraction on the residues suggested that the metals were more available in the NGR than the NLR. The iron (hematite) in the NLR is very stable while that in the NGR is less stable (iron hydroxides). The trace metals, nickel, copper, cobalt and zinc are associated not only with the hematite in the NLR but also with other minerals or phases resulting in a significant portion of these metals being more susceptible to weathering. During treatment and disposal of the residues it will be

important to consider the metals associated with all the phases present in particular those that are more susceptible to weathering. This study provides information on the micro-structure, mineralogy and stability of trace metals in these residues, further work is required to confirm these results and to determine the weathering properties of the sulfur-bearing phases present particularly in the NLR.

3.5 REFERENCES

Alpers, C.N., Blowes, D.W. Nordstorm, D.K., Jambor, J.L. (1994). Secondary minerals and acid mine-water chemistry. In *Environmental Geochemistry of Sulfide Mine Wastes* (short course). Minerals Association of Canada, 257-270.

Belzile, N., Chen, Y., Cai, M., Li, Y. (2004). A review of pyrrhotite oxidation. *Journal of Geochemical Exploration*, 84, 65-76.

Berg, D., Borve, K. (1996). The disposal of iron residue at Norzink and its impact on the environment. Proceedings: Second International Symposium of Iron Control in Hydrometallurgy, Ottawa, Oct.20-23, 1996, In J.E., Dutrizac, G.B., Harris (Eds.) *Iron Control and Disposal*, Ottawa, ON: CIM., 627-641.

Berner, R.A. (1967). Thermodynamic stability of sedimentary iron sulfides. *American Journal of Science*, 265, 773-785.

Bruckard, W.J., Woodstock, J.T. (2004). Characterization of Metal-Containing waste products in relation to re-treatment methods for metal recovery and recycling. In *International Conference on Sustainable Processing of Minerals, Green Processing Conference* (May 10-12, 2004). Fremantle, WA, 217-224.

Burns, R.G., Fisher, D.S. (1990). Iron –sulfur Mineralogy of Mars: Magmetic evolution and chemical weathering products, *Journal Geophysical Research*, 95, 14415-14421.

Chen, T.T., Cabri, L.J. (1986). Mineralogical overview of iron control in hydrometallurgy. In Dutrizac, J.E., Monhemius, A.J., (Eds.), *Iron Control in Hydrometallurgy,*. Chichester, U.K.: Ellis Horwood Ltd., 19-55.

Chen, T.T., Dutrizac, J.E., Poirier, G., Kerfoot, D.G., Singhal, A. (2006). Characterization of the iron-rich residues generated during the pressure oxidative leaching of Voisey's Bay nickel sulphide concentrate. In *Proceedings Conference of Metallurgy 2006*, Montreal, Oct 1-4, 2006, 429-445.

Claassen, J.O., Meyer, E.H.O., Rennie, J., Sandenbergh, R.F. (2002). Iron precipitation from zinc-rich solutions: Defining the Zincor Process. *Hydrometallurgy,* 67(1-3), 87-108.

Cornell, R.M., Schwertmann, U. (2003). The Iron Oxides, 2nd ed. VCH, Weinheim.

Corwin, D.L. Davis, A., Goldberg, S. (1999). Mobility of arsenic from Rocky Mountain arsenal area. *Journal of Contaminant Hydrology,* 39, 35-58.

Domenech, C., Ayora, C., de Pablo, J. (2002) Sludge weathering and mobility of contaminants in soil affected by the Aznalcollar tailing dam spill (SW Spain). *Chemical Geology*, 190, 355-370.

Dutrizac, J.E. (1980). The physical chemistry of iron precipitation in the zinc industry. In: Proceedings Lead--Zinc--Tin 80'; Las Vegas, Nev; 24-28 Feb. 1980., 532-564.

Dutrizac, J.E., Chen, T.T. (2001). Characterization of hematite residues from commercial zinc circuits, Waste Processing and Recycling in Mineral and Metallurgical Industries IV, In S.R. Rao, L.M., Amaratunga, P.D., Kondos, G.G. Richards, N. Kuyucak and J.A., Kozinski (Eds), *The Canadian Institute of Mining, Metallurgy and Petroleum*, Montreal, Canada, 2001, 269-296.

Dzombak, D.A., Morel, F.M. (1990). *Surface Complex Modeling- Hydrous ferris oxide*. New York: John Wiley & Sons.

Evangelou, V.P. (1998). *Environmental Soil and Water Chemistry, Principles and Applications.* New York: John Wiley and Sons.

Filgueiras, A.V., Lavilla, I., Bendicho, C. (2002). Chemical sequential extraction for metal partitioning in environmental solid samples. *Journal of Environmental Monitoring*, 4, 823 – 857.

Jambor, J.L., Blowes, D.W. (1991). Mineralogy study of low-sulfide, high carbonate, arsenic bearing tailings from the Delnite minesite, Timmins area, Ontario. In: *Proceedings of the Second International Conference of Acidic Drainage*, MEND Secretariat, Ottawa, Ontario. 4, 173-198.

Jambor, J.L. (1994). Mineralogy of sulfide-rich tailings and their oxidation products, In *Environmental Geochemistry of Sulfide Mine Wastes*, (short course, Chapter 3). Minerals Association of Canada, 22, 59-102.

Jambor, J.L, Dutrizac, J.E. (1998). Occurrence and constitution of natural and synthetic ferrihydrite, a widespread iron oxy-hydroxide. *Chemical Reviews*, 98, 2549-2585.

Jansen, M.P., Nicholson, R.V. (1997). The role of enhanced particle surface area, crystal, structure and trace metal content on pyrrhotite oxidation rates in tailings. In *Proceedings of the Fourth International Conference on Acid Rock Drainage (ICARD)*, Vancouver, B.C., May 31-June 6, 1997.V2. Richmond, B.C.: Bi-Tech Publishers.

Lahtinen, M., Svens, K. Lehtinen, L. (2006). Hematite versus jarosite precipitation in zinc production. In: *Proceedings Conference of Metallurgy 2006*, Montreal, Oct 1-4, 2006, 93-111.

Loan, M. Parkinson, G.M., Newman, O.G.M., Farrow, J.B. (2000a). Iron oxy-hydroxide crystallization in a hydrometallurgical residue. *Journal of Crystal Growth,* 235, 482-488.

Loan, M. Parkinson, G.M., Newman, O.G.M., Farrow, J.B. (2000b). Identifying nanoscale ferrihydrite in hydrometallurgical residues. *Journal of Minerals, Metals and Materials Society,* 54(12), 40-43.

Nicholson, R. V., Sharer, J. M. (1990). Laboratory studies of pyrrhotite oxidation kinetics, In C.N. Alpers, D.W. Blowes (Eds.), *Environmental Geochemistry of Sulfide Oxidation* (pp. 14-30). American Chemical Society, Symposium Aug 23-28, 1992.

McGregor, R.G., Blowes, D.W., Jambor, J.L., Robertson, W.D. (1998). The solid-phase controls on the mobility of heavy metals at the Copper Cliff tailings area, Sudbury, Ontario, Canada. *Journal of Contaminant Hydrology,* 33, 247-271.

Mohapatra, M., Anand, S., Das, R.P., Upadhyay, C.; Verma, H. C. (2002). Preparation and characterization of Cu(II), Ni(II) or Co(II) ion-doped goethite samples and their conversion to magnetite in NH_3-$FeSO_4$-H_2O medium. *International Journal of Hydrometallurgy*, 66(1), 125-134.

Price, W.A., Morin, K, Hutt, N. (1997). Guidelines for the prediction of acid rock drainage and metal leaching for mines in British Columbia: Part I general procedures and information requirements. In *Proceedings of the Fourth International Conference on Acid Rock Drainage (ICARD).* May 31-June 6 1997, Vancouver, BC, Canada. MEND Secretariat CANMET, Ottawa, Ontario. 1, 15-30.

Price, W. A. (2005). *List of potential information requirements in metal leaching and acid rock drainage assessment and mitigation work.* (MEND report 5.10E. MMSL No. 601856. CANMET Mining and Minerals Sciences Laboratory.

Romero, M., Rincon, J.M. (1997). Microstructural characterization of a goethite waste from zinc hydrometallurgical process, *Materials Letters*, 31(1-2), 67-73.

Sammut, D., Welham, N.J. (2002). The Intec Copper Process: a detailed environmental analysis. In *Proceedings Green Processing Conference*, May 29-31, 2002, Cairns, Qld., 115-124.

Scott, J.D., Donyina, D.K., Mouland, J.E. (1986). Iron the good with the bad- Kidd Creek zinc plant experience. In Dutrizac, J.E., Monhemius, A.J., (Eds.), *Iron Control in Hydrometallurgy*, Chichester, U.K: Ellis Horwood Ltd. 657-675.

Takayama, T., Campolina, C., Dutra, F. (2006). Environmental aspects of the generation and disposal of iron residues at the Votorantim zinc refinery in Brazil. In: *Proceedings Conference of Metallurgy*, Oct 1-4, 2006. Montreal, 723-735.

Tessier, A., Campbell, P.G.C., Bisson, M. (1979). Sequential extraction procedure for the speciation of particulate trace metals. *Analytical Chemistry,* 51(7), 844-851.

Vega-Farfan, J. L., Tamargo, F. (1996). Bentonites as a material for controlling contamination related to zinc hydrometallurgy. Proceedings of the Second International Symposium for Iron Control in Hydrometallurgy, Ottawa, Oct.20-23, 1996, In J.E., Dutrizac, G.B., Harris (Eds.) *Iron Control and Disposal* (pp.565-579). CIM, Ottawa, ON.

VINL (2006). *Voisey's Bay Nickel Company Project Description and Project Registration for a Commercial Processing Plant.* Retrieved September 15, 2006, from http://www.vbnc.com/NewsItems.asp?EffectiveYear=2006,

Webster, J.G., Nordstrom, D.K., Smith, K.S. (1994). Transport and natural attenuation of Cu, Zn, As and Fe in the acid mine drainage of Leviathan and Bryant Creeks. In: Alpers, C.N., Blowes, D.W. (Eds.), ACS Symposium Series 550, *Environmental Geochemistry of Sulfide Oxidation.* ACS, Washington DC, pp. 244-260.

Wilkin, R.T., Barnes, H.L. (1997). Formation of framboidal pyrite. *Geochimica et Cosmochimica Acta,* 61(2), 323-339.

Zinck, J.M., Dutrizac, J.E., (1998). The behavior of zinc, cadmium, thallium, tin and selenium during ferrihydrite precipitation from sulphate media. *CIM bulletin 91* (1019), 94-100.

CHAPTER 4

ANALYSIS OF RESULTS FROM SHAKE FLASK EXPERIMENTS CONDUCTED ON RESIDUES FROM HYDROMETALLURGICAL PROCESSES

A. Steel, K. Hawboldt[a], F. Khan[a]

[a] *Faculty of Engineering and Applied Science, Memorial University of Newfoundland, St. John's, Newfoundland, Canada.*

Received 5 May 2008; revised 28 August 2008; accepted 1 September 2008

ABSTRACT: *Hydrometallurgical facilities processing sulfide based ores, produce waste residues in the form of sludges that contain concentrations of metals as well as metal-sulfides. As part of the waste characterization and risk assessment process, a statistical design of experiment was used to assess the significant factors and interactions in the residue leaching process. Two shake flask experiments, a 2^4 factorial design and 2^3 Central Composite Design (CCD), were employed to evaluate the effect of mixing time, test pH, solid/liquid ratio and residue type on acidity, alkalinity, sulfate and metal concentration and pH of the resulting filtered leachate. The results indicate that of the variables tested mixing time and solid/liquid ratio most strongly affect metal concentration in the filtrate from waste residue samples tested over a moderate test pH range. When tests were conducted over a longer test period and at lower test pH values, test pH and residue type were dominant factors contributing to residue filtrate metal concentration.*

This paper has been published in the journal *International Journal of Environmental Science and Technology*. The lead author is Abigail Steel and the co-authors are Dr. Kelly Hawboldt and Dr. Faisal Khan. Ms. Steel's contribution to this paper is as follows:

- Wrote the paper
- Performed all laboratory testing and analysis (except ICPMS analysis)

- Calibrated and verified the experimental techniques
- Conducted interpretation of experimental results
- Performed all literature searches required for background information.

Dr. Hawboldt and Dr. Khan provided technical guidance and editing of the manuscript. The figure and table numbers and reference formats have been altered to match the formatting guidelines set out by Memorial University. The Editor-in-Chief for *International Journal of Environmental Science and Technology* is aware that this manuscript will be published in this thesis and has given permission.

4.1 INTRODUCTION

The ore at the Voisey's Bay mine site in Newfoundland and Labrador exists mainly as a nickel sulfide (pentlandite). Traditionally, when a smelter is employed to refine nickel sulfides the deleterious minerals are removed from the matte in the form of a slag containing large quantities of iron and the sulfur is partitioned from the matte to the air in the form of SO_2, which is a major source of acid deposition. Vale Inco and Voisey's Bay Nickel Company (VBNC) is testing a novel hydrometallurgical process to refine its nickel, cobalt and copper from the nickel sulfide concentrate. In this work, solid residue from this process is tested through shake flask experiments in order to provide relevant information related to the prediction of metal release to the environment. Initial testing of the Vale Inco Pressure Oxidative Leach (POL) process was conducted at a 1:1000 scale plant (mini-plant) at Vale Inco's Sheridan Park facility in Mississauga, Ontario. A larger scale (1:100) Demonstration Plant was constructed in Argentia, Newfoundland and operated between October 2005 and June 2008 and the full-scale facility is expected to be under construction by 2009 and operational by 2011. In the hydrometallurgical process a significant amount of the sulfur from the ore is dissolved and is neutralized then precipitated out largely in the form of $CaSO_4 \cdot 2H_2O$ (VBNC, 2006a). The process eliminates SO_2 emissions, and transfers the sulfur into wastewater and residue. Residue and liquid wastes are easier to handle from a pollution control perspective, but this does not eliminate the sulfur. In addition, as there has been limited experience in the use of hydrometallurgy to process nickel sulfide concentrate the characterization information on process residue is limited.

Although, the process residue will be neutralized before it is sent for disposal, it is important to perform both short and longer term tests on the residue as it contains a significant percentage of sulfur and its compounds. The tests will assist in determining its acid generating potential and metal leaching capacity with time and provide information to determine optimal treatment/mitigation/disposal options and the associated risks. These shake flask experiments are one of the established, kinetic tests used to predict release of metals from mine waste to the environment (MEND, 1991).

The methodology to conduct both static and kinetic testing on mine waste is well documented (Price and Errington, 1998; MEND, 2000; Morin and Hutt, 2001) and assists in predicting drainage chemistry. The kinetic tests assess the influence of time on the leachate characteristics of the mine materials and can include: shake flask, humidity cell, column and lysimeter tests and large test cells. A comparison of different types of kinetic tests has been conducted by Bradham and Caruccio (1991) and different humidity cell methodologies were investigated by Frostad et al. (2000). Humidity cell experiments are often used to simulate weathering conditions experienced by subaerial disposal of waste rock and mine tailings and resulting acid rock drainage (Lappako, 2003; Morin and Hutt, 2000; Verburg et al., 2000 and Li and Bernier, 1999). Column tests are also widely used to assess mine leachate either through submerged tailings or after simulated "rain events" as reported by Li and St. Arnaud (1997), Doepker (1991) and Chapman et al. (2000). Lysimeter tests provide additional control of water flow through and across subaqueously deposited mine waste material and have been described by Dave and Paktunc (2003) and Tabouda et al. (1997).

The shake flask experiment is simple and inexpensive to set up and typically a shorter duration test than the humidity cell, column or lysimeter. Variations in experimental methodologies have been used with examples described by Gleisner and Herbert (2002) and Filipek et al. (1991). The shake flask experiment has been conducted to assess the leaching conditions of specific minerals, waste rock or tailings (Marchand and Silverstein, 2000 and 2002; Renman et al., 2006 and Harahuc et al., 2000). Frostad (2003) used shake flask experiments to aid in the interpretation of kinetic test results. Darkwah et al. (2000), Bilgin et al. (2004) and Johnson and Bridge (2002) considered the effect of strains of bacteria on sulfide mineral oxidation while Widerland et al. (2005) used shake flask experiments to examine the effect of adding fresh water to an existing tailings impoundment. Results from this type of test on hydrometallurgical residues have not, to the author's knowledge, been widely reported in the literature. The shake flask experiments were conducted on the campus of Memorial University, St. John's, Newfoundland, Canada during July through August, 2006 and November, 2006 through January, 2007.

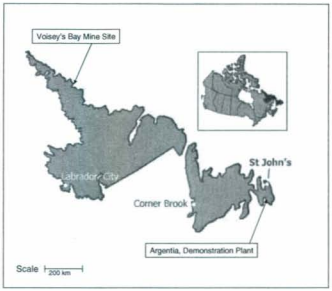

Figure 4.1: Location of Argentia Demonstration Site and Voisey's Bay Mine site.

Sampling Site Description

The hydrometallurgical plant concentrate feed is shipped from the mine site at Voisey's Bay, located on Labrador's North coast to the hydrometallurgical demonstration plant situated approximately 150 km west of St. John's, Newfoundland in Argentia (Fig. 4.1) in close proximity to the proposed location of the full-scale facility.

Hydrometallurgical residue samples were taken from test campaigns conducted during the period of March through October 2006. The residues from the plant are derived through either precipitation processes or pressure leaching and are in the form of sludges. The three main sources of sludges/residues are:

1) The solids remaining, Neutralized Leach Residue (NLR), when the pulp from the pressure leaching is washed by Counter Current Decantation (CCD);

2) The precipitate, Neutralized Gypsum Residue (NGR), formed during the iron removal and neutralization stage;

3) A final source of sludge is the precipitated metals impurities stripped from solution after the cobalt, copper and nickel have been removed. Under current strategy this stream will not be combined with the residues.

Each of these sludges has a solid and liquor portion. The solid waste from the hydrometallurgical process is approximately 60 % NLR, 40 % NGR and minor amounts of solids from water treatment processes. The current plan for the full-scale facility is to combine the NLR and NGR as a Neutralized Combined Residue (NCR) prior to disposal. The NCR will be mixed with wastewater (Process Effluent Neutralization, PEN) to approximately 40 % solids and the slurry pumped to the residue disposal pond where the waste will remain under a water cover (Vale Inco, 2008).

The amount of residue predicted to be produced from the demonstration plant is 3500 tonnes/yr while the full-scale facility is approximately 375,000 tonnes/yr (VBNC, 2002; VBNC, 2006b). For the full-scale plant, Vale Inco has proposed the NCR PEN slurry be neutralized then pumped into an existing natural pond for disposal (Vale Inco, 2008). Any discharge from the pond will be treated to meet regulatory guidelines. The waste residue from the plant will contain a high percentage of sulfur and sulfur compounds as well as a small percentage of non-processed sulfide minerals. There is potential that the sulfur and sulfur compounds present could oxidize to form acid and subsequently cause leaching of metals from the residue or bedrock and acidification of disposal pond surface water. The oxidation of the iron sulfide mineral, pyrite, on exposure to dissolved oxygen

and by ferric iron has been described by Evangelou (1998). Pyrite oxidation has been well documented in the literature and is well understood in comparison to that of pyrrhotite which is the main iron sulfide mineral present in the concentrate (Belzile et al., 2004; Nicholson and Sharer, 1990). Nicholson and Sharer (1990) have reported on the oxidation pyrrhotite.

4.2 MATERIALS AND METHODS

Two shake flask experiments have been conducted on the Demonstration Plant hydrometallurgical residues. The objective of these shake flask experiments is to assess how the chemical properties of water changes when exposed to differing concentrations of NGR and NLR over relatively short term.

Residue Composition

Scanning Electron Microscope (SEM), X-Ray Diffraction (XRD) and elemental analysis (Steel et al., 2006) indicates that the NGR contains a high percentage of gypsum particles and small percentage of iron hydroxide particles with minor quantities of nickel hydroxides and other metal hydroxide compounds as well as metals adhered to the iron hydroxides. The NLR appears to consist primarily of Fe_2O_3 and amorphous iron sulfide, and small quantities of unprocessed concentrate and sulfur.

The residues contain relatively high concentrations of nickel (0.2 - 1.1 %), copper (0.05 - 0.6 %) and lead (0.008 - 0.011 %) and the sulfur content of the NGR and NLR are in the order of 20 to 27 % respectively with sulfate concentration 54 % and 6 %, respectively.

The metals appear to be, for the most part, associated with the iron hydroxides in the NGR and iron oxides in the NLR.

Experimental Design

A factorial design of experiment was used in all shake flask experiments to optimize the required number of runs. The objective of the first experiment (experiment #1), a 2^4 factorial, was to explore the effect of various factors on the basic chemistry and metals concentration of the residue filtered leachate (filtrate) solution. The objective of the second experiment (experiment #2), a 2^3 Centre Composite Design (CCD), was to explore the effect of longer mixing times and a broader pH range and to verify and to improve relationships between the factors tested and the responses of the filtrate solution. The factors involved in the two experiments are outlined in Table 4.1; they were pH of test solution, mixing time, solids ratio (i.e. the mass of solids/mass of liquids) and residue type. Twenty separate test runs were conducted for experiment #1 and twenty-four for experiment #2 with the factor levels as in Table 4.1.

Experimental Procedure

The glass and plastic labware used for the shake flask experiments was soaked in 2N HNO_3 for at least 24 hours, after soaking in acid all equipment was triple rinsed in nano pure distilled, de-ionized water. In this paper the filtrate refers to liquid from the experiment that has been filtered using sterile disposable Millipore® 0.45 μm syringe-type filters. One blank was run for every 10 samples for periodic checks on test procedures.

The test procedure was as follows: the samples of NLR and NGR were air dried, 10 g, 38 g or 50 g of solids were weighed into separate 250 ml erlmeyer flasks to which 200 g, 200 g and 150 g, respectively, of nano pure water was added to provide solids ratios of 0.05, 0.19 and 0.33. The pH of the nano pure water was adjusted to the test pH by addition of hydrochloric acid as measured by the pH meter (Oakton, pH2100 series meter). Next, the flasks were secured on a shaker table (VWR OS-500 shaker table) set at speed 4.5 (relative 4.5/10) for the predetermined mixing period (2, 8, 14 or 26 days). The residue and water was fully mixed for the duration of the test period. At the end of the mixing time, the samples were allowed to settle and the supernatant was filtered through 0.45 μm filters into plastic containers. The types of responses measured on the filtrate are outlined in Table 4.2 along with the parameter normal range and the method of analysis. The measured metal concentrations included: iron, nickel, copper, cobalt, zinc and lead concentration. Sulfate and ferrous iron were measured by spectrophotometric methods with Hach DR/2000 spectrophotometer. Acidified samples were stored at approximately 4 ºC until the individual metals analysis was conducted in duplicate by Varian Inc. atomic absorption graphite furnace. Approximately 20 % of the metals results were verified through ICMPS (Inductively Coupled Mass Spectrometer) and duplicate runs were made of 25 % of the samples. Also indicated in Table 4.2 is the measurement resolution for each response.

Table 4.1: Summary of shake flask experimental conditions

Summary of Experimental Conditions for 2^4 Experiment #1				
Factor Name	Units	Low Level	Mid Level	High Level
Test pH		3	4	5
Mixing Time	days	2	8	14
Solids/Liquid Ratio		0.05	0.19	0.33
Residue Type		NLR		NGR
Summary of Experimental Conditions for 2^3 Experiment #2				
Factor Name	Units	Low Level	Mid Level	High Level
Test pH		2	3.5	8
Mixing Time	days	2	14	26
Residue Type		NLR		NGR

Table 4.2: Experimental responses on filtrate solution

Response Name	Units	Normal Instrument Range (Resolution)	Method/Equipment
pH		1-14 (0.005)	Oakton pH1100/2100 combination pH electrode
Electrical Conductivity	mS/cm^2	200-1999 $\mu S/cm^2$ (5% full scale: 300 $\mu S/cm^2$)	Hach CO150 conductivity meter
Redox Potential	mV	-2000 to +2000 (1mV)	ExTech orp Electrode with Oakton pH1100/2100 meter
Acidity	mg/L $CaCO_3$	0-500 typical (5 mg/L $CaCO_3$)	Titration with NaOH to 8.3 endpoint
Alkalinity	mg/L $CaCO_3$	0-500 typical (5 mg/L $CaCO_3$)	Titration with HCl to 4.3 endpoint
Sulfate Concentration	mg/L	0-70 (3 mg/L without dilution)	Spectrophotometric: barium sulfate method
Ferrous Iron Concentration	mg/L	0-3.00 (0.03 mg/L)	Spectrophotometric: 1,10 phenanthroline method
Other Metals	ppb	Variable 10-500 ppb (15%)	Varian graphite furnace AA, ICPMS

4.3 RESULTS AND DISCUSSION

The data points from experiment #1 were initially entered in Stat-Ease Design Expert® for assessment of main effects, interactions, analysis of variance, determination of regression equations, evaluation of diagnostic plots and model graphs. As a first approach, the response relationships for experiment #1 were assumed to be linear. Using this analysis, the main trends and interactions from experiment #1 were determined. Example plots of the results are shown in Figs. 4.2, 4.3 and 4.4. The data scatter evident in the plots can be attributed to: the heterogeneity of the samples, the difficulty in controlling the test water pH especially at lower test pH values, the error associated with diluting samples (sulfate measurement), and potential interference from other dissociated species (ferrous iron measurement).

The second experiment was conducted to assess the filtered leachate response over a wider test pH range (pH 2 to pH 8) and longer test times (2 to 26 days); while the solid to liquid ratio was held constant. In this experiment intermediate data points were also added. Sample graphs of the results are provided in Figs. 4.5 and 4.6. The duplicate sample results are not included in these plots due to the number of points but the data showed the same trends. In general, the main factor affecting the responses was the test pH.

In experiments #1 and #2 the effect of various factors on the chemistry of the filtered leachate solution from the hydrometallurgical plant residue was explored. Each of the experimental factors is now considered separately and discussed, then to assist in understanding the experimental responses the geochemical modeling code PHREEQC

(Parkhurst and Appelo, 1999) is used to consider the response of individual minerals in solution as well as the response of the minerals mixed in proportions similar to that found in each residue.

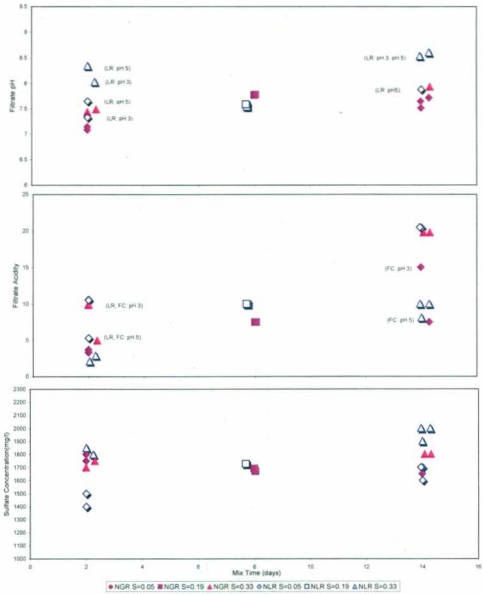

Figure 4.2: Plots of mix time versus filtrate pH, acidity and sulfate concentration at varying solids ratios from Experiment #1.

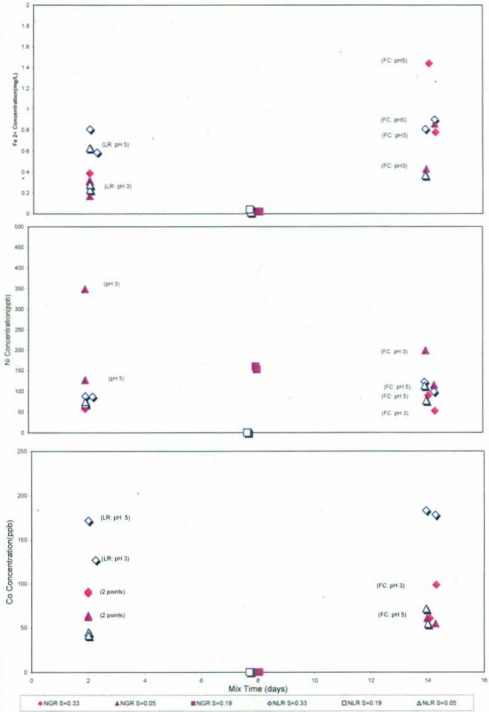

Figure 4.3: Plots of mix time versus metal concentrations from Experiment #1

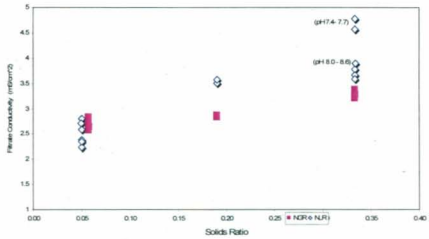

Figure 4.4: Plot of solids ratio versus filtrate conductivity from Experiment #1

Experimental Results

The solids ratio varied from 0.05 to 0.38 and had a strong effect on most parameters measured in experiment #1 while being held constant in experiment #2. It was the most significant factor in terms of pH and conductivity for NLR and sulfate concentration of the filtrate for both residues. The interaction of the residue type and solids ratio was the most significant factor for filtrate acidity, alkalinity and cobalt concentration for both residues and nickel concentration for the NGR. Mix time and solids ratio was the main interaction factor affecting iron concentration. Increasing the solids ratio causes an increase in the conductivity and sulfate concentration for both residues through increased ions in solution. NGR alkalinity decreases slightly with increasing solids ratio and the reverse is true for acidity. It was found that NGR acidity increases and NLR acidity decreases with increasing solids ratio. As the NLR is highly neutralized with lime, a higher solids ratio translates to a higher lime content which in turn rapidly goes into

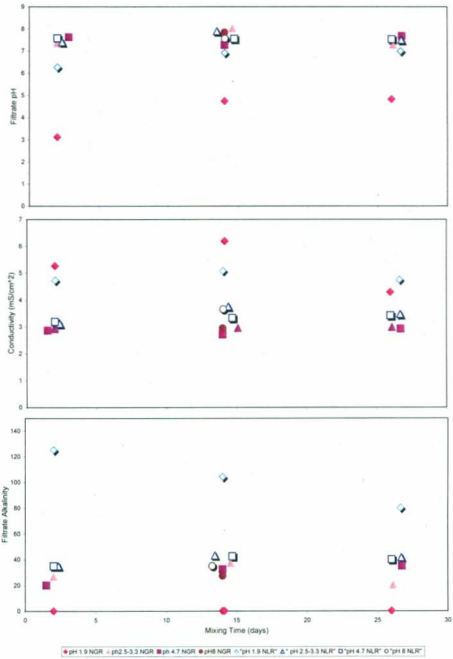

Figure 4.5: Plots of mix time versus filtrate pH, conductivity and alkalinity at varying test pH values from Experiment #2.

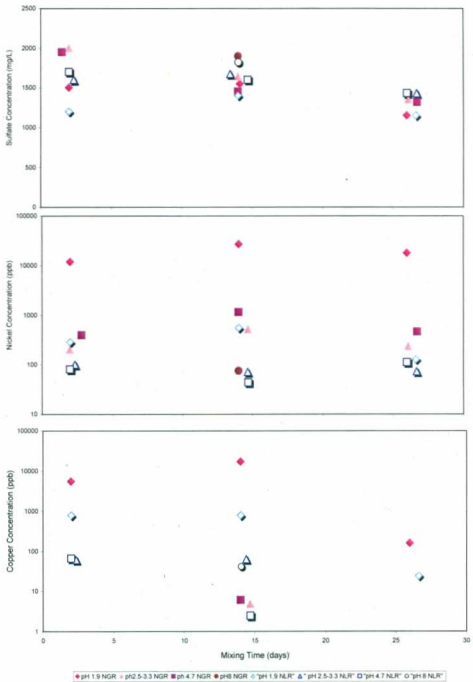

Figure 4.6: Plots of mix time versus filtrate sulfate, nickel and copper concentration at varying test pH values from Experiment #2

solution to reduce acidity in the short term. For the NLR, cobalt and ferrous iron concentration increases with increasing solids ratio and to a lesser extent nickel follows the same trend. For the NGR residue this trend is not as dramatic although the metal concentration is generally elevated with higher solids ratio. Dissolution of calcite in the NLR follows reaction (4.1), therefore, an increase in calcite concentration produces an increase in solution alkalinity and pH.

$$CaCO_3 + H_2O \rightarrow Ca^{2+} + HCO_3^- + OH^- \qquad (4.1)$$

The mix time varied from 2 to 14 days for experiment #1 and from 2 to 26 days for experiment #2. Mix time was not the primary factor for any of the responses, however it did impact the pH response, ferrous iron concentration, acidity and sulfate concentration (NLR only) for experiment #1. Increasing mix time caused a slight increase in pH response. This is initially due to the pH of the filtrate being driven by the test pH then with longer test times the test solution was neutralized by the gypsum in the NGR and the lime in the NLR. Mix time permitted more ferrous iron to go into solution. As the NLR mix time increased, the pH of the initially highly neutralized solution could drop due to the oxidation of sulfide minerals. With the wider experimental pH range (pH 2 to pH 8) of experiment #2, mix time was significant only for filtrate sulfate concentration (decreasing slightly after the 14 day mix time). The effect of mix time has to be considered with the neutralizing capacity of the residues and the role of the sulfide minerals. The slight decrease in the residue filtrate sulfate concentration after 14 days could be in part due to sulfate being adsorbed on to the walls of the glass container or sulfate combining with other available ions in solution. Further experimental work on

mixed residue results from humidity cells tests will confirm the effect of extended mix times.

In experiment #2, when the test pH drops below pH 2.5 it is the most significant model term for filtrate pH, conductivity, sulfate, acidity and metals concentration. Extending the test pH to pH 8 from pH 5 had limited effect on measured responses with the most noticeable being on sulfate concentration. Generally the sulfate concentration was higher, the redox lower, the acidity lower and metals concentration lower with higher test pH. These results indicate that an elevated pH, as encountered when residue is disposed initially in a disposal pond, may initially prevent metals from going into solution. As indicated previously, residue type is involved in the significant interaction effect for response pH, conductivity, acidity, alkalinity and metal concentration for experiment #1 and #2. The NLR metals may be less available than in the NGR for two reasons. The NLR is strongly neutralized with lime slurry prior to disposal, at short mixing times this will have a strong impact on responses. In addition, the metals in the NLR may be more strongly bound by the micro-structure of the iron oxide particles (Chen et al., 2006; Steel et al., 2006) than in the metal hydroxide particles of the NGR. The NGR, on the other hand, is disposed without further treatment therefore is more strongly impacted by changes in the leach pH, the mix time and solids ratio.

Modeling Results

The geochemical modeling code PHREEQC has been used to assess the impact that changes in the pH of water added to the main residue minerals has on the concentration of dissolved species and final solution pH. Initially individual minerals were studied, then

minerals were combined in similar ratios as those estimated to be present in the actual residue and this modeled residue was evaluated. The minerals included were: goethite, gypsum, calcite, hematite, magnetite, pyrite, pyrrhotite, pentlandite, chalcopyrite, sulfur and FeS(ppt) (a freshly precipitated, less stable and more crystalline mackinawite). FeS(ppt) is used to represent the amorphous iron sulfide in the NLR. As both Fe_2O_3, modeled as hematite, and iron sulfide, modeled as FeS(ppt), appear to be present in the NLR in an amorphous form, the database equilibrium formulations may not accurately represent the compounds present. In addition, the PHREEQC batch simulations are equilibrium based which may not be achieved in the relatively short duration of the experimental shake flask experiments. However, this work reveals the long-term trends of the minerals present.

PHREEQC results indicate when one mole of the individual minerals was added to one litre of pure water the minerals least affected by changes in test pH were hematite and goethite while gypsum, ferrihydrite, magnetite and FeS(ppt) gave final pH values slightly higher than that of the test pH. Pyrite, sulfur, pyrrhotite, pentlandite and chalcopyrite were not greatly affected by changes in test pH and resulted in final pH values between pH 2 and pH 5. Calcite was somewhat affected by test pH and final solution pH values ranged from pH 8 to pH 10.

Next the NGR minerals gypsum and goethite were equilibrated with water at pH 2 through pH 8 at molar ratios similar to that found in the actual NGR. The final pH values were slightly higher than the test pH and ferrous iron concentration decreased with

increasing test pH, sulfate concentration was fairly stable, hematite saturation index was above zero.

A non-neutralized NLR mineral composition was approximated with the minerals hematite, magnetite, sulfur, FeS(ppt) and a very minor amount of pyrrhotite, pentlandite and chalcopyrite to represent the portion of unprocessed concentrate. Again mineral molar ratios were similar to that found in the actual NLR. The high oxidizing strength of the sulfur and sulfide minerals dominated the composition of the resultant solution at all test pH values resulting in a final solution exhibiting a pH below 5. In general, the test pH only affected the concentration of ions in solution at lower test pH values. When 10 % calcite mineral was added to the NLR composition, the final solution pH was elevated above a pH of 5 at all test pH conditions. Gypsum, CO_2 and pyrite were supersaturated when calcite was added to the NLR. Only pyrite was supersaturated without the calcite mineral. The value in the PHREEQC simulations was to gain an understanding of the minerals having the greatest impact on final solution pH over a range of initial pH values and to identify compounds that precipitate out of solution.

The trace metals associated with the residues could exist in several different forms including: sorbed to surfaces of the minerals, part of the unprocessed concentrate, precipitated hydroxides or oxides, or within the crystal structure of the minerals. It is expected solution activity of trace metals will follow that of the minerals with which they are associated: gypsum, iron hydroxides, iron oxyhydroxides, iron oxides, unprocessed concentrate and iron sulfide. To summarize, of the factors considered, including solids ratio, mix time, test pH and residue type; the test pH and residue type were the main

factors that affected the majority of filtered leachate experimental responses. Residue type was a main factor in most of the responses over a range of test pH values; this reflects the importance of considering the very different nature of the two residues. Test pH was the most significant factor when the test pH was lowered to pH 2. Results suggest a significant drop in solution pH is required before a noticeable change in metal concentrations unless the solution solids ratio is elevated. In several cases it was the interaction between two factors (such as residue type and pH) that constituted the main effect on the response. Solids ratio had a significant effect on the filtrate metal and sulfate concentration and conductivity and alkalinity. Mix time was not a significant factor for most of the responses, probably due to the relatively short test duration and the strong effect of the other factors on the responses of the fresh residues.

Tests of this nature are valuable in the understanding of factors having shorter-term affects on the chemistry of waters containing appreciable amounts of residue such as the surface water in a residue disposal pond. Further shake flask experimental work will be conducted on mixed residue (NGR and NLR) at proportions similar to that proposed for disposal at the future hydrometallurgical plant to elucidate the effect of longer mix times and the synergistic effects due to the mixed residue chemistry. Geochemical modeling is a useful tool to highlight the minerals most affected by pH variations and driving changes in solution pH.

4.5 REFERENCES

Belzile, N., Chen, Y., Cai, M., Li, Y. (2004). A review of pyrrhotite oxidation. *Journal of Geochemical Exploration*, 84(2),65-76.

Bilgin, A.A., Silverstein, J., Jenkins, J. D. (2004). Iron respiration by Acidiphilium cryptum at pH 5. *Federation of European Microbiological Societies*, 49, 137-143.

Bradham, W., Caruccio, F. T. (1991). A comparative study of tailings analysis using acid/base accounting, cells, columns, and soxhlets. In *Proceedings of the Second International Conference on the Abatement of Acidic Drainage*, 1. MEND, Natural Resources Canada, Ottawa, Ontario, 157-173.

Chapman, J., Paul, M., Jahn, S., Hockley, D. (2000). Sulphide and carbonate availability and geochemical controls established for long-term column tests. In *Proceedings of the fifth International Conference on Acid Rock Drainage (ICARD)*, Society for Mining, Metallurgy and Exploration, Littleton, Colorado. 1, 581-601.

Chen, T.T., Dutrizac, J.E., Poirier, G., Kerfoot, D.G., Singhal, A. (2006). Characterization of the iron-rich residues generated during the pressure oxidative leaching of Voisey's Bay nickel sulphide concentrate. In *Proceedings Conference of Metallurgy 2006*, Montreal, Oct 1-4, 2006.

Darkwah, L., Rowson, N.A., Hewitt, C.J. (2005). Laboratory scale bioremediation of acid mine water drainage from a disused tin mine. *Biotechnology Letters*, 27,1251-1257.

Dave, N.K., Paktunc, A.D. (2003). Surface reactivity of high-sulfide copper mine tailings under shallow water cover conditions. Cairns, In *Proceedings of the Sixth ICARD*, QLD, Jul12-18, 2003, 241-251.

Doepker, R.D. (1991). Column leach study IV: factors affecting the dissolution of metals from sulfidic metal-mine tailings. In *Proceedings of the Second International Conference on Abatement of Acidic Drainage*, 1, 115-138.

Evangelou, V.P. (1998). *Environmental Soil and Water Chemistry, Principles and Applications.* New York: John Wiley and Sons.

Filipek, L.H., Gormley, J., Ewing, R., Ellsworth, D. (1991). Kinetic acid-prediction studies as aids to waste-rock and water management during advanced exploration of a massive sulfide deposit. In *Proceedings of the Second International Conference on Abatement of Acidic Drainage,* 3, 191-208.

Frostad, S., Klein, B., Lawrence, R.W. (2000). Kinetic testing I. Effects of protocol variables on rates of weathering. In *Proceedings from the Fifth International Conference on Acid Rock Drainage (ICARD)*. Society for Mining, Metallurgy and Exploration, Littleton, Colorado, 1, 641-649.

Frostad, S. (2003). Operational prediction of the ARD and metal leaching potential of a strongly oxidized, low NP waste rock. In *Proceedings from the Sudbury 2003, Mining*

and the Environment Conference. May 25-28, 2003, Laurentian University, Sudbury, ON.

Gleisner, M., Herbert, R.B. (2002). Sulfide mineral oxidation in freshly processed tailings: Batch experiments. *Journal of Geochemical Exploration,* 76, 139-153.

Harahuc, L., Lizama, H.M., Suzuki, I. (2000). Selective Inhibition of the Oxidation of Ferrous Iron or Sulfur in Thiobacillus ferrooxidans. *Applied and Environmental Microbiology*, 6(3), 1031-1037.

Johnson, D.B., Bridge, T.A.M. (2002). Reduction of ferric iron by acidophilic heterotrophic bacteria: evidence for constitutive and inducible enzyme systems in Acidiphilium spp. *Journal of Applied Microbiology*, 92, 315-321.

Lapakko, K. A. (2003). Developments in humidity cell tests and their application. In J.L. Jambor, D.W. Blowes, A.I.M. Ritchie (Eds.). *Environmental Aspects of Mine Wastes* (pp.147-164), Minerals Association of Canada.

Li, M., St. Arnaud, L. (1997). Hydrogeochemistry of secondary mineral dissolution: column leaching experiment using oxidized waste rock. In *Proceedings of the Fourth International Conference on Acid Rock Drainage (ICARD). (May 31- June 6, 1997 Vancouver, B.C.).* MEND, Natural Resources Canada, Ottawa, Ontario, 465-477.

Li, M.G., Bernier, L.R. (1999). *Contributions of carbonates and silicates to neutralization observed in laboratory tests and their field implications.* In D. Goldsack, N. Belzile, P. Yearwood, and G. Hall (Eds.). Proceedings of Sudbury '99, Mining and the Environment II, Vol.1, Sudbury, Canada, September 13-15, 1999, 59-68.

Marchand, E.A., Silverstein J. (2000). Remediation of acid rock drainage by inducing biological iron reduction. In *Proceedings from the Fifth International Conference on Acid Rock Drainage.* Society for Mining, Metallurgy and Exploration, Littleton, Colorado, 1, 1201-1207.

Marchand, E. A., Silverstein J. (2002). Influence of heterotrophic microbial growth on biological oxidation of pyrite. *Environmental Science and Technology,* 36, 5483-5490.

MEND (1991). *Acid Rock Drainage Prediction Manual*, MEND project 1.16.1b, prepared for NAMET-MSL division. MEND, Natural Resources Canada, Ottawa, Ontario.

MEND (2000). *MEND Manual, Volume 3- Prediction*, G.A. Tremblay and C.M. Hogan, (Eds.), *MEND Project* 5.4.2c. MEND, Natural Resources Canada, Ottawa, Ontario.

Morin, K.A., Hutt, N.A. (2000). Lessons learned from long-term and large-batch humidity cells, *Proceedings of the Fifth International Conference on Acid Rock Drainage (ICARD)*. Society for Mining, Metallurgy and Exploration, Littleton, Colorado, 1, 661-671.

Morin, K.A., Hutt, N.M. (2001, 2nd edition). *Environmental Geochemistry of Minesite Drainage: Practical Theory and Case Studies*. MDAG Publishing, Vancouver, Canada.

Nicholson, R.V., Sharer, J. M. (1990). Laboratory studies of pyrrhotite oxidation kinetics, In C.N. Alpers, D.W. Blowes (Eds.), *Environmental Geochemistry of Sulfide Oxidation*, 14-30. American Chemical Society, Symposium Aug 23-28, 1992.

Parkhurst, D.L. Appelo, C.A.J. (1999). User's guide to PHREEQC (Version 2) A computer program for speciation, batch reaction, one-dimensional transport and inverse geochemical calculations, U.S. Geol. Surv. Water Resources Investigation Report, 99-4259.

Price, W.A., Errington, J.A. (1998). *Guidelines for Metal Leaching and Acid Rock Drainage at Minesites in British Columbia*. Ministry of Energy and Mines. British Columbia.

Renman, R., Jiankang, W., Jinghe, C. 2006., Bacterial heap-leaching: practice in Zijinshan copper mine. *International Journal of Hydrometallurgy*, 83(1-4), 77-82.

Steel, A., Hawboldt, K., Khan, F. (Oct. 2006). *A microstructural and geochemical comparison of residues from hydrometallurgical processes*. Poster session presented at Conference of Metallurgy 2006, Montreal, Oct. 1-4, 2006.

Tabouda, A. G., Pinto, A. C. P., Nepomuceno, A. L. (1997). Lysimeter test: A method to optimize environmental forecasting the Rio Paracatu Mineracao experience. *Proceedings of the Fourth International Conference on Acid Rock Drainage (ICARD)*, (May 31-June 6, 1997 Vancouver, B.C.). MEND Secretariat CANMET, Ottawa, Ontario. 3, 1611-1626.

Vale Inco (2008). *Environmental Impact Statement, Long Harbour Commercial Processing Plant, April 2008*. Retrieved August 14, 2008, from http://www.env.gov.nl.ca/env/Env/EA%202001/Project%20Info/1243.htm.

VBNC (2002). *Argentia Hydrometallurgical Demonstration Plant Project Registration*, Retrieved January 11, 2006, from http://www.vbnc.com/Reports.asp.

VBNC (2006a). *Hydromet Development and Commercial Nickel Processing Plant Update*, presentation CIMM St. John's, NL, Nov. 3/06.

VBNC (2006b). *Voisey's Bay Nickel Company Project Description and Project Registration for a Commercial Processing Plant.* Retrieved January 1, 2006, from http://www.vbnc.com/NewsItems.asp?EffectiveYear=2006

Verburg, R., Atkin, S., Hansen, B., McWharter, D. (2000), Subaqueous and subaerial kinetic testing of paste tailings. *Proceedings of the Fifth International Conference on Acid Rock Drainage (ICARD)* May 21-24, 2000, Denver Colorado). Society for Mining, Metallurgy and Exploration, Littleton, Colorado, 2, 877-889.

Widerlund, A., Shcherbakova E., Carlsson E., Holmström H., Öhlander B. (2005). Laboratory study of calcite-gypsum sludge – water interactions in flooded tailings impoundments at the Kristineberg Zn-Cu mine, northern Sweden. *Journal of Applied Geochemistry*, 973-987.

CHAPTER 5

AN APPROACH TO NUMERICAL MODELING OF PROCESS RESIDUE IMPOUNDMENT DECANT WATER

A. Steel, K. Hawboldt[a], F. Khan[a]
[a] *Faculty of Engineering and Applied Science, Memorial University of Newfoundland, St. John's, Newfoundland, Canada*

ABSTRACT: *Nickel hydrometallurgical facilities produce large quantities of waste residues in the form of sludges which contain concentrations of sulfur, metal oxides and hydroxides, as well as minor quantities metal sulfides present in both crystalline and amorphous form. Although, the waste is neutralized before it is sent for disposal, it is critical to assess its acid generating and metal leaching potential with time in order to determine optimal treatment/mitigation/disposal options and associated risks. The waste is disposed of in an impoundment as a slurry consisting of a combination of Neutralized Combined Residue (NCR), residue liquor and Process Effluent Neutralization (PEN) solution. A geochemical code is used to model the geochemical processes occurring in the hydrometallurgical residue and to predict the impact on decant water in the residue impoundment in the short and longer term. Laboratory and field data are used to calibrate the model. Factors that affect the modeled chemistry of impoundment decant water are explored. For example, the effect of varying wastewater composition, considering closed and open scenarios and reaction kinetics. Finally, a sensitivity analysis of the model is conducted.*

This paper has been submitted to the journal *Canadian Geotechnical Journal* and is currently under review. The lead author is Abigail Steel and the co-authors are Dr. Kelly Hawboldt and Dr. Faisal Khan. Ms. Steel's contribution to this paper is as follows:

- Wrote the paper
- Performed all laboratory testing and analysis (except where noted)
- Conducted all numerical modeling work

- Conducted interpretation of results
- Performed all literature searches required for background information.

Dr. Hawboldt and Dr. Khan provided technical guidance and editing of the manuscript. The figure and table numbers and reference formats have been altered to match the formatting guidelines set out by Memorial University. The Editor-in-Chief for *Canadian Geotechnical Journal* is aware that this manuscript will be published in this thesis and has given permission.

5.1 BACKGROUND AND INTRODUCTION

The ore at the Voisey's Bay mine site in Newfoundland and Labrador exists mainly as a nickel sulfide (pentlandite). Traditionally, a smelter is used to refine nickel sulfides and waste minerals are removed from the matte in the form of a slag. During the smelting process sulfur is partitioned to the air in the form of SO_2 and has been a major source of acid deposition.

Vale Inco Newfoundland and Labrador (VINL) is testing a novel hydrometallurgical process to refine its nickel, cobalt and copper from the nickel sulfide concentrate. This Pressure Oxidative Leach (POL) process is expected to realize a reduction in energy demands compared to the traditional pyrometallurgical (smelting and refining) process and an increase in nickel and cobalt recovery (VINL, 2006). Initial testing was conducted at a 1:1000 scale plant (mini-plant) at Vale Inco's research facility in Mississauga, Ontario. A larger scale (1:100) plant has since been constructed in Argentia, Newfoundland, Canada.

The hydrometallurgical process eliminates SO_2 emissions and transfers the sulfur into wastewater and solid waste residue. There has been limited experience in the use of hydrometallurgy to process nickel sulfide concentrate, thus the characterization information on process residue is not widely reported. It is known to contain significant quantities of sulfur, sulfur-bearing phases and minor quantities of nickel, copper and cobalt (Steel et al., 2006, 2009a). Although, the waste will be neutralized before it is sent for disposal, it will be important to assess its acid generating potential and metal leaching capacity with time in order to determine optimal treatment/mitigation/disposal options

and associated risks. The work described is the task of modeling of hydrometallurgical residue such that the modeled residue can be used to further understand the decant water chemistry in the residue impoundment in the short and longer term. The model is calibrated with field data and laboratory data. Numerical modeling is employed to determine factors that affect specific residue processes and the resulting affect on the decant chemistry.

Although modeling studies on hydrometallurgical residue are not available in the open literature, numerous studies have been completed and reported on Acid Rock Drainage (ARD) from mill tailings (Nordstrom and Alpers, 1999; Kimball et al., 2003; Mayer et al., 1999 and 2002; Glynn and Brown, 1996; Hecht et al., 2002; Sharer et al., 1994; Bain et al. 2000 and Frind and Molson, 1994). Prediction of groundwater chemistry from waste rock composition has also been widely investigated (Morin and Cherry, 1988; Brown et al., 2000; Hoth et al., 2000; Filipek at al., 1999). To effectively simulate sulfide-mineral oxidation and pH buffering it is necessary to incorporate reaction kinetics. Mayer et al. (1999, 2000, 2003) describes inclusion of kinetic processes in the models and calibration of models with field data with the code MIN3P. STEADYQL (Furrer et al., 1989) classifies reactions kinetics into three categories; very fast, very slow and moderate. In this code it is the moderate rate reactions that employ kinetic expressions as illustrated in Stromberg and Banwart (1994), Salmon and Malmstrom (2004), Brown et al. (2000) and Fernandes et al. (2000). PHREEQC, is one of the geochemical reactive transport codes that has been frequently applied to the study of

leachate composition from tailings or waste rock (Shcherbakova, 2006; Filipek et al., 1999; Brown at al., 1999 and Hoth et al., 2001).

This work focuses on modeling the residue as closely as possible to the residue, using minerals, phases and metals adhered to surfaces, and comparing predicted chemistry to laboratory and modeled batch experiments as well as field measurements of impoundment decant water. Some of the residue model limitations include: the residues contain minerals in small quantities that have not been included, the residue mineral composition changes, in some cases the thermodynamic properties of the phases/minerals present are not clearly established, it was challenging to accurately model how metals are attached to minerals and modeling sulfur adsorption to minerals was not possible at this time. In addition, the code may not include all the reactions that are occurring. After calibrating the model, a sensitivity analysis on various factors affecting the model results is conducted. It should be noted that although the residue impoundments (also called disposal ponds) at the Demonstration Plant are fully lined and monitored they are for temporary storage of the process residue and all decant water is treated to ensure discharge effluent meets applicable regulatory guidelines before discharge.

5.2 SAMPLING SITE DESCRIPTION

The hydrometallurgical plant concentrate feed is shipped by barge from the mine site at Voisey's Bay, located on Labrador's North coast to the hydrometallurgical Demonstration Plant situated approximately 150 km west of St. John's, Newfoundland in Argentia (Fig. 5.1). The hydrometallurgical Demonstration Plant was operational from October, 2005 until June, 2008.

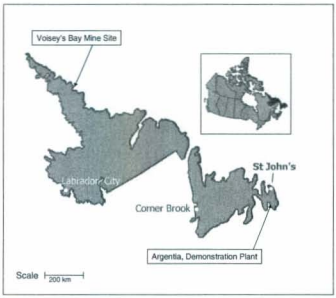

Figure 5.1: Location of Argentia demonstration plant site and Voisey's Bay mine site.

Hydrometallurgical residue samples were taken from test campaigns conducted during the period of March through October, 2006. The residues from the plant are derived through either precipitation processes or pressure leaching and are in the form of sludges. The two main sources of sludges/residues are: 1) the solids remaining when the pulp from the pressure leaching (Neutralized Leach Residue, NLR) is washed by Counter Current Decantation (CCD) and 2) the precipitate (Neutralized Gypsum Residue, NGR) formed during the iron removal and neutralization stage. Each of these sludges has a solid and liquor portion. The Neutralized Combined Residue (NCR) to be disposed of at the proposed full-scale plant will be approximately 55 % NLR and 45 % NGR (VINL, 2006). The amount of residue predicted to be produced from the demonstration plant is 3500 tonnes/yr while the amount predicted to be produced from a full-scale facility would be in

the order of 375,000 tonnes/yr (VINL, 2006, 2008). At the Demonstration Plant the solid and liquor waste exited the plant either separately or mixed into one of four lined disposal ponds that retained the solids and the liquids were further neutralized in treatment and finishing ponds.

As the waste residue from the plant contains a high percentage of sulfur and sulfur-bearing phases there is potential that the sulfur oxidize to form acidic drainage. Pyrite oxidation has been well documented in the literature (Evangelou, 1998) and is well understood in comparison to that of pyrrhotite which is the main iron sulfide mineral present in the concentrate and present in minor quantities in the residue (Belzile et al. 2004; Nicholson and Sharer, 1990). As described by Nicholson and Sharer (1990), the overall reaction for the oxidation of pyrrhotite by oxygen is written as;

$$Fe_{1-x}S_{(s)} + (2-\frac{x}{2})O_2 + xH_2O \rightarrow (1-x)Fe^{2+} + SO_4^{2-} + 2xH^+ \qquad (5.1)$$

The ferrous iron can be further oxidized to produce acid as follows;

$$Fe^{2+} + \frac{1}{4}O_2 + \frac{5}{2}H_2O \rightarrow Fe(OH)_{3(s)} + 2H^+ \qquad (5.2)$$

5.3 METHODS OF INVESTIGATION

5.3.1 Representing the Residue

The NLR and NGR were subjected to various tests to assist in determining how the residue should be modeled. Results from sample analysis with the Scanning Electron Microscope (SEM), X-Ray Fluorescence Spectrometer (XRF), and X-Ray Diffractometer (XRD) were used to determine mineral composition and microstructure of each residue

(Steel et al., 2006, 2009a). Inductively Coupled Mass Spectrometer (ICPMS) was used for elemental analysis in the residue and residue liquor (Chapter 8).

5.3.2 Field and Laboratory Studies

Decant samples were regularly taken, by VINL personnel, from residue disposal ponds (Fig. 5.2) at the Demonstration Plant site. The decant water in one of the four disposal ponds (5D) was not neutralized as a temporary test case; the remaining impoundments were kept neutralized. Sample analytical results were available, from VINL, for a five month period in 2007 and included: metals analysis, pH, conductivity and total dissolved solids. Additionally, to assess pH and conductivity conditions in a temperature and humidity controlled environment, a slurry of Neutralized Combined Residue (NCR), a mixture of NGR and NLR, was stored in the laboratory and the supernatant chemistry monitored for more than six months.

Figure 5.2: VINL demonstration plant main residue lined disposal pond

A series of shake flask experiments (Fig. 5.3) have been conducted on the NGR and NLR and reported elsewhere (Steel et al., 2009b). The shake flask experiments entailed adding distilled, de-ionized water to the weighed portions of dried residues then placing the flask on a shaking table for sets time periods (2, 7, 14 and 21 days). The supernatant chemistry (pH, conductivity, alkalinity, acidity, sulfate concentration and trace metals) was measured at the end of each test period.

Figure 5.3: Shake flask experimental set-up

5.3.3 Numerical Modeling

A conceptual model of the proposed full-scale disposal pond is provided in Fig. 5.4 and the focus of this work is the decant water above the residue. The decant water in the disposal pond will be approximately 1 m in depth (VINL, 2008). Due to the typically strong winds in the area and the shallow water depth in comparison to the size of the impoundment; it is modeled as a batch reactor as a worst case scenario involving high suspended solids.

The objective for the modeling work is to model the residue and to study factors that affect the decant water chemistry employing the modeled residue. A staged approach is used to model the disposal pond decant water; 1) each residue is modeled with consideration of its elemental and mineral composition and known properties, 2) the modeled residue is used in batch reactions and results compared with the results of shake flask experiments, 3) the adjusted modeled residue is then used to predict the decant water chemistry and results compared to that of the Demonstration Plant site conditions and 4) predictions are derived for differing disposal pond conditions.

Numerous codes are capable of modeling surface water chemistry including: MINTEQ, PHREEQC, STEADYQL, MIN3P, TOUGHREACT, CHEMSAGE and HYDROGEOCHEM, Geochemists Workbench. Not many codes can perform the batch reactions with solid minerals while considering effects such as redox, complexation, sorption/de-sorption, precipitation/dissolution, ion exchange and one or two dimensional transport. Due to its flexibility PHREEQC (Parkhurst and Appelo, 1995, 1999) was selected for this application.

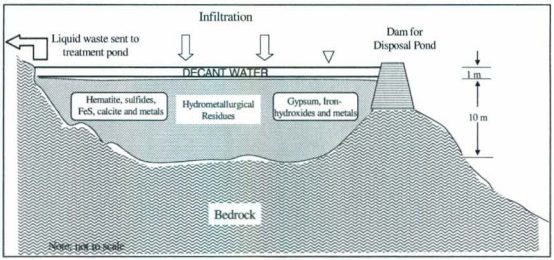

Figure 5.4: Conceptual model of typical full-scale residue disposal pond

Shake Flask Experiment

The shake flask experiment is a fully mixed batch experiment and is similar to the CSTR model of the decant water in the disposal pond at times between residue placement. To simulate this experiment with the code PHREEQC, first the batch test equilibrium model is run without metals then metals are added and the model is run again.

Impoundment Decant Water

The next objective is to model the neutralized combined residue (NCR) in a solution similar to that that will be used in the proposed full-scale plant. To do this a modeled NCR is developed in PHREEQC and tested in a batch reaction with three solutions: distilled water, residue liquor chemistry water and finally Process Effluent Neutralization (PEN) chemistry water. The resulting solutions are compared to the chemistry of the decant water in the two Demonstration Plant impoundments. At the Demonstration Plant the NCR and residue liquor was mixed with PEN before discharge the majority of the time. Residue liquor is the liquid portion of the residue slurry and PEN solution is the neutralized plant effluent after the target metals have been removed. For the full-scale plant the residue will be mixed with PEN solution prior to disposal. As the decant water above the residue will become diluted with slightly acidic rainwater over time, an acidic distilled water combined with NCR is also tested.

Next the modeled NCR is tested by considering open and closed cases, changes in mineral content, PEN solution concentration and mineral reaction kinetics. The open

case represents conditions in the decant water; while the closed case conditions that could be present at depth in the residue where oxygen is limited. Changes in mineral content and PEN solution are considered to understand the factors driving the results. As PHREEQC models equilibrium conditions it is also valuable to assess conditions not at equilibrium.

5.4 EXPERIMENTAL RESULTS AND DISCUSSION

5.4.1 Modeled Residue

Residue Composition

The residue composition is considered by way of chemical assay results, mineralogy and observed field conditions. When neutralization is maintained, chemical analysis of the decant water composition shows: the calcium concentration is high (400-600 mg/L), the dissolved iron is relatively low (0.1-4 mg/L) and the metal concentration is relatively low (0.03-0.3 mg/L (nickel)). The pH decreases with time when the decant water is left to acidify (pH 9.8 to pH 2.8) and the iron and other metals increase in concentration as expected.

SEM, XRD and elemental analysis indicates that the principal residue minerals, present in crystalline or amorphous form, are: gypsum, iron hydroxides, and iron oxides with residual sulfur and sulfides in the forms of FeS , chalcopyrite, pyrrhotite and pentlandite. Specifically the NGR contains large needle-shaped (maximum size ~300 μm) gypsum particles and smaller (<5 μm), sub-rounded iron hydroxide particles with minor quantities of nickel hydroxides and other metal hydroxide compounds. The NLR appears to consist

primarily of Fe_2O_3, an iron sulfur phase, unreacted concentrate and sulfur; the sulfur is present in elemental form and as part of compounds. The main minerals judged to be present in crystalline or amorphous form in the NGR and NLR of the hydrometallurgical residue are shown below in Table 5.1. These minerals were determined through XRD analysis with additional information provided from SEM work. Further information on the mineralogy of the residue is provided in Steel et al. (2006, 2009a).

Table 5.1: Examples of compound/minerals present in NGR and NLR.

Filter Cake (NGR)		**Leach Residue (NLR)**	
Compounds/ minerals[a]	Chemical Formula	Compounds/ minerals[a]	Chemical Formula
Gypsum	$CaSO_4 \cdot 2H_2O$	Hematite	Fe_2O_3
Ferrihydrite	$Fe(OH)_3$ or $Fe_2O_3 \cdot 9H_2O$	Magnetite	Fe_3O_4
Goethite	FeO(OH)	FeS	Fe S
Nickel & other metal hydroxides		Sulfur	S
Metal sulfides		Pyrrhotite	$Fe_{(1-x)}S$
Ni, Cu, Co adhered to iron hydroxides		Pentlandite	$(Fe,Ni)_9S_8$
		Chalcopyrite	Cu,FeS_2
		Calcite	$CaCO_3$
		Sulfur (associated with Fe_2O_3)	
		Plagioclase	ie. $CaAl_2Si_2O_8$
		Ni, Cu, Co adhered to iron oxides	

Note: [a] Minerals may be present in crystalline or amorphous form.

Table 5.1 does not represent all minerals present and the target metals (in this case nickel, copper and cobalt) appear to be, for the most part, associated with the iron hydroxides in the filter cake and iron oxides in the leach residue (Steel et al., 2009a). Table 5.2 outlines the percentage of target metals and sulfur associated with each of the residues based on four separate analyses.

Table 5.2: Select metal and sulfur concentrations in hydrometallurgical residues

	Weight Percentage (%)		
Analyte	**NLR**	**NGR**	**NCR**
Nickel	0.4-1.1	0.2-0.6	0.5-0.6
Copper	0.2-0.3	0.07-0.2	0.2-0.3
Cobalt	0.02	0.002-0.005	0.01
Total Sulfur	27-28	20-21	25-26

Modeled Residue

In order to model the residues, initially as many of the minerals present as possible are included. Table 5.3 provides the approximate fraction of the minerals present in each modeled residue. These minerals contribute either to the ion concentration in solution, the precipitated minerals or the acidity of the solution. The residues contain concentrations of nickel, copper and cobalt; these are incorporated by inclusion in the minerals and/or by surface adsorption. From the range of metal concentration in bulk samples (Table 5.2), the moles of the target metals in an 180 g sample (shake flask experiment sample size) is calculated (Table 5.4).

Table 5.3: Mineral fraction in modeled residues

Compounds/minerals present in crystalline or amorphous form	Mineral Weight Fraction		
	NLR	NGR	NCR[a]
Gypsum $CaSO_4 \cdot 2H_2O$	0	0.93	0.4
Goethite FeO(OH)	0	0.0375	0.02
Ferrihydrite $Fe(OH)_3$	0	0.0375	0.02
Iron(III) oxide Fe_2O_3	0.7	0	0.4
Iron(II,III) oxide Fe_3O_4	0.05	0	0.03
FeS	0.08	0	0.05
Sulfur S	0.02	0	0.005
Pyrrhotite $Fe_{(1-x)}S$	0.02	0	0.005
Pentlandite $(Fe,Ni)_9S_8$	0.015	0	0.0005
Chalcopyrite Cu,FeS_2	0.01	0	0.005
Calcite $CaCO_3$	0.1	0	0.4-0.1
Total	0.995	1.01	1.035

Note: [a] NCR weight percentage is estimated at 55 % NLR and 45 % NGR

Table 5.4: Trace metals in modeled residues

Residue Type	Metal	Total Metals (moles/kg)	Modeled Metals Attached to Surface[c] (mole/kg)	Amount of Metals in Sample (moles/sample)
NLR[a]	Nickel	0.17	8.50E-02	1.53E-02
	Copper	0.09	4.50E-02	8.10E-03
	Cobalt	0.0034	3.40E-03	6.12E-04
NGR[a]	Nickel	0.1	1.00E-01	1.80E-02
	Copper	0.31	3.10E-02	5.58E-03
	Cobalt	0.00078	7.80E-04	1.40E-04
NCR[b]	Nickel	0.102		1.22E-02
	Copper	0.047		5.64E-03
	Cobalt	0.0017		2.04E-04

Notes:
[a] NLR and NGR = 0.180 kg sample in 1 L of water, solids ratio=0.18
[b] NCR = 0.120 kg of sample in 1 L of water, TSS = 120 g/L
[c] 50 % of the copper and nickel is attached via surfaces to the minerals while 100 % of the cobalt is attached by surfaces
Sample size: NLR and NGR= 0.180kg, NCR=0.120 kg

5.4.2 Comparison of Modeled Residue and Shake Flask Experimental Results

To model metal release from the residues in PHREEQC it is possible that the metals are either attached to ferrihydrite in the case of the NGR or attached to ferrihydrite and within the structure of the residues minerals such as pentlandite and chalcopyrite in the NLR. For the NLR it is assumed that half the target metals are present in the mineral structure and half sorbed to surfaces. To model the correct amount of metals in the residue, a solution containing target metals in solution is placed in equilibrium with either NGR or NLR (Step 1) then the resulting solution and minerals are equilibrated with ferrihydrite surfaces (Step 2). The exposed surface area of the minerals, site density and solution metal concentration is varied until the amount of metals on surface is in the same range as that in Table 5.4. Next, these minerals and surfaces are equilibriated with pure water at a pH of 6.0 in a batch reaction at the correct ratio to simulate the shake flask experiment (Step 3). The schematic in Fig. 5.5 illustrates the process used in PHREEQC to model the metals and minerals in the shake flask experiment. The resulting concentration of metals in solution is compared to that measured in the shake flask experiments. The values listed for the shake flask experiment in Table 5.5 are based on analyses completed during experiments conducted for 14 or 26 days and at a solution pH of either 4.8 or 8.0.

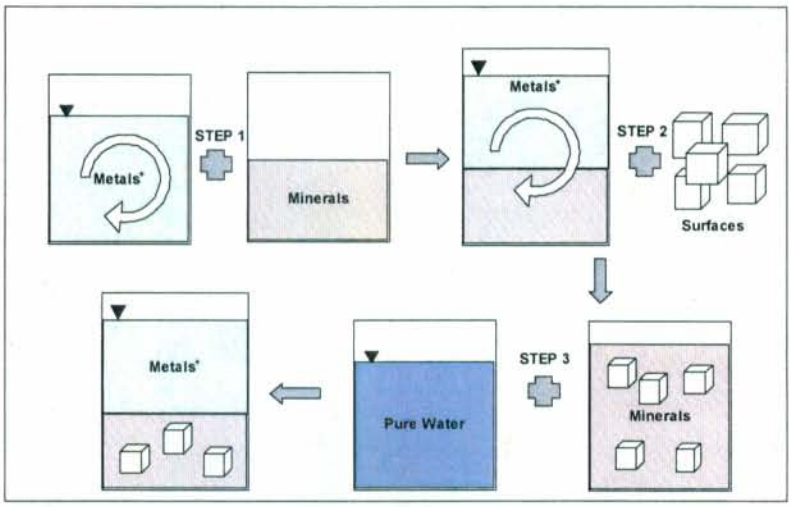

Figure 5.5: Schematic of modeling residue with surfaces and minerals in PHREEQC

Table 5.5: Comparison of shake flask solution composition with modeled residue and actual residue

	Modeled Residue Batch Test Predicted Solution Composition		**Laboratory Shake Flask Experiment Solution Composition**	
Parameter	**NLR**	**NGR**	**NLR**	**NGR**
pH	7.3	5.9	7.5	7.6
HCO_3^-	1.5E-01	4.3E-03	NA	NA
CO_3^{-2}	3.8E-04	2.7E-07	Very low	Very low
Ca^{+2}	92	11	NA	NA
Fe^{+2}	0.0	0.0	7.0E-04	9.0E-04
Fe^{+3}	0.0	0.0	NA	NA
SO_4^{-2}	100	11	18	18
conductivity	NA	NA	3.4	2.9
Ni	8.1	0.86	1.4	5.8
Cu	9.0E-03	8.4E-04	0.87	9.0E-02
Co	0.38	6.4E-02	NA	4.0E-02
alkalinity	NA	NA	38	27
acidity	NA	NA	12	9

Note: NA: not available
Concentrations in mmoles/L and total metals ions in solution reported
Alkalinity in mg/L $CaCO_3$

The objective of this exercise was to assess a geochemical reactive transport code's ability to model the residue and predict the supernatant chemistry. From the results in Table 5.5, the following generalizations can be made: the predicted pH is lower in the modeled NGR, the nickel and cobalt concentrations are in the correct range while the predicted copper concentration is two orders of magnitude lower than that found in the shake flask experiments. The sulfate concentration in the modeled NGR is close to that of the experiment while that with the modeled NLR is higher. This may be due to elemental sulfur in the NLR adhering to the glass flask. Also the predicted concentration of ferrous iron is much lower than that analysed. In the modeled NLR batch test the following minerals show saturation indices (SI) exceeding zero or close to zero: anhydrite, gypsum, H-jarosite, $FeOH_{2.7}Cl_{0.3}$ and $CoFeSO_4$. For the NGR: cupric and cuprous ferrite, $CoFeO_4$, hematite, magnetite, lepidocrocite and anhydrous have SI greater than or close to zero.

In general, it is more difficult to model the NLR. The lower predicted copper or ferrous iron concentrations could be due to metal complexes precipitating in the modeled solution while not in the actual experiments as suggested by the SI indices. PHREEQC assumes equilibrium conditions and it is likely that the solution is not at equilibrium after the 14 or 26 day test period. The PHREEQC equilibrium conditions will produce the lower pH value in the NLR due to the sulfur and sulfide mineral oxidation. Also the amorphous iron oxides and sulfur-bearing phase are likely not correctly represented by the mineral dissociation constants from in the database. Finally the way in which the trace metals are attached to ferrihydrite mineral surfaces and the mineral percentages is a

rough approximation of what was evident through mineralogical characterization of the residues (Steel et al., 2006, 2009a). One of the difficulties encountered is that the NLR was strongly neutralized with a lime slurry prior to discharge in the field, to model this calcite ($CaCO_3$) is added to the NLR minerals. This is not entirely accurate but provides the neutralizing effect evident with the NLR.

5.4.3 Numerical Modeling of Impoundment Decant Water

There are three sources of metals for this modeling exercise: metals attached to surfaces in both the NLR and NGR, metals within the structure of the minerals (such as pentlandite and chalcopyrite) and metals in solution. As with the shake flask experiment the modeled residues with surfaces and metals attached to the surfaces (Steps 1-3, Fig. 5.5) are equilibrated with pure water, NCR liquor or PEN solution and then resulting solution is compared to that of the impoundment decant water. The amount of solids in comparison to liquid was determined based on the maximum Total Suspended Solids (TSS) measurement from the Demonstration Plant residue impoundment as a worst case scenario.

The composition of the modeled NCR is provided in Tables 5.3 and 5.4 and an analysis of the mixed residue liquor and PEN solution from the Demonstration Plant is shown in Table 5.6. As with the shake flask experiment the ability to model the target metal concentration and pH was the main focus. The disposal pond consists of fresh water, PEN solution and residue liquor and the chemistry of these three solutions are run with the modeled residue to determine which provides the best fit to the measured decant water metal concentration. Fig. 5.6 shows the concentration of nickel, copper, cobalt,

lead and cadmium in solution with each of the three solutions and the average field measurements, with more detailed information provided in Table 5.7. In this case the decant water that has been neutralized is used for comparative purposes. As the pure water solution does not contain lead and cadmium those metals are not present in the resulting solution. The model using the PEN solution provides the best prediction of the trace metals selected but largely underestimates the lead concentration. Various proportions of PEN solution and residue liquor were tested to enhance the results. Saturation indices of the solution exceeded zero for cobalt oxides, anhydrite and $FeOH_{2.7}Cl_{0.3}$.

Table 5.6: PEN and NCR liquor solution composition

Analyte	PEN (mg/L)	Liquor NCR (mg/L)
Ca	733	458
Mg	127	4.5
S	1884	1109
Na	1630	NA
Cl	763	55
Fe	1	1.3
Ni	<0.5	79.5
Cu	1	26.6
Co	1	3.0
Pb	10	<0.006
Cd	19	<0.002

Note: PEN values from an average of three readings taken February –April 2008
NA: Not Available

Table 5.7: Comparison of modeled and actual impoundment decant water chemistry

	Field Measurements of Decant Water				Modeled-Disposal Pond Decant Water		
Analyte	5D-Impoundment (Not Neutralized) May-Nov., 2007		Impoundment (Neutralized) May-Nov., 2007		NCR + water	NCR + Residue Liquor	NCR + PEN
	range (mmol/L)		range (mmol/L)		(mmol/L)	(mmol/L)	(mmol/L)
pH	2.8	3.4	7.1	9.8	7.7	7.6	7.6
Ca	7.5E+00	1.7E+01	1.1E+01	1.6E+01	1.2E+01	1.3E+01	1.5E+01
Mg	1.2E-01	3.3E-01	5.8E-01	1.8E+00	0.0E+00	9.3E-02	2.7E+00
Fe	9.1E-02	8.1E-01	1.8E-03	6.8E-02	0.0E+00	0.0E+00	0.0E+00
Ni	5.3E-02	1.2E-01	5.1E-04	4.3E-03	1.5E-02	2.8E-02	2.2E-02
Cu	7.4E-03	3.1E-02	1.6E-04	9.4E-04	5.1E-05	7.4E-05	5.7E-05
Co	1.5E-02	3.3E-03	8.5E-05	2.1E-03	3.2E-03	6.0E-03	6.2E-03
Pb	2.4E-05	1.9E-04	9.7E-06	9.7E-06	0.0E+00	6.3E-12	9.3E-09
Cd	4.4E-06	1.6E-05	8.9E-07	8.9E-06	0.0E+00	2.8E-09	1.9E-04

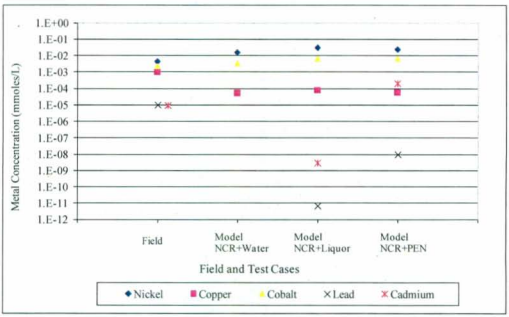

Figure 5.6: Comparison of trace metal concentration in field and modeled residue mix solution

Two conditions modeled are the not-neutralized decant water and the closed or low oxygen system. Fig. 5.7 shows these conditions for pH and a selection of trace metals. The field not-neutralized measurements were taken in the impoundment where the decant water pH was not controlled. When the decant water in the impoundment is allowed to acidify the metal concentration is approximately one order of magnitude higher than that found in the pH controlled impoundment. These conditions are simulated by reducing the amount of the calcite in the NCR from 0.095 to 0.06 moles/L. Generally the metal concentration increases (amount depending on the metal) with decreasing amounts of calcite; as expected due to the neutralizing effect of the calcite. A calcite concentration of 0.095 moles/L approximates the metal conditions found at the site. The modeled and measured pH for the not neutralized scenario is closer at a calcite concentration of 0.075 moles/L.

The closed or anaerobic case is similar to conditions that exist near the base of the impoundment when oxygen has been depleted. The closed case shows the reduction in nickel and copper concentration with lower oxygen conditions compared to the base case (calcite concentration equal to 0.095 moles/L) as less pentandite and chalcopyrite is oxidized.

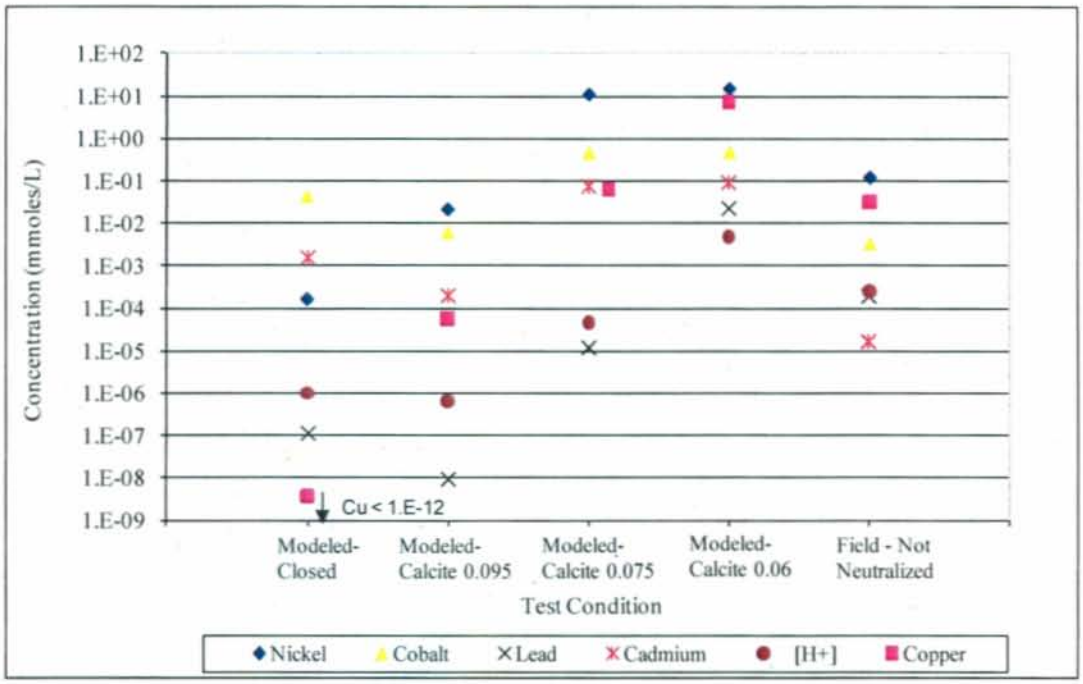

Figure 5.7: Trace metal concentration versus field and model solutions with variable test conditions

5.4.4 Comparison of Acidification of Disposal Pond Decant Water and Laboratory Measurements

As indicated previously, in one of the four Demonstration Plant impoundments the decant was not treated after residue disposal as a test case. The chemistry of this decant water was monitored by VINL. Fig. 5.8 provides a comparison between pH readings from this disposal pond and that measured in a laboratory set-up for a period of approximately six months. The laboratory results were measured from the supernatant of a 15 L bucket half filled with mixed residue slurry. The pH drop for each solution shows a very similar trend over time. The majority of the decrease occurs within the first 50 days at which point most of the readily available sulfur has been oxidized.

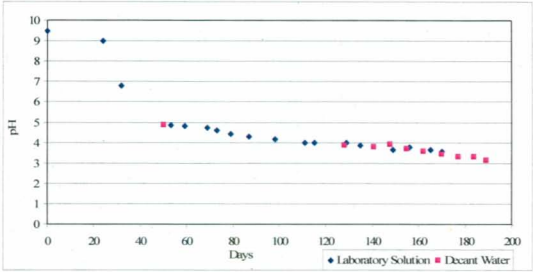

Figure 5.8: Comparison between pH of Demonstration Plant and laboratory decant water

5.4.5 Sensitivity Analysis

The sensitivity analysis consisted of three different methods; the total mineral percentage in comparison to the weight of solution was altered, individual mineral percentages as a portion of the solids were increased, and the concentration of the analytes in the PEN solution was increased. Fig. 5.9 shows the effect, on the predicted trace metal concentration, of increasing the amount of minerals present, except calcite, in the solution by 10, 15 and 20 percent. Calcite was not increased as it canceled the effect of increasing the mineral concentration. The cobalt concentration tended to level off while the other metals increased proportionally. As shown by Fig. 5.10, increasing the PEN solution analyte concentrations did not appreciably alter the concentration of metals in solution and increases in concentration of any one mineral did not appreciably increase metal concentration in the modeled decant water with the exception of FeS and pyrrhotite

which caused increases in concentration of all trace metals above that of the base case. Changes in the concentration of FeS had the largest single effect on the modeled decant water trace metal concentration. This is due to the thermodynamics of its formation/ dissolution reaction and the direct generation of hydrogen sulfide ions.

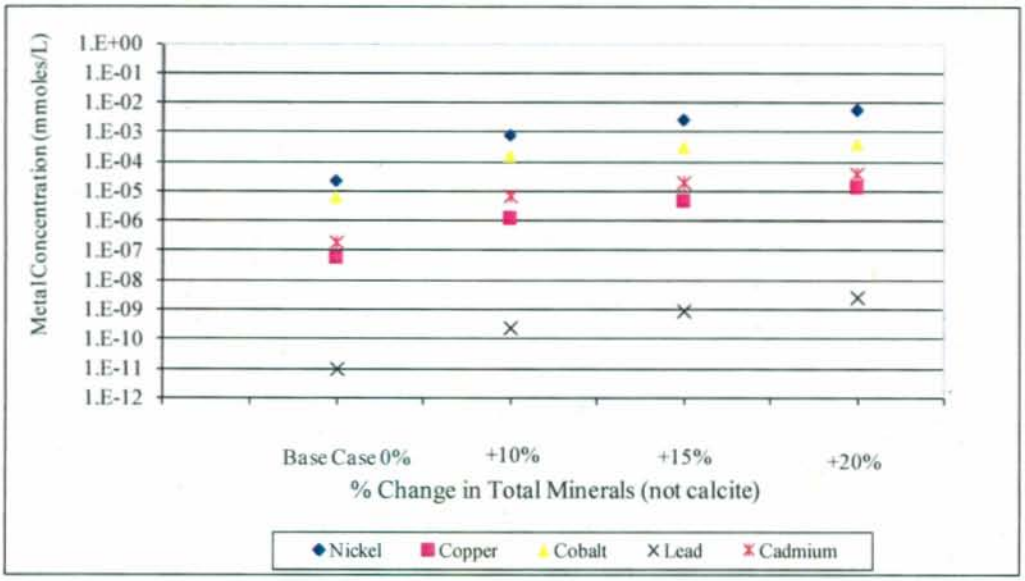

Figure 5.9: Effect of change in total minerals on predicted metal concentration

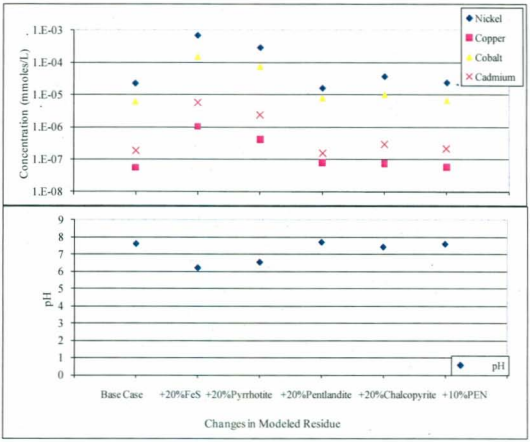

Figure 5.10: Effect of changes in percent of individual minerals on predicted metals concentration

5.4.6 Role of Kinetics in Modeling Decant Water in the Disposal Pond

Modeling the residue minerals with equilibrium expressions provides information on the long-term status in the impoundment. It is also of interest how the chemistry of the decant water may be alter with time. When considering the kinetics of mineral dissolution reactions the minerals can be grouped into three categories. There are minerals that react so slowly that they need not be considered in the modeling exercise; an example of this is hematite. Second, there are reactions that occur very rapidly and for

which the equilibrium expression is an appropriate approximation of reality. Finally there are those minerals for which the kinetics of the reactions is important to consider. In PHREEQC the dissolution – precipitation reactions are modeled, unless stated, by equilibrium expressions while in the geochemical reactive transport code MIN3P (Mayer et al., 1999) they are based solely as kinetically controlled reactions. The code MIN3P is used to model changes in pore water chemistry in a residue-filled column (Chapter 6) and is used in this work to provide further understanding of reaction kinetics in the decant solution. Table 5.8 summarizes the rate expressions employed in the model when considering the kinetics of mineral dissolution and the residue. A shrinking core model (Davis and Ritchie, 1986; Wunderly et al., 1996) is used to describe the rate expression for the sulfide minerals. Pentlandite and chalcopyrite rates are dependent on oxygen concentration while the pyrrhotite rate expression is a function of both ferric iron and oxygen concentration. Calcite has a surface area controlled, reversible reaction that has three pathways (including carbonic acid concentration and pH). Hematite is not included in the model as it does not dissolve readily. The remainder of the minerals (magnetite, goethite, gypsum, sulfur, ferrihydrite and FeS) are described by simple reversible rate expressions based on their saturation index. In the cases of sulfur, ferrihydite and FeS a high rate constant is used to ensure these phases reach equilibrium quickly, as suggested by others (Furrer et al., 1989, 1990). The residue minerals were modeled in a batch reaction with MIN3P in a solution with decant water chemistry and in proportions similar to that found in the field. Table 5.9 indicates the saturation status of the residue minerals and the trend of the saturation index with time. In addition an estimate is provided of the

time to a stable saturation index. It should be noted that the quasi-stable saturation index for ferrihydrite, goethite and pyrrhotite was less than zero. FeS, ferrihydrite, magnetite and calcite exhibited the highest dissolution/precipitation rates for the mineral volumes and solution modeled. Using the shrinking core rate expression the sulfide minerals reached quasi-stability in approximately two years while other minerals took 20 years. The shrinking core model describes the decrease in reactivity of sulfide minerals observed during oxidation. Wunderly et al. (1986) has attributed this phenomenon to the formation of oxide coatings on surfaces. The decrease in reactivity is based on the radius of the unreacted core and causes a quasi-stability after two years.

5.4.7 Limiting Factors

There are many sources of error for this type of work. They include using database minerals and their thermodynamic equilibrium expressions to approximate the minerals (sometimes amorphous in nature) present in the residues. The percentage of each of the minerals present in the residues has not been clearly established. In addition, at the beginning of the two and half year life of the Demonstration Plant operation the residues were disposed in batch format and separately in the first impoundments (5C and D). Later the residues were mixed prior to disposal and the residue composition could vary due to optimization of the plant process. The NLR was always neutralized with lime slurry prior to disposal and the NGR was neutralized during from the iron removal process. For impoundment 5C and D the chemistry of the decant water over time could vary depending on which residue had most recently gone for disposal, its placement and the solution chemistry as well as other factors. Other influences that also could affect the

Table 5.8: Rate expressions for minerals in the hydrometallurgical residue

Mineral	Rate Expression (mol dm^{-3} s^{-1})	Reference
Chalcopyrite	$R=-(\frac{r_p}{(r_p-r_r)r_r})10^{-9.9}\{O_2(aq)\}$	Wunderly et al., 1986
Pentlandite[b]	$R=-(\frac{r_p}{(r_p-r_r)r_r})10^{-10.5}\{O_2(aq)\}$	Wunderly et al., 1986
Pyrrhotite[b]	$R=-(\frac{r_p}{(r_p-r_r)r_r})10^{-9.62}\{O_2(aq)\}+10^{-11.92}\{Fe^{+3}(aq)\}^{0.6}\left[1-\frac{IAP}{10^{-134.7}}\right]$	Wunderly et al., 1986
Calcite[c]	$R=-S(10^{-0.051}\{H^+\}+10^{-3.301}\{H_2CO_3(aq)\}+10^{-6.187}\{H_2O\})\left[1-\frac{IAP}{10^{-8.5}}\right]$	Chou et al., 1989
Magnetite	$R=-1.0x10^{-10}\left[1-\frac{IAP}{10^{-3.74}}\right]$	See note a)
Goethite	$R=-2.0x10^{-11}\left[1-\frac{IAP}{10^{-1.0}}\right]$	Ball, Nordstrom, 1991
Gypsum	$R=-1.0x10^{-11}\left[1-\frac{IAP}{10^{-4.58}}\right]$	Ball, Nordstrom, 1991
Ferrihydrite	$R=-1.0x10^{-9}\left[1-\frac{IAP}{10^{3.191}}\right]$	Equilibrium based
Sulfur	$R=-1.0x10^{-9}\left[1-\frac{IAP}{10^{-2.1449}}\right]$	Equilibrium based
FeS	$R=-1.0x10^{-9}\left[1-\frac{IAP}{10^{-2.95}}\right]$	Equilibrium based
Hematite	Not included	

Notes:
[a] Estimated based on existing information
[b] r_p= radius of particle (set to 69μm) and r_r= radius of unreacted core (set to 68.9μm) (Brookfield et al., 2006).
[c] S = surface area

modeling exercise and field conditions include: the site conditions of temperature and precipitation, generation of thiosalts in the residue, mineral reaction kinetics, the effect of

non-dominant minerals or analytes and generation of secondary minerals or phases either by the model or in the field.

Table 5.9: Mineral saturation information in neutralized decant solution

Mineral	Saturation Index	Trend with time	Time to Quasi-Equilibrium
Chalcopyrite	Negative	Increasing	2 yr
Pentlandite	Positive	Decreasing	2 yr
Pyrrhotite	Negative	Decreasing	2 yr
Calcite	Positive	Decreasing	3 yr
Magnetite	Positive	Decreasing	20 yr
Goethite	Negative	Decreasing	7 yr
Gypsum	Positive	Decreasing	20 yr
Ferrihydrite	Negative	Decreasing	7 yr
Sulfur	Positive to Negative	Decreasing	Very short
FeS	Negative to Positive	Increasing	Very short
Hematite	NA		NA

NA: not applicable, not included in model

5.5 CONCLUSIONS

From the work completed it has been shown how it is possible to model hydrometallurgical residue using minerals in a geochemical reaction code and use it to predict metal concentrations in a batch test situation such as shake flask experiment. Care must be taken to consider the formation of secondary minerals within the code and its subsequent affect on solution composition. Not surprisingly due to the complex nature of the residue the NLR was much more difficult to model that the NGR. The modeled residue was useful in predicting decant water chemistry and was used to consider factors affecting the chemistry. The modeled NCR residue and PEN solution gave the best approximation of metal concentration in the decant water. Removing oxygen from the reaction, similar to subsurface conditions, generated significantly reduced concentrations

of nickel and copper in the decant water. Sensitivity analysis indicated that the modeled residue was very sensitive to the amount of neutralization it received from calcite and to the amount of FeS and pyrrhotite in the modeled NCR. As PHREEQC's default is to use equilibrium expressions for mineral dissolution and precipitation it considers long term conditions. The kinetics of mineral dissolution/ precipitation reactions was considered using the code MIN3P and provided insight into the time to quasi-equilibrium and the saturation index of the residue minerals and its trend with time. Metal sorption appears to play a strong role in the actual residue and was able to be modeled in a simple manner with PHREEQC. More work is required on the characterization of the residue and determination the reaction kinetics and equilibrium thermodynamics of its particular minerals and phases in order to better represent the residue in a geochemical code.

5.6 REFERENCES

Bain, J.G., Blowes, D.W., Robertson, D., Find, E.O. (2000). Modelling sulfide oxidation with reactive transport at a mine drainage site. *Journal of Contaminant Hydrology*, 41, 23-47.

Ball, J.W., Nordstrom, D.K. (1991). *User's manual for WATEQ4F, with revised thermodynamic database and test cases for calculating speciation of major, trace and redox elements in natural waters*. US. Geological Survey, Open-File Report 91-183, 189pp.

Belzile, N., Chen, Y., Cai, M., Li, Y. (2004). A review of pyrrhotite oxidation. *Journal of Geochemical Exploration*, 84, 65-76.

Brookfield, A.E., Blowes, D.W., Mayer, K.U. (2006). Integration of field measurements and reactive transport modeling to evaluate containment transport at a sulfide mine tailings impoundment, *Journal of Contaminant Hydrology*, 88, 1-22.

Brown., G.B., Bassett, R.L., Glynn, P.D. (1999). Reactive transport of metal contaminants in alluvium-model comparison and column simulation. *Applied Geochemistry*, 15, 35-49.

Brown, P.L, Ritchie, A.I.M., Bennett, J.W., Comarmond, M.J., Timms, G.P. (2000). Geochemical kinetic modelling of acid rock drainage, In *Proceedings ICARD 2000, Fifth International Conference Acid Rock Drainage*, Denver, Colorado, USA, 21-24, May, 2000, 1, 289-296.

Chou L., Garrels R. M. and Wollast R. (1989). Comparative study of the kinetics and mechanisms of dissolution of carbonate minerals. *Chemical Geology*, 78, 269–282.

Davis, G.B., Ritchie, A.I.M. (1986). A model of oxidation in pyretic mine wastes: Part1. Equations and approximate solution. *Applied Mathematical Modelling*, 10, 314-322.

Evangelou, V.P. (1998). *Environmental Soil and Water Chemistry, Principles and Applications.* New York: John Wiley and Sons.

Fernandes, H.M, Franklin, M.R., 2001. Assessment of acid rock drainage pollutants release in the uranium mining site of Pocos de Caldas, Brazil, *Journal Environmental Radioactivity*, 54, 5-25.

Filipek, L. H., Gormley, J., Ewing, R., Ellsworth, D. (1991). Kinetic acid-prediction studies as aids to waste-rock and water management during advanced exploration of a massive sulfide deposit. In *Proceedings of the Second International Conference on Abatement of Acidic Drainage,* 3, 191-208.

Frind, E. O. Molson, J. W. (1994). Modelling of Mill-Tailings Impoundments, In J.L. Jambor, D.W. Blowes (eds.) *Short Course Handbook on Environmental Geochemistry of Sulfide Mine Waste.* Minerals Association of Canada, Nepean.V.22.

Furrer, G., Westall, J., Sollins, P. (1989). The study of soil chemistry through quasi-steady state models: I. Mathematical definition of model. *Geochimica et Cosmochimica Acta*, 53, 595-601.

Furrer, G., Westall, J., Sollins, P. (1990). The study of soil chemistry through quasi-steady state models: I. Mathematical definition of model. *Geochimica et Cosmochimica et Acta*, 53, 2363-74.

Glynn, P., Brown, J. (1996). Reactive transport modeling of acidic metal-contaminated ground water at a site with sparse spatial information. In P.C. Litchner, C.I.,

Steefel, E.H. Oelkers (Eds.), *Reactive Transport in Porous Media*, Reviews in Mineralogy, 34, 377-438.

Hetcht, H., Kolling, M., Geishas, N. (2002). "DiffMod7 – Modelling oxygen diffusion and pyrite decomposition in the unsaturated zone based on ground, air and oxygen distribution." In H.D. Schultz, G. Teutsch (Eds.), *Geochemical processes-conceptual models for reactive transport in soil and groundwater* (Research Report) (pp.55-77). Weinheim, Germany: Wiley – VCH.

Hoth, N., Wagner, S., Hafner, F. (2001). Predictive modeling of dump water impact on the surroundings of the lignite dump site Janschwalde (Eastern Germany), *Journal of Geochemical Exploration*, 73(2), 113-121.

Kimball, B. A, Runkel, R. C., Walton-Day, K. (2003). Use of field-scale experiments and reactive solute-transport modelling to evaluate remediation alternatives in streams affected by acid mine drainage. In J.L. Jambor, D.W. Blowes, A.I.M. Ritchie (Eds.), *Environmental Aspects of Mine Wastes*, Vol. 31. 261-282, Minerals Association of Canada.

Mayer, K.U., Benner, S.G., Blowes, D.W. (1999). The reactive transport Model MIN3P: application to acid mine drainage generation and treatment – Nickel Rim Mine Site, In *Proceedings Sudbury Ontario. Sudbury'99, Mining and the Environment*, 1, 145-154.

Mayer, K.U., Blowes, D.W., Frind, E.O. (2000). Advances in reactive-transport modeling of contaminant release and attenuation from mine-waste deposits. In J.L. Jambor, D.W., Blowes (Eds.), *Environmental Aspects of Mine Wastes,* Vol.31, Minerals Association of Canada.

Mayer, K.U., Frind, E.O., Blowes, D.W. (2002) Multicomponent reactive transport modeling in variably saturated porous media using a generalized formulation for kinetically controlled reactions. *Water Resources Research*, 38(9), 1174-1195.

Morin, K.A, Cherry, J.A. (1988). Migration of Acidic Groundwater Seepage from Uranium-Tailings Impoundments: 3. Simulations of the Conceptual Model with Application to seepage Area A. Contaminant Hydrology, *Journal of Contaminant Hydrology,* 6(2), 323-342.

Nicholson, R.V., Sharer, J.M. (1990). Laboratory studies of pyrrhotite oxidation kinetics, In C.N. Alpers, D.W. Blowes (Eds.), *Environmental Geochemistry of Sulfide Oxidation* (pp. 14-30). American Chemical Society, Symposium Aug 23-28, 1992.

Nordstrom, D.K., Alpers, C.N. (1999). Geochemical modeling of water rock interactions in mining environments. In Plumlee Logsdon (Eds.) *Environmental Geochemistry*

of Mineral Deposits (Part A: Processes Techniques and Health Issues). Reviews in Economic Geology, (Vol. 6A). Society of Economic Geologists Inc.

Parkhurst, D. L., Engesgaard, P., Kipp, K.L. (1995). Coupling the geochemical model PHREEQC with a 3D multi-component solute transport model. In Proceedings *Fifth Annual V.M. Goldschmidt Conference*, Pen State University, University Park, Penn. *Geochem. Soc.*, Retrieved from http://brr.cr.usgs/gov/projects/GWC_coupled/phast/.

Parkhurst, D. L. Appelo, C. A. J. (1999). *User's guide to PHREEQC (Version 2) A computer program for speciation, batch reaction, one-dimensional transport and inverse geochemical calculations*, U.S. Geological Survey Water Resources Investigation Report, 99-4259.

Salmon, U.S., Malmstrom, M.E. (2004). Geochemical processes in mill tailings deposits: modeling of groundwater composition. *Applied Geochemistry*, 19, 1-17.

Sharer, J.M., Nicholson, R.V., Halbert, B., Snodgrass, W.J. (1994). A computer program to assess acid generation in pyretic tailings. In C.N. Alpers, D.W. Blowes, (Eds.), *Environmental Geochemistry of Sulfide Oxidation*. American Chemical Society symposium series, Washington, D.C., USA. 550(11), 132-152.

Shcherbakova, E. (2006). Geochemical and hydrological aspects of interactions between water and mine waste. Licentiate thesis, Lulea University of Technology, Department of Chemical Engineering and Geosciences, Division of Applied Geology.

Steel, A., Hawboldt, K., Khan, F. (2006). A microstructural and geochemical comparison of residues from hydrometallurgical processes. Poster session presented at *Conference of Metallurgy*, Montreal, Oct. 1-4, 2006.

Steel, A., Hawboldt, K., Khan, F. (2009a). Assessment of minerals and iron-bearing phases present in hydrometallurgical residues from nickel sulfide concentrate and residue associated metals. *International Journal of Hydrometallurgy,* accepted.

Steel, A., Hawboldt, K., Khan, F. (2009b). Results of shake flask experiments on hydrometallurgical residues. *International Journal of Environmental Science and Technology*, 6(1), 57-68.

Stromberg, B., Banwart, S. (1994). Kinetic modeling of geochemical processes at the Aitik mining waste rock site in northern Sweden. *Applied Geochemistry*, 9, 583-595.

VINL (2006). *Voisey's Bay Nickel Company Project Description and Project Registration for a Commercial Processing Plant.* Retrieved January 6, 2006, from http://www.vbnc.com/NewsItems.asp?EffectiveYear=2006.

VINL (2008). *Environmental Impact Statement, Long Harbour Commercial Nickel Processing Plant, Vol1.* Project Description, 174pp. Retrieved July 15/08, from http://www.env.gov.nl.ca/env/Env/EA%202001/pages/active%20projects.htm#Environmental%20Impact%20Statements.

Wunderley, M.D., Blowes, D.W., Frind, E.O., Ptacek, C.J. (1996). Sulfide mineral oxidation and subsequent reactive transport of oxidation products in the mine tailings impoundments. *Water Resources Research*, 32, 3173-3187.

CHAPTER 6

NUMERICAL MODELLING OF TWO DISPOSAL OPTIONS FOR MINING PROCESS RESIDUE

A. Steel[a], *K. Hawboldt*[a], *F. Khan*[a]
[a] *Faculty of Engineering and Applied Science, Memorial University of Newfoundland, St. John's, Newfoundland, Canada A1B3X5*

ABSTRACT: *In order to encourage more sustainable mining practices a methodology has been developed to assist in determining optimum disposal options for potentially environmentally deleterious waste at the design stage of the project. In this case two disposal options are considered for mining process residue. For both subaqueous and subaerial residue disposal options, a geochemical reactive transport code is used to predict the changes in residue pore water chemistry with depth and with time in a modeled column. The numerical models are calibrated against site data and are used to predict full-scale conditions. Sensitivity analysis is conducted to assess dominant model variables. Nickel hydrometallurgical waste residue was selected for this research. The waste considered in this study is mostly comprised of iron oxides and hydroxides, gypsum and sulfur with minor amounts of metal sulfides. Although, the waste is neutralized before it is sent for disposal, it is critical to assess its acid generating and metal leaching potential with time in order to determine optimal treatment/mitigation/disposal options.*

This paper has been submitted to the *International Journal of Applied Geochemistry.* The lead author is Abigail Steel and the co-authors are Dr. Kelly Hawboldt and Dr. Faisal Khan. Ms. Steel's contribution to this paper is as follows:

- Wrote the paper
- Conducted all numerical modeling work
- Conducted interpretation of results
- Performed all literature searches required for background information.

Dr. Hawboldt and Dr. Khan provided technical guidance and editing of the manuscript. The figure and table numbers and reference formats have been altered to match the formatting guidelines set out by Memorial University.

6.1 INTRODUCTION

The treatment and disposal of base metal ore waste is challenging however more sustainable mining practices are achieved by integration of long-term disposal implications of a waste at the design stage of a project. In this study, sulfidic waste residue produced by a novel nickel hydrometallurgical process is under consideration. If this type of hydrometallurgical residue is exposed to atmospheric oxygen, it produces acidic drainage as with Acid Mine Drainage (AMD). Oxidation of sulfide minerals and subsequent generation of AMD mainly occurs as oxygen diffuses through the unsaturated zone of tailings or waste rock deposits (Blowes and Jambor 1990; Robertson, 1994). The oxidation mobilizes metals in the tailings and potentially the underlying bedrock.

Recently, multi-component reactive transport models have been used to model many of the complexities involved with AMD including interactions between physical, chemical and biological processes. Modeling of AMD aids in understanding the site and deposit; specifically development, duration and attenuation of AMD. Elberling et al. (1994); Wunderly et al. (1996); Frind and Molson (1994) and Bain et al. (2000) have considered oxygen diffusion through simplified modeled tailings. The rates of chemical reactions can be a significant factor in the development of AMD as shown by Sharer et al. (1994); Nicholson and Sharer (1990); Mayer et al. (1999, 2000 and 2002) and Lichtner (1996). Work by Salmon and Malmstrom (2004) focused on biogeochemical processes that contribute to leachate composition in a tailings deposit. The affect of acid neutralizing reactions on pH and reduced metal mobility has been studied by Blowes and Ptacek (1994) and Stromberg and Banwart (1999). Numerical modeling of sulfide oxidation in

mine waste rock and heap leach piles has been examined by Jaynes et al. (1984); Davis and Ritchie (1986) and Fernandes and Franklin (2001).

In this study MIN3P, a multi-component reactive transport code (Mayer et al., 1999), is used to simulate drainage through hydrometallurgical process residue at a proposed full-scale disposal site. The method is to use characterization data collected on the residue to develop a modeled mineralogical assemblage which in turn is used in a geochemical reactive transport model to simulate two disposal conditions (subaerial and subaqueous) and predict groundwater conditions with depth and time. The two modeled disposal scenarios are calibrated with field data collected at the nickel hydrometallurgical Demonstration Plant site.

MIN3P considers solute and gas transport in variably saturated porous media in one, two or three dimensions. This code permits advective-dispersive transport in aqueous phase and diffusive gas transport. The model formulation was based on the global implicit approach which considers reaction and transport processes simultaneously (Steefel and Lasaga, 1994). Previous studies in which it has been used include: the impact of flooding a former underground uranium mine (Bain et al., 2001), performance of a permeable reactive barrier for remediation (Mayer et al., 2001), quantification of acid neutralization reactions in a column experiment (Jurjovec et al., 2004) and simulation of reactive solute transport through a tailings impoundment (Brookfield et al., 2006).

6.2 PHYSICAL AND HYDROGEOLOGICAL SETTING

Hydrometallurgical plant concentrate feed was shipped, between 2005 and 2008, from the mine site at Voisey's Bay, in Labrador to the site of a 1:100 scale Demonstration Plant site, in Argentia, situated approximately 150 km west of St. John's, Newfoundland (Fig. 6.1). The proposed full-scale plant located in Long Harbour, near Argentia, Newfoundland will commence construction in 2009. At the proposed full-scale facility the residue will be disposed subaqueously.

Two main methods were considered for the disposal of the residue. In subaerial disposal the waste is disposed of in an impoundment with proper site drainage and runoff treatment. In this case the waste remains unsaturated during and after disposal. In subaqueous disposal, the waste is placed in the disposal site such that it remains saturated under a water cover during placement and after disposal. A head of water is maintained above the waste at all times, limiting the supply of oxygen to the waste. Subaqueous disposal can either be in an existing water body or developed through an excavation. Fig. 6.2 provides a schematic of the subaqueous disposal option in a pond and the theoretical subsurface flow regime.

The proposed full-scale residue disposal pond will cover an area of approximately 74 hectares (VINL, 2006, 2008) and will extend an average estimated depth of 10 m when complete. The bedrock at the site is precambrian volcanic flows and tuffs and pyroclastic and clastic sedimentary rocks (VINL, 2006, 2008; King, 1988). As indicated in Fig. 6.2 the simplified water balance for the impoundment considers only infiltration and contribution to groundwater.

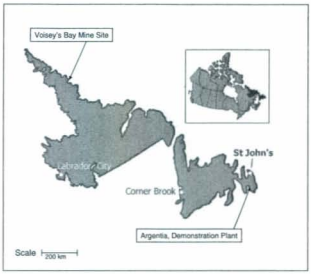

Figure 6.1: Location of Argentia Demonstration Plant and Voisey's Bay mine site

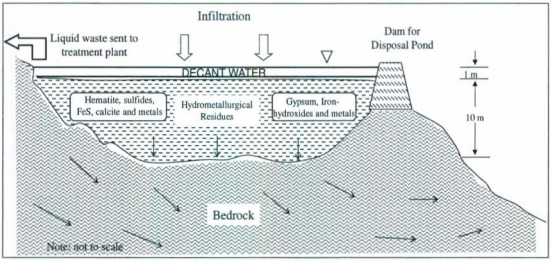

Figure 6.2: General conceptual model of a typical subaqueous residue disposal pond

6.3 MODEL DEVELOPMENT

6.3.1 Conceptual Model Development

In this study geochemical reactive transport modeling is used to analyze waste disposal options. The model utilizes available site information; assumes representative values for other parameters and calibrates the model scenarios against site data. Pore water chemistry predictions are made using several assumptions and limiting factors (Section 6.4.4) and therefore are for illustration purposes. They are not expected to represent actual full-scale conditions at the site. Details of various aspects of the model are provided in the following sections.

6.3.2 Process Residue

The residues from the Demonstration Plant are derived through either pressure leaching or precipitation processes and are in the form of sludges. The two main sources of sludges/residues are: 1) the solids, or the Neutralized Leach Residue (NLR), remaining when the pulp from the pressure leaching is washed by counter current decantation and neutralized with lime and 2) the precipitate, or the Neutralized Gypsum Residue (NGR), formed during the iron removal and neutralization stage. The Neutralized Combined Residue (NCR) consists of approximately 55 % NLR and 45 % NGR (VINL, 2006). The NLR and NGR were subjected to various tests to determine its mineralogy, structure and metal leaching capacity. Scanning Electron Microscope (SEM), X-Ray Fluorescence Spectrometer (XRF), and X-Ray Diffractometer (XRD) sample analyses were used to determine residue mineral composition and microstructure (Steel et al., 2006, 2009a). Inductively Coupled Mass Spectrometer (ICPMS) was used for elemental analysis in the

residue. Results of Acid Base Accounting analysis, shake flask experiments, humidity cell experiments, sequential extractions and Toxicity Characteristics Leaching Procedure tests were used to determine its acid generating and metal leaching capabilities and are described in Steel et al. (2009a, 2009b) and Chapter 8.

The filter cake contains mainly gypsum ($CaSO_4 \cdot 2H_2O$) and iron hydroxide particles (FeO(OH) and $Fe(OH)_3$) with minor quantities of nickel hydroxides and other metal hydroxide compounds. The leach residue appears to consist primarily of Fe_2O_3 and sulfur with minor amounts of amorphous FeS and unreacted concentrate. The sulfur is present in elemental form and attached to other compounds. The principle minerals present in crystalline or amorphous form in the NGR and NLR of the hydrometallurgical residue are shown in Table 6.1 (Steel et al., 2009a). In order to model the residues, as many of the minerals present as possible were included initial analysis. Table 6.1 also provides percentages of the minerals present in each modeled residue. The residues contain concentrations of nickel, copper and cobalt; these were considered by inclusion in the minerals. Table 6.2 outlines the percentage of target metals (nickel, copper and cobalt) and sulfur associated with each residue.

Table 6.1: Examples of compound/minerals present in NGR, NLR and NCR and weight fractions

Compounds/minerals (either crystalline or amorphous)	Mineral Weight (Fraction)		
	NLR[b]	NGR[a]	NCR[c]
Gypsum $CaSO_4 \cdot 2H_2O$	0	0.93	0.4
Goethite FeO(OH)	0	0.0375	0.03
Ferrihydrite $Fe(OH)_3$	0	0.0375	0.03
Iron(III) oxide Fe_2O_3	0.7	0	0.4
Iron(II,III) oxide Fe_3O_4	0.05	0	0.03
FeS	0.08	0	0.05
Sulfur S	0.02	0	0.01
Pyrrhotite $Fe_{(1-x)}S$	0.02	0	0.03
Pentlandite $(Fe,Ni)_9S_8$	0.015	0	0.005
Chalcopyrite Cu,FeS_2	0.01	0	0.005
Calcite $CaCO_3$	0.1	0	0.04
Total	0.995	1.01	1.03

Notes:
[a] NGR: Nickel and other metal hydroxides containing Cu, Al, Si and/or Cl were present.
[b] NLR: Spheres containing iron, sulfur and oxygen with minor Ca, Si, Ni, Cu, Al were present.
[c] NCR weight percentage is estimated at 55% NLR and 45% NGR

Table 6.2: Select metal and sulfur concentrations in hydrometallurgical residues

Analyte	Metal/Sulfur Weight (%)		
	NLR	NGR	NCR
Nickel	0.4-1.1	0.2-0.6	0.5-0.6
Copper	0.2-0.3	0.07-0.2	0.2-0.3
Cobalt	0.02	0.002-0.005	0.01
Total Sulfur	27-28	20-21	25-26

6.3.3 Geochemical Processes

The compounds present (in both amorphous and crystalline form) in the hydrometallurgical residue are subjected to oxidation upon disposal. The main reactions that are predicted to occur in the NCR deposit are provided in Table 6.3. When oxidized the sulfides release sulfate and ferrous iron (Table 6.3, reactions 10-13) and produce hydrogen ions. Oxidation of released ferrous iron (Fe(II)) produces ferric iron (Fe(III)) (Table 6.3, reaction 3) which can precipitate to form ferric hydroxide and hydrogen ions (Table 6.3, reaction 2). As a strong oxidant, ferric iron can also be used to catalyse reactions (Table 6.3, reaction 10). Secondary processes such as reaction 2) may also occur within the residue deposit and contributes to the groundwater pH and concentration of dissolved ions (Blowes and Ptacek, 1994; Nordstrom and Alpers, 1999). Release of target metals is caused by oxidation of sulfide minerals such as pentlandite and chalcopyrite (Table 6.3, reactions 12 and 13) and by weakened surface adsorption caused by changes in pH (Table 6.3, reaction 6). The dissolution of the carbonates, calcite and gypsum contributes to the natural control of the pH in the residue leachate (Table 6.3, reactions 1 and 7) (Blowes and Ptacek, 1994). Dissolution of the minerals calcite and pyrrhotite can occur without the presence of oxygen. If pH increases metal sulfates, carbonates or hydroxides may form (Table 6.3, reactions 4 and 5).

With subaerial residue disposal the diffusion of oxygen through the pore space is anticipated to be the primary source of oxygen for reactions in the deposit as it is with tailings deposits (Elberling and Nicholson, 1996). The rate of diffusion is highly dependent of the degree of saturation of the deposit and well as its effective porosity

Table 6.3: Chemical reactions of interest

1. Gypsum precipitation/dissolution $CaSO_4 \cdot 2H_2O \leftrightarrow Ca^{2+} + SO_4^{2-} + 2H_2O$
2. Iron hydroxides $FeOOH_{(s)} + 3H^+ \leftrightarrow Fe^{3+} + 2H_2O$ (Geothite)
$Fe(OH)_{3(s)} + 3H^+ \leftrightarrow Fe^{3+} + 3H_2O$ or $Fe_3HO_8 \cdot 4H_2O_{(s)} + 3H^+ \leftrightarrow Fe^{3+} + 3H_2O$ (Ferrihydrite)
3. Ferric/Ferrous iron formation $4Fe^{2+} + O_2 + 4H^+ \leftrightarrow 4Fe^{3+} + 2H_2O$
4. as pH increases $Fe^{2+} + CO_3^{2-} \leftrightarrow FeCO_3$; $Fe^{2+} + SO_4^{2-} \leftrightarrow FeSO_{4(aq)}$
5. Nickel/copper hydroxides $Ni(OH)_{2(s)} \leftrightarrow Ni^{2+} + 2OH^-$; $Cu(OH)_{2(s)} \leftrightarrow Cu^{2+} + 2OH^-$
6. Release of metals from Fe_2O_3 $Fe_2O_{3(s)} + Ni_xO_{a(s)} + Cu_yO_{b(s)} + Co_zO_{c(s)} + 2(3+a+b+c)H^+$
$\leftrightarrow 2Fe^{2+} + xNi^{x+} + yCu^{y+} + zCo^{z+} + (3+a+b+c)H_2O$
7. Calcite dissolution/precipitation $CaCO_3 + H^+ \leftrightarrow Ca^{2+} + HCO_3^-$;
$CaCO_3 + H_2O \leftrightarrow Ca^{2+} + HCO_3^- + OH^-$; $CaCO_3 + H_2CO_3 \leftrightarrow Ca^{2+} + 2HCO_3^-$
8. Formation of amorphous $FeS_{2(s)}$ $Fe^{2+} + 2S^{2-} \leftrightarrow FeS_{2(s)}$
9. Pure sulfur oxidation $2S_{(s)} + 3O_{2(aq)} + 2H_2O \leftrightarrow 2H_2SO_4$
10. $FeS_{(s)}$ oxidation $FeS - O_2 + O_2 \rightarrow Fe^{2+} + SO_4^{2-}$ (Mackinawite)
$FeS_{2(s)} + 3.5O_{2(aq)} + H_2O \rightarrow Fe^{2+} + 2SO_4^{2-} + 2H^+$ (Pyrite)
11. $FeS_{1-x(s)}$ oxidation $FeS_{1-x(s)} + (2-0.5x)O_{2(aq)} + 2H_2O \rightarrow (1-x)Fe^{2+} + SO_4^{2-} + 2xH^+$
12. $(FeNi)_9S_{8(s)}$ oxidation $(FeNi)_9S_{8(s)} + 16.5O_{2(aq)} + 2H^+ \rightarrow 4.5Fe^{2+} + 4.5Ni^{2+} + 8SO_4^{2-} + 0.5H_2O$
13. $CuFeS_{2(s)}$ oxidation $CuFeS_{2(s)} + 4O_{2(aq)} \rightarrow Fe^{2+} + Cu^{2+} + 2SO_4^{2-}$
14. Transformation of $Fe_{1-x}S_{(s)}$ to $FeS_{2(s)}$
$2Fe_{1-x}S_{(s)} + (0.5-x)O_{2(aq)} + (2-4x)H^+ \rightarrow FeS_2 + (1-2x)Fe^{2+} + (1-2x)H_2O$
15. Formation water $H^+ + OH^- \leftrightarrow H_2O_{(l)}$
16. Hematite $Fe_3O_4 + 8H^+ \rightarrow 2Fe^{3+} + Fe^{2+} + 4H_2O$

(Hermann et al., 2002). Oxidation of sulfide minerals is expected to occur more readily in the unsaturated zone where oxygen availability is higher. As acid in produced by sulfide mineral oxidation, the acid may be partially neutralized by the dissolution of carbonate minerals. Above the water table both of these processes will be very active

however the amount of carbonate minerals may not be sufficient to neutralize the acidity. The unsaturated zone will be a main source of dissolved species to the underlying saturated zone.

In the saturated zone, oxygen availability is limited due to infilling of interconnected pore space with groundwater which has a diffusion coefficient several orders of magnitude lower than air (Nordstrom and Ball, 1989). The oxidation of sulfide minerals will be limited in the saturated deposit and below the water table in the subaerial deposit. The presence of dissolved ferrous iron, other metals and high sulfate concentration in the pore water are indicators of sulfide oxidation products. Oxidation of ferrous iron leads to the precipitation of secondary phases such as iron hydroxides and hydroxy-sulfates, reduces ferric iron concentration and alkalinity. High sulfate concentration may lead to precipitation of secondary minerals such gypsum and jarosite (Jurjovec et al., 2002).

6.3.4 Equilibrium and Kinetic Processes

To effectively simulate sulfide-mineral oxidation and pH buffering it is necessary to incorporate reaction kinetics. Mayer et al. (1999, 2000, 2002) describes inclusion of kinetic processes in the models and calibration of models with field data with the code MIN3P. STEADYQL (Furrer et al., 1989, 1990) classifies reactions kinetics into three categories; very fast, very slow and moderate. In this code it is the moderate rate reactions that employ kinetic expressions as described in Stromberg and Banwart (1994), Salmon and Malmstrom (2004), Brown et al. (2000) and Fernandes and Franklin (2001). PHREEQC (Parkhurst and Appelo, 1999) is also able to incorporate mineral reaction

kinetics in geochemical modeling, but cannot model in two dimensions, model unsaturated conditions or include a variety of boundary conditions.

Compared to the residence time in the deposit many of the reversible geochemical processes that occur are much faster and were assumed to exist at chemical equilibrium by the authors. Slower processes or reactions were represented in the model as kinetically controlled reactions. A shrinking core model is used to describe the rate expression for the sulfide minerals (pentlandite, chalcopyrite and pyrrhotite) which are dependent on oxygen concentration (Davis and Ritchie, 1986; Wunderly et al., 1996). The pyrrhotite rate expression is a function of both ferric iron and oxygen concentration (Mayer et al., 2002). Calcite has a surface area controlled, reversible reaction that has three pathways (including carbonic acid concentration and pH) (Chou et al., 1989). Magnetite, goethite and gypsum are described by simple reversible rate expressions based on the saturation index. Hematite is not included in the model as it typically does not react readily. The remainder of the minerals/elements (sulfur, ferrihydrite and FeS) are assumed to go to equilibrium by assuming high rate constants, as is common with kinetic modeling (Furrer et al., 1989 and 1990). For this study, the empirical rate expressions were selected from weathering experiments on mineral samples reported in the literature as shown in Table 6.4. The rates of reactions for reactions (10) –(13) and reaction (3) (Table 6.3) may be significantly increased by iron oxidizing bacteria (Nordstrom and Southam, 1997; Stumm and Morgan 1981; and Nicholson, 1994). Also the reducibility of amorphous or poorly crystalline ferric iron takes place more rapidly than crystalline phases (Christensen et al.,

2000). Steel et al. (2009c) provides further information relating to reaction kinetics involving the hydrometallurgical residue and decant water and is provided in Chapter 5.

Table 6.4: Rate expressions used in the model

Mineral	Rate Expression (mol dm^{-3} s^{-1})	Reference
Chalcopyrite	$R = -(\frac{r_p}{(r_p - r_r)r_r})10^{-9.9}\{O_2(aq)\}$	Wunderly et al., 1986
Pentlandite[b]	$R = -(\frac{r_p}{(r_p - r_r)r_r})10^{-10.5}\{O_2(aq)\}$	Wunderly et al., 1986
Pyrrhotite[b]	$R = -(\frac{r_p}{(r_p - r_r)r_r})10^{-9.62}\{O_2(aq)\} + 10^{-11.92}\{Fe^{+3}(aq)\}^{0.8}\left[1 - \frac{IAP}{10^{-134.7}}\right]$	Wunderly et al. 1986
Calcite[c]	$R = -S(10^{-0.051}\{H^+\} + 10^{-3.308}\{H_2CO_3(aq)\} + 10^{-6.187}\{H_2O\})\left[1 - \frac{IAP}{10^{-8.5}}\right]$	Chou et al., 1989
Magnetite	$R = -1.0x10^{-10}\left[1 - \frac{IAP}{10^{-3.74}}\right]$	See note a)
Goethite	$R = -2.0x10^{-11}\left[1 - \frac{IAP}{10^{-1.0}}\right]$	Ball and Nordstrom, 1991
Gypsum	$R = -1.0x10^{-11}\left[1 - \frac{IAP}{10^{-4.58}}\right]$	Ball and Nordstrom, 1991
Ferrihydrite	$R = -1.0x10^{-9}\left[1 - \frac{IAP}{10^{3.191}}\right]$	Equilibrium based
Sulfur	$R = -1.0x10^{-9}\left[1 - \frac{IAP}{10^{-2.1449}}\right]$	Equilibrium based
FeS	$R = -1.0x10^{-9}\left[1 - \frac{IAP}{10^{-2.95}}\right]$	Equilibrium based
Hematite	Not included	

Notes:

[a] Estimated based on existing information

[b] r_p= radius of particle (set to 69um) and r_r= radius of unreacted core (set to 68.9um) (Brookfield et al., 2006)

[c] S = surface area

6.3.5 Model Set-up and Calibration

MIN3P (Mayer et al.,1999, 2000) was used to simulate different residue disposal methods. The model input for the code is provided in Table 6.5. The model was calibrated for both subaerial and subaqueous disposal methods through data available from the site in order to predict full-scale disposal conditions. In the model, the residue deposit was assumed to be constant in porosity, water content, hydraulic conductivity and mineral content and the flow was vertically downward through a residue-filled column. For the subaerial disposal scenario, calibration data was available from two subaerial test plots located on the site, one containing NGR and one NLR, measuring approximately 3 m by 3 m by 0.5 m depth. The concentration of dissolved constituents from the test plot leachate was compared to that derived by the model. The model assumed that the water table was 0.1 m from the base of a 0.5 m column of residue. In the model, water (with rainwater composition) infiltrated the surface of the residue column and exited out the base.

The subaqueous disposal scenario was calibrated with piezometer sampling data collected from the base of a lined subaqueous residue impoundment at the Demonstration Plant. The site impoundments were approximately 10 m by 10 m and 3 m in depth with 0.2 m of decant water cover. The decant water consists of treated plant effluent mixed with residue slurry and rain water that has collected in the impoundment and may include products from reactions in water column. The subaqueous model consisted of 3.0 m column of modeled residue with 0.2 m of water (with decant water composition) above the residue. A low flow was maintained out the base of the column. In the subaerial

disposal case, the initial condition assumed Process Effluent Neutralization (PEN) solution present within the pore space in the residue below the water table as this most closely resembled initial field disposal conditions. The PEN solution is treated plant effluent that has had target metals removed. In the subaqueous disposal case, the residue slurry will be mixed with decant solution during disposal therefore the solution chemistry used for initial conditions was a mixture of the plant PEN solution and decant solution. The composition of the decant water and PEN solution used in the model is provided in Table 6.6. It should be noted that all waste water from the Demonstration Plant was treated before being released and met applicable discharge guidelines.

Table 6.5: Model parameter values for saturated and unsaturated disposal conditions

Average Volumetric Fractions of Minerals				
Gypsum	1.45E-01	FeSppt		1.02E-02
Ferrihydrite	4.21E-03	Sulfur		4.69E-02
Magnetite	4.66E-03	Pyrrhotite		1.73E-03
Goethite	4.21E-03	Chalcopyrite		9.53E-04
Calcite	9.73E-03	Pentlandite		1.17E-03
Model Parameters				
Parameter	**Value**		**Units**	
Porosity	0.50			Measured
Residue density	1.100		g/cm^3	Measured
Residue surface area	1.0E-06		m^2/g	Estimated
Hydraulic conductivity	1.0E-06		m/s	Estimated
Saturated Case	**(full scale)**			
Inflow head	3.1 (10.5)		m	Estimated from site
Outflow flux	1.0E-13 (5.0E-09)		m/s	Estimated
Column height	3.0 (10.0)		m	Estimated
Longitudinal dispersivity	3.0E-01 (1.0E-01)			Estimated
Unsaturated Case	**(full scale)**			
Inflow head	5.0E-08		m/s	Envir. Canada, 2009
Outflow head	0.1 (2.5)		m	Estimated from site
Column height	0.5 (10.0)		m	Estimated
Longitudinal dispersivity	5.0E-02 (1.0E-01)			Estimated
Residual saturation	0.05			Estimated

Note: (…) Model parameters for full-scale disposal impoundment.

Table 6.6: Composition of modeled initial condition and boundary condition solution

Analyte	Model Initial Condition Solution (PEN) (mg/L)	Model Boundary Condition Solution (Decant Water) (mg/L)	Model Boundary Condition Solution (not neutralized) (mg/L)
Cu	1 (0.1[a])	0.0238	1
Ni	1 (0.1[a])	0.107	5.16
Co	1 (0.1[a])	0.015	0.14
Pb	10 (1.0[a])	0.002	0.023
Cd	10	0.0001	0.0007
Zn	5	0.0061	0.12
Fe	1	0.89	24.3
Ca	733	574	519
Mg	127	24.2	5.19
S	1884	NA	NA
SO4	5652	7000[b]	NA
Na	1630	NA	NA
Cl	763	500[b]	NA
pH	7.0[b]	9.2	3.2

Note: [a] Concentrations used for subaqueous case.
[b] Estimated based on typical values; NA: not available

6.4 MODEL RESULTS AND DISCUSSION

6.4.1 Comparison of Field and Modeled Results of Subaerial Test Cell

The subaerial column was modeled for four months, three years and 19 years. Fig. 6.3 compares the modeled concentration of select components (at partial pressure of oxygen PO_2=0.21 atm) and the average of those taken during four months of field measurements. For the model the influx rate was based on the average rainfall for the area. Field measurements were taken at the base of the disposal test cell while the column model simulations are from the base of the 0.5 m column with the bottom 0.1 m below the water table. The full oxygen saturation condition caused higher oxidation rates for sulfide minerals and resulted in higher concentrations of metals in the leachate than lower saturation levels. In general the model predictions of analyte concentrations were in good

agreement with those measured in the field. All field measurements were within one order of magnitude of the model predictions with the exception of lead concentration which was about 60 times higher in the model than in the field and may be due to formation of secondary lead phases (such as oxides or sulfates) in the field. The ferrous iron concentration is generally high in both the field and model as it is generated during oxidation of sulfide minerals. The iron field measurements are actually total iron concentration. In the model the predicted ferric iron concentration is significantly lower than that of ferrous iron as ferric hydroxides precipitates readily.

Figure 6.3: Comparison of modeled and field measurements at base of cell (0.5 m) for subaerial disposal method

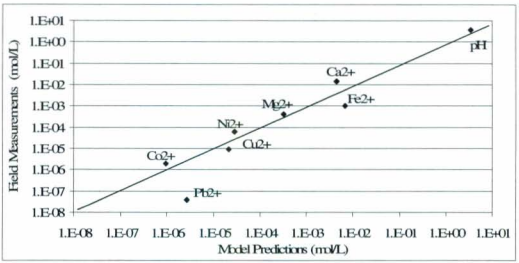

Fig. 6.4 illustrates the model predictions of aqueous geochemistry of the pore water over the depth of the test cell four months after disposal. The nickel and copper concentration decreases with depth as sulfide mineral oxidation decreases and cobalt and lead concentration actually increases with depth as the rainwater influx dilutes the

concentration of these metals near the surface. The pH of the pore water remains low throughout the depth of the cell. Ferrous iron generally decreases with depth. Sulfate remains fairly constant with depth. Very near the surface, there is a dilution effect due to the influx of rainwater as is evident in a number of the metals (ferrous iron, nickel and copper). Calcium and carbonate concentration increases with depth as it is consumed by neutralizing the acid in the upper portion of the deposit where oxidation takes place. Hydrogen monosulfide is constant below 0.45 m depth.

Figure 6.4: Predicted analyte concentrations with depth for subaerial test cell; time 4 months

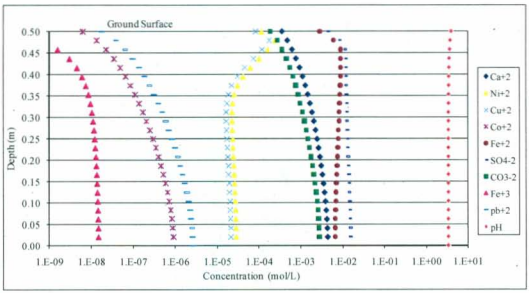

6.4.2 Comparison of Field and Modeled Results of Subaqueous Residue Impoundment

The subaqueous column was modeled for periods of one, three and nineteen years. Fig. 6.5 shows fairly good agreement between the predicted and field observations of subsurface pore water concentration after one year however the agreement was not as strong agreement as the subaerial case (Fig. 6.3). This case was different to model; there was no flow from the base of the lined impoundment and the model used a very low base flux (Table 6.5). The model over predicted the concentrations of magnesium, copper and lead and under predicted ferrous iron concentration. As the predicted pH was 5.6 and the actual pH was 9.6 this caused the modeled metal concentrations in some cases to be higher than that in the field. The lower measured lead concentration may be due to secondary phases forming or lead adsorption on mineral surfaces. In the model, the initial condition pore water metal concentration is high and due to the lack of subsurface flow the initial pore water chemistry is not significantly diluted with infiltration. Full saturation of the residue greatly reduced the oxidation of the sulfide minerals except in the top 1 m of the impoundment.

Fig. 6.6 shows model predictions of analyte concentration with depth for the Demonstration Plant impoundment. In general, the metal concentration in the pore water was lower in the upper 0.5 m and then increased rapidly and leveled off for the remaining 2.5 m depth of residue. The calcium and sulfate concentration was fairly constant with depth and was not strongly affected by pH changes. The metal concentrations were lower near the surface where the pH was higher due to the influx of decant solution which has a

Figure 6.5: Comparison of modeled and field measurements at base of impoundment (3.0 m) for subaqueous disposal method (time one year)

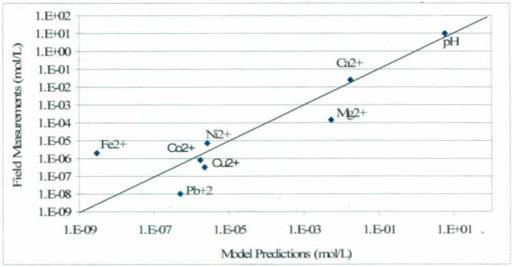

Figure 6.6: Predicted analyte concentrations with depth for subaqueous impoundment; time 1 year

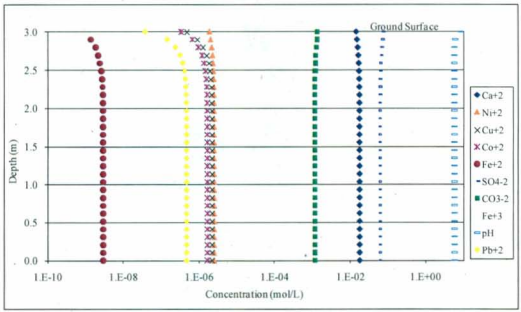

higher pH and generally lower metal concentration. At depth the metal concentration is similar to that of the interstitial PEN solution.

6.4.3 Prediction of Full Scale Subaerial and Subaqueous Disposal Pond Subsurface Chemistry

The modeled residue from the two field calibrated disposal scenarios was used to predict the pore water chemistry at proposed subaerial and subaqueous full-scale disposal sites. The model was run for 50 days and six, 19 and 27 years. Plots for the subaerial disposal case and the first three times versus deposit depth are provided in Fig. 6.7. As shown by Fig. 6.7a), initially nickel, copper, cobalt and lead concentrations are similar and the pH is fairly low (3.5-4.7) throughout. There is a slight decrease in metal concentration below the water table. With time the pH decreases as sulfide oxidation progresses through the deposit and then pH stabilizes (Fig. 6.7c) at 5.1. After several years (Fig. 6.7b) and continued mineral oxidation the metal concentration is higher below the water table, potentially due to accumulation from the sulfide oxidation occurring above the water table and leaching down into the groundwater. In addition, rainwater influx will dilute dissolved ions near the surface. At 19 years, the nickel and copper concentration remains fairly high, compared to the initial case, throughout the deposit however there's a lower generation rate of oxidation products due to the sulfide mineral shrinking core kinetic expressions. In the model, the lead and cobalt concentration are not contained in the minerals present thus their concentration in the groundwater is diluted over time. Calcium concentration increases with depth as it is consumed near the surface by acid neutralization and generated below the water table by calcite dissolution. Ferrous iron

concentration changes significantly and generally decreases with depth. Initially it is high near the surface where oxidation is occurring then as oxidation progresses with time the ferrous iron concentration is high deeper into the residue deposit (Fig. 6.7a and 6.7b). At 19 years the ferrous iron concentration is high throughout the depth of the residue deposit, as is shown in Fig. 6.7c.

The results of modeling the full-scale subaqueous residue disposal pond with depth and time are provided in Fig. 6.8. The results are provided for 50 days, six years and 19 years in Fig. 6.8a, b and c respectively. In general, little change with time is evident for many of the dissolved species. The pH of the deposit increases with time from approximately 4.4 to 6.5 after 19 years. The metal species have a lower concentration in the upper 0.5 to 1.0 m of the deposit at all modeled times, reflecting the influx of decant solution, increased oxygen concentration and potential formation of secondary phases. The metal concentrations (copper, nickel, lead and cobalt) do not vary considerably over the model time periods. The ferrous iron concentration decreased from initial conditions due to influx of decant water and reduction in dissolved oxygen then generally increased with time from six to 19 years (Fig. 6.8b and 6.8c) reflecting the increase of sulfide mineral oxidation products. Ferric iron concentration was low compared to ferrous iron and decreased with modeled time. Hydrogen monosulfide also increased in concentration with time as a result primarily of sulfur or sulfur compound dissolution. When the hydraulic conductivity of the deposit and/or the flux of the pore water from the deposit base were varied there was corresponding change in the extent of the upper zone (i.e. the depth over which large changes occur in pore water metal concentration).

Figure 6.7: Predicted analyte concentrations with depth for full-scale subaerial disposal site; time 50 days, 6 years, 19 years

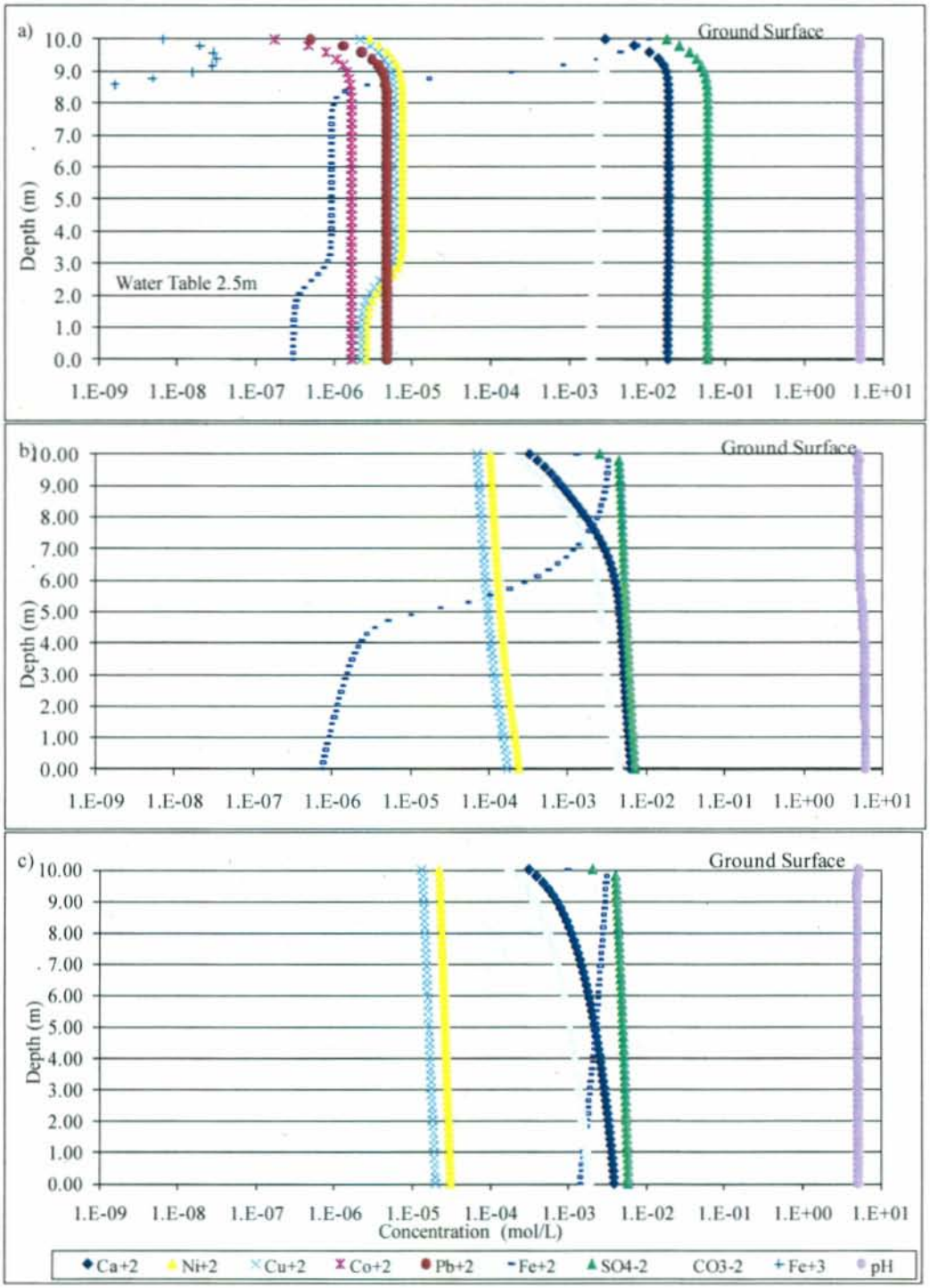

Figure 6.8: Predicted analyte concentrations with depth for full-scale subaqueous disposal site; time 50 days, 6 years, 19 years

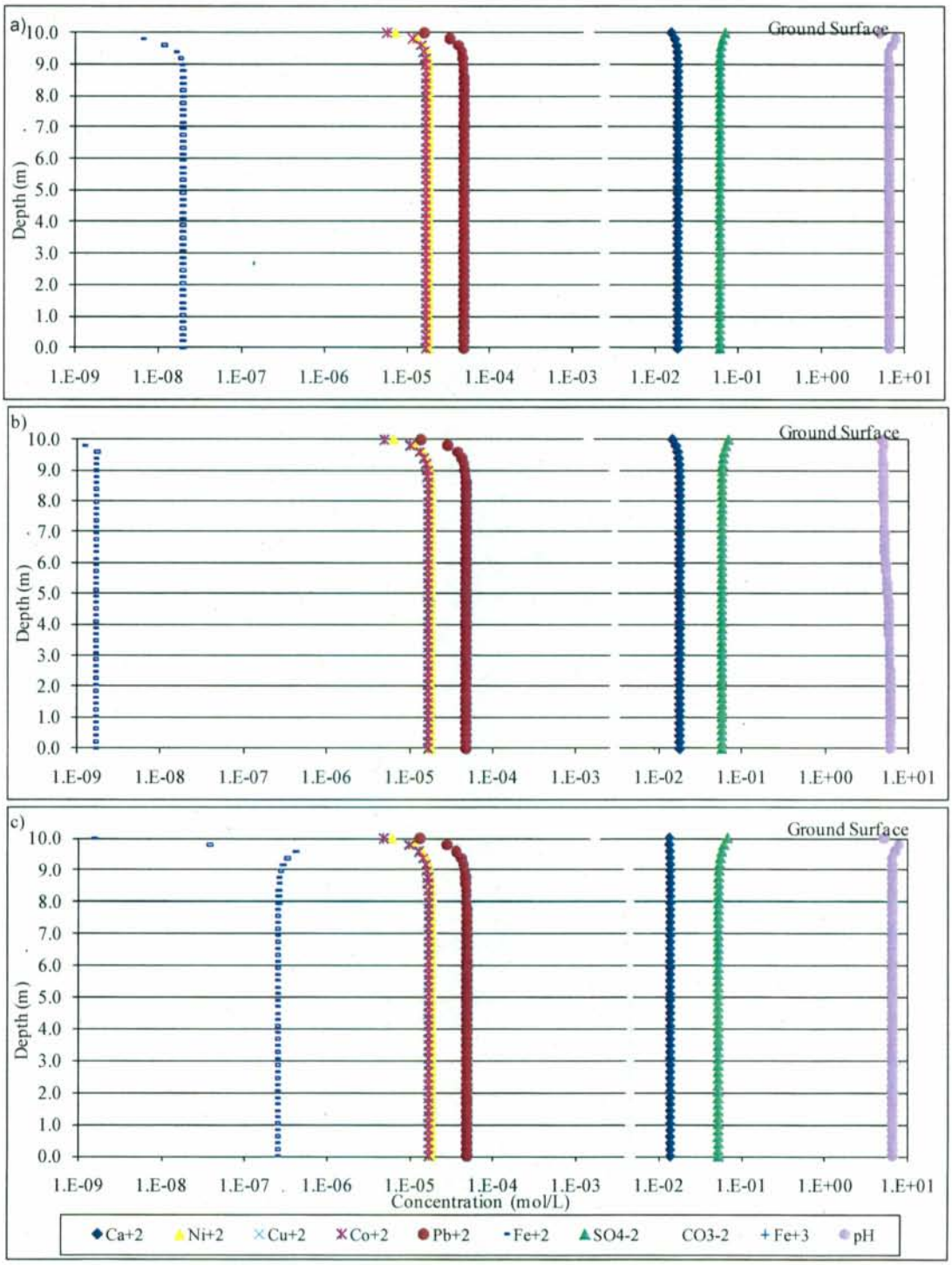

6.4.4 Sensitivity Analysis and Limiting Factors

Model variables assessed during sensitivity analysis included: hydraulic conductivity, dispersivity and porosity of the deposit, mineral volume fraction and surface area, reaction kinetics, flux from deposit, oxygen availability and modeled time. For the subaerial and subaqueous cases, consideration was given to the effect of removing one of the minerals which contributes to the residue's neutralizing or acid generating capacity as well as varying hydrogeologic input parameters. The subaerial base case used for sensitivity analysis was a 10 year time and the 0.5 m column. From Fig. 6.9 the dominant factors are changes in the flux into the column and removal of the mineral calcite. The subaqueous base case was a 19 year time and the 3.0 m column. Fig. 6.10 and Fig. 6.11 illustrate the dominant factors at the base of the column and 0.4 m from the residue surface respectively. The main model factors affecting the selected subaqueous pore water chemistry are changes in the flux from the column, deposit porosity, surface area or reaction rate of calcite and pyrrhotite, initial condition solution composition, and selection of mineral to model FeS. As expected, the hydrologic parameters were significant to the chemistry of the upper deposit.

Limiting Factors

There are many potential limiting factors with this model that could cause the discrepancies between the modeled and field measurements. First, there are the limitations of the field data/observations. Little data was available, both temporally and spatially, from the two locations used for model calibration. In addition, the placement and type of residue for the Demonstration Plant impoundment was not well controlled.

Figure 6.9: Factors affecting geochemistry of modeled subaerial pore water

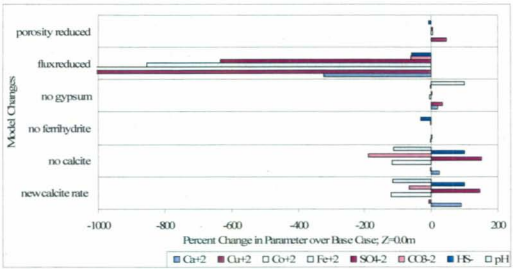

Second, limits in the model and model inputs. Several of the inputs for the calibrated scenarios and full-scale conditions were assumed due to lack of available data (see Table 6.5). The residue was assumed to be composed of ten minerals this is an over simplification of what actually exists in the residue and participates in reactions. The model only included the phases assumed to be dominating the groundwater geochemistry, especially metal concentrations. For example FeS, represented as the mineral mackinawite ($FeS\text{-}O_2$), may be present in amorphous form, thus it's thermodynamic and reaction kinetics may not be as represented in the code database. The kinetics of mineral dissolution/precipitation was derived from experiments conducted by others (Chou et al., 1989; Wunderly et al., 1996; Brookfield et al., 2006) and not on the actual minerals present. In addition, the reactive surface area for the minerals was assumed based on previous studies. Other compounds present in the residue could include metal oxides,

hydroxides and sulfates such as $Ni(OH)_2$, $Cu(OH)_2$, $CuSO_4$, furthermore the target metals may also be present adhered to the surfaces of other minerals such as ferrihydrite, magnetite and hematite. As the lead and cobalt and other metals exist also as metal oxides, hydroxides and sulfates and attached to surfaces, it is likely that these metals will leach more slowly into the groundwater. Due to competing reactions it was difficult to accurately model ferrous and ferric iron in the system as it was involved in many kinetically controlled reactions in the simulation, this may have resulted in the lower pH predictions in the saturated scenario.

Figure 6.10: Factors affecting geochemistry of modeled subaqueous pore water; Z=0.0m

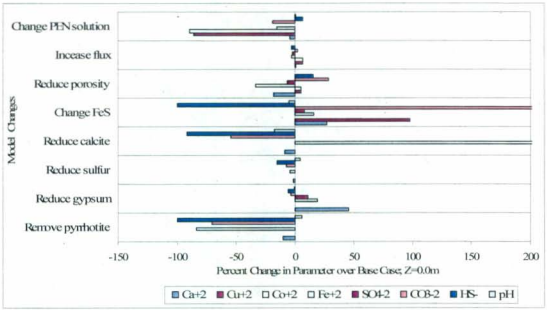

Figure 6.11: Factors affecting geochemistry of modeled subaqueous pore water; Z=2.6 m

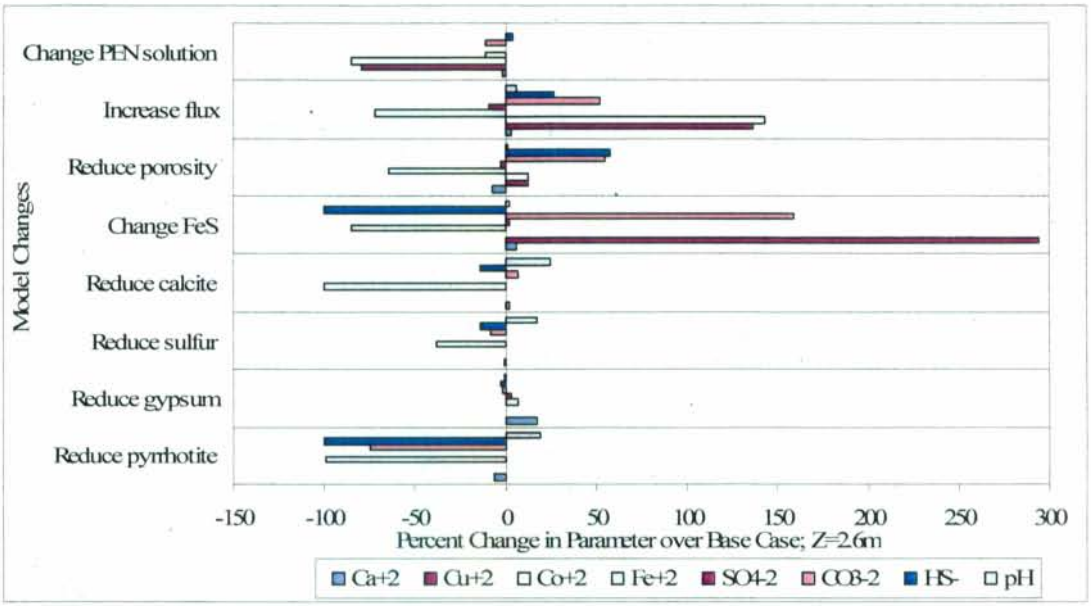

6.5 CONCLUSIONS

To enhance our ability to assess and subsequently optimally design mine waste disposal systems, it is beneficial to incorporate conceptual modeling and reactive transport simulations as one of the tools used at the design stage of the project. In this work a conceptual model of two disposal options for hydrometallurgical residue was developed which included developing a mineralogical assemblage that represents the hydrometallurgical residue, running simulations using a geochemical reactive transport code, calibrating the model against field data then predicting full-scale conditions. There was relatively good agreement between the model and the limited field measurements for both the subaerial and subaqueous disposal cases although it was difficult to model the ferrous iron concentrations and the high pore water pH evident in the subaqueous

scenario. Many factors contributed to the discrepancy between field measurements and model predictions, they include: lack of representative rate equations for minerals present, limited mineralogical expression of the residue, presence of amorphous minerals and metals attached to mineral surfaces, lack of information on mineral reactive surface areas, potentially inaccurate model flow system data.

The conceptual model was able to provide insight into some of the dominant reactions and influences on groundwater geochemistry in the residue impoundment. The model demonstrated the following dominant processes: the sulfide mineral oxidation, the neutralizing effect of the gypsum and calcite, the strong effect of initial pore water conditions in disposal situations with limited baseflow, the strong effect of oxygen availability as evident through the subaerial disposal method. From the work it is apparent that subaerial disposal can result in low pore water pH and high metal concentrations throughout the deposit in a relatively short period of time. The subaqueous case resulted in a higher deposit pH and reduced dissolved metal concentrations for the period modeled. Also there was a complex interdependence between the decant water chemistry, the initial interstitial pore water chemistry and the reactive minerals in the case of subaqueous disposal. For subaerial disposal, where rainwater infiltrates the deposit the chemistry is somewhat simpler. In both cases the conceptual model and reactive transport modeling was valuable in assessing some dominant reactions and predicting subsurface geochemical trends that could potentially occur with these disposal options.

6.6 REFERENCES

Bain, J.G., Blowes, D.W., Robertson, D., Find, E.O. (2000). Modelling sulfide oxidation with reactive transport at a mine drainage site. *Journal of Contaminant Hydrology*, 41, 23-47.

Bain, J.G., Mayer, K.U., Blowes, D.W., Frind, E.O., Molson, J.W.H., Kahnt, R., Jenk, U. (2001) Modelling the closure related geochemical evolution of groundwater at a former uranium mine. *Journal of Contaminant Hydrology*, 52, 109-135.

Ball, J.W., Nordstrom, D.K. (1991). *User's manual for WATEQ4F, with revised thermodynamic database and test cases for calculating speciation of major, trace and redox elements in natural waters*. US. Geological Survey, Open-File Report 91-183, 189pp.

Blowes, D.W., Jambor, J.L. (1990). The pore-water geochemistry and mineralogy of the vadose zone of sulphide tailings, Waite Amulet, Quebec, Canada. *Applied Geochemistry*, 5, 327-346.

Blowes, D.W., Ptacek, C.J. (1994). Acid neutralization mechanisms in inactive mine tailings. In Jambor, J.L., Blowes, D.W., (Eds.) *Environmental chemistry of sulphide mine wastes*, Mineral Association of Canada, Nepean, Canada. 271-292.

Brookfield, A.E., Blowes, D.W., Mayer, K.U. (2006). Integration of field measurements and reactive transport modeling to evaluate containment transport at a sulfide mine tailings impoundment. *Journal of Contaminant Hydrology*, 88(2006) 1-22.

Brown, P.L., Ritchie, A.I.M., Bennett, J.W., Comarmond, M.J., Timms, G.P. (2000). Geochemical kinetic modelling of acid rock drainage. In *Proceedings ICARD 2000, Fifth International Conference Acid Rock Drainage,* Denver, Colorado, USA, May, 21-24, 2000, 1, 289-296.

Chou, L., Garrels R. M. and Wollast R. (1989). Comparative study of the kinetics and mechanisms of dissolution of carbonate minerals. *Chemical Geology.* 78, 269–282.

Christensen, T.H., Bjerg, P.L, Banwart, S.A., Jakobsen, R., Heron, G., Albreschtsen, (2000). Characterization of redox conditions in groundwater contaminant plume. *Journal of Contaminant Hydrology,* 45, 165-241.

Davis, G.B., Ritchie, A.I.M. (1986) A model of oxidation in pyretic mine wastes: Part1. Equations and approximate solution. *Applied Mathematical Modelling*, 10, 314-322.

Elberling, B., Nicholson, R.V., Sharer, J.M. (1994). A combined kinetic and diffusion model for pyrite oxidation in tailings: a change in controls with time. *Journal of Hydrology,* 157, 47-60.

Elberling, B. (1996). Gas phase diffusion coefficient in cemented porous media. *Journal of Hydrology*, 178, 93-108.

Environment Canada, National Climate Data and Information Archive, Retrieved March 15, 2009, from http://www.climate.weatheroffice.ec.gc.ca.

Fernandes, H.M, Franklin, M.R. (2001). Assessment of acid rock drainage pollutants release in the unranium mining site of Pocos de Caldas, Brazil, *Journal of Environmental Radioactivity*, 54, 5-25.

Frind, E.O. Molson, J.W. (1994). Modelling of Mill-Tailings Impoundments, In J.L. Jambor, D.W. Blowes (eds.) *Short Course Handbook on Environmental Geochemistry of Sulfide Mine Waste.* Minerals Association of Canada, Nepean.V.22.

Furrer, G., Westall, J., Sollins, P. (1989). The study of soil chemistry through quasi-steady state models: I. Mathematical definition of model. *Geochimica et Cosmochimica Acta*, 53, 595-601.

Furrer, G., Westall, J., Sollins, P. (1990). The study of soil chemistry through quasi-steady state models: II. Acidity of soil solution. *Geochimica et Cosmochimica Acta*, 53, 2363-74.

Hermann, K.H., Polhlmeier, A., Gembris, D., Vereecken, H. (2002). Three-dimensional imaging of pore water diffusion and motion in porous media by nuclear magnetic imaging. *Journal of Hydrology,* 267, 244-257.

Jaynes, D.B., Rodowski, A.S., Pionke, H.B. (1984). Acid mine drainage from reclaimed coal strip mines 1. Model decription . *Water Resources Research*, 20, 233-242.

Jurjovec, J., Ptacek, C.J., Blowes, D.W., (2002) Acid neutralization mechanisms and acid release in mine tailings: a column experiment. *Geochimica et Cosmochimica Acta*, 60(9), 1511-1522.

Jurjovec, J., Blowes, D.W., Ptacek, C.J., Mayer, K.U. (2004) Multicomponent reactive transport modeling of acid neutralization reactions in mine tailings. *Water Resources Research*, 40 (11).

King, A.F. (1988) Geology of the Avalon Peninsula, Newfoundland. Newfoundland Department of Mines, Mineral development Division, Map 88-01.

Lichtner, P.C. (1996). Continuum formulation of multi-component multi-phase reactive transport. In: Lichtner, P.C., Steefel, C.I., Oelkers, E.H., (Eds), *Reactive Transport in Porous Media*. Reviews of Mineralogy, Mineralogical Society of America, Washington, DC, USA, 1, 1-81.

Mayer, K.U., Blowes, D.W., Frind, E.O. (1999). Advances in reactive-transport modeling of contaminant release and attenuation from mine-waste deposits. In. J.L. Jambor, D.W., Blowes (Eds.), *Environmental Aspects of Mine Wastes* (Vol.31), Minerals Association of Canada.

Mayer, K.U., Blowes, D.W., Frind, E.O. (2000). Numerical modelling of acid mine drainage and subsequent reactive transport. In *Proceedings ICARD 2000, Fifth International Conference Acid Rock Drainage*, Denver, Colorado, USA, May, 21-24 2000, 1, 135-141.

Mayer, K.U., Blowes, D.W., Frind, E.O. (2001). Reactive transport modelligh of an insitu reactive barrier for the treatment of hexavalent chromium and trichloroethlylene in groundwater. *Water Resources Research*, 37(12), 3091-3103.

Mayer, K.U., Frind, E.O., Blowes, D.W. (2002) Multicomponent reactive transport modeling in variably saturated porous media using a generalized formulation for kinetically controlled reactions. *Water Resources Research*, 38(9), 1174-1195.

Nicholson, R.V., Sharer, J.M. (1990). Laboratory studies of pyrrhotite oxidation kinetics, In C.N. Alpers, D.W. Blowes (Eds.), *Environmental Geochemistry of Sulfide Oxidation*, American Chemical Society, Symposium Aug 23-28, 1992., 14-30.

Nicholson, R.V. (1994). Iron-sulfide oxidation mechanisms: laboratory studies. In Jambor.J.L., Blowes, D.W., (Eds.), *Short Course Handbook on Environmental Geochemistry of Sulfide Oxidation*. ACS Symposium Series 550, 172-189.

Nordstrom, D.K., Ball, J.W. (1989). Mineral saturation states in natural waters and their sensitivity to thermodynamic and analytical errors. *Sciences Geologiques Bulletin*, 42, 269-280.

Nordstrom, D.K., Southam, G. (1997). Geomicrobiology of sulfide mineral oxidation. In Banfield, J.F., Nealson, K.H. (Eds.) *Geomicrobiology: Interactions Between Microbes and Minerals*. Reviews Mineralogy, Mineralogical Soc. Am., Washington, D.C., USA, 11, 361-390.

Nordstrom, D.K., Alpers, C.N. (1999). Geochemical modeling of water rock interactions in mining environments. In Plumlee Logsdon (Eds.) *Environmental Geochemistry of Mineral Deposits (Part A: Processes Techniques and Health Issues)*. Reviews in Economic Geology, (Vol. 6A). Society of Economic Geologists Inc.

Parkhurst, D. L. Appelo, C. A. J. (1999). *User's guide to PHREEQC (Version 2): A computer program for speciation, batch reaction, one-dimensional transport and inverse geochemical calculations.* U.S. Geological Survey Water Resources Investigation Report, 99-4259.

Robertson, J.D. (1994). The physical hydrology of mill-tailings impoundments. In: Jambor, J.L., Blowes, D.W., (Eds.), *Short Course Handbook on Environmental Geochemistry of Sulfide Mine-Wastes*. Mineralogical Association of Canada Short Course Handbook, 22, 1-17.

Salmon, U.S., Malmstrom, M.E. (2004). Geochemical processes in mill tailings deposits: modeling of groundwater composition. *Applied Geochemistry, 19, 1-17.*

Sharer, J.M., Nicholson, R.V., Halbert, B., Snodgrass, W.J. (1994). A computer program to assess acid generation in pyretic tailings. In C.N. Alpers, D.W. Blowes, (Eds.), *Environmental Geochemistry of Sulfide Oxidation.* American Chemical Society symposium series, Washington, D.C., USA. 550(11), 32-152.

Steefel, C.I., Lasaga, A.C. (1994). A couple model for transport of multiple chemical species and kinetic precipitation/dissolution reactions with application to reactive flow in single phase hydrothermal systems. *American Journal of Science*, 294, 529-592.

Steel, A., Hawboldt, K., Khan, F. (2006). A microstructural and geochemical comparison of residues from hydrometallurgical processes. Poster session presented at Conference of Metallurgy 2006, Montreal, Oct. 1-4, 2006.

Steel, A., Hawboldt, K., Khan, F. (2009a). Assessment of minerals and iron-bearing phases present in hydrometallurgical residues and availability of their associated metals. *International Journal of Hydrometallurgy,* accepted.

Steel, A., Hawboldt, K., Khan, F. (2009b). Results of shake flask experiments on hydrometallurgical residues. *International Journal of Environmental Science and Technology*, 6(1), 57-68.

Steel, A., Hawboldt, K., Khan, F. (2009c). An approach to numerical modeling of process residue impoundment decant water. *Canadian Geotechnical Journal*, submitted.

Stromberg, B., Banwart, S. (1994). Kinetic modeling of geochemical processes at the Aitik mining waste rock site in northern Sweden. *Applied Geochemistry*, 9, 583-595.

Stumm, W., Morgan, J.J. (1981). *Aquatic chemistry: An Introduction Emphasizing Chemical Equilibria in Natural Waters*, (2nd ed), Wiley, New York, US.

VINL (2006). *Voisey's Bay Nickel Company Project Description and Project Registration for a Commercial Processing Plant*. Retrieved September 15, 2006, from http://www.vbnc.com/NewsItems.asp?EffectiveYear=2006.

VINL (2008). *Environmental Impact Statement, Long Harbour Commercial Nickel Processing Plant, Vol1. Project Description* , 174pp. Retrieved July 15, 2008, from http://www.env.gov.nl.ca/env/Env/EA%202001/pages/active%20projects.htm#Environmental%20Impact%20Statements.

Wunderly, M.D., Blowes, D.W., Frind, E.O., Ptacek, C.J. (1996). Sulfide mineral oxidation and subsequent reactive transport of oxidation products in the mine tailings impoundments. *Water Resources Research*, 32, 3173-3187.

CHAPTER 7

AN INTEGRATED, RISK-BASED APPROACH TO THE DESIGN OF MINE WASTE LONG-TERM DISPOSAL FACILITIES

A. Steel, K. Hawboldt[a], F. Khan[a]
[a] Faculty of Engineering and Applied Science, Memorial University of Newfoundland, St. John's, Newfoundland, Canada

***ABSTRACT**: Base metal mines produce large quantities of waste in the form of tailings and sludges which contain metals as well as metal sulfides and oxides. Although, the waste is neutralized before disposal, it has high acid generating and metal leaching potential and therefore it is important to determine optimal treatment/mitigation/disposal methods and their associated risks in order to protect human health and the environment. A risk-based approach is proposed to determine the optimal disposal methodology for mine waste. The main steps include: hazard identification, characterization, geochemical transport modeling, exposure affect modeling, risk estimation/characterization and risk management. To demonstrate the applicability of this method, a case study illustrating four mine waste disposal options with three potential sources of Contaminants of Concern (COC) are considered. Based on the selected COC's, the human health and ecological risk is evaluated against acceptance criteria for each design option. A multi-criteria decision making analysis framework is used to optimize the waste disposal options based on criteria which includes risk, costs and environmental protection.*

This paper will be submitted to the *International Journal of Stochastic Environmental Research and Risk Assessment.* The lead author is Abigail Steel and the co-authors are Dr. Kelly Hawboldt and Dr. Faisal Khan. Ms. Steel's contribution to this paper is as follows:

- Wrote the paper
- Performed all laboratory testing and analysis (except where noted)

- Conducted all numerical modeling work
- Conducted interpretation of results
- Performed all literature searches required for background information.

Dr. Hawboldt and Dr. Khan provided technical guidance and editing of the manuscript. The figure and table numbers and reference formats have been altered to match the formatting guidelines set out by Memorial University.

7.1 INTRODUCTION

Ecological or human health risk assessment is a common approach to derive environmental quality criteria or to serve as a basis for remediation decisions. However, a risk-based approach to waste management is not often used at the design stage of a project. This work proposes a methodology for employing a risk-based approach to mine waste disposal management. This approach could also be applied to industrial waste or mining-related waste. The advantage of such an approach is the reduced long-term costs and liability of a project and the reduced environmental effects. Waste management involves balancing competing objectives of minimizing risks and waste management costs within the constraints of the project. In general, the lower the risk level the higher the costs involved and vice versa. There is an optimum combination of risk level and cost for a set level of acceptance (Asante-Duah, 1993). Part of a risk management program is to compare risks, benefits and costs for various strategies. Liu et al. (2004) is an example where risk time curves were employed for decision making, the benefit being the immediate indication of periods of elevated societal risk.

There has been considerable use of risk assessment as a decision making tool for remediation options. Khan and Husain (2003) reported the evaluation of petroleum hydrocarbon contaminated sites using risk-based monitored natural attenuation. Volosin et al. (1997) described risk assessment in the remediation of acid rock drainage. The use of risk-based assessment of soil and groundwater quality relative to remediation strategies was described by Swartjes (1999). This Netherlands-based study determined target values and intervention values based on potential risks to human health and

ecosystems. Bonano et al. (2000) also considered risk assessment in the decision analysis of environmental remediation alternatives. Nitzche et al. (2000) investigated database uncertainty in reactive transport modeling through Monte Carlo simulations.

On the topic of disposal of materials Proctor et al. (2002) considered the human health and ecological risk posed by steel slag in the environment. A stochastic analysis was conducted to assess variability and uncertainty in the inhalation risk estimates associated with environmental applications of slag. Other work on waste disposal included Sadiq et al. (2004), who presented a decision framework for selection of the best drilling waste disposal option, which included quantification of uncertainties in risk, cost and technical feasibilities through the use of fuzzy numbers. Other examples on risk related to groundwater contamination include: Maxwell et al. (2003), who used a risk-based approach to account for the differences in risk to individuals arising from: variability in individual physiology and water use; the uncertainty in estimating chemical carcinogens, and uncertainties and variability in contaminant concentration in groundwater. A risk assessment approach to assist in the management of petroleum contaminated sites in western Canada was described by Liu et al. (2004). The project framework included a multi-phase, multi-component transport model and an ELCR (Excess Lifetime Cancer Risk) - based human health risk assessment. Ibrahim et al. (2003) discussed some of the limitations of cost-benefit analysis in an integrated approach for management of contaminated groundwater resources using health risk assessment and economic analysis. The approach in this work involves characterization of mine waste for use in a contaminant fate and transport model to determine the exposure of receptors to selected

COC's. A probabilistic approach is then used to estimate the risk to receptors based on different waste disposal options. Finally, a multi-criteria risk-based decision making methodology integrates risk with other disposal criteria. This approach assimilates the data/information to determine the most effective mine waste disposal systems (Fig. 7.1). After detailing the methodology of the above approach, a case study is presented. This case study does not represent a particular site location and results cannot be used to infer assessment of a specific location or waste but rather used as an application of the described methodology. Results from any risk-based decision making process are site specific thus results will change with site location and waste characteristics.

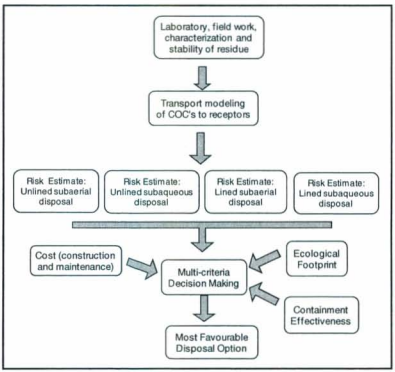

Figure 7.1: Schematic of study plan

7.2 RISK ASSESSMENT METHODLOGY

The main steps involved in the determination of ecological and human health risk follow and are described in detail in the following section.

1. Hazard identification: identification of potential sources of COC's, release mechanisms and receiving environment.
2. COC identification and characterization: estimating characteristics of identified hazards such as source concentration, species at source, chemical human health and ecological toxicity data.
3. Modelling transport of COC's from sources to receptors: Geochemical reactive advective-dispersive transport models as well as simplified models.
4. Exposure modeling: modeling potential exposure routes to receptors (i.e. inhalation, dermal, food chain, ingestion and estimating exposed concentration).
5. Risk estimation: estimation of risk potential based on the exposed concentration and allowable concentration (reference dose) for human and ecological receptors.
6. Uncertainty analysis
7. Risk-based decision making: selection of an appropriate disposal design/technique which exhibits acceptable risk. The disposal options will be evaluated using multi-criteria decision making including ecological and human health risk.

Based on most common options two main disposal methods were evaluated. 1) Subaerial disposal where waste is placed in a lined or unlined site with proper site drainage and treatment of site drainage. In this case the waste remains unsaturated during and after disposal. 2) Subaqueous disposal, where waste is saturated under a water cover during

placement and after disposal. A head of water is maintained above the waste at all times, limiting the supply of atmospheric oxygen to the waste. Subaqueous disposal can either be in an existing water body or developed through a lined excavation. For each disposal case a lined and unlined disposal site was considered.

7.2.1 Hazard Sources, Release Mechanism and Receiving Environment

The fault tree in Fig. 7.2 shows the three potential routes (surface water, groundwater and air transport) and release mechanisms for contaminants to enter the environment. For this work, only two sources of contaminants were considered; the decant water, and the mine waste in the disposal site. The air transport of mine waste particulates is not considered. Potential mechanisms of release considered are: 1) decant water release by overtopping of the impoundment dam and 2) leaching of contaminants into the groundwater through the base of the disposal site.

Given that the release mechanisms under consideration; the two main receiving environments are surface water and groundwater. The potential receptors are humans or ecological receptors which are in contact with groundwater or the receiving surface waters. Exposure from the decant water and leachate in the soil, sediment and air was beyond the scope of this work.

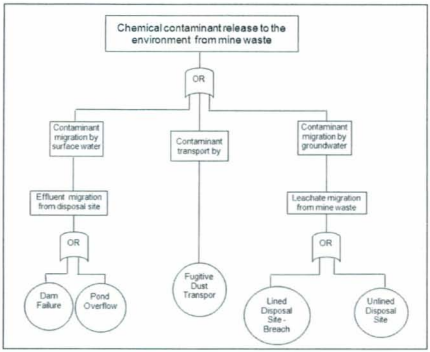

Figure 7.2: Fault tree of routes for contaminants from mine waste entering environment and release mechanisms

7.2.2 PCOC, COPEC Identification and Characterization

The selection of PCOC's (Potential Contaminants of Concern) and COPEC's (Contaminants of Potential Ecological Concern) is based on a number of factors including: assay results on the mine waste and waste liquor, acid producing potential of the waste, mineralogy and transport modeling. The mine waste assay results can be compared with Canadian Council of Minister of the Environment (CCME) Soil Quality Guidelines (SQG) (CCME, 1999) and the waste liquor compared to CCME Freshwater Aquatic Life (FAL) (CCME, 2003), provincial effluent guidelines and background and baseline surface water quality. Treated wastewater from the mine waste disposal site must meet provincial water and sewage regulations and surface and groundwater and

must comply with Canadian Council of Ministers of the Environment's (CCME) FAL or Marine Aquatic Life (MAL) regulations, (CCME, 2006). The CCME limits for Freshwater Aquatic Life are often used as a first step to determine whether surface water or groundwater is contaminated. It will be important to consider background surface and groundwater quality when considering whether the mine waste or decant water are affecting the local environment.

The presence of sulfur in mine waste can result in pH depression due to its acid generating potential. Preliminary Acid Base Accounting (Sobek et al., 1978) analyses and batch tests on samples will indicate whether the mine waste will be acid generating in the long term. The mine waste may be neutralized before it is sent for disposal however pH can still be considered a COPEC.

For the assessment, the concentration (range and average) of each COC in the decant water and in groundwater at the base of the disposal site is determined. The concentration of COC's in the groundwater is provided for the two main disposal options investigated.

Human Health Toxicity Data

In human health risk assessment non-carcinogenic chemicals are governed by threshold limits such as "Acceptable Daily Intake" (ADI) or Reference Dose (RfD) and cancer causing chemicals use unit cancer risk (UCR) or cancer slope factor parameters (SF). The appropriate values of RfD and SF are determined for each PCOC during the hazard assessment. Depending on the cancer classification of a chemical it may or may not be assessed for carcinogenic risk. The hierarchy from EPA used for the determination of

slope factors and RfD values is: the Integrated Risk Information System (IRIS), Provisional Peer Reviewed Toxicity Values (PPRTV), and other databases such as the US EPA Superfund Human Effects Assessment Summary Tables (HEAST) (RAIS, 2007) and American Conference of Government Industrial (ACGIH, 2009).

Determination of Non-carcinogenic Threshold Limits

If RfD values are not reported for the PCOC's then RfD may be calculated through determination of No Observed Adverse Effect Level (NOAEL) and the Lowest Observed Adverse Effect Level (LOAEL) levels from dose response animal studies (Equation (7.1)). The applied uncertainty factors (UF) or modifying factors (MF) can include several factors such as: the quality of the study, animal to human extrapolation, dose extrapolation and variability in results (U.S. EPA, 1993).

$$RfD = \frac{NOAEL}{\sum_{i=1-n}^{n} UF_i \cdot MF} \text{ or } RfD = \frac{LOAEL}{\sum_{i=1-n}^{n} UF_i \cdot MF} \qquad (7.1)$$

Determination of Carcinogenic Slope Factor

Carcinogenic risk is determined through dose-response assessment. It is a process of quantitatively evaluating the toxicity information and characterizing the relationship between the dose of a contaminant received and the incidence of adverse health effects such as cancer. Fig. 7.3 shows a typical dose response curve.

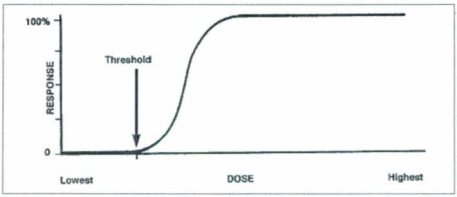

Figure 7.3: Dose response curve showing threshold level

For the simplest case:

$$R=k[C] \qquad (7.2)$$

where k - Rate constant

R - Response

C - Concentration of COC

Where the slope of the curve is a straight line, a slope factor is often used to describe the curve. EPA uses a Linearized Multi-Stage Model (LMS) to yield a cancer slope factor ($mg/kg \cdot day^{-1}$) through a linear extrapolation from the zero threshold to the 95% upper confidence level of the lowest dose to produce cancer in an animal test.

Ecological Toxicity Data

During the toxicity assessment the dose-response relationship for each chemical species on laboratory or captive animals is assessed in order to determine an acceptable exposure level. The aquatic toxicological data is available through U.S. EPA ECOTOX (U.S. EPA, 2006) database.

In this case:

$$NOEC < BC\,(TRV) < LOEC \qquad (7.3)$$

where LOEC - Lowest Observed Effects Level

NOEC - No Observed Effects Level

TRV - Toxicity Reference Value

BC - Benchmark Concentration

The TRV's or BC can also be selected based on CCME Freshwater or Marine Aquatic Quality guidelines (CCME, 1996, 1997, B.C. MOE 2006), similar provincial regulations or EPA water quality guidelines. The Office of Water Regulations and Standards suggests BC is applied to lowest 5th percentile of species ranked by sensitivity.

The US EPA Office of Solid Wastes uses:

$$BC = MATC/SafetyFactor \qquad (7.4)$$

where MATC - Maximum Acceptable Toxic Concentration

SafetyFactor – Factor used to consider effect of data quality, sensitivity of the species and other influences.

The procedure used to determine TRV for this project was similar to that of the Office of Water Regulations and Standards (U.S. EPA, 1987). NOEC data from the U.S. EPA ECOTOX database for the aquatic species and metal species of interest is selected and plotted as a probability density function. If sufficient data is not available LOEC or LC50 data can be converted to NOEC values by dividing by an appropriate factor. From the cumulative density function the 5 percentile exceedance value is derived, this

value is used for the TRV for the species and metal unless it exceeds the CCME FAL guidelines; in which case FAL is used for TRV.

As an initial screening the predicted freshwater and sea water COPEC concentrations can be compared to that of the CCME guidelines. If the predicted values are less than that of the guidelines (Exposure Ratio (ER)<1.0), then that metal and pathway is not deemed to be a concern for aquatic life at the receptor location and further screening is not completed on this COPEC and pathway. Those metals with ER greater than 1.0 are brought forward for further assessment.

7.2.3 Modelling Transport of PCOC's and COPEC's from Sources to Receptors

The scenarios considered for this study follow and are explained in this section.

1) A larger water body downgradient of the disposal site that is impacted by a contaminated stream.
2) A stream immediately downgradient of the site that is impacted by leachate from the disposal site.
3) A stream immediately downgradient of the site that is impacted by dam overtopping.
4) A downgradient groundwater well that is impacted by leachate from the disposal site.

If a dam on the impoundment overtops due to extreme weather conditions the decant water will likely enter the downgradient stream and eventually the larger body of water. The concentration of COC's in the larger body of water is determined by assuming the

body of water is a Continuously Stirred Tank Reactor (CSTR). In that case the following relationship (Dehling, 2007) is used.

$$V\frac{dC}{dt} = Q_{in}C_{am}(t) - Q_{out}C_{mix} - KVC_{mix} + S(t) \qquad (7.5)$$

where:

V - Volume of water in water body

Q - Flow or discharge

t - Time

S - Storage

C_{am}, C_{mix} - Concentration of COC (ambient or mixture)

K - Decay constant

Assuming Q_{in} equals Q_{out}, there is no COC decay and no storage;

$$C_3Q_3 = C_1Q_1 + C_2Q_2 \qquad (7.6)$$

where:

C_1, C_2 - Concentration of COC's entering water body

C_3 - Concentration of COC's exiting water body

Q_1, Q_2 - Discharge of streams entering water body

Q_3 - Discharge of stream leaving water body

The concentration of metals in the stream due to leachate migration can be calculated using the stream hydrograph and groundwater advective dispersive transport modeling. The groundwater contribution to the stream can be estimated by considering the percentage of the base-flow (groundwater) with respect to the total stream discharge. The

leachate concentration at the stream location can be calculated by using a simple advective dispersive subsurface transport code or assuming a very short flow path and a maximum potential concentration.

If impoundment dam overtops due to extreme weather conditions the decant water will enter a downgradient stream. The concentration of COC's due to dam overtopping is calculated by assuming the dam would overtop when the water elevation was 1.0 cm higher than the dam. At this point the volume of water available to overtop the dam would be equal to the surface area of the impoundment times the height of water above the dam.

Leachate from the mine waste site could also migrate to the base of the impoundment into the groundwater in the bedrock, where it will be dispersed and transported in the direction of groundwater flow. The concentration of COC's in a groundwater well used for human consumption, at a specific location downgradient of the disposal site, can be modeled through a code such as such as SESOIL (Environmental Software Consultants Inc, 2006) combined with AT123D (Yeh et al., 1987).

7.2.4 Exposure Modelling for Human Health and Ecological

Human Health Exposure Modelling

The human receptors for PCOC's in the groundwater and surface water are considered separately. The human exposure to surface water could occur through dermal adsorption (fishing, ingestion and/or swimming). Groundwater metal concentration should be considered for ingestion and dermal absorption.

Determination of Chronic Daily Intake for Dermal Contact and Ingestion

U.S. EPA (1988, 1989a, 1989b, 1992a) risk assessment guidelines are followed and standard default exposure assumptions are used to calculate the dose for each COC in each scenario and application. Site specific information is used when available in addition to US EPA exposure assessment guidance (U.S. EPA, 1997). Consistent with U.S. EPA risk assessment guidelines (1989a) Chronic Daily Intake (CDI) in mg/kg/day is determined for non-carcinogens and Lifetime Average Daily Dose (LADD) for potential carcinogens. The equations used for dermal contact and ingestion follow.

CDI or LADD via dermal contact as is a function of several factors (U.S. EPA, 1989a, 1992a, 1997) including: concentration in water (CW), dermal adsorption (DA_{event}), skin absorption rate (Kp), fraction absorbed (FA), surface area (SA), exposure frequency (EF), exposure duration (ED), event frequency (EV), bodyweight (BW) and averaging time (AT) and can be expressed by the equations (7.7) and (7.8).

$$CDIorLADD = (DA_{event} \cdot SA \cdot EV \cdot ED \cdot EF) / (BW \cdot AT) \qquad (7.7)$$

$$DA_{event} = FA \cdot Kp \cdot CW \qquad (7.8)$$

The CDI or LADD for ingestion of drinking water is a function of many of the parameters included in equation (7.7) as well as amount ingested (IR), bioavailability (ABSs), fraction ingested (FI) and can be expressed by the equation (7.9).

$$CDIorLADD = (CW \cdot IR \cdot FI \cdot ABs \cdot EF \cdot ED) / (BW \cdot AT) \qquad (7.9)$$

The CDI or LADD formulation for dermal contact through showering is the same as has been provided in the previous section for swimming.

Ecological Exposure Modeling

For this study COPEC's affecting ecological receptors are assessed for two cases 1) a downgradient stream and 2) a downgradient larger water body. COPEC's concentration in the stream downgradient of the impoundment is derived from two sources the decant water through dam overtopping and mine waste leachate through groundwater migration. In Canada environmental effects assessment uses the Valued Ecosystem Component (VEC) approach (Beansland and Duiker, 1983). The selection of VEC's can be extensive and can include many species or even a food web. It is recommended that the species selected have ecological relevance, relevance to management goals, are located within study area and have potential to be impacted (U.S. EPA 1998, CCME, 1996). The exposure of metals to the aquatic species is assumed to be equal to the concentration of the COPEC's in the fresh water or marine environment, however bioconcentration and biomagnification is should be taken into account (LeGrega et al., 1994)

7.2.5 Risk Estimation Human Health and Ecological

Human Risk Estimation

Non-carcinogenic Risks

The total Hazard Index (HI) provides an estimate of the level of risk to human health due to non-carcinogenic hazards as described by equation (7.10). HI varies between from 0 to greater than 1.0, levels greater than 1.0 are considered unacceptable risk.

$$\textit{Total Hazard Index} \quad HI = \sum_{i}^{n} (CDI_i / RfD_i) \qquad (7.10)$$

where CDI_i - exposure level for the i^{th} COC (mg·kg/day)

RfD_i - Acceptable reference dose for each COC (mg·kg/day)

n - Total number of contaminants

and $HQ = CDI / RfD$) (individual hazard)

Carcinogenic Risks

According to LeGrega et al. (1994) and U.S.EPA (2005) the human health total carcinogenic risk at a site should be below the range of $1x10^{-7}$ to $1x10^{-4}$. The total carcinogenic risk is described by equation (7.11). SF is the slope of the dose response curve and can be determined through reported values as indicated previously or read directly off an appropriate dose response curve.

$$TotalCarcinogenicRisk = \sum_{i}^{n} (LADD_i \cdot SF_i) \qquad (7.11)$$

Where $LADD_i$= Lifetime Average Daily Dose for ith contaminant

SF_i= Slope factor for ith COC

n= Total number of COC

Ecological Risk Estimation

The aquatic risk characterization for the COPEC's and VEC's selected consists of comparing the total estimated Environmental Exposure Concentration (EEC) of each chemical to that of the appropriate threshold Toxicity Reference Value (TRV) or Benchmark Concentration (BC) through equation (7.12) or (7.13).

$$\textit{Exposure Ratio (ER)} = \frac{\textit{Estimated Exposure Concentration (EEC)}}{\textit{TRV}} \qquad (7.12)$$

In addition with multiple chemicals assume the 1/TRV term is additive, where by:

$$ER = \sum (EEC/TRV) \qquad (7.13)$$

EEC is derived from exposure modeling and various methods are available to calculate TRV or BC (CCME, 1996 and 1997, U.S. EPA 1992). ERA standard practice in North America is that an ER of 1.0 represents the benchmark of safety (CCME, 1996) although this approach has several weaknesses (Burns, 1991). ER less than 1.0 suggests risk that is slight and little or no action is required, while ER near 1.0 represents uncertainty in risk estimate and additional data is required. If the ER exceeds 1.0, it implies the risk is greater and adverse effects could possibly occur; further assessment is required to evaluate the uncertainty represented and conservative assumptions (CCME, 1996).

7.2.6 Uncertainty Analysis

Uncertainty analysis provides a fuller understanding of the limitations and implications of the risk assessment. This work evaluates uncertainty associated with the risk assessment, providing methods of dealing with the uncertainty and prioritizing the most critical components of the risk assessment. To consider uncertainty and their effects on a given decision, a probabilistic approach is used.

Uncertainty in risk characterization needs to be clearly identified by source and magnitude. Barnthouse and Suter (1986) suggest three sources of uncertainty in modeling ecological risk assessment: inherent variability, parameter uncertainty and model errors. Methods that can be used to help identify and minimize uncertainty

include: probabilistic analysis including Monte Carlo simulation, sensitivity analysis and model calibration with monitoring data. Depending on the approach used the most critical source of uncertainty may vary; this work considers parameter uncertainty. When considering uncertainty it is important to determine whether one component of the risk assessment has a much higher level of precision that another. There should be a balance between level of precision and importance of component in the overall risk assessment process. A sensitivity analysis will bring to the forefront the most critical processes and input parameters. It is also important to consider correlations amongst parameters (Fordham and Reagan, 1991) and focus on pathways and contaminants likely to dominate the risk assessment.

Finally, in order to have accuracy in the risk characterization model verification, calibration and validity is required. Calibration of the model with monitoring data or laboratory studies will assist significantly in reducing the level of uncertainty.

According to Hammonds et al. (1994), to assess parameter uncertainty in exposure modeling first, list all uncertain parameters and specify a maximum range of potential values with respect to the endpoint. Next, assign a probability distribution for each specified value. After assessing correlations among parameters; use analytical or numerical procedures (such as Monte Carlo simulations) to produce a probability distribution of the model predictions based on parameter distributions. Finally, derive quantitative statements of uncertainty of excess cancer risk and Hazard Index and rank parameters contributing most to uncertainty.

7.2.7 Risk-based Decision Making

Multi-criteria decision making (MCDM) analysis integrates probabilistic health and ecological risk assessment. This process enables consideration of several factors to identify the best processing or mine waste disposal method at the design stage of the project. The key objectives of this MCDM are: to minimize construction cost and long-term maintenance costs, minimize human health and ecological risk, to reduce the ecological footprint and to maximize containment effectiveness. The proposed methodology provides six decision criteria: 1) construction cost, 2) long-term maintenance costs, 3) human health risk, 4) ecological risk, 5) containment effectiveness and 6) ecological footprint. Ecological footprint can be defined as the amount of land required to produce materials used to create a product along with the amount of land required to safely dispose of the product. Regulatory compliance was not included in these criteria as assessment results should be independent of regulatory requirements in cases where options may be presented to regulators; and applications to consider alternatives to standard procedures are often presented to regulators.

Various systematic analysis methodologies exist to synthesize data and rank the alternatives in a decision matrix. Outranking (Kangas et al. 2001) is a method used when one dominant alternative is assessed against another to identify the extent of preference in terms of one criterion over others. This method works best when criteria measurements are not readily comparable. Other decision making methods include: multi-attribute utility theory (MAUT) and analytical hierarchy process (AHP). These methods use numerical scores to permit alternative comparison. Decision criteria are assigned a utility

value and weighting function, to permit comparison of numerical and non-numerical criteria. AHP (Saaty, 1980; Schmoldt et al., 2001) uses quantitative approach with pair-wise comparison of decision criteria. For this work the AHP methodology was selected as its method permits straight forward comparison of qualitatively and quantitatively described criteria. The decision hierarchy is shown in Fig. 7.4.

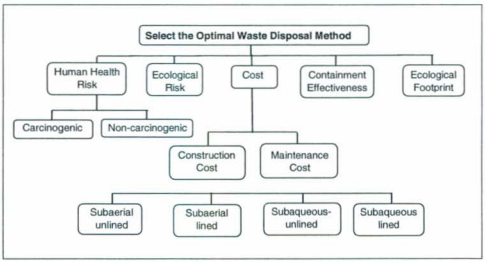

Figure 7.4: Decision hierarchy for selection of waste disposal method

The steps to conduct the AHP include: definition of problem, develop a decision hierarchy tree, define the alternatives for the goal, construct pair-wise comparison matrices for each criterion, and use priorities from the comparison to weigh priorities for each alternative and criterion. Each criterion is compared with other criteria with respect to the goal and each alternative is compared with other alternatives with respect to each criterion and subcriterion. To make comparisons a scale of 1-9 is used to determine the importance or dominance of one element over another with respect to the particular

criterion. For this case 12 matrices are constructed; one comparing the four alternatives, seven comparing each disposal alternative with respect to the seven criteria, one each comparing human health risk and total costs subcategories, one comparing the five main criteria and finally one synthesis matrix collating the priority results from other matrices and determining the overall priorities.

The advantages of this system include: relative ease with which the researcher can compare two options or criteria, ability to assign a numerical value to all criteria thus compare non-numeric and numeric qualities and the ability to integrate the alternative assessments and criteria assessments. A worked example is provided in the case study.

7.3 CASE STUDY – SITE ABC

This case study provides an example of the methodology, described in the previous section, to assess mine waste disposal methods at the design stage of a project. The location of the site (ABC) is non-specific and all values used in reference to the mine waste and the site are for solely for illustration purposes. The results of this assessment will change with site location and mine waste characteristics.

7.3.1 PCOC and COPEC Identification

As indicated in Section 7.2 first the results of solid mine waste assay are compared with CCME SQG and liquid mine waste assay compared with CCME FAL guidelines as well as background and baseline data.

For this mine waste, prior to treatment the liquid waste constituents that exceed one of the guidelines include: aluminum, nickel, copper, lead, selenium, and cadmium. The location

baseline groundwater metal concentrations consistently exceed FAL for iron, aluminum, cadmium and copper in the proximity of the disposal site location. Based on previous mine waste assays and our analysis the following metals or compounds exceed the CCME SQG: nickel, copper, cadmium, chromium and selenium. The mine waste contains a high percentage of sulfur thus there is potential that the sulfur could oxidize and form acid rock drainage causing leaching of metals from the waste or bedrock. Preliminary Acid Base Accounting (ABA) (Sobek et al., 1978) analyses on the waste and batch tests indicate it will be acid generating in the long term (Chapter 8). Mineralogical characterization and kinetic testing of the mine waste provides further information on its acid generation and metal leaching capacity (Chapter 3 and 4). Although the waste will be neutralized before it is sent for disposal, pH is considered a COPEC for the ecological risk assessment.

From a comparison of the assay results on solid and liquid mine waste with guidelines, and baseline metals concentrations the metals selected as potential COC's were nickel, cobalt, copper, lead and pH. Cadmium and chromium were not selected as they are close to the SQG, selenium was close to its detection limit in the liquid waste. Iron was not selected as it has a more limited effect on human health. It was noted that copper, nickel and lead have the highest percent exceedance of the FAL guideline.

7.3.2 Human Health Risk Assessment –Site ABC

7.3.2.1 PCOC Characterization

The concentration of each COC at each source, either in the decant water above the mine waste in the impoundment or in the groundwater at the base of the disposal site, is summarized in Table 7.1. Concentrations (range and average values) are provided for a representative decant water when it is neutralized and as a worst case scenario when it is not neutralized. The predicted concentration of COC's in the groundwater below the mine waste is provided for the two main disposal options: 1) subaerial disposal 2) subaqueous disposal. All groundwater concentrations are based on common values derived from reduced-scale field conditions and numerical modeling.

Table 7.1: Concentrations of COC's at source

COC	Decant Water-Neutralized (mg/L)	Decant Water-Not-Neutralized (mg/L)	Groundwater[a]-Subaqueous (mg/L)	Groundwater[a] - Subaerial (mg/L)
	Subaqueous	**Subaqueous**	**Subaqueous**	**Subaerial**
Copper	0.01-0.14 (0.024)	0.47-1.59 (1.1)	0.01-0.03 (0.02)	0.02-1.09 (0.55)
Lead	0.002 (0.002)	0.002-0.037 (0.023)	0.002-0.003 (0.003)	0.002-0.016 (0.006)
Nickel	0.03-0.25 (0.11)	3.08-7.33 (5.2)	0.256-0.558 (0.4)	0.205-7.481 (3.5)
pH	7.1-9.7 (9.2)	2.8-6.4 (3.2)	9.2-9.8 (9.6)	3.1-4.2 (3.6)

Notes: [a] Groundwater concentrations taken at base of test disposal site.
(…) average values

Table 7.2 provides the toxicity information for the PCOC's identified in the previous section. A summary of the carcinogenic class is also provided in Table 7.2. Of the PCOC's considered only lead is listed, by the U.S. EPA, as a probable human carcinogen (class B2). A chemical specific dose response relationship was used to characterize the health effects of lead.

Table 7.2: Hazard Information for selected COC's

Chemical	CASRN Number	Carcinogen Class	Route	Toxicity Reference Value		Critical Effect	Principal Study	Regulatory Agency
				Type	Value			
Nickel (soluble salts)	007440-48-4	NC- not classified (Oral /dermal)	Oral	RfD	0.02 mg/kg bw/day[b]	Decreased body and organ weights (rats)	Ambrose et al., 1976[b]	IRIS, U.S. EPA 1991
					0.025 ppm			PWQO
					0.1 ppm			
			Dermal (chronic)[1]		0.02 mg/kg bw/day			IRIS, U.S. EPA 1991
Lead	7439-92-1		Oral	RfD	0.0036 mg/kg bw/day	Neurobehavioral & neurodevelopmental effects (child)	Ziegler et al., 1978 in WHO, 1995	Health Canada, 2004
				RfD	no threshold level[f]			EPA, 1988[c]
				Action level	0.015 mg/L	Delays in physical and mental development in infants and children		U.S. EPA, National Primary Drinking Water Regulations, 2009
			Dermal (chronic)[1]		see Section 3.2			IRIS, U.S. EPA 1991
		Group 2A - probably carcinogenic	Oral					IARC, 2006[e]
		B2- probable human carcinogen	Oral			Rental tumors and reduced weight gain, in rat bioassays and mouse assay, human evidence inadequate	Azar et al., 1973, Kasprzak, 1985, Koller, 1986 in IRIS, U.S. EPA, 1991	IRIS, U.S. EPA 1991
Copper	7440-50-8		Oral	TRV	0.091 mg/kg bw/day (female toddler)	Upper intake level: maximum daily nutrient level	IOM, 2001	Health Canada, 2006
			Oral	Action Level	1.3ppm			U.S. EPA, 2009
			Oral, acute and intermediate	Internal MRL[1]	0.01 mg/kg bw/day	Gastrointestinal disturbances in people tested.	Pizarro et al.1999, Araya et al. 2003 in ATSDR, 2004	ATSDR, 2004
			Dermal (chronic)[1]		0.01 mg/kg bw/day			
		D- not classified	Oral/dermal					IRIS, U.S. EPA 1991

Notes:

a) TRV's exist generally for the oral and inhalation routes of exposure. No dermal limits have been identified for the COC's for this HHRA. Regulatory guidance U.S. EPA 1989, 1992 on route to route extrapolation typically dermal limits are determined from oral limits. It is common to multiply the oral RfD by a factor to represent the percent of the COC absorbed dermally. In this case, to be conservative, 100% skin absorption of COC in water was assumed; thus the dermal RfD through water contact was assumed to be equal to the oral RfD.

b) Ambrose, A.M., P.S. Larson, J.R. Borzelleca and G.R. Hennigar, Jr. 1976. Long-term toxicologic assessment of Ni in rats and dogs. J. Food Sci. Technol. 13: 181-187.

c) Lead (EPA, 1988):*A great deal of information on the health effects of lead has been obtained through decades of medical observation and scientific research. This information has been assessed in the development of air and water quality criteria by the Agency's Office of Health and Environmental Assessment (OHEA) in support of regulatory decision-making by the Office of Air Quality Planning and Standards (OAQPS) and by the Office of Drinking Water (ODW). By comparison to most other environmental toxicants, the degree of uncertainty about the health effects of lead is quite low. It appears that some of these effects, particularly changes in the levels of certain blood enzymes and in aspects of children's neurobehavioral development, may occur at blood lead levels so low as to be essentially without a threshold. The Agency's RfD Work Group discussed inorganic lead (and lead compounds) at two meetings (07/08/1985 and 07/22/1985) and considered it inappropriate to develop an RfD for inorganic lead.*

U.S. EPA: National Primary Drinking Water Regulations: http://epa.gov/safewater/contaminants/index.html#listmcl

d) MRL: Minimal Risk Level

e) IARC, 2006: International Agency for Research on Cancer

As a slope factor is not provided for lead by the U.S. EPA, a dose response curve (Figure A.2, Appendix V) summarizing the results from a representative study on rats fed lead acetate or lead subacetate (U.S. EPA, 2006) was used to derive a SF of $2x10^{-4}$ $mg/kg/bw{\cdot}d^{-1}$ using the LMS model described in Section 7.2.

7.3.2.2 Human Health Transport Modeling and Exposure Modeling of PCOC's

As indicated in Section 7.2 only receptors involving surface water and groundwater concentrations are considered. At site ABC the human receptors for fresh water could include fishers and swimmers. As a child is the most vulnerable receptor, for conservative analysis a child swimming in the downgradient larger water body was selected as one receptor. Based on typical mine surroundings a light industrial park may be located downgradient from the disposal site. A worker receptor at the industrial park exposed to COC's through groundwater usage was selected as a second receptor. Assuming limited flow in a stream immediately downgradient of the disposal site, human contact with COC's in this stream surface water is assumed to be limited and has not been considered.

In the following sections the COC concentration at receptors is provided for two cases 1) a larger body of water downgradient of site ABC and 2) groundwater near the location of a proposed light industrial park adjacent and downgradient of the site. The metal concentration is used to determine exposure due to 1) dermal absorption while swimming in the larger water body and 2) and water ingestion and dermal adsorption due to drinking

and showering using groundwater. For human health risk assessment solely lead and nickel are considered as COC's.

CASE 1: Exposure through Dermal Absorption- Swimming

Fig. 7.5 illustrates the flow of COC's from the site to a larger water body in the case of dam overtopping and subaqueous disposal. The metal concentrations in the larger water body is determined by assuming: 1) complete mixing in the water body, 2) the flow into equals the flow out of the water body and 3) the concentration of COC's in the outflow is proportional to discharges and COC concentrations of contributing inflows (Fig. 7.6).

As a worst case scenario the concentration of metals in the stream during overtopping is equal to that in the decant water. A summary of the concentration of COC's in the larger water body at site ABC due to overtopping of the impoundment is provided in Table 7.3 along with water quality guideline and baseline concentration data. Although predicted concentrations are less than the water quality guideline used the risk to receptors is calculated to illustrate the methodology.

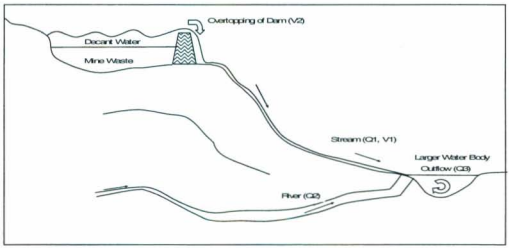

Figure 7.5: Schematic of dam overtopping and entering stream and larger water body

CASE 1: Contaminated Stream Entering Larger Water Body	
Assumptions:	**Data Source**
Stream discharge (Q_1) = 0.1-0.2 m3/s	measured
River discharge (Q_2) = 5 m^3/s	assumed
Outflow from water body = Q_3	calculated
C_1= metal concentration in stream during overtopping	estimated
C_2= metal concentration in river	assumed based on site data
C_3= metal concentration in larger water body	predicted
Complete mixing of inlet	
Calculations	
$Q_1+Q_2 = Q_3$	
0.2 + 5.0 = 5.2 m^3/s	
$Q_1C_1+Q_2C_2 = Q_3C_3$	
$C_3= (Q_1C_1+Q_2C_2)/Q_3$	
$C_3= (0.2C_1+5.0C_2/5.2$	

Figure 7.6: Assumptions and calculations for dam overtopping affecting larger water body

Table 7.3: Predicted metal concentrations in downgradient larger water body due to dam overtopping.

COC	Water Quality Guideline[b] (µg/L)	Baseline Concentration[a] - Larger Water Body (µg/L)	Predicted COC Concentration in Larger Water Body (µg/L)	
			DW1[c]	DW2[d]
Copper	2	0.2-1.5	0.2-1.4	0.21-1.5
Lead	2	0.1-0.4	0.1-0.39	0.1-0.4
Nickel	8.3	<0.5	0.48-0.49	0.6-0.8
pH	NGA	NA	7.5-7.6	7.3-7.5

Notes:

a. ERA for proposed development

b. Water Quality Guideline: B.C. MOE, 2006

c. DW1: stream concentration due to overtopping of dam with neutralized decant water

d. DW2: stream concentration due to overtopping of dam with acidic decant water

NGA: no guideline available NA: not available

Exposure Calculation: The exposure parameters for swimming are summarized in Table 7.4 and CDI and LADD are calculated through equations (7.7) and (7.8). A range of values is provided where data are available along with the assumed parameter distributions. The assumptions made relating to the exposure parameters are provided in the footnotes of the Table 7.4. The concentration of COC's in the larger water body was determined for two sources both neutralized and acidic decant water (DW1 and DW2). As the calculated concentrations in the larger water body were similar for each case only one set of values were used as input for the exposure determinations. The exposure concentrations were approximately equal to that of the baseline concentrations.

Table 7.4: Exposure parameters for swimming in larger water body (dam overtopping)

Human Health Exposure Parameters	Distribution Description	Child (7-12years)	
		50 Percentile Values	5%-95% Confidence Limit
Chemical Concentration (CW) Lead (mg/L- water)	lognormal (1.5E-4,1.0E-4) shift(0.00006)	1.8E-04	1.0E-04 - 4.0E-04
Chemical Concentration (CW) Nickel (mg/L- water)	lognormal (1.0E-4,1.2E-4) shift(0.00005)	5.6E-04	5.0E-04 - 8.0E-04
Dermal Adsorption Dose (DA-event) Lead (mg/cm^2-event)	NA	6.0E-08	NA
Dermal Adsorption Dose (DA-event) Nickel (mg/cm^2-event)	NA	5.2E-04	NA
Exposure Frequency-swimming (EF) (days/year)	normal μ=15 σ=1.8	15	12-18
Exposure Duration-swimming (ED) (years)	constant	6	NA
Body Surface Area (SA) (cm^2)	constant	11300	NA
Event Frequency (EV) swimming (hr/day)	constant	1	NA
Fraction Absorbed (FA) (fraction)	constant	1	NA
Skin permeability coefficient lead in water (Kp) (cm/hr)	normal μ=4.0E-06 σ=5.0E-07	4.0E-06	3.2E-06- 4.8E-06
Skin permeability coefficient nickel in water (Kp) (cm/hr)	normal μ=1.0E-4 σ=1.3E-04	1.0E-04	0.8E-04- 1.2E-04
Body Weight (BW) (kg)	constant	32.9	NA
Averaging Time (AT) (days) -CDI	constant	1825	NA
Averaging Time (AT) (days) - LADD	constant	25550	NA
CDI Lead swimming (child) (mg/kg/day)		1.40E-11	
CDI Nickel swimming (child) (mg/kg/day)		1.20E-09	
LADD Lead swimming (child) (mg/kg/day)		9.70E-13	

Notes

EF-swimming: assume swimming 3 months/year, 1/week for each month= 15/year

(USEPA 1997: age: 5-11, 5/month 50% frequency)

ED-swimming: 6 years (USEPA)

EV: Exposure time swimming: 1 hour USEPA 1997, 50 percentile swimming fresh water pools.

FA: 1.0 assumed

BW -child: USEPA 1997, average weight age 7-12, 50 percentile of distribution

AT: 70 years for LADD= 25550 days

AT: 5x365 for CDI= 1825 days

NA: not applicable

CASE 2: Exposure through Ingestion and Dermal Absorption of Groundwater

Fig. 7.7 illustrates the migration of COC's from the disposal site to the receptor at a proposed industrial facility through the groundwater. SESOIL combined with AT123D, is used to predict the migration of the leachate plume from the base of the disposal site to the receptor for both subaerial and subaqueous disposal cases. Input for the code is provided in Fig. 7.8. Advective-dispersive transport can be described according to equations (7.14, 7.15 and 7.16) (Robertson, 1974 in Environmental Software Consultants Inc., 2006).

$$\frac{\partial C}{\partial t} = \nabla \bullet (\overline{\overline{K}} \bullet \nabla C) - \nabla \bullet \bar{U} C - \left(\frac{K}{R_d} + \lambda \right) C + \frac{\dot{M}}{n_e R_d} \qquad (7.14)$$

where:

$\dot{M}$ – Contaminant source release rate
C - Dissolved contaminant concentration
t - Time
$\overline{\overline{K}}$ - Retarded dispersion tensor
∇ - Gradient (wrt. x,y,z)
$\bar{U}$ - Retarded seepage velocity vector
K - Chemical degradation rate
R_d - Retardation factor
λ - Radioactive decay constant

$$R_d = 1 + \frac{\rho_b K_d}{n_e} \qquad (7.15)$$

$$\overline{\overline{K}} = \frac{\overline{\overline{D}}}{R_d} \qquad (7.16)$$

K_d - Distribution coefficient
η_e - Effective porosity
ρ_b - Bulk density of the soil
$\overline{\overline{D}}$ - Hydraulic dispersion coefficient tensor

Figure 7.7: Schematic of leachate migration from disposal site into groundwater

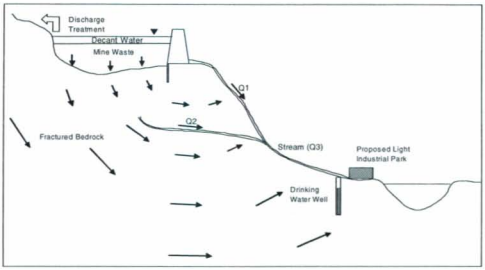

Assuming a hydraulic conductivity of the bedrock of 5.0E-06 m/s, the maximum concentration of contaminant in the plume reached the receptor (1200 m) in between 145-151 years depending on the metal and the initial concentration. If the hydraulic conductivity was reduced to 1.0E-6 m/s the maximum concentration in the plume arrived at 600 m in 289 years and using 1.0E-05 m/s the peak concentration reached the receptor in 60 years. The arrival time is very sensitive to the hydraulic conductivity or extent of fractures in the bedrock which will in turn affect the concentration of contaminants at the receptors.

Figure 7.8: Calculations and assumptions of leachate migration affecting groundwater quality

CASE 2: Groundwater Discharge Towards Well	
Assumptions	**Reference**
Bedrock permeability range = 5.0E-06 m/s	Assumed
Average gradient from disposal site to assumed well = 0.01	Typical
Distance from disposal site to assumed well = 1200 m	Typical
Longitundinal dispersivity= 100 m	Assumed
Tranverse dispersivity = 33 m	Assumed
retardation factor=1.0; retarded darcy velocity=7.2E-04	Assumed
soil density=1700 kg/m^3	Assumed
2-D advection, dispersion model no chemical interaction	
Calculations	
Employed SESOIL with AT123D	

Table 7.5: Predicted metal concentrations in groundwater due to leachate migration

COC	Water Quality Guideline (µg/L)	Background Concentration[a] (µg/L)	Baseline Concentration[a] (µg/L)	Predicted Groundwater Metal Concentration in Well (µg/L)	
				GW1[b]-subaerial	GW2[c]- subaqueous
Lead	1-7	<1	<0.5	1.3E-03-9.8E-03	1.3E-03-1.95E-03
Nickel	25	<1	<2-3.0	0.163-4.8	0.163-0.33

Notes:

a. ERA for proposed development

Water Quality Guideline: CCME, 2006 for lead and nickel

b. GW1: stream concentration due to metal migration from subaerial disposal

c. GW2: stream concentration due to metal migration from subaqueous disposal

Concentration of Metals in Groundwater due to Leachate Migration from Impoundment

A summary of the concentration of metals in the groundwater due to leachate migration from the base of the disposal site for both disposal cases is provided in Table 7.5 along with the water quality guideline, background and baseline concentration data.

Exposure parameters: The exposure parameters for ingestion (drinking water) and dermal absorption (showering) are summarized in Tables 7.6 and 7.7. Calculations for

CDI and LADD use equations (7.7), (7.8) and (7.9) for adsorption and ingestion. Although concentrations are below FAL guidelines CDI and LADD values are calculated in order to demonstrate this part of the study methodology.

Table 7.6: Exposure Parameters for Ingestion

Human Health Exposure Parameters	Distribution Description	Adult	
		50 Percentile Values	5%-95% Confidence Limit
Chemical Concentration (CW) Lead (mg/L- water) - subaerial	lognormal (4.0E-6,3.0E-6) shift(3.0E-07)	4.3E-06	1.3E-06- 9.8E-06
Chemical Concentration (CW) Nickel (mg/L- water) - subaerial	lognormal (1.6E-3,1.9E-3) shift(0.0)	1.6E-03	0.16E-3- 4.8E-03
Chemical Concentration (CW) Lead (mg/L- water) - subaqueous	lognormal (1.7E-7,3.0E-7) shift(1.35E-06)	1.5E-06	1.3E-06- 1.95E-06
Chemical Concentration (CW) Nickel (mg/L- water) - subaqueous	lognormal (2.4E-4,0.5E-4) shift(0.0)	2.4E-04	1.6E-04-3.26E-04
Intake Rate (IR or CR) (ml/kg bodyweight-day)	constant	34	NA
Fraction Ingested (FI) (fraction)	constant	1	NA
Gastrointestinal Absorption (ABS) (fraction)	normal μ=1.0 σ=0.1	1	0.9-1.1
Exposure Frequency (EF) (days/year)	constant	260	NA
Exposure Duration (ED) (years)	constant	39.8	NA
Body Weight (BW) (kg)	constant	70	NA
Averaging Time (AT) (days) - CDI	constant	10400	NA
Averaging Time (AT) (days) - LADD	constant	25550	NA
CDI Lead drinking water (adult) -subaerial (mg/kg/day)		1.4E-07	
CDI Nickel drinking water (adult) -subaerial (mg/kg/day)		5.4E-05	
LADD Lead drinking water (adult) -subaerial		5.5E-08	
CDI Lead drinking water (adult) -subaqueous (mg/kg/day)		5.8E-08	
CDI Nickel drinking water (adult) -subaqueous (mg/kg/day)		8.1E-06	
LADD Lead drinking water (adult) -subaqueous		2.3E-08	

Notes:
IR: USEPA, 1997: 90th percentile, 34ml/kg-day
FI: all water from well water
ED: total working hours (8hrs) and working lifetime of workers (39.8 yrs).
AT: 70 years 25550 days (LADD)
AT: 260*40= 10400 days (CDI)
BW: 70 Kg average male U.S. EPA 1997
NA: not applicable

Table 7.7: Exposure Parameters for Dermal Contact (showering –adult)

Human Health Exposure Parameters	Distribution Description	Adult	
		50 Percentile Values	5%-95% Confidence Limit
Chemical Concentration (CW) Lead (mg/L- water) - subaerial	lognormal (4.0E-6,3.0E-6) shift(3.0E-07)	4.3E-06	1.3E-06- 9.8E-06
Chemical Concentration (CW) Nickel (mg/L- water) - subaerial	lognormal (1.6E-3,1.9E-3) shift(0.0)	1.6E-03	0.16E-3- 4.8E-03
Chemical Concentration (CW) Lead (mg/L- water) - subaqueous	lognormal (1.7E-7,3.0E-7) shift(1.35E-06)	1.5E-06	1.3E-06- 1.95E-06
Chemical Concentration (CW) Nickel (mg/L- water) - subaqueous	lognormal (2.4E-4,0.5E-4) shift(0.0)	2.4E-04	1.6E-04-3.26E-04
Dermal Adsorption Dose (DA-event) Lead (mg/cm^2-event)	NA	1.6E-08	NA
Dermal Adsorption Dose (DA-event) Nickel (mg/cm^2-event)	NA	1.6E-04	NA
Exposure Frequency-showering (EF) (days/year)	normal μ=260 σ=26	260	217-303
Exposure Duration-showering (ED) (years)	constant	40	NA
Body Surface Area (SA) (cm^2)	constant	23,000	NA
Event Frequency (EV) showering (events/day)	constant	0.74	NA
Shower Duration (ED-dermal) (hr/event)	constant	0.1733	NA
Fraction Absorbed (FA) (fraction)	constant	1	NA
Skin permeability coefficient lead in water (Kp) (cm/hr)	normal μ=4E-06 σ=5E-07	4.0E-06	3.2E-06- 4.8E-06
Skin permeability coefficient nickel in water (Kp) (cm/hr)	normal μ=1E-04 σ=1.3E-05	1.0E-04	0.8E-04- 1.2E-04
Body Weight (BW) (kg)	constant	70	NA
Averaging Time (AT) (days) - CDI	constant	10400	NA
Averaging Time (AT) (days) - LADD	constant	25550	NA
CDI Lead showering (adult) - subaerial (mg/kg/day)		6.7E-13	
CDI Nickel showering (adult) - subaerial (mg/kg/day)		6.7E-09	
LADD Lead showering (adult) - subaerial		2.8E-13	
CDI Lead showering (adult) - subaqueous (mg/kg/day)		2.9E-13	
CDI Nickel showering (adult) - subaqueous (mg/kg/day)		1.0E-09	
LADD Lead showering (adult) - subaqueous		1.2E-13	

Notes

EV-showering: assume 0.74 /day (US DHUD, 1984).

AT: 70 years for LADD= 25550 days

AT: 40 years for CDI= 10400 days

ED-showering: 10.4 minutes (US DHUD, 1984)

FA: estimated at maximum

SA- adult= 95th percentile= 23000, 50th percentile=20,000

NA: not applicable

7.3.2.3 Human Health Risk Estimation

Using equations (7.10) and (7.11) values for HI and excess carcinogenic risk are derived for four options: 1) subaerial and lined; 2) subaqueous lined; 3) subaerial and unlined and 4) subaqueous and unlined (Table 7.8 and 7.9). For this exercise, the lined ponds are assumed to be leak proof. To account for variations in the dose response test results, RfD values for lead (0.0036 mg/kg bw/day) and nickel (0.02 mg/kg bw/day) (Table 7.2) and the SF_{lead} (2.0E-04 mg/kg/ bw-day $^{-1}$) were described by a normal distribution. The range values provided in Tables 7.10 and 7.11 are the 95% and 5% confidence limits of the CDF along with the 50% value of the CDF which are derived through Monte Carlo simulations with the code @RISK (Palisade Corporation, 1991). A sample plot of an HI CDF is provided in Fig. 7.9. In general, the disposal options in order of lowest HI and carcinogenic risk values to highest were: lined subaerial, lined subaqueous, unlined subaqueous and unlined subaerial. The highest HI values were for nickel ingestion at HI=2.7E-03 for subaerial and 4.1E-04 for subaqueous unlined cases. The excess carcinogenic risk values were higher for subaerial unlined disposal than subaqueous unlined. The highest carcinogenic risk value was that for ingestion of groundwater at 1.1E-11 in the subaerial unlined case.

Table 7.8: Hazard Indices for PCOC's lead and nickel and select disposal methods

Disposal Method	Exposure Route	HI		HI		Total HI
		Lead[a]	Distribution[b]	Nickel[a]	Distribution[b]	
Subaerial-lined	Assuming no leakage and no decant water	-		-		0
Subaqueous-lined	Swimming (Marine)	3.8E-09	1.8E-09-8.0E-09	5.1E-08	3.3E-08-7.5E-08	5.5E-08
Subaerial-unlined	Ingestion (groundwater)	3.8E-05	1.3E-05-9.5E-05	2.7E-03	0.3E-03-8.2E-03	2.7E-03
	Showering (groundwater)	1.9E-10	0.6E-10-4.8E-10	3.4E-07	0.46E-07-9.7E-07	
Subaqueous-unlined	Ingestion (groundwater)	1.6E-05	1.1E-05-2.0E-05	4.1E-04	2.7E-04-6.0E-04	4.3E-04
	Showering (groundwater)	8.0E-11	4.9E-11-10.3E-11	5.1E-08	3.0E-08-7.8E-08	
	Swimming (Marine)	3.8E-09	1.8E-09-8.0E-09	5.1E-08	3.3E-08-7.5E-08	

Notes: a) 50 percentile value, b) range 5-95 percentile

Table 7.9: Carcinogenic Risk for COC's lead and nickel and select disposal methods

Disposal Method	Exposure Route	Carcinogenic Risk (lead)[a]	Distribution[b]	Total Carcinogenic Risk (lead)
Subaerial- lined	Assuming no leakage and no decant water	0.0E+00	-	0.0E+00
Subaqueous-lined	Swimming (Marine)	1.9E-16	0.92E-16-3.9E-16	1.9E-16
Subaerial-unlined	Ingestion (Groundwater)	1.1E-11	0.35E-11-2.8E-11	1.1E-11
	Showering (Groundwater)	5.5E-17	1.7E-17-13.0E-17	
Subaqueous-unlined	Ingestion (Groundwater)	4.7E-12	3.1E-12-5.6E-12	4.7E-12
	Showering (Groundwater)	2.4E-17	1.6E-17-3.4E-17	
	Swimming (Marine)	1.9E-16	0.92E-16-3.9E-16	

Notes: a) 50 percentile, b) range 5-95 percentile

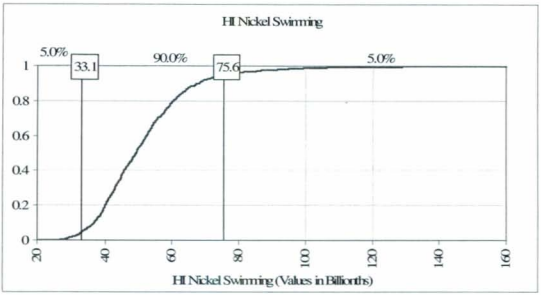

Figure 7.9: CDF of HI for nickel with swimming pathway

7.3.2.4 Uncertainty in Human Health Risk Assessment

The uncertainty associated with select parameters in this assessment is shown for each pathway in Table 7.9. The spearman rank was used to evaluate the contribution these parameters. From these results the PCOC concentration (CW) is the most dominant factor for most of the lead and nickel exposures for HI and carcinogenic risk for all three pathways. The exceptions were: Kp (skin absorption rate) and showering; ABS and SF for carcinogenic risk from ingestion. For HI CW was the dominant factor except Kp and swimming for nickel; and Kp and showering for lead.

There has not been an attempt made to address uncertainty in all the exposure parameters. Examples of a few other influences on results include: site location; waste type; bedrock type, permeability and fracturing; subsurface and surface water chemical reactions; and liner permeability.

Table 7.10: Spearman rank of select HI and Carcinogenic Risk parameters

Pathway	Parameter	HI				Excess Carcinogenic Risk	
		Lead		Nickel		Lead	
		SAR[a]	SAQ[b]	SAR[a]	SAQ[b]	SAR[a]	SAQ[b]
Swimming	EF	0.24	NA	0.47	NA	0.24	NA
	KD	0.23	NA	0.51	NA	0.23	NA
	CW	0.88	NA	0.48	NA	0.87	NA
	RfD/SF	-0.19	NA	-0.38	NA	0.17	NA
Ingestion	CW	0.97	0.57	0.99	0.8	0.97	0.49
	ABS	0.22	0.48	0.1	0.36	0.1	0.54
	RfD/SF	-0.15	-0.55	-0.1	-0.40	0.19	0.54
Showering	EF	0.15	0.47	0.1	0.35	0.16	0.47
	KD	0.21	0.58	0.17	0.4	0.21	0.57
	CW	0.95	0.37	0.98	0.69	0.95	0.37
	RfD/SF	-0.2	-0.44	-0.14	-0.35	0.13	0.45

Notes:
a) SAR: Subaerial disposal method,
b) SAQ: Subaqueous disposal method
NA: Not Applicable

7.3.3 Ecological Risk Assessment

7.3.3.1 COPEC Identification and Characterization

For this study the COPEC concentration in the downgradient stream are derived from two sources the decant water through dam overtopping and mine waste leachate through groundwater migration. Details of these calculations are provided in the following section. The predicted metal concentration in the downgradient larger water body was considered under the human health risk assessment for the site (Section 7.3.2).

For this work rainbow trout and brook trout were selected as the VEC's for the freshwater environment. TRV was determined as described in Section 7.2.2.2. NOEC

data from the U.S. EPA ECOTOX database (U.S. EPA, 2006) for the aquatic species and metal speciation of interest was selected and plotted as a probability density function. From the cumulative density function (Fig. 7.10) the 5 percentile exceedance value is derived for the species and metal as shown in Table 7.11 with CCME guidelines. The estimated TRV was selected from the lower of that determined from NOEC values and the CCME FAL guideline and is provided in Table 7.11.

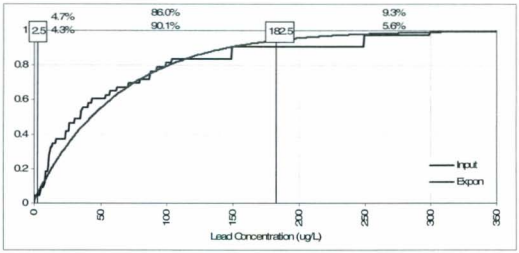

Figure 7.10: Example CDF plot for lead effects on rainbow and brown trout

Table 7.11: Summary of ECOTOX Data and CCME guidelines on COPEC's for Aquatic Receptors

COC	CCME FAL[b] guideline (µg/L)	CCME MAL[b] Guideline (µg/L)	Estimated 5% exceedance of NOEC values[a] (µg/L)	Estimated TRV[a] (µg/L)
Cu	2.0	2	2.5	2.0
Ni	25	8.3	10	10
Pb	1.0	2	2.5	1.0
pH	6.5-9	NA	NA	NA

Notes: a) for freshwater trout
b) CCME, 2006
NA- not applicable

7.3.3.2 Ecological Transport Modeling of COPECs

CASE 1a): Exposure through Surface Water Contamination – Dam Overtopping

Fig. 7.5 illustrates the overtopping of the decant water into a downgradient stream. The assumptions and calculations for the concentration of COPEC in the stream are provided in Fig. 7.11.

Figure 7.11: Calculations and assumptions of dam overtopping into downgradient Stream

CASE 1a): Dam Overtopping into Downgradient Stream

Assumptions

Flow in stream= 0.1-0.2 m^3/s, peak 0.7m^3/s (typical)

Shape of streambed: depth=0.25m, width= 4.0m, length 2000m (typical)

Surface area of impoundment = 50 hectares (500000 m^2) (typical)

Depth of decant water= 1.0 m

Complete mixing

Calculations (using data above)

Volume of water along length of Stream at any one time (V1) = 0.25m*4m*2000m= 2000m^3

If average elev. of water is 0.01 m above dam when it overtops water released (V2) = 0.01*500000m2=5000m^3

Ratio of released overtopping water volume to water volume in Stream = 5000m^3/2000m^3 = 2.5 or 250%

If average elev. of water is 0.05 m above dam when it overtops water released (V2) = 0.05*500000m^2=25000m^3

Ratio of released overtopping water volume to water volume in Stream = 25000m3/2000m3 = 12.5 or 1250%

Overtopping Volume as a percent of Stream volume = 250% - 1250%

$V_1C_1+V_2C_2 = V_TC_T$ where V_T = volume of water in stream when overtopping occurs (V_1+V_2)

C_1, C_2, C_T = concentration of metals in Stream (C_1), decant water (C_2) and stream with overtopping (C_T)

$C_T = (V_1C_1+V_2C_2)/(V_1+V_2)$

CASE 1b): Exposure through Surface Water Contamination – Groundwater Migration

As indicated previously, when leachate migrates through the mine waste and base of the impoundment into the groundwater in the bedrock, the regional groundwater flow system will disperse and transport the leachate in the direction of groundwater flow (see Fig. 7.7). For this case study, groundwater is a major contributor to the discharge volume of the downgradient stream. As leachate from the base of the impoundment enters the groundwater it subsequently contributes to the base-flow of the stream. The COPEC concentration in the stream due to leachate in the groundwater is determined based on the contribution of baseflow to the overall stream discharge (see Fig. 7.12).

Figure 7.12: Assumptions and calculations for groundwater flow contribution to Stream

CASE 1b) Contaminated Groundwater as Baseflow for Stream
Assumptions
Stream average discharge (Q3) = 0.1-0.2 m^3/s (typical)
1/3 stream flow from confluent stream
Stream average discharge above confluent stream (Q1) = 2/3*average discharge= 0.067-0.133 m^3/s
Stream baseflow (from stream hydrograph) = 0.05 m^3/s
Assume lower average stream discharge (Q1)= 0.067 m^3/s (worse case scenario)
Estimated stream baseflow above confluent stream = 0.0335 m^3/s
Assume 100% of baseflow from groundwater from immediately below disposal site (worse case scenario)
Complete mixing
Calculations
Q1C1+Q2C2 = Q3C3; C3= (Q1C1+Q2C2)/Q3
Baseflow as % of Stream Discharge = [0.05 m^3/s/(0.133m^3/s)]*100 to [0.05 m^3/s/ (0.067m^3/s)]*100 = 38% to 75%

A summary of the concentration of COPECs in the Stream due to dam overtopping and leachate migration from the base of the impoundment is provided in Table 7.12 along with the water quality guideline and groundwater baseline concentration data. Predicted average copper, nickel and lead concentrations in the stream due to dam overtopping

(with decant water neutralized and not neutralized) and leachate migration (for the subaerial and subaqueous case) exceed the CCME water quality guidelines and ER is greater than 1.0. The pH measurement for the cases of: DW2 (not neutralized) and GW-1 (subaerial) had pH ranges outside that of CCME guideline for freshwater aquatic life. Copper, nickel, lead and pH are brought forward for further assessment for freshwater aquatic life.

Table 7.12: Predicted metal concentrations in Stream due to dam overtopping and leachate migration

COC	Water Quality Guideline (µg/L)	Background Concentration[a] (µg/L)	Baseline Concentration[a] (µg/L)	Predicted Stream Metal Concentration from Various Sources (µg/L)			
				Dam Overtopping		Leachate Migration	
				DW1- neutralized	DW2- not neutralized	GW1- subaerial	GW2- subaqueous
Copper	2	<1-2 (1.1)	<1-14 (2.1)	7.6-110 (35)	360-920 (540)	6.8-370 (95)	3.4-19 (9)
Lead	1	<1	<1-10 (1.75)	1.5-1.7 (1.6)	1.5-21 (6.8)	0.74-6.0 (2.3)	0.74-1.74 (1.2)
Nickel	25	<1	<1-3 (1.2)	23-190 (65)	2300-4200 (3150)	69-2500 (550)	8.6-190 (53)
pH	6.5-9	NA	5.74	6.8-8.7	3.5-4.7	4.9-5.2	6.9-7.1

Notes:
a. ERA for facility
Water Quality Guideline: CCME, 2006 for copper, lead and nickel
DW1: stream concentration due to overtopping of dam with neutralized surface water
DW2: stream concentration due to overtopping of dam with acidic surface water
GW1: stream concentration due to metal migration from subaerial disposal
GW2: stream concentration due to metal migration from subaqueous disposal
(50 percentile value)
NA: Not available

CASE 2: Exposure in Larger Water Body - Dam Overtopping

The concentration of metals in the larger water body was derived previously (see Figs. 7.5 and 7.6, Table 7.3). As is evident from Table 7.3 the predicted concentrations for

copper, lead and nickel are below CCME marine water quality guidelines therefore ER is less than 1.0 and the concentrations are very close to the baseline concentrations in the larger body of water therefore these specific COPEC's, pathway and receptor are not considered further in this ecological risk assessment.

7.3.3.3 Risk Estimation and Uncertainty: Ecological

Using equations (7.12) and (7.13) values for ER and total ER are derived for the four disposal options: subaerial and subaqueous lined and unlined disposal options (Table 7.13). To consider the uncertainty associated with the predicted stream COPEC concentrations each COPEC concentration range in Table 7.12 is described using the 95 % and 5 % confidence limits of the CDF lognormal distribution. The TRV values are also described using a normal distribution. A sample plot of the ER CDF is provided in Fig. 7.13. The 50 percentile exposure ratios for rainbow trout and COPEC's copper, nickel and lead are derived using these distributions (Table 7.13) for each of the four disposal methods. In general, the disposal options in order of lowest ER values to highest for the COPEC's and pathways selected are: lined subaerial, unlined subaerial, lined subaqueous and unlined subaqueous. The ER values were above 1.0 for each scenario, COPEC and both pathways except the lined subaerial. The highest ER values are for the COPEC's copper and nickel, the pathway dam overtopping with non-neutralized decant water. The third highest ER value was with the COPEC nickel with subaerial disposal and contaminated groundwater. The cases of dam overtopping with non-neutralized decant water and groundwater contamination with subaerial disposal both predicted pH values that are outside the range of the CCME FAL guidelines and

baseline pH values. It is expected that both of these scenarios will have negative effects on aquatic freshwater life in the downgradient stream. For this ecological risk assessment uncertainty associated with specific model parameters is not determined.

Table 7.13: Exposure ratios for COEPC's and rainbow trout

Disposal Method	Exposure Route	ER (50 Percentile Value)			ER	Total ER
		Copper	Nickel	Lead	pH	
Subaerial-unlined	Groundwater - GW1	50	55	2.3	>1.0	107
Subaqueous-unlined	Dam Overtopping- DW1	18	6.5	1.6	<1.0	37; 598
	Dam Overtopping- DW2	265	315	6.75	>1.0	
	Groundwater - GW2	4.4	5.3	1.2	<1.0	
Subaerial- lined	No leakage and no decant water	0	0	0	<1.0	0
Subaqueous-lined	Dam Overtopping- DW1	18	6.5	1.6	<1.0	26; 587
	Dam Overtopping- DW2	265	315	6.75	>1.0	

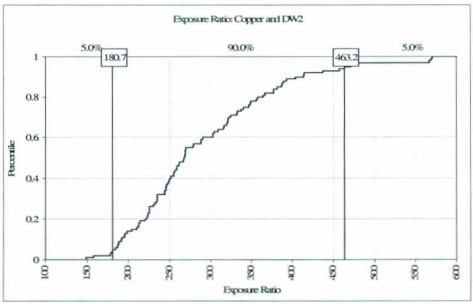

Figure 7.13: CDF of Exposure Ratio for Copper in Stream due to Dam Overtopping

7.4 MULTI-CRITERIA RISK-BASED DECISION MAKING

The decision hierarchy for this case was already provided in Fig. 7.4. Using the AHP methodology for optimization seven alternative matrices, two pair-wise matrices, one goal matrix and a synthesis matrix were developed. Examples of the matrices along with the synthesis matrix are provided (Tables 7.14-7.16) and in entirety in Appendix V. The values (1-9) and reciprocals used to compare the alternatives are based on the authors judgment and used mainly for illustration purposes. From the results of the synthesis matrix which includes all decision criteria, the order of preference for disposal methods from highest to lowest is: lined subaqueous, lined subaerial, unlined subaqueous, unlined subaerial.

Table 7.14: Containment Effectiveness Matrix

	Unlined Subaerial	**Lined Subaerial**	**Unlined Subaqueous**	**Lined Subaqueous**	**Priorities**
Unlined Subaerial	1.000	0.143	1.000	0.143	0.066
Lined Subaerial	7.000	1.000	5.000	1.000	0.404
Unlined Subaqueous	1.000	0.200	1.000	0.143	0.068
Lined Subaqueous	7.000	1.000	7.000	1.000	0.462

Table 7.15: Decision Goal Matrix

	Human Health Risk	**Ecological Risk**	**Cost**	**Containment Effectiveness**	**Ecological Footprint**	**Priorities**
Human Health Risk	1.000	2.000	3.000	2.000	2.000	0.347
Ecological Risk	0.500	1.000	2.000	1.000	2.000	0.225
Cost	0.333	0.500	1.000	0.500	0.500	0.098
Containment Effectiveness	0.500	1.000	0.500	1.000	2.000	0.173
Ecological Footprint	0.500	0.500	2.000	0.500	1.000	0.156

Table 7.16: Synthesis matrix for optimal mine waste disposal method

	Human Health Risk		Cost		Ecological Risk	Containment Effectiveness	Ecological Footprint	Overall Priority
	0.347		0.098		0.225	0.173	0.156	
Disposal Options	Carcinogenic risk	carcinogenic risk	Construction cost	Maintenance Cost				
	0.667	0.333	0.167	0.833				
Unlined Subaerial	0.088	0.088	0.532	0.063	0.055	0.066	0.062	0.078
Lined Subaerial	0.213	0.213	0.099	0.250	0.166	0.404	0.205	0.235
Unlined Subaqueous	0.153	0.153	0.297	0.143	0.201	0.068	0.139	0.148
Lined Subaqueous	0.546	0.546	0.071	0.545	0.578	0.462	0.594	0.538

7.5 CONCLUSIONS

The risk-based approach to decision making was used to employed disposal options for typical mine waste and provided effective decision making. Mine waste characterization data and contaminant fate and transport modeling to predict exposure to potential receptors. A probabilistic approach permitted estimation of the risk to the receptors based on different mine waste disposal options. Multi-criteria risk-based decision making, which integrates risk assessment with other disposal criteria, was used to determine the optimal disposal option.

It is interesting to note, three different disposal priority rankings were determined for the four disposal options depending on whether the ranking was based on human health risk, ecological risk or the multi-criteria decision making process. The ecological risk had a different disposal ranking than the human health risk; due to the inclusion of risk to the VEC's in the Stream and the dominant effect of the non-neutralized decant water.

According to the predicted ER values for the Stream, the VEC's would be affected both by leachate migration and dam overtopping. The metals and the pH would negatively affect the Stream VEC's. For this case study, in order to protect the stream it would be important to eliminate leachate migration from the impoundment. With subaerial disposal there is no risk of dam overtopping thus one less factor contributing to the total risk. Although not considered, it is anticipated that any subaerial disposal site will require a cover to protect the local environment from air transport of the waste. For this case study, leachate migration was not predicted to cause a significant risk for users of a downgradient well thus also not for exposures to the larger water body further from the source. The actual ranking of disposal options is site and waste specific and can incorporate additional factors and decision criteria.

When considering uncertainty with the Spearman ranking, the COC concentration was the most dominant parameter in modeling HI or excess cancer risk for this case study. This was in part due to the wide range associated with the assumed concentration. As indicated previously there are many other parameters that deserve more detailed consideration or preliminary consideration when evaluating disposal methods. They could include but are not limited to: bedrock type, permeability and fracturing; site location; waste characteristics; subsurface and surface water chemical reactions; leakage and degradation rate and type of liner system; and modeling of COC transport. The results from the risk assessment were integrated with other criteria in the MCDM analysis. For this case study, human health risk and ecological risk had the highest score of the five decision criteria. This analysis helped to demonstrate the significance of these

risks and the corresponding importance of the longterm integrity of the disposal site on the selection of an optimal waste disposal method.

7.6 REFERENCES

ACGIH. (2009). *TLVs and BEIs Threshold Limit Values for Chemical Substances and Physical Agents and Biological Exposure Indicies*. American Conference of Government and Industrial Hygienists Inc. Cincinnnati, OH.

Ambrose, A.M. Larson, P.S., Borzelleca, J.R., Hennigar, G.R. (1976). Long-term toxicological assessment of Ni in rates and dogs. *Journal of Food Science Technology*, 13, 181-187.

Asante-Duah, D. K. (1993). *Hazardous Waste Risk Assessment*, Florida: Lewis Publishers, CRC Press.

ASTDR (Agency for Toxic Substances and Disease Registry) (2004). *Toxicological Profile for Copper*, U.S. Department of Health and Human Services, Retrieved January 5, 2009, from http://www.atsdr.cdc.gov/toxprofiles/tp132.pdf.

B.C. MOE (2006). *British Columbia Approved Water Quality Guidelines*. Science and Information Branch. Ministry of Environment. Retrieved January 5, 2009, from http://www.waterquality.ec.gc.ca/EN/navigation/3297/3300/3305.htm .

Barnthouse, L. W., Suter, G. W. (1986). *User's manual for ecological risk assessment*. Prepared for U.S. EPA, Office of Research and Development, Oak Ridge, TN: Oak Ridge National Laboratory.

Beansland, G.E., Duinker, P.N. (1983). *An ecological framework for ecological Risk Assessment in Canada. Institute for Research and Environmental Studies*, Federal Environmental Assessment Review Office., Halifax, NS.

Bonano, E.J., Apostolakis, G.E., Salter, P. F., Ghassemi, A., Jennings, S. (2000). Application of risk assessment and decision analysis to the evaluation, ranking and selection of environmental remediation alternatives. *Journal of Hazardous Materials*,71(1-3), 35-57.

Burns, L.A. (1991). *PIRANHA Pesticide and Industrial Chemical Risk Analysis and Hazard Assessment*. Ver. 2.0, U.S. EPA, Environmental Research Laboratory, Office of Research and Development, Athens, GA.

CCME (Canadian Council of Ministers of the Environment) (1996). *A Framework for Ecological Risk Assessment: General Guidance.* Winnipeg, Canada: CCME Subcommittee on Environmental Quality Criteria for Contaminated Sites, The National Contaminated Sites Remediation Program, Winnipeg, MB. PN1195.

CCME (1997). *A framework for Ecological Risk Assessment: Technical Appendices.* Winnipeg, Canada: CCME Subcommittee on Environmental Quality Criteria for Contaminated Sites.

CCME (1999). Canadian soil quality guidelines for the protection of environmental and human health: In *Canadian Environmental Quality Guidelines, 1999.* Canadian Ministers of the Environment, Winnipeg, MB.

CCME (2003). Canadian water quality guidelines for the protection of aquatic life: In *Canadian Environmental Quality Guidelines, 1999,* Canadian Ministers of the Environment, Winnipeg, MB.

CCME (2006). *Canadian Environmental Quality Guidelines, Summary Table – Update 2006.* Retrieved September 15, 2008, from http://www.ccme.ca/assets/pdf/e1_06.pdf.

Dehling, H., Gottschalk, T., Hoffman, A. (2007). *Stochastic Modelling in Process Technology.* Elsevier, Amsterdam, NL, pp279.

Environmental Software Consultants Inc. (2006). *SEVIEW: Integrated Contaminant Transport and Fate Modeling System: User's Guide Version 6.3, January 2006.* Madison Wisconsin. USA.

Fordham, C. L., Regan, D. P. (1991). Pathways analysis method for estimating water and sediment criteria at hazardous waste sites. *Environmental Toxicology and Chemistry,* 10, 949.

Hammonds, J.S, Hoffman, F.O., Bartell, S.M. (1994). *An introductory guide to uncertainty analysis in environmental and health risk assessment.* Dec. 1994., SENES Oak Ridge Inc., Oak Ridge National Laboratory, Oak Ridge, Tennessee, USA, 34pgs.

Health Canada (2004). *Lead Information Package,* Retrieved January 15, 2009, from http://www.hc-sc.gc.ca/ewh-semt/contaminants/lead-plomb/exposure-exposition-eng.php#a37.

Health Canada (2006). *Copper Technical Document,* Retrieved January 15, 2009, from http://www.hc-sc.gc.ca/ewh-semt/pubs/water-eau/copper-cuivre/index-eng.php.

Ibrahim, M. K., Kaluarachchi, J. J. (2003). Multi-criteria analysis with probabilistic risk assessment for the management of contaminated ground water. *Environmental Impact Assessment Review*, 23, 683-721.

IARC (International Agency for Research on Cancer) (2006). *Monographs on the Evaluation of Carcinogenic Risks to Humans.* Vol. 87 (2006) (Inorganic and Organic Lead Compounds), 506pp., Retrieved from, http://monographs.iarc.fr/ENG/Monographs/vol87/index.php retrieved 01/05/09.

Kangas, A., Kangas, J., Pykalainen, J. (2001). Outranking methods as tools in strategic natural resource planning. *Silva Fennica*, 35(2), 215-227.

Khan, F. I., Husain, T. (2003). Evaluation of a petroleum hydrocarbon contaminated site for natural attenuation using 'RBMNA' methodology. *Journal of Environmental Modelling and Software*, 18, 179-194.

LaGrega, M.D., Buckingham, P. L., Evans, J.C. (1994). *Hazardous Waste Management.* New York, McGraw-Hill Inc.

Liu, I., Huang, G. H., Hao, R. X., Cheng, S. Y. (2004). An integrated subsurface modeling risk assessment approach for managing the petroleum-contaminated sites. *Journal of Environmental Sciences and Health*, A39, 11, 3083-3113.

Maxwell, R. M., Carle, S. F., Tompson, A. F. (2003). *Contamination, Risk, and heterogeneity: On the Effectiveness of Aquifer Remediation.* Geosciences and Environmental Technologies Division, Lawrence Livermore National Laboratory.

Nitzche, O., Meinrath, G., Merkel, B. (2000). Database uncertainty as a limiting factor in reactive transport prognosis. *Journal of Contaminant Hydrology*, 44, 223-237.

Palisade Corporation. (1991). *@RISK Analysis and Simulation Add-in for Microsoft Excel: User's Guide.* Newfield, New York. USA.

Proctor, D. M., Shay, E. C., Fehling, K. A., Brent, L. F. (2002). Assessment of human health and ecological risks posed by the uses of steel-industry slags in the environment. *Journal of Human and Ecological Risk Assessment*, 8(4), 681-711.

RAIS. (2007). Risk Assessment Information System. Chemical Specific Factors, Oak Ridge National Laboratory. Retrieved January 5, 2009 from, http://rais.ornal.gov.

Robertson, J.B. (1974). *Digital modeling of radioactive and chemical waste transport in the Snake River Plain Aquifer at the National Reactor Testing Station, Idaho.* U.S.G.S., Open-File report IDO-22054.

Saaty,T. (1980). Decision making with analytic hierarchy process. *International Journal Services Sciences*, 1, 1, 83-98.

Sadiq, R., Husain, T., Veithch, B., Bose, N. (2004). Risk-based decision-making for drilling waste discharges using a fuzzy logic synthetic evaluation technique. *Ocean Engineering*, 31, 1929-1953.

Schmoldt, D., Kangas, J., Mendoza, G.A, (2001). Basic principles of decision making in natural resources and the environment, In Schmoldt et al (Eds.) *The Analytic Hierarchy in Natural Resource an Environmental Decision Making*, 1-13, Kluwer Academic Publishers, Netherlands.

Sobek, A. A., Schuller, W. A., Freeman, J. R., Smith, R. M. (1978). *Field and Laboratory Methods Applicable to Overburdens and Minesoils*. U.S. EPA 600/2-78-054. Washington, DC.

Swartjes, F. A. (1999). Risk-based assessment of soil and groundwater quality in the Netherlands: standards and remediation urgency. *Risk Analysis*, 19(6), 1235-1249.

U.S. Environmental Protection Agency (EPA) (1987). *Quality Criteria for Water, Update#2, May 1987*, Office of Water Regulation and Standard, Washington D.C. EPA440/5-98-001.

U.S. EPA (1988) *Superfund exposure assessment manual*. Office of Emergency and Remedial Measures Response, Washington, D.C., EPA/540/1-88/001.

U.S. EPA (1989a). *Risk assessment guidance for Superfund. Vol1, Human health evaluation manual (Part A)*. Office of Emergency and Remedial Measures Response, Washington, D.C., EPA/540/1-89/002

U.S. EPA (1989b). *Risk assessment guidance for Superfund. Vol2, Environmental evaluation manual (Part A)*. Office of Emergency and Remedial Measures Response, Washington, D.C., EPA/540/1-89/001.

U.S. EPA (1991). Nickel Soluble Salts, Lead and Copper (CASRN Various). *United States Environmental Protection Agency Integrated Risk Information System*. Retrieved January 5, 2009, from http://www.epa.gov/iris/subst/0271.htm.

U.S. EPA (1992a). *Dermal Exposure Assessment: Principles and Applications, Interim Report January1992*, Office of Health and Environmental Assessment, EPA/600/8-91/011B, 389pgs.

U.S. EPA (1992b). *Framework for Ecological Risk Assessment,* Risk Assessment Forum, Feb 1992, Washington, D.C. EPA/630/R-92/001

U.S. EPA (1993). Reference Dose (RfD): Description and Use in Risk Assessments, Background Document 1A, March 15, 1993. Retrieved January 10, 2009 from http://www.epa.gov/iris/rfd.htm.

U.S. EPA (1997). *Exposure Factors Handbook*. Retrieved January 5, 2009, from http://cfpub.epa.gov/ncea/cfm/recordisplay.cfm?deid=12464.

U.S. EPA (1998). *Guidelines for Ecological Risk Assessment*. EPA/630/R-95/002F. Risk Assessment Forum, U.S. Environmental Protection Agency, Washington, D.C.

U.S. EPA (2005). *Guidelines for Carcinogenic Risk Assessment*. EPA/630/P-03/001F, March 2005, Risk Assessment Forum, U.S. Environmental Protection Agency, Washington D.C.

U.S. EPA (2006). *U.S. Environmental Protection Agency ECOTOX database*. Retrieved January 5, 2009, from http://cfpub.epa.gov/ecotox/.

U.S. EPA (2007). *Framework for Metals Risk Assessment*. Office of the Science Advisor, Risk Assessment Forum, U.S. Environmental Protection Agency, Washington, D.C., EPA 120/R-07/001. March 2007.

U.S. EPA (2009). *National Primary Drinking Water Regulation, EPA816-F-09-004, May, 2009*. Retrieved July, 2009, from http://www.epa.gov/safewater/consumer/pdf/mcl.pdf.

U.S. DHUD. (1984). *Residential Water Conservation Projects: Summary report*. Report Number HUD-PDR-903. Washington, DC: U.S. Department of Housing and Urban Development, Office of Policy Development and Research.

Volosin, J. S., Cardwell, R. D., Wisdom. C. S. (1997). Use of risk assessment in the remediation of acid rock drainage, In *Proceedings of the Fourth International Conference on Acid Rock Drainage (ICARD)*, (May 31-June 6, 1997 Vancouver, B.C.). MEND Secretariat CANMET, Ottawa, Ontario.

Yeh, G.T., Trussel, H., Hoopes, J. (1987). *AT123D: Analytical transient one, two and three dimensional simulation of waste transport in the aquifer system*. Wisconsin Department of Natural Resources.

CHAPTER 8

HUMIDITY CELL, WEATHERING AND STATIC TESTS

8.1 INTRODUCTION

In this chapter results are provided from two kinetic tests and two static tests conducted on the residues from the VINL hydrometallurgical plant. The static tests include the ABA analysis and TCLP analysis both explained in Chapter 2. The kinetic tests, the humidity cell experiment and field weathering tests, are also described briefly in Chapter 2. Each test methodology and results is presented separately.

8.2 HUMIDITY CELL TEST

The humidity cell test simulates weathering conditions through control of air, temperature and moisture. It is a widely accepted method in Canada and the United States and results tend to compare favorably with field and other prediction tests. The tests take a long time to complete are high cost and result interpretation can be complex. Other tests that will compliment the humidity cell experiments are oxidizing batch tests, sequential extractions (Steel et al., 2009b; Chapter 3) and field weathering tests (Section 8.3).

Humidity cell tests last approximately 12 months are conducted to assess drainage chemistry. Leached oxidation products in solution are analyzed to calculate mass load, rates of acid generation and sulfide oxidation and the concentration of metals and other species as a function of time (breakthrough curves). Results are generally presented graphically. The cell usually holds approximately 1 kg of sample.

8.2.1 Humidity Cell Test Methodology

As indicated in the ASTM procedure, "this accelerated weathering test method is designed to increase the geological-chemical-weathering rate for selected 1000-g solid material samples and produce a weekly effluent that can be characterized for solubilized weathering products. This test method is performed on each sample in a cylindrical cell. Multiple cells can be arranged in parallel; this configuration permits the simultaneous testing of different solid material samples. The test procedure calls for weekly cycles comprised of three days of dry air (less than 10% relative humidity) and three days of water-saturated air (approximately 95% relative humidity) pumped up through the sample, followed by a leach with water on Day 7. A test duration of 20 weeks is recommended. The purpose of this accelerated weathering procedure is to determine the following: (*1*) whether a solid material will produce an acidic, alkaline, or neutral effluent, (*2*) whether that effluent will contain diagnostic cations (including trace metals) and anions that represent solubilized weathering products formed during a specified period of time, and (*3*) the rate at which these diagnostic cations and anions will be released (from the solids in the effluent) under the closely controlled conditions of the test" (ASTM, 2001).

The specific test conditions for the Memorial University humidity cell experiments are provided in Table 8.1. The drainage analysis includes: pH, conductivity, redox, acidity, alkalinity, metals, sulfide, sulfate and thiosalts. Four tests cells are set up, one containing each of the following: Neutralized Combined Residue (NCR), Neutralized Leach Residue

(NLR), Neutralized Gypsum Residue (NGR) and submerged NCR. Fig. 8.1 shows the experimental set-up.

Figure 8.1: Humidity cell set-up with humidifier and NLR, NGR and NCR cells

Table 8.1: Test conditions for humidity cell experiments

Test Parameter	After ASTM D5744-96 and Morin &Hutt (1997)
Particle Size	<6.3 mm
Sample Size	1 kg
Cell Diameter	20.3
Cell Length	10.2
Temperature	25 C
Humidity	controlled
Airflow rate	1-10 L/min
Dry air cycle	<10% RH for 3 days over sample
Wet air cycle	95% RH for 3 days over sample
Leachate Volume	500mL
Contact time	4 hours, stirred for 1 minute
Test duration	40 weeks or more
Cell contents	NCR, NLR and NGR

The standard (ASTM, 2001) humidity cell set-up and test procedure was modified in several ways to account for the fact that the material being tested is very fine grained. The following test modifications were made some of which were recommended by Morin and Hutt (1997, 2000) in their testing of mine tailings.

- The dry and moist air is directed over the surface of the residue due to the low porosity and permeability of the residues.
- When the leach water was added it was added all at once and stirred with the top 1 cm of the residue. This action prevented water from infiltrating cracks developed on the residue surface.
- A separatory funnel was not used in applying the leach water.
- The leach water applied was left to stand for four hours before permitting drainage out of the bottom of each cell.

8.2.2 Humidity Cell Test Results and Discussion

The graphs in Fig. 8.2 through 8.4 present the results of the experiment for the three residues. The release rates of sulfur for the residues are provided in Table 8.2.

Table 8.2: Total sulfur release rates for residues from humidity cells tests

Residue	4-10 Weeks (mg Sulfur/week)	17-31 Weeks (mg Sulfur/week)	38-43 Weeks (mg Sulfur/week)
NLR	147	113	203
NGR	195	240	350
NCR	328	220	230

To determine release rates of cations or sulfur first, weekly loads are calculated (equation (8.1)) then the cumulative load is determined (equation (8.2)) and finally the slope of the cumulative curve is calculated (equation (8.3)).

$$L_e = (C_e \times V_e) \qquad (8.1)$$

Where:

L_e - Loading constituent of interest in the effluent (mg)

C_e - Concentration of the constituent in the effluent (mg/L)

V_e - Litres of the weekly collected effluent (L)

$$L_n = \sum_{i=0}^{n} (C_i \times V_i) \qquad (8.2)$$

$$R_n = \frac{(L_{n2} - L_{n1})}{(n_2 - n_1)} \qquad (8.3)$$

R_n - Release rate of constituent for n weeks between and including the inflection points, mg/g/week.

L_{n2} , L_{n1} - Constituent cumulative load, the final and initial week of n weeks.

n_2 , n_1 - Final week and initial week of n weeks.

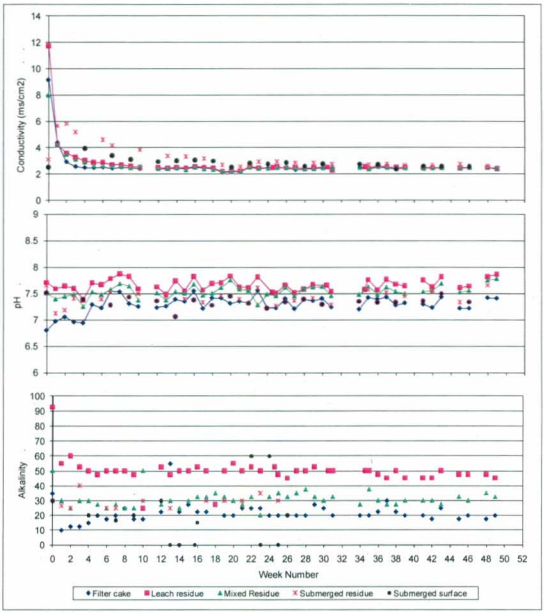

Note: Alkalinity in mg/L $CaCO_3$

Figure 8.2: Conductivity, pH and alkalinity results on leachate from humidity cell tests on residue samples

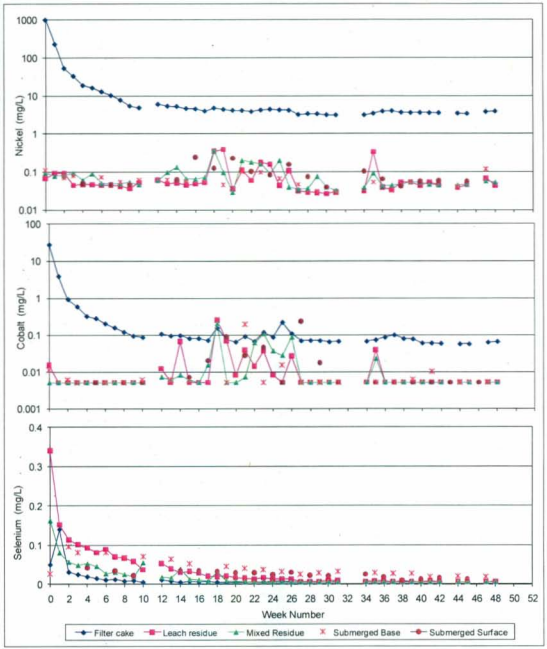

Figure 8.3: Nickel, cobalt and selenium concentrations on leachate from humidity cell tests on residue samples.

Figure 8.4: Total sulfur and cumulative sulfur in leachate from humidity cells tests.

8.3 FIELD WEATHERING TESTS ON NGR AND NLR

8.3.1 Field Weathering Test Methodology

Samples were taken from the test cells at the Argentia demonstration plant to consider the change in metal concentration through the depth of the deposit and the change in metal concentration after approximately a year of weathering. The depth samples, removed from two locations, were taken after the residue had been in place approximately two years (Table 8.3) at depths of 1 cm, 15 cm and 25-30 cm from the

surface. The samples taken at the 25-30 cm depth were close to saturation. The initial weathering sample was taken approximately two months after placement of the residue in the test cell, the second sample was taken about 11 months later (Table 8.4). Each sample was analyzed with the ICPMS.

Table 8.3: Concentrations of analytes in NLR and NGR with depth in test cells

Sample (Type-SA#)	Depth (cm)	S ppm	Ca 43 ppm	Fe 57 ppm	Co ppm	Ni ppm	Cu ppm	Pb ppm
NLR-1	1	290144	74984	320115	259	7946	3800	23
NLR-2	1	350515	45618	441494	209	7439	3884	30
NLR-1	15	340598	33071	453849	276	8855	4561	30
NLR-2	15	289250	54184	381056	262	8038	4021	31
NLR-1	25-30	345161	28064	466661	332	10075	4633	30
NLR-2	25-30	348220	28807	477089	472	13432	5499	30
NGR-1	1	257724	219904	9457	70	2961	481	8
NGR-2	1	277580	211023	12060	78	3626	581	7
NGR-1	15	256520	227868	11812	21	1049	497	8
NGR-2	15	257164	194000	12704	23	1040	489	6
NGR-1	30	245564	207612	13189	29	1291	557	8
NGR-2	30	219168	158617	10281	18	817	384	5

8.3.2 Field Weathering Tests Results

The results from the samples analyzed through the depth of the deposit showed the following trends for the limited sampling conducted. For the NLR, the sulfur concentration was more constant near the water table and varied in concentration in the upper 25 cm. Calcium concentration decreased with depth. The metals iron, cobalt, nickel and copper generally increased with depth while lead was fairly constant for the

samples analyzed. In the NLR samples the lower metal concentration in the samples taken closer to the surface was probably due to the metals leaching from the residue due to oxidation of the sulfide minerals. At the lowest sampling depth the residue is saturated limiting the oxidation process and metal leaching. For the NGR, sulfur concentration decreased slightly with depth while calcium remained fairly constant. Cobalt and nickel decreased in concentration at the upper two sampling depths. The concentrations of iron and copper showed no clear trends for the samples and depths tested and the lead concentration was fairly constant. There was a significant change in colour of the NGR with depth: near the surface the sample was pale in colour with depth it became the typical orange-red shade. This effect suggests either leaching of the iron hydroxides from the surface or precipitation of oxidation products.

Table 8.4 indicates the NLR weathered samples had higher cobalt, nickel, copper and zinc concentrations than when the residue was placed. In contrast the NGR weather samples had lower cobalt, copper and zinc concentrations after approximately one year of weathering. The NGR weathers more readily and the metals are more available attached iron hydroxides as suggested by sequential extractions (Steel et al., 2009b). The higher metal concentrations in the weathered NLR samples could due to the following: analytical error, sampling inconsistencies or the dissolution of lime used to the neutralized the NLR.

Table 8.4: Concentration of analytes in residue after 11 months of weathering

Sample	S	Ca 42	Fe 57	Co	Ni	Cu	Zn	Pb
	ppb	ppb	ppb	ppb	ppb	ppb	ppb	ppb
NLR Dec/06	3.29E+08	2.86E+07	4.86E+08	2.27E+05	1.05E+07	4.36E+06	6.95E+04	3.34E+04
NLR Nov/07	3.13E+08	2.20E+07	4.66E+08	5.31E+05	1.98E+07	6.55E+06	1.26E+05	3.13E+04
NGR Dec/06	2.10E+08	2.29E+08	1.32E+07	7.43E+04	5.33E+06	5.91E+05	6.96E+04	8.40E+03
NGR Nov/07	2.09E+08	2.26E+08	1.04E+07	3.11E+04	ERR	5.22E+05	4.79E+04	9.61E+03

8.4 ABA ANALYSIS

8.4.1 ABA Analysis Methodology

To conduct an ABA test hydrochloric acid is added to a known weight of sample, once the reaction is complete the excess amount of acid remaining is determined through titration with sodium hydroxide and the amount of acid consumed is calculated. The value of acid consumed is compared with the amount of acid that could be produced if all the sulfur in the sample was converted to sulfuric acid. The ABA test includes the following analysis or calculations: sulfur analysis (total, sulfate-sulfur, sulfide-sulfur, organic sulfur) and Acid Potential (AP) calculation, bulk Neutralization Potential (NP), Carbonate Neutralization Potential (Carbonate-NP), pH and Net Acid Generation (NAG) (Peroxide) test results.

8.4.2 ABA Analysis Results

Preliminary results of ABA analysis on the demonstration plant hydrometallurgical residues are presented in Table 8.5.

Table 8.5: ABA analysis results on demonstration plant hydrometallurgical residues

Waste Type	Paste pH	Sulfur Speciation				Modified Sobek Method				Total Carbon (%)
		Stot (%)	S^o (%)	SO_4-S (%)	S^{2-} S (%)	NP	AP (calc)	Net NP (calc)	NP/AP (calc)	
NCR	3.53	25.4	24.6	13.2	15.8	0.1	494	-494	0.001	0.126
	3.28					-38.7	494	-505	-0.002	
Leach[a] Residue	2.96	27.5	31.3	5.9	17.3	-63.1	540	-603	-0.117	0.095
	2.86					-24.9	540	-579	-0.070	
NGR	5.35	20.2	2	57.2	8.2	-6.5	258	-264	0.025	0.06
	5.29					-38.1	258	-296	-0.148	

Legend
Stot: total sulfur
SO4-S: sulfate sulfur
S2-: sulfide sulfur
NP: Neutralization Potential
AP: Acid Potential
NNP: Net Neutralization Potential
NP/AP: NPR
[a] Leach Residue is not neutralized

For the standard ABA procedure a sample is classified as a potential source of acidic drainage if Net Neutralization Potential (NNP) is -5 tonnes of $CaCO_3$ or more negative (MEND, 1991). Another indication of acid producing potential is the Neutralization Potential Ratio (NP/AP). If this ratio is less than 3:1 then the sample has potential to be acid generating (MEND, 1991). The interpretation of ABA procedure results is best conducted with knowledge of test procedure limitations, experience and after consideration of other predictive tools and site specific information. In addition, kinetic testing or field results may indicate that waste is not acid producing although the NNP

value is negative. The universal ABA criteria for predicting the pH range of mine site drainage is provided in Table 8.6 (Morin and Hutt, 1997).

For the VINL residues the NNP values are negative and the NP/AP ratio (NPR) values are less than one thus the residues have acid generating potential. The neutralized residue was not tested at this time.

Table 8.6: Universal Criteria for ABA Assessment

Criteria	Prediction/Current Condition
Paste/Rinse pH	
Paste/rinse pH <5.0	Currently acidic; future unknown
5.0 ≤ paste/rinse pH ≤ 10.0	Currently neutral; future unknown
Paste/rinse pH > 10.0	Currently alkaline; future unknown
*x*NPR or *x*NNP	
*x*NPR< 1.0 or NNP< 0.0 t CaCO3/1000t	Eventually acidic
1.0 ≤ *x*NPR ≤ 2.0 or 0 ≤ NNP ≤ 20	Uncertain future
*x*NPR > 2.0 or NNP > +20 tCaCO3/1000 t	Indefinitely near-neutral or alkaline

Note: Many exceptions are known, so kinetic tests are needed to refine predictions

8.5 TCLP WASTE CLASSIFICATION TEST

8.5.1 TCLP Methodology

Waste classification tests provide a classification to the material based on a set of testing protocols and guidelines as prescribed by regulatory agencies. In the United States a waste can be described as "toxic" or "hazardous" in terms of subtitle C or D of the Resource Conservation Recovery Act (RCRA). In general, the tests consist of placing a set amount of sample (i.e. 50 g) in a flask, adding one litre of extractant, agitating the sample for 24 hours and analyzing the filtered leach from the flask. The analytical results are compared to a set of criteria and if there are exceedances the waste is described as

"toxic" or "hazardous". This type of test may also be used to assess metal leaching from mine wastes.

8.5.2 TCLP Results

Results of the TCLP on the hydrometallurgical waste residue from the demonstration plant are provided in Table 8.7. The results from this test indicate that the concentrations of the selected metals are well below the U.S. EPA guideline for waste disposal (U.S. EPA, 1996). Further tests of this nature, as indicated above, should be conducted for comparative purposes.

Table 8.7: TCLP results on demonstration plant hydrometallurgical residues

TCLP Metals	TCLP Regulatory limit (mg/L)	Material		
		Leach Residue (mg/L)	Filter Cake (mg/L)	Mixed Residue (mg/L)
As	5	<0.03	<0.03	<0.03
Ba	100	0.02	0.04	0.04
Cd	1	<0.02	<0.02	<0.02
Cr	5	<0.3	<0.3	<0.3
Pb	5	<0.00	0.01	<0.00
Hg	0.2	<0.01	<0.01	<0.01
Se	1	<0.13	<0.14	<0.15
Ag	5	<0.00	<0.00	<0.00

CHAPTER 9

SUMMARY AND RECOMMENDATIONS

The objective of this research was to characterize the mobility of heavy metals and sulfur compounds from hydrometallurgical residue to the subsurface environment through assessment of its mineralogy, static and kinetic testing and numerical modeling then integrate the data in a risk-based approach to select the most favourable mine waste disposal design. This research targeted ore metals nickel, cobalt and copper as well as sulfur compounds in the waste residues from the hydrometallurgical demonstration plant in Argentia, Newfoundland.

This thesis is comprised of six sections:

1) literature review (Chapter 2);
2) characterization of the VINL residue mineralogical assemblage (Chapter 3);
3) assessment of residue metal and acid generating potential (Chapters 4 and 8);
4) geochemical reactive modeling of residue impoundment decant water (Chapter 5);
5) geochemical reactive transport modeling of two residue disposal options (Chapter 6); and
6) risk-based and multi-criteria decision making (MCDM) methodology to determine optimal mine waste disposal design (Chapter 7).

Literature Review

There is very limited data relating to the characterization of nickel sulfide hydrometallurgical residue in the open literature. However the procedure for characterizing mine tailings and the mineralogy of zinc process residues has been well

documented. Zinc process residues are produced through hydrometallurgical treatment of zinc sulfide ores and the resulting residues, although not similar in nature to the VINL residue, provide important information relative to testing methodologies. Mineralogy work associated with hydrometallurgy has focused on problems with the removal of iron during hydrometallurgical process and issues surrounding the disposal of zinc process residue jarosite. A variety of typical static tests conducted on tailings and mine waste have been described. Kinetic tests, used to assess metal leaching of tailings and waste rock have also described with a focus on those tests applicable to the hydrometallurgical residue.

While extensive literature exists relating to geochemical models and transport models, less is available in the area of geochemical reactive transport models focusing on metals in layered, saturated or partially saturated porous media. Examples have been provided of geochemical reactive transport codes used to model mine tailings and waste rock which are mineralogically simpler materials than process residue. For the risk assessment work, a review has been provided of 1) risk assessment processes and associated decision-making, 2) the Canadian Council of Ministers of the Environment (CCME) ecological risk assessment (ERA) process, 3) human health risk assessment and 4) other authors' approaches to risk assessment applied to site remediation and risk-based disposal management.

Mineralogical Assessment of the VINL Residue

The mineralogical assessment, through SEM and XRD analyses, was able to reveal characteristics of the hydrometallurgical residues valuable in understanding how it will

weather on disposal. NLR (Neutralized Leach Residue) exists mainly as very small framboidal, spherical particles comprised largely of iron with varying and significant quantities of oxygen, calcium and sulfur. A total of 16 different phases were identified in the NLR by SEM analysis. They include: Fe-S phases, pure sulfur and several Fe-O phases. XRD analysis was not able to fully interpret the NLR due to the amorphous nature of some of its minerals. The NGR (Neutralized Gypsum Residue) consists of gypsum and a small percentage of an iron hydroxides minerals as well as target metal hydroxides. The SEM and XRD work indicated that, except for variations in the gypsum percentages, the mini-plant and demonstration plant residues were largely similar in micro-structure and composition which could be beneficial when conducting weathering and treatment studies.

The results of the five-step sequential extraction on the residues suggested that metals were more available in the NGR than the NLR. The target metals associated with the residues could exist in several different forms including: sorbed to surfaces of the minerals or phases; precipitated hydroxides, oxides or sulfates; or within the crystal structure of the minerals. It is expected dissolution activity of target metals will follow that of the minerals or phases with which they are associated: gypsum, iron hydroxides, iron oxides, unprocessed concentrate and FeS. The iron (hematite) in the NLR is very stable while that in the NGR is less stable (iron hydroxides). The trace metals, nickel, copper, cobalt and zinc are associated not only with the hematite in the NLR but also with other minerals or phases resulting in a significant portion of these metals being more susceptible to weathering. During treatment and disposal of the residues it will be

important to consider the metals associated with all the phases present in particular those that are more susceptible to weathering.

Residue Kinetic Testing

Kinetic tests conducted on the residue included shake flask experiments, humidity cell experiments and field weathering tests while static tests comprised assays, ABA analysis and TCLP tests. Shake flask experiments are valuable in the understanding of factors having shorter-term affects on the chemistry of waters containing appreciable amounts of residue such as the decant water in a residue disposal pond. The factors considered during the shake flask experiments included: solids ratio, mix time, test pH and residue type. The test pH and residue type were the main factors that affected the majority of filtered leachate experimental responses. Residue type was a main factor in most of the responses over a range of test pH values; this reflects the importance of considering the very different nature of the two residues. Test pH was the most significant factor when the test pH was lowered to pH 2. Results suggest a significant drop in solution pH is required for a noticeable change in metal concentrations unless the solution solids ratio is elevated. In several cases it was the interaction between two factors (such as residue type and pH) that constituted the main effect on the response. Solids ratio had a significant effect on the filtrate metal and sulfate concentration and conductivity and alkalinity. The PHREEQC simulations conducted provided an understanding of which individual minerals have the greatest impact on final solution pH over a range of initial pH values and to identify compounds that precipitate out of solution.

The humidity cell experiments provided information of sulfur generation rate and metal leaching capacity of the residues over the test period while the field weathering tests show the strong weathering affects on the residues with time and deposit depth.

Geochemical Reactive Modeling

With the knowledge of the minerals and phases present in the residue and how the metals may be associated with the minerals, it was possible to model hydrometallurgical residue using the geochemical reaction code PHREEQC and predict metal concentrations in a batch test situation such as the shake flask experiment. Not surprisingly due to the complex nature of the residue the NLR was much more difficult to model that the NGR. The modeled residue was also useful in predicting decant water chemistry and was used to consider factors affecting its chemistry. The modeled NCR (Neutralized Combined Residue) and PEN solution gave the best approximation of metal concentration in the decant water. Removing oxygen from the reaction, similar to subsurface conditions, generated reduced nickel and copper concentrations in the decant water as would be expected. Sensitivity analysis indicated that the modeled residue was very sensitive to the amount of neutralization it received from calcite and to the percentage of FeS and pyrrohotite in the modeled NCR. The kinetics of mineral dissolution/ precipitation reactions was considered using the code MIN3P and provided insight into the time to quasi-equilibrium and the saturation index of the residue minerals and its trend with time. Metal sorption appears to play a strong role in the actual residue and was able to be modeled in a simple manner with PHREEQC.

Numerical Modeling of Residue Disposal Options

In this work a conceptual model of two disposal options for hydrometallurgical residue was developed which included developing a mineralogical assemblage that represents the hydrometallurgical residue, running simulations using a geochemical reactive transport code (MIN3P), calibrating the model against field data and then predicting full-scale conditions. There was relatively good agreement between the model and the limited field measurements for both the subaerial and subaqueous disposal cases although it was difficult to model the ferrous iron concentrations and the high pore water pH evident in the subaqueous scenario.

The model was able to provide insight into some of the dominant reactions and influences on groundwater geochemistry in the residue impoundment. The model demonstrated the dominant processes: sulfide mineral oxidation; the neutralizing effect of the gypsum and calcite; the strong effect of initial pore water conditions on disposal situations with limited base-flow; and the strong effect of oxygen availability as evident through the subaerial disposal method. From the work it is apparent that subaerial disposal can result in low pore water pH and high metal concentrations throughout the deposit in a relatively short period of time. The subaqueous case resulted in a higher deposit pH and reduced dissolved metal concentrations for the period modeled. Also there was a complex interdependence between the decant water chemistry, the initial interstitial pore water chemistry and the reactive minerals in the case of subaqueous disposal. For subaerial disposal, where rainwater infiltrates the deposit the subsurface chemistry is relatively simpler.

Risk-based Decision-making for Residue Disposal Design

A multi-criteria, risk-based methodology was used to assess disposal options for mine waste and provide effective decision-making. Three different disposal priority rankings were determined for the four disposal options depending on human health risk, ecological risk and the multi-criteria decision making process. The ecological risk had a different disposal ranking than the human health risk; largely due to the inclusion of risk to the VEC's in the Stream. For this case study, in order to protect the VEC's in the stream it would be important to eliminate leachate migration from the impoundment. With subaerial disposal there is no risk of dam overtopping thus one less factor contributing to the total risk. In this case, leachate migration was not predicted to cause a significant risk for users of a downgradient well; nor for users of a larger water body located further from the source. The results from the risk assessment were integrated with other criteria in the MCDM analysis. Human health risk and ecological risk had the highest score of the five decision criteria when applied to the case study. This analysis helped to demonstrate the significance of these risks and the corresponding importance of long-term integrity of the disposal site on the selection of an optimal waste disposal method. The determination of risks associated with disposal options and ranking of disposal options is site and waste specific.

This research assists with ensuring the long-term stability of the residue by augmenting the understanding of its mineralogy, weathering, metal leaching and reactivity. The risk-based approach integrates developed data and provides an effective methodology for waste disposal system evaluation and decision-making.

RECOMMENDATIONS

1) This research provided information on the micro-structure, mineralogy and stability of trace metals in the VINL residues, further work is now required to confirm the results and to focus on determining the stability of specific sulfur-bearing phases present particularly in the NLR.

2) Additional shake flask experimental work is required on the NCR to elucidate the synergistic effects due to the mixed residue chemistry; and the consequence of longer mix times, changes in dissolved oxygen and addition of microorganisms (for example *Acidithiobacillus ferrooxidans*). The humidity cells experiments should be extended with the addition bacteria. The field weathering tests should be repeated with mineralogy work conducted on samples taken at different depths to augment understanding of the weathering processes.

3) The geochemical model needs to be enhanced by more accurate representation of the residue in the reactive geochemical code. The present residue code has limited mineralogical expression and work is required on how to better represent the amorphous minerals and metals attached to different mineral surfaces. Experimental work should also be conducted to determine mineral reactive surface areas; and reaction rate expressions and equilibrium thermodynamics of particular minerals and phases in the residues. Thiosalt reaction expressions should be included in the code and the model could be further calibrated with additional site data. Finally, the model flow system requires further refinement.

4) In the risk analysis, there are many parameters that deserve more detailed consideration or preliminary consideration when evaluating disposal methods. These include but are not limited to: bedrock type, permeability and fracturing; site location; waste characteristics; subsurface and surface water chemical reactions; type, leakage rate and degradation rate of liner system; and modeling of COC transport. Due to the higher ecological risk, it would be important to consider areas of greater uncertainty in ecological risk determination and to assess ecological risk management alternatives.

5) To optimally design the "best" treatment/disposal options, the waste treatment should be considered as part of the entire facility design. The method developed here can be used once the process is designed, but to use it optimally it should be used as a tool in process design to optimize process selection and operations.

STATEMENT OF ORIGINALITY

1) As there is very limited experience in the processing of nickel sulfide concentrate through hydrometallurgy the high sulfur, process residue is generally not well characterized. The mineralogical and sequential extraction work provided key residue mineral and microstructure information; suggested how target metals are present in the residue minerals and phases; and provided metal partitioning results which are important in understanding the residues metal leaching potential. The static and kinetic testing conducted further characterized the residues by assessing their acid generating and metal leaching capacity.

2) Geochemical modeling of process residues is not widely reported in the literature due in part to the complexity of the mineralogical assemblage. This work, through calibrated models, was successfully able to model the residue that led to a greater understanding of factors impacting the chemistry of groundwater and surface water and enabled the prediction of longer term subsurface conditions in the residue impoundment.

3) The design of a mine waste disposal site is waste and site specific and is complex. Using a risk-based decision-making to assess design options for a mine waste disposal project is novel and effective approach. This approach integrated the results from the mineralogical characterization and contaminant fate and transport modeling and included uncertainty in the human health and ecological risk analysis; then incorporated this risk analysis in a MCDM analysis to evaluate the optimal mine waste disposal alternative.

REFERENCES

Agatzini, S., Kontopoulos, A., Maraboutis, P., Xenidis, A. (1986). Removal of iron from iron-nickel-cobalt solutions. In Dutrizac, J.E., Monhemius, A.J., (Eds.), *Iron Control in Hydrometallurgy* (pp. 353-376). Chichester, U.K.: Ellis Horwood Ltd.

Allison, J.D., Brown, D.S., Novo-grade, K.J. (1991). *MINTEQAC2/PRODEFA2, A Geochemical Assessment Model for Environmental Systems: Ver 3.0 Users Manual*. U.S. EPA, EPA/600/3-91/021.

Appelo, C.A., Postma, D. (1993). *Geochemistry, Groundwater and Pollution*. Rotterdam, Brookfield, A.A. Balkema, 563pp.

ASTM (2001). D5744-96 *Standard Test Method for Accelerated Weathering of Solid Materials Using a Modified Humidity Cell.* Developed by Subcommittee: D34.01.04 Book of Standards Volume: 11.04.

ASTM (2004). *D5284-93 (2004) Standard Test Method for Sequential Batch Extraction of Waste with Acidic Extraction Fluid.* Developed by Subcommittee: D34.01.04 Book of Standards Volume: 11.04.

ASTM (2006). *D4874-95 (2006) Standard Test Method for Leaching Solid Material in a Column Apparatus.* Developed by Subcommittee: D34.01.04 Book of Standards Volume: 11.04.

Asante-Duah, D. K. (1993). *Hazardous Waste Risk Assessment*, Florida: Lewis Publishers, CRC Press.

Au-Yeung, S. C., Bolton, G.L. (1986). Iron control Sherrit Gordon Mines. In Dutrizac, J.E., Monhemius, A.J., (Eds.), *Iron Control in Hydrometallurgy*, Chichester,U.K., Ellis Horwood Ltd.,131-151.

Bear, J. (1972). *Dynamics of Fluids in Porous Media.* New York: Elsevier.

Belzile, N., Chen, Y., Cai, M., Li, Y. (2004). A review of pyrrhotite oxidation. *Journal of Geochemical Exploration*, 84, 65-76.

Berg, D., Borve, K., (1996). The disposal of iron residue at Norzink and its impact on the environment. Proceedings Second International Symposium of Iron Control in Hydrometallurgy, Ottawa, Oct.20-23, 1996, In J.E., Dutrizac, G.B., Harris (Eds.) *Iron Control and Disposal.* Ottawa, ON: CIM., 627-641.

British Columbia Acid Mine Drainage Task Force (1989), *Draft Acid Rock Drainage Guide*. Vancouver, British Columbia: BiTech Publishers Ltd.

British Columbia (Province of) (1992). *Waste Management Act: Special Waste Regulation Schedule 4, Parts 1 and 2*, Queen's Printer, Victoria, BC, 72-79.

Bruckard, W. J., Woodstock, J. T. (2004). Characterization of Metal-Containing waste products in relation to re-treatment methods for metal recovery and recycling. In *International Conference on Sustainable Processing of Minerals, Green Processing Conference* (May 10-12, 2004). Fremantle, WA, 217-224.

Bruynesteyn, A. and Hackel, R.P. (1984). Evaluation of Acid Production Potential of Mining Waste Materials, *Minerals and the Environment,* 4, 5-8.

Buckle, R. L., Lorenzen, L. (1996). The stabilization and disposal of jarosite. In Proceedings Second International Symposium Iron Control in Hydrometallurgy, Ottawa, Oct.20-23, 1996, In J.E., Dutrizac, G.B., Harris (Eds.) *Iron Control and Disposal*, CIM, Ottawa, ON. 597-611.

Burnmaster, D. E., Anderson, P. D. (1994). Principles of good practice for the use of Monte Carlo techniques in the human health and ecological risk assessment. *Risk Analysis*, 14(4), 477-481.

CCME (Canadian Council of Ministers of the Environment) (1996). *A framework for ecological risk assessment: General guidance*, Winnipeg, Canada: CCME Subcommittee on Environmental Quality Criteria for Contaminated Sites, PN1195.

CCME (Canadian Council of Ministers of the Environment) (1997). *A framework for Ecological Risk Assessment: technical appendices*, Winnipeg, Canada: CCME Subcommittee on Environmental Quality Criteria for Contaminated Sites.

CGSB (Secretary of Canadian General Standards Board). *Leachate Extraction Procedure 164-GPIMP.*, Ottawa, Ontario: CGSB, (1987).

Chen, T.T., Dutrizac, J. E., Poirier, G., Kerfoot, D. G., Singhal, A. (2006). Characterization of the iron-rich residues generated during the pressure oxidative leaching of Voisey's Bay nickel sulphide concentrate. In *Proceedings Conference of Metallurgy 2006*, Montreal, Oct 1-4, 2006.

Creamer's Media Miner's Weekly on-line, (Sept 2006), Retrieved November, 2006 from, http://www.miningweekly.co.za/min.

Defreyne, J., Grieve, W., Jones, D., Mayhem, K. 2006. The role of iron in the CESL process. In *Proceedings Conference of Metallurgy 2006*, Montreal, Oct 1-4, 2006.

Dave, N. K., Lim, T. P., Home, D., Boucher, Y., Stuparyk, R. (1997). Water cover on reactive tailings and wasterock: Laboratory studies of oxidation and metal release characteristics. In *Proceedings of the Fourth International Conference on Acid Rock Drainage (ICARD),* May 31-June 6 1997, Vancouver, BC, Canada. MEND Secretariat CANMET, Ottawa, ON, 779-794.

Davis, G.B., Ritchie, A.I.M. (2003). Surface reactivity of high-sulfide copper mine tailings under shallow water cover conditions. *Proceedings of Sixth International Conference on Acid Rock Drainage (ICARD),* QLD, Cairns, Jul12-18, 2003, 241-251.

Dzombak, D.A, Morel, F.M. (1990). *Surface Complex Modeling: Hydrous Ferris Oxide.* New York, John Wiley and Sons.

Evangelou, V.P. (1998). *Environmental Soil and Water Chemistry, Principles and Applications.* New York: John Wiley and Sons.

Fetter, C. W. (1999). *Contaminant Hydrogeology.* 2nd Ed., New York: Prentice Hall Inc. 500pp.

Foged, S., Vandekeybus, J., Menthens, G. (2006). How to substantially improve the life of a 30 Ha tailings pond at Umicore zinc plant. In *Proceedings Conference of Metallurgy 2006,* Montreal, Oct 1-4, 2006.

Frind, E. O. Molson, J. W. (1994). Modelling of Mill-Tailings Impoundments, In J.L. Jambor, D.W. Blowes (eds.) *Short Course Handbook on Environmental Geochemistry of Sulfide Mine Waste.* Minerals Association of Canada, Nepean.V.22.

Geldart, J., Ferron, C. J., Fleming, C. A. (1996). Hydrothermal processing of Kidd Creek jarosite for stabilization and metal recovery. Proceedings of the Second International Symposium on Iron Control in Hydrometallurgy, Ottawa, Oct.20-23, 1996, In: J.E., Dutrizac, G.B., Harris (Eds.) *Iron Control and Disposal* (pp.659-673). Ottawa, ON: CIM.

Glynn, P., Brown, J. (1996). Reactive transport modeling of acidic metal-contaminated ground water at a site with sparse spatial information. In P.C. Litchner, C.I., Steefel, E.H. Oelkers (Eds.), *Reactive Transport in Porous Media,* Reviews in Mineralogy, 34,377-438.

Hage, Scheiling. (1996). An integrated jarosite and sludge treatment process. Proceedings of the Second International Symposium on Iron Control in Hydrometallurgy, Ottawa, Oct.20-23, 1996, In J.E., Dutrizac, G.B., Harris (Eds.) *Iron Control and Disposal* (pp.659-673). Ottawa, ON: CIM.

Hetcht, H., Kolling, M., Geishas, N. (2002). "DiffMod7 – Modelling oxygen diffusion and pyrite decomposition in the unsaturated zone based on ground, air and oxygen distribution." In H.D. Schultz, G. Teutsch (Eds.), *Geochemical processes-conceptual models for reactive transport in soil and groundwater* (Research Report) (pp.55-77). Weinheim, Germany: Wiley – VCH.

Hutt, N., Morin, K. (1999). The international static database (ISD). In *Proceedings of Sudbury '99, Mining and the Environment II (pp.* 363-370). Minesite Drainage Assessment Group (MDAG) Publishing, Vancouver, British Columbia.

Ibrahim, M. K., Kaluarachchi, J. J. (2003). Multi-criteria analysis with probabilistic risk assessment for the management of contaminated ground water. *Environmental Impact Assessment Review*, 23, 683-721.

Jambor, J. L. (1994). Mineralogy of sulfide-rich tailings and their oxidation products, In *Environmental Geochemistry of Sulfides*, (short course, Chapter 3). Minerals Association of Canada.

Kimball, B. A, Runkel, R. C., Walton-Day, K. (2003).Use of field-scale experiments and reactive solute-transport modelling to evaluate remediation alternatives in streams affected by acid mine drainage. In J.L. Jambor, D.W. Blowes, A.I.M. Ritchie (Eds.), *Environmental Aspects of Mine Wastes*, Vol. 31. 261-282, Minerals Association of Canada.

Knapp, R. B. (1989). Spatial and temporal scales of local equilibrium in dynamic fluid-rock systems. *Geochimica et Cosmochimica Acta*, 53, 1955-1964.

Lahtinen, M., Lehtinen, L. (2006). Hematite versus jarosite precipitation in zinc production. In *Proceedings Conference of Metallurgy 2006*, Montreal, Oct 1-4, 2006.

Lapakko, K. A. (2002). *Metal mine rock waste and characterization tools: an overview.* Report to Minnesota Department of Natural Resources (No.67) April 2002, Mining Minerals and Sustainable Development. 31p. http://www.iied.org/mmsd/mmsd_pdfs/067_mftf-f_lapakko.pdf

Lapakko, K. A. (1993). *Evaluation of tests for predicting mine waste drainage pH.* Report to the western governor's Assoc. Minnesota Depart. Nat. Res., Div of Minerals, St. Paul, MN.

Lapakko, K., Wessels, J., Antonson, D. (1995). *Long term Dissolution Testing of Mine Waste.* Minnesota Department of Natural Resources, Report to the US EPA, EPA 530-R-95-040, PB 95-260287.

Lawrence, R. W. (1990). Prediction of the behavior of mining and processing wastes in the environment. In *Mining and Mineral Processing Wastes. Proceedings of Western Regional Symposium on Mining and Mineral Processing Wastes,* Littleton, CO: Soc. for Mining, Metallurgy and Exploration, 115-121.

Lawrence, R. W., Wang, Y. (1996). *Determination of Neutralization Potential for Acid Rock Drainage Prediction.* MEND Project 1.16.3, Natural Resources Canada, Ottawa, Ontario, 149p.

Lawrence, R.W., Wang, Y. (1997). Determination of neutralization potential in the prediction of acid rock drainage. In *Proceedings of the Fourth International Conference on Acid Rock Drainage (ICARD),* May 31-June 6, 1997, Vancouver, B.C., MEND Secretariat CANMET, Ottawa, Ontario. 449-464.

Li, M., St. Arnaud, L. (1997). Hydrogeochemistry of secondary mineral dissolution: column leaching experiment using oxidized waste rock. In *Proceedings of the Fourth International Conference on Acid Rock Drainage (ICARD). (May 31-June 6, 1997 Vancouver, B.C.).* MEND, Natural Resources Canada, Ottawa, Ontario. 465-477.

Li., M., Catalan, L. J., St.-Germain, P. (2000). Rates of oxygen consumption by sulphide tailings under shallow water covers- f ield measurement sand modelling. In *Proceedings of the Fifth International Conference on Acid Rock Drainage (ICARD).* Society for Mining, Metallurgy and Exploration, Littleton, Colorado. 913-920.

Lindvall, M. Erikssen, N. (2003). Investigation of weathering properties of tailings from Boliden's Aitik copper mine, Sweden. A summary of twelve years investigations, In *Proceedings of the Sixth International Conference on Acid Rock Drainage* (ICARD), July 12-14, 2003 Cairns, 725-731.

Liu, I., Huang, G. H., Hao, R. X., Cheng, S. Y. (2004). An integrated subsurface modeling risk assessment approach for managing the petroleum-contaminated sites, *Journal of Environmental Sciences and Health*, A39, 11, 3083-3113.

Lottermoser, B. (2003). *Mine Wastes, Characterization, Treatment and Environmental Impacts*, Springer-Verlag, Berlin, Heidelberg.

Marcus, J. J. (1997) *Mining Environmental Handbook, Effects of mining on the environment and American environmental controls on mining*: Imperial College Press.

Maxwell, R.M., Carle, S.F., Tompson, A. F. (2003). *Contamination, Risk, and heterogeneity: On the Effectiveness of Aquifer Remediation.* Geosciences and Environmental Technologies Division, Lawrence Livermore National Laboratory.

Mayer, K.U., Blowes, D.W., Frind, E.O. (1999). Advances in reactive-transport modeling of contaminant release and attenuation from mine-waste deposits. In J.L. Jambor, D.W. Blowes (Eds.), *Environmental Aspects of Mine Wastes* (Vol 31, short course). Minerals Association of Canada.

Mayer, K.U., Frind, E. ., Blowes, D.W. (2003). Multi-component reactive transport modeling in variably saturated porous media using formulation for kinetically controlled reactions. *Water Resources Research.*

MEND (1991). *Acid Rock Drainage Prediction Manual*, MEND project 1.16.1b, prepared for NAMET-MSL division.

MEND (2000). *MEND Manual, Volume 3- Prediction.*,(G.A. Tremblay and C.M. Hogan, (eds.). *MEND Project* 5.4.2c. MEND, Natural Resources Canada, Ottawa, Ontario.

Menge, R., Van Driessche, R., Mentens, G. (2006). Closing a goethite pond at the Umicore Balen, Belgium. In *Proceedings Conference of Metallurgy 2006*, Montreal, Oct 1-4, 2006.

Merkel, R.J., Planar-Friedrich, B. (2005). *Groundwater Geochemistry: A practical Guide to Modeling of Natural and Contaminated Aquatic Systems* D.R. Nordstrom (Ed.). Berlin: Springer-Verlag, 200pp.

Miller, S. D., Jeffery, J. J., Wong, J. W. (1991). Use and misuse of the acid-base account and 'AMD' prediction, In *Proceedings of the Second International Conference on Abatement of Acid Drainage*, Montreal, Sept. 1991.

Miller, S., Robertson, A., Donohue, T. (1997). Advances in acid drainage prediction using the net acid generation NAG test. In *Proceedings of the Fourth International Conference on Acid Rock Drainage* (ICARD). (May 31-June 6, 1997 Vancouver, B.C.). MEND Secretariat CANMET, Ottawa, Ontario.

Ministry of the Environment (1985). "*Regulation 309/Leachate Extraction Procedure*," Government of Ontario.

Ministre de L'Environnement (1985). "*Procedure d'evaluation des characteristiques des dechets solides et des boues pompables*," Ministre de L'Environnement, Quebec, Canada.

Morin, K. A, Cherry, J. A, Dave, N. K., Lim, T. P. Vivyurka, A. J. (1988). Migration of Acidic Groundwater Seepage from Uranium-Tailings Impoundments: 1. Field Study and Conceptual Hydrogeochemical Model Contaminant Hydrology, *JCOHE,* 6, 2, 271-303.

Morin, K.A., Hutt, N.A. (1997) *Environmental Geochemistry of Minesite Drainage: Practical Theory and Case Studies*. MDAG Publishing, Vancouver, Canada.

Morin, K.A., Hutt, N.A. (2000). Lessons learned from long-term and large-batch humidity cells, In *Proceedings of the Fifth International Conference on Acid Rock Drainage (ICARD)*. Society for Mining, Metallurgy and Exploration, Littleton, Colorado, (1), 661-671.

Muir, D. M., Jamieson, E. (2006). Precipitation of iron oxides form iron (II)/(III) chloride media at ambient temperatures using caustic, lime or magnesia. In *Proceedings* Conference of Metallurgy 2006, Montreal, Oct 1-4, 2006.

Nicholson, R.V., Sharer, J.M., (1990). Laboratory studies of pyrrhotite oxidation kinetics. In C.N. Alpers, D.W. Blowes (Eds.), *Environmental Chemistry of Sulfide Oxidation*, American Chemical Society, Symposium Aug 23-28, 1992, 14-30.

Nordstrom, D.K., Alpers, C. N. (1999). Geochemical modeling of water rock interactions in mining environments. In Plumlee Logsdon (Eds.) *Environmental Geochemistry of Mineral Deposits (Part A: Processes Techniques and Health Issues).* Reviews in Economic Geology, (Vol 6A). Society of Economic Geologists Inc.

Norecel Environmental Consultants (1992). *Field QA/QC Protocols for Monitoring and Predicting Impacts of Acid Rock Drainage*. Resource Management Branch, BC, Ministry of Energy, Mines and Petroleum Resources.

Palmer, C. M., Johnson, G.D. (2005). The Activox ® Process: Growing Significance in the Nickel Industry, *Journal of Metallurgy*, July, 40-47.

Parker, G., Roberston, A. (1999). *Acid Drainage*. Australian Minerals and Energy Environment Foundation, 200p.

Parkhurst, D.L. Appelo, C.A.J. (1999). *User's guide to PHREEQC (Version 2)- A computer program for speciation, batch reaction, one-dimensional transport and inverse geochemical calculations*, U.S. Geological Survey Water Resources

Investigation Report, 99-4259.

Peacey, J., Guo, X. J., Robles, E. (2004). *Copper Hydrometallurgy: Current status, preliminary economics, future direction and positioning versus smelting.* Hatch Associates, Retrieved from, http://www.hatch.ca/Non_Ferrous/articles/copper_hydrometallurgy.pdf

Pophanken, H. (1996). Constructing, operating and capping of the jarosite pond, Galing1. Proc. 2nd Int. Symp. Iron Control in Hydrometallurgy, Ottawa, Oct.20-23, 1996, In: J.E., Dutrizac, G.B., Harris (Eds.) *Iron Control and Disposal*, CIM, Ottawa, ON. 613-625

Price, W. A. (1997). *DRAFT Guidelines and Recommended Methods for the Prediction of Metal Leaching and Acid Rock Drainage at Minesites in British Columbia*, British Columbia Ministry of Employment and Investment, Energy and Minerals Division, Smithers, BC, (April), 143p.

Price, W. A., Morin, K, Hutt, N. (1997). Guidelines for the prediction of acid rock drainage and metal leaching for mines in British Columbia: Part I general procedures and information requirements. In *Proceedings of the Fourth International Conference on Acid Rock Drainage (ICARD).* May 31-June 6 1997, Vancouver, BC, Canada. MEND Secretariat CANMET, Ottawa, Ontario. Vol 1, 15-30.

Price, W. A. (2005). *List of potential information requirements in metal leaching and acid rock drainage assessment and mitigation work.* (MEND report 5.10E. MMSLNo. 601856. CANMET Mining and Minerals Sciences Laboratory, 24p.

Proctor, D. M., Shay, E. C., Fehling, K. A., Brent, L. F. (2002). Assessment of human health and ecological risks posed by the uses of steel-industry slags in the environment, *Journal of Human and Ecological Risk Assessment*, 8, 4,681-711.

Ptacek, C. J., Blowes, D. W. (1994). Geochemistry of concentrated waters at mine-waste sites. In J.L. Jambor, C.J. Blowes, A.I.M. Ritchie (Eds.) *Environmental Aspects of Mine Wastes*. Minerals Association of Canada. 31, 239-261.

Queneau, P. B., Wier, D. R. (1986). Iron control hydrometallurgical processing of nickel-ferrous laterite ores. In Dutrizac, J.E., Monhemius, A.J., (Eds.), *Iron Control in Hydrometallurgy* (pp.76-105). Chichester, U.K.: Ellis Horwood Ltd.

Ritchey, G. M. (1989). *Tailings Management, Problems and Solutions in the Mining Industry*. Amsterdam, NL: Elsevier Science Publishers.

Robertson, J. D. (1991). Subaqueous disposal of reactive mine waste: an overview of the practice with case studies. *Proceedings of the Second International Conference on Abatement of Acidic Drainage*, 3, 185-200.

Saaltink, M. U., Carrera, J., Ayora, C. (2001). On the behavior of approaches to simulate reactive transport. *Journal of Contaminant Hydrology*, 48, 213-235.

Salmon, U. S. (2003). *Geochemical Modelling of Acid Mine Drainage in Mill Tailings: quantification of kinetic processes from laboratory to field scale* (report). KTH Land and Water Resources Engineering. 61p.

Salomons, W. (1995). Environmental impact of metals derived from mining activities-processes, predictions prevention, *Journal of Geochemical Exploration*, 52 (1-2), 5-23.

Sammut, D., Welham, N. J. (2002). The Intec Copper Process: a detailed environmental analysis. In *Proceedings Green Processing Conference*, May 29-31,2002, Cairns, Qld. 115-124

Scott, J. D., Donyina, D. K., Mouland, J. E. (1986). Iron the good with the bad- Kidd Creek zinc plant experience. In Dutrizac, J.E., Monhemius, A.J., (Eds.), *Iron Control in Hydrometallurgy,* Chichester, U.K, Ellis Horwood Ltd., 657-675.

Skousen, J. G., Renton, J. Brown, H., Evans, P., Leavitt, B., Brady, K., Cohen, L., Ziemkiewicz, P. (1997). Neutralization potential of overburden samples containing siderite. *Journal of Environmental Quality*, 26(3), 673-681.

Smith, A. (1997). Waste rock characterization. In J.J. Marcus, (Ed.), *Mining Environmental Handbook,* London, Imperial College Press, p. 287-293.

Sobek, A. A., Schuller, W. A., Freeman, J. R., Smith, R. M. 1978. *Field and Laboratory Methods Applicable to Overburdens and Minesoils*. U.S. EPA 600/2-78-054. Washington, DC.

Steel, A., Hawboldt, K., Khan, F., 2006. A microstructural and geochemical comparison of residues from hydrometallurgical processes. Poster session presented at *Conference of Metallurgy 2006*, Montreal, Oct. 1-4, 2006.

Steel, A., Hawboldt, K., Khan, F., 2009a. Results of shake flask experiments on hydrometallurgical residues. *International Journal of Environmental Science and Technology*, 6(1), 57-68.

Steel, A., Hawboldt, K., Khan, F., 2009b. Assessment of minerals and iron-bearing phases present in hydrometallurgical residues from nickel sulfide concentrate and of residue associated metals. *International Journal of Hydrometallurgy,* accepted.

Stefel, C.T., MacQuarrie, K.T.B. (1996). Approaches to modeling of reactive transport in porous media, In P.C. Lictner, C.I., Stefel, E.H. Oilkus (Eds.), *Reactive Transport in Porous Media.* Review Mineralogy, 34, 83-129

Stefel, C. I., VanCappellen, P. (1998). Reactive transport of natural systems (Editorial in 'Special Issue'). *Journal of Hydrology,* 209, 1-7.

Suter, G. W., II (1993). *Ecological Risk Assessment.* MI: Ann Arbor, Lewis Publishers.

Takayama, T., Campolina, C., Dutra, F. (2006). Environmental aspects of the generation and disposal of iron residues at the Votorantim zinc refinery in Brazil. In *Proceedings Conference of Metallurgy* 2006, Montreal, Oct 1-4, 2006.

Tindall, G.P., Muir, D.M. (1996). Transformation of iron oxide in nickel laterite processing. Proceedings of the Second International Symposium of Iron Control in Hydrometallurgy, Ottawa, Oct.20-23, 1996, In: J.E., Dutrizac, G.B., Harris (Eds.) *Iron Control and Disposal,* CIM, Ottawa, ON., 249-262

U.S. EPA (1989a). *Risk assessment guidance for Superfund. Vol1, Human health evaluation manual (Part A).* Office of Emergency and Remedial Measures Response, Washington, D.C.. EPA/540/1-89/002

U.S. EPA (1989b). *Risk assessment guidance for Superfund. Vol2, Environmental evaluation manual (Part A).* Office of Emergency and Remedial Measures Response, Washington, D.C., EPA/540/1-89/001.

U.S. EPA (1996). *Test Methods for Evaluating Solid Waste - Physical/Chemical Methods (SW-846),* USEPA, Washington, DC.

Uuipaaralniemi, E., Karlman, S.G., Takala, H. (1996). Handling of iron at the zinc plant in Kokkola. Proceedings Second International Symposium Iron Control in Hydrometallurgy, Ottawa, Oct.20-23, 1996, In J.E., Dutrizac, G.B., Harris (Eds.) *Iron Control and Disposal,*. CIM, Ottawa, ON, 101-115.

Vale Inco (2008). *Environmental Impact Statement, Long Harbour Commercial Processing Plant, April 2008. Project Description,* Retrieved August 14, 2008, from http://www.env.gov.nl.ca/env/Env/EA%202001/Project%20Info/1243.htm.

VBNC (1997). *Voisey's Bay Mine/Mill Project Environmental Impact Statement, Dec. 1997.* Retrieved August 15, 2006, from http://www.vbnc.com/Reports.asp.

VBNC (2002). *Argentia Hydrometallurgical Demonstration Plant Project Registration.* Retrieved January 11, 2006, from http://www.vbnc.com/Reports.asp.

VBNC (2006). *Voisey's Bay Nickel Company Project Description and Project Registration for a Commercial Processing Plant.* Retrieved August 15, 2006, from http://www.vbnc.com/NewsItems.asp?EffectiveYear=2006.

Vega-Farfan, J. L., Tamargo, F. (1996). Bentonites as a material for controlling contamination related to zinc hydrometallurgy. Proceedings of the Second International Symposium for Iron Control in Hydrometallurgy, Ottawa, Oct.20-23, 1996, In: J.E., Dutrizac, G.B., Harris (Eds.), *Iron Control and Disposal*, CIM, Ottawa, ON. 565-579

Verburg, R., Atkin, S., Hansen, B., McWharter, D. (2000), Subaqueous and subaerial kinetic testing of paste tailings. In *Proceedings of the Fifth International Conference on Acid Rock Drainage (ICARD)* May 21-24, 2000, Denver Colorado). Society for Mining, Metallurgy and Exploration, Littleton, Colorado, 2, 877-889.

Wunderley, M.D., Blowes, D.W., Frind, E.O., Ptacek, C.J. (1996). Sulfide mineral oxidation and subsequent reactive transport of oxidation products in the mine tailings impoundments. *Water Resources Research*, 32, 3173-3187.

Yeh, G. T, Tripathi, V. S. (1989). A critical evaluation of recent developments in hydrogeochemical transport models of reactive multichemical components. *Water Resources Research*, 25, 93-108.

Yeh, G.T, Tripathi, V.S. (1990). *HYDROGEOCHEM: A coupled model of HYDROlogic transport and GEOCHEMical equilibria in reactive multi-component systems.* Oak Ridge National Laboratory, Oak Ridge, TN.

Zhu, C., Anderson, G. (2002). *Environmental Applications of Geochemical Modeling.* Cambridge: Cambridge University Press.

APPENDIX I

Vale Inco Hydrometallurgical Process and Residue Production

The Inco hydrometallurgical process consists of nine main steps: 1) the concentrate is crushed and fine ground, 2) a chlorine pre-leach, followed by a pressure oxidative leach (with hydrochloric acid) of the concentrate occurs in the autoclave resulting in a pregnant solution containing nickel, copper and cobalt in solution and a leach residue, 3) a Counter Current Decantation (CCD) is employed to dissolve all of the target metals within the leach residue 4) iron is precipitated from the pregnant solution through addition of limestone, lime, and air resulting in an iron gypsum filter cake, 5) solvent extraction is used to selectively remove copper which is plated through electrowinning, 6) further precipitation of iron is accomplished through addition of a lime slurry, 7) the impurities stream is precipitated through pH adjustment and addition of soda ash (Na_2CO_3), 8) cobalt is removed through solvent extraction and electrowinning and finally 9) the remaining nickel in the pregnant solution is removed by electrowinning. A process flow diagram is provided in Figure A.1 (VBNC, 2002).

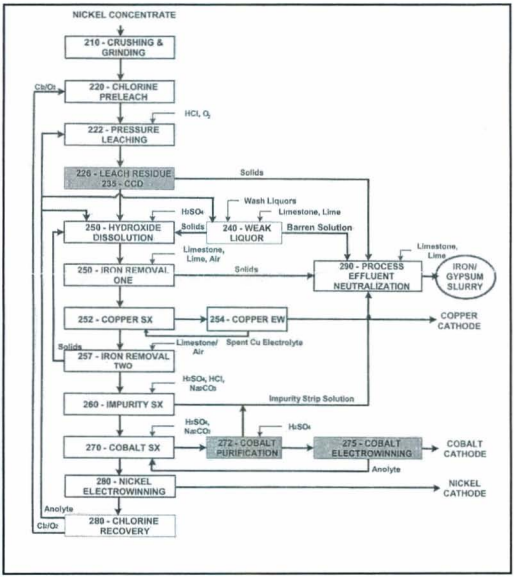

Figure A.1: Process flow diagram for VBNC hydrometallurgical plant

APPENDIX II

Rate of Pyrite Oxidation and Role of Carbonates and Silicates

Pyrite and Pyrrhotite Minerals and the Weathering Process

Pyrite (FeS_2) is the most abundant of the sulfide minerals and pyrite oxidation has been extensively studied, while less literature exists on other sulfides (including pyrrhotite, galena, sphalerite and chalcopyrite). In general, sulfides are stable under reducing conditions and under oxidizing conditions they breakdown. Iron, micro-organisms and oxygen availability play critical roles in pyrite oxidation as described by the following four methods (Lottermoser, 2003):

- Oxidation by O_2 direct, abiotic
- Oxidation by O_2 with micro-organisms, direct, biotic
- Oxidation by O_2 and Fe, indirect, abiotic
- Oxidation by O_2 with Fe and micro-organisms, indirect, biotic

The oxidation of iron sulfide minerals (as shown by pyrite) on exposure to dissolved oxygen follows the following chemical reactions (Evangelou, 1998):

$$FeS_2 + 7/2O_2 + H_2O \rightarrow Fe^{2+} + 2SO_4^{2-} + 2H^+ \quad (A.1)$$

$$Fe^{2+} + 1/4O_2 + H^+ \rightarrow Fe^{3+} + 1/2H_2O \quad (A.2)$$

$$Fe^{3+} + 3H_2O \rightarrow Fe(OH)_3(s) + 3H^+ \quad (A.3)$$

$$FeS_2 + 14Fe^{3+} + 8H_2O \rightarrow 15Fe^{2+} + 2SO_4^{2-} + 16H^+ \quad (A.4)$$

Pyrite can be oxidized by oxygen and Fe^{3+} as indicated by reactions (A.1) and (A.4). Reaction A.1 shows the oxidation of pyrite by oxygen producing Fe^{2+} (ferrous iron). The ferrous iron can oxidizes to produce Fe^{3+} (ferric iron) (reaction A.2). At low pH values,

the ferric iron precipitates from solution creating an iron hydroxide. This reaction is reversible thus can serve as a source or sink for the ferric iron. The reaction (A.2) is considered the rate limiting step as ferric iron can oxidize pyrite at a much faster rate than oxygen and is therefore the main oxidation reaction under anaerobic conditions such as below the depth of oxygen diffusion (Davis and Ritchie, 1986). Below the oxidation zone ferric iron is consumed by reaction (A.3) and (A.4). Nordstrom and Alpers (1999) (in Lappako, 2002) suggest that the bacterially mediated (such as by Thiobacillus (T.) ferrooxidans) rate of pyrite oxidation by ferric iron is roughly two to three orders of magnitude faster than the abiotic oxidation by oxygen at pH 2. The role of Thiobacillus ferrooxidans at neutral and alkaline pH is very limited.

Rate of Pyrite Oxidation

Pyrite oxidation has been well documented in the literature and is well understood in comparison to that of pyrrhotite (Belzile et al., 2004, Nicholson, Sharer, 1990). At Voisey's Bay pyrite is present however pyrrhotite makes up 70% of the minerals present in the ovoid zone. Pyrrhotite has the general formula $Fe_{(1-x)}S$ where x can vary from 0.125 (Fe_7S_8) to 0.0 (FeS). As pyrrhotite is iron-deficient it has a more complicated chemistry than pyrite. The oxidation of pyrrhotite under aerobic and anaerobic conditions has been described by Nicholson and Sharer (1990), and in Chapter 3.

The kinetics of a reaction depends on mineralogical properties and chemical, physical and biological factors. The mineralogical properties include: particle size, porosity, surface area, crystallography, trace element content of pyrite. Other external factors are:

presence of other sulfides, presence of micro-organisms, O_2 and CO_2 concentration, temperature, pH, Fe^{2+} /Fe^{3+} ratio of weathering solution.

Nicholson and Sharer (1990) have reported oxidation rates of pyrrhotite at 22ºC and with oxygen saturation as 20 to 100 times faster than values reported for pyrite oxidation at 25ºC. In general, this was in agreement with the higher reactivity of pyrrhotite evident in the field. It is thought that the iron deficiency could result in lower stability and the higher oxidation rates. They also indicated oxidation rates increased with the fraction of pyrrhotite in a mixture of pyrite and pyrrhotite. Much of what affects the oxidation rate of pyrite also applies to pyrrhotite. Lottermoser (2003) describes a number of factors that affect the rate of pyrite oxidation.

- Large pyrite surface area, small particle size increase reactivity. Framboidal pyrite is more reactive;
- Poor pyrite crystal structure is more susceptible to oxidation;
- Trace elements can be present in pyrite in the form of inclusions and chemical impurities.
- Sulfide minerals with the lowest electrode potential are weathered more strongly. If pyrite, galena and sphalerite are present, sphalerite has lowest electrode potential and is preferentially weathered.
- Oxidation of pyrite (and pyrrhotite) is exothermic and this encourages growth of thermophilic micro-organisms. As pyritic waste gets warmer through oxidation this promotes more rapid oxidation. The rate doubles every 10ºC increase in temperature.

- Certain bacteria grow well in pH 2 to pH 3 environments (acidophilic bacteria) and work in the conversion of Fe^{2+} to Fe^{3+} and the oxidation of sulfur and sulfur compounds. The resulting increase in Fe^{3+} production oxidizes the pyrite and accelerates acid formation. The aerobic bacteria T. ferroxidans and Leptospirillum ferroxidans oxidize Fe^{2+} to Fe^{3+} while T.thioxidans and ferrobacillus sulfooxidans oxidize sulfur and sulfur compounds. Generally, abiotic chemical oxidation is dominant over the biotic oxidation of pyrite. Also 95 % of bacteria associated with AMD is not T. ferroxidans.
- Pyrite oxidation occurs in water and air and the oxidation rate increases with O_2 concentration. If oxidation takes place in water or saturated pores under cover, reactivity is affected by concentration and rate of transport of O_2 in water. Concentration O_2 in water is temperature dependant and varies from 0 mg/L to 8mg/l at 25 ℃, while in air O_2 concentration is 21 percent by volume or 286 mg/L at 25℃. Therefore pyrite oxidation in water much less than air. In flooded mine workings with no dissolved O_2 pyrite oxidation can be negligible.
- Sulfur oxidizing anaerobic bacteria utilize CO_2 as their sole source of carbon for growth. CO_2 is produced in sulfur waste dumps as a result of carbonate dissolution and release of CO_2 in pore spaces. Thus pyrite oxidation is heightened in pore spaces due to favourable anaerobic bacteria conditions.
- The pH of the solution adjacent to the pyrite surface is important. Below pH 3 sulfide oxidation becomes faster. Water is an important transport medium as it

removes oxidation products exposing fresh pyrite for further oxidation. Alternating wetting and drying pyrite surface accelerates oxidation.

- The most efficient oxidant for pyrite is dissolved Fe^{3+} not O_2 as Fe^{3+} oxidizes pyrite more rapidly than O_2. The oxidation of Fe^{2+} to Fe^{3+} is considered the rate limiting step in indirect abiotic oxidation of pyrite. The precipitation of Fe^{3+} places a limit on the amount of dissolved Fe^{3+} available and the rate of oxidation.

Role of Carbonates and Silicates

The majority of minerals on the earth's crust are silicates and silicate minerals which consume hydrogen ions by complete dissolution (congruent weathering) and silicate alteration (incongruent weathering). During the weathering of silicates dissolved cations, silicic acid (H_4SiO_4) and secondary minerals are produced. The silicic acid of silica may also precipitate from solution during the weathering process if it doesn't it is a very weak acid and doesn't contribute significantly to acidity of the solution.

Carbon dioxide may or may not be present in the mine waste environment depending on whether the pore water is in contact with the atmosphere or not. When carbon dioxide is present there is increased calcite dissolution as more bicarbonate is produced. The weathering of other carbonates (dolomite, ankerite and magnesite) is similar to the process above with the addition of magnesium ions being generated along with carbonate, bicarbonate and carbonic acid. In contrast, siderite ($FeCO_3$), which is commonly found in metal ores, under well oxidized conditions has a net zero effect on solution neutralization (Ptacek and Blowes, 1994). With the oxidation of pyrite there is a release of H^+ ions to solution and a corresponding increase in the solution's acidity unless

the hydrogen is consumed by buffering reactions. This buffering typically occurs through reaction with gangue minerals in the waste. The buffering is largely a result of weathering of silicates, carbonates and hydroxides. The individual gangue minerals dissolve at different pH ranges. In the case of Voisey's Bay concentrate the gangue minerals include: plagioclase, olivine, pyroxene and biotite and hornblende may be present in small quantities.

Carbonates contribute significantly to acid buffering reactions. Calcite ($CaCO_3$) is the most important neutralizing agent as it's prevalent in the environment and it reacts rapidly. Calcite neutralizes acid by dissolving and forming bicarbonate (HCO_3^-) and carbonic acid (H_2CO_3) (Ptacek and Blowes, 1994). In weakly acidic environments bicarbonate is produced while in strongly acidic conditions carbonic acid is produced. This results in a neutralization of acidity and increase in pH and alkalinity. Re-precipitation can occur with changes in conditions such as temperature or carbon dioxide.

$$CaCO_{3(s)} + H^+_{(aq)} <-> Ca^{2+}_{(aq)} + HCO_3^-{}_{(aq)} \qquad (A.5)$$

$$CaCO_{3(s)} + 2H^+_{(aq)} <-> Ca^{2+}_{(aq)} + H_2CO_{3(aq)} \qquad (A.6)$$

APPENDIX III

Table A.1: Summary Table of Reactive Transport Models Applicable to Evaluation of Mine Drainage Quality

Name of Software	Description
MINTRAN; MIN3P	Law of Mass Action, 1-D oxygen diffusion in general purpose reactive transport model includes kinetically controlled sulfide oxidation. PLUME2D and MINTEQA2 with two step coupling method. Applied to the Nickel Rim tailings impoundment near Sudbury (Bain et al. 2000). University of Waterloo, also developed MINTOX (diffusion of oxygen into tailings), PYROX (pyrite), MIN3P (3-D transport).
PHREEQC-2	USGS model with speciation, solubility, reaction path model, inverse mass balance modeling, 1-D advective dispersive reactive transport capabilities. Coupled transport and thermodynamic equilibrium model with a two step method. PHREEQC-2 models sorption processes using surface complexation concept and dissolution/precipitation and kinetic reactions. Takes analytical uncertainties into account. Has been coupled with 2-3D transport models: HST3D (to create PHAST), MTS-DMS (to create PHT3D) & PHREEQM-2D.
MINTEQ 4.02 (MINTEQA2)	U.S. EPA supported software. Geochemical equilibrium speciation software for dilute solution uses DDL diffuse double layer, a surface complexation model. Calculates mass distribution between dissolved, adsorbed and gas phases. Can include multiple solid and gas phases. Seven adsorption models are available. Widely used with a comprehensive database.
TOUGHREACT TOUGH2-CHEM	Set of models that can simulate acid mine drainage generation and buffer reactions in unsaturated porous or fractured heterogeneous media. Accommodates chemical species in solids, liquid or gas phase. Two solutions: one based on SIN and one based on simultaneous solution of flow, transport and reaction processes. Model can simulate pyrite oxidation and kinetically controlled dissolution-precipitation, and sorption and surface complexation processes. Distributed by Rockware: TOUGHREACT $1200, PetraSim $1200 single license.

Table A.1: Summary Table of Reactive Transport Models Applicable to Evaluation of Mine Drainage Quality (continued)

Name of Software	Description
HYDROGEOCHEM	Coupled equilibrium model with flow and transport models, coupling technique is 1 and 2 step. Simulates transient and steady-state distribution of reactive chemical species. For transport, subsurface flow in multi-component multi-species systems in either 2 or 3D. Applicable for saturated, unsaturated and partially saturated multi-layer environments. Includes equilibrium, complexation, redox, sorption, precipitation/dissolution, ion exchange and transport processes. Cost~$1500 not sure about academic pricing.
STEADYQL and STEADYSED1	Quasi –steady state model, includes both kinetic reaction, equilibrium and advective transport modeling. Applications in waste rock, tailings, impoundments and underground mines. Not readily available.
RATAP	Developed for CANMET. Used for assisting to predict acid generation and heavy metal release from tailings due to sulfide oxidation. Accounts for physical and biogeochemical processes. Quasi steady state model has one month time steps, can model seasonal variations in temperature and precipitation. Can enter data in probabilistic mode. Applications eg. Lin and Quarfort 1996, Nicholson, 2000. Poor documentation must be calibrated for each site, not user friendly, not on the market, complex.
MIGRATE	Models contaminant transport from multiple sources, either at the surface or buried in 2D. MIGRATE does not require the use of a "time-marching" procedure. MIGRATE uses a finite-layer technique that provides numerically accurate and stable results. ~$750 with discount. Good graphics but only includes sorption and decay, advective and dispersion.

Table A.2: Summary of Geochemical Reactive Transport Models

Name	Description
RETRASO**	Simulates flow and transport in column experiments using unsaturated contaminated soil.
SULIDOX**	Developed at ANSTO. Developed for environmental mining issues particularly related to waste rock and heap leach piles.
MT3D-IPD* (MT3-DM3)	3D reactive transport model, IPD finite difference for inter-particle diffusion. (Simulates advection, dispersion/diffusion, source/sink mixing and chemical reactions.
DiffMod7*	Shrinking core model. Model O2 diffusion FeS_2 oxidation in unsaturated zone.
STEADYQL and STEADYSED1	Quasi –steady state model, includes both kinetic reaction, equilibrium and advective transport modeling. Applications in waste rock, tailings, impoundments and underground mines.
NETPATH*	USGS produced. And inverse mass balance modeling program for net geochemical mass balance reactions in hydrologic flow path. Good for fractionation.
MINEQL* Version4	Uses MINTEQA2 Thermodynamics. Windows interface model composition good, good viewing of results. Used by aquatic chemists and engineers.
MINTEQA2*	EPA supported software. Speciation modeling (redox,ion-exchange, surface complexation). Geochemical speciation software uses DDL diffuse double layer, a surface complexation model
Geochemists Workbench*	Collection of five geochemical programs capable of performing all except couple reactive transport. Has graphical output. www.rockware.com (Law of mass action model.)
RATAP	Used for assisting to predict acid generation and heavy metal release from tailings due to sulfide oxidation. Accounts for physical and biogeochemical processes. Quasi steady state model has one month time steps, can model seasonal variations in temperature and precipitation. Can enter data in probabilistic mode. Applications eg. Lin and Quarfort 1996, Nicholson, 2000.

Table A.2: Summary of Geochemical Reactive Transport Models (continued)

Name	Description
HYTEC	Reactive transport model coupled with geochemical code CHESS used in saturated groundwater.
MODEL MAKER	Dynamic system silmulator. Simultaneously solves, transport and kinetics. Optimization software and reactive model.
SMART	One-D streamtube model. Streamtube Model Advective Reactive Transport. Lagrangian approach discretising a heterogeneous model domain
TBC	Multi-species reactive transport model, finite difference approach
CARRY	Physically based reactive transport model
CoTReM	Simulates 1-D transport of solutes and solid phases and their interactions driven by bio-geochemical reactions and thermodynamic equilibria occurring in natural environments. (includes 30 species) Based on operator-spitting, mixing cell approach.
HDROGEO-CHEM	Coupled equilibrium model with flow and transport models, coupling technique 1 and 2 step. For transport, subsurface flow in multi-component multi-species systems.
CHEM-FLUX	2D contaminant transport modeling software including advection, diffusion, adsorption and decay
PHAST	Simulates multi-component reactive transport in 3-D in saturated groundwater system.
CHESS	Simulates equilibrium state for complex solution of minerals, colloids, organics and gases.
AT123D	Generalized 3-D groundwater transport and fate model with contaminant transport in 1-D includes advection, dispersion, adsorption and biodegradation.
MIGRATE	Contaminant transport from multiple sources, either at the surface or buried, 2D. MIGRATE does not require the use of a "time-marching" procedure. MIGRATE uses a finite-layer technique that provides numerically accurate and stable results. ~$750 with discount. Good graphics but only includes sorption and decay, advective and dispersion.

APPENDIX IV

Geochemical Algorithms

Examples of how speciation and geochemical reactions are incorporated into a geochemical code are briefly outlined in this section through a review of PHREEQC. Initially, for most modeling codes a few basis species (or master species, components) are selected. These species are the minimum number of chemical formulas required to describe the composition of all the phases and all species. Mineral or gas phases are also included in the basis. The modeling program determines the secondary species based on stoichiometry linking the secondary species to the basis species and the reaction equilibrium constant.

Distribution of Aqueous Species

The distribution of species is calculated from data bases using two different approaches:

i) The determination of the thermodynamically most stable state by minimization of Gibbs free energies of reaction (CHEMSAGE is an example of a tool that uses this approach).

ii) Solving a set of non-linear equations from equilibrium constants and mass balances (PHREEQC, EQ3/6,WATEQ4F and MINTEQA2 use this approach).

For a given chemical reaction described by mass-action law:

$$aA+bB<->cC+dD \qquad (A.7)$$

$$K = \frac{a_c^c \, a_d^d}{a_a^a \, a_b^b} \qquad (A.8)$$

Where

K= temperature dependent equilibrium constant

a_i = activity of species *i*

Given $a_i = \gamma_i m_i$ and $n_i = m_i W_{aq}$

γ_i = activity coefficient

n_i = number of moles

m_i = molality

W_{aq} = weight of water in 1 kg of aqueous solution

The general mass action equation can be written as:

$$K_i = a_i \prod_{m}^{M_{aq}} a_m^{-c_{m,i}} \quad \text{(Parkhurst and Appelo, 1999)} \qquad (A.9)$$

where M_{aq} = the total number of aqueous master species

$c_{m,i}$ = stoichiometric coefficient of master species *m* in species *i*

In this case, the total moles can be expressed as:

$$n_i = K_i W_{aq} \frac{\prod_{m}^{M_{aq}} a_m^{c_{m,i}}}{\gamma_i} \qquad (A.10)$$

Ion Activities and Activity Product

The commonly employed approach to describe water-gas-soil-rock interaction in aquatic systems is the ion dissociation theory or the ion interaction theory. In PREEQC, activities can be calculated based on variations of the DeBye-Huckel equation for low concentration solution or the Davies equation for solutions of higher ionic strengths.

$$\log \gamma_i = -Az_i^2 \left(\frac{\sqrt{\mu}}{1+\sqrt{\mu}} - 0.3\mu \right) \quad \text{(Davies equation)} \qquad (A.11)$$

where $\mu = 0.5 \sum m z^2$ = ionic strength

z= ionic charge of the species *i*

A= temperature dependent constant

Solubility Index

The solubility of a product is defined by the Solubility Index (SI); if SI is positive the compound is supersaturated in the solution.

$SI = \log(IAP) - \log(Ksp) = \log(IAP/Ksp)$ (A.12)

Where $IAP = \{A\}\{B\}$

A and B are components of the compound in solution

Ksp = solubility product

Ion Exchange

PHREEQC allows for multiple exchangers (exchange assemblages) to exist in equilibrium with the aqueous phase. Ion exchange reactions are modeled with the Gaines-Thomas convention and equilibrium constant derived from Appelo and Postma (1993). The approach uses mass-action expressions based on half-reactions between aqueous species and the fictive exchange site.

For example for exchange species CaX_2 the reaction is $Ca^{2+} + 2X^- = CaX_2$ where X- is the exchange master default species.

Surface Complexation

Surface complexation reactions in PHREEQC are modeled with a generalized two-layer model (Dzombak and Morel, 1990) incorporating surface complexation constants from Dzombak and Morel (1990) and Allison et al. (1991) (MINTEQA2) and others.

In PHREEQC, kinetically controlled reactions and solid solutions can be defined using rate expressions and a Basic ™ interpreter.

Background of PHREEQC

Early versions of PHREEQC calculated of element concentration, molalities, activities of aquatic species, pH, pe, saturation index and mole transfers to achieve equilibrium as a function of the specified reactions. Improvements in the algorithm included accounting for elements in solids, aqueous and gas phase, use of redox couples for definition of redox state calculations, mole balance with hydrogen and oxygen to account mass of water in aqueous phase and identification of stable phase assemblages from the list of candidate phases.

The PHREEQC equations for speciation and forward modeling are defined by algebraic equations that define the thermodynamic activities of aqueous species, ion-exchange species, surface complexation species, gas-phase components, solid solutions and pure phases. First, thermodynamic activities and mass-action equations are described for aqueous, exchange and surface species. Then, a set of functions are defined that are solved simultaneously to determine equilibrium conditions. The functions are derived for the most part from mole balance equations for each element or element valence state, exchange site and surface site or from mass-action equations for pure phases and solid solutions. Additional functions are derived for: alkalinity, activity of water, aqueous charge balance, gas-equilibria, ionic strength and surface complexation. Each function is reduced to contain a minimum number of variables and at equilibrium all functions are equal to zero. PHREEQC uses a modified Newton-Raphson method to solve the simultaneous non-linear Jacobian matrix equations.

In PHREEQC, the advective transport is calculated first by finite difference, then the chemical reactions are calculated as indicated in the previous paragraphs. Next dispersive

transport is determined through central difference this is followed by chemical reaction calculation. The one-dimensional transport models such as PHREEQC do not take into consideration transverse dispersion.

APPENDIX V

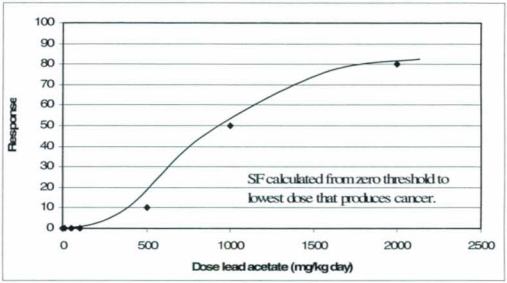

Figure A.2: Dose response curve for renal tumors in rats

Analytical Hierarchy Process Alternative Matrix Tables

Longterm Maintenance Cost

	Unlined Subaerial	Lined Subaerial	Unlined Subaqueous	Lined Subaqueous	Priorities
Unlined Subaerial	1	0.2	0.5	0.1428571	0.062733
Lined Subaerial	5	1	1	0.3333333	0.249635
Unlined Subaqueous	2	1	1	0.2	0.142973
Lined Subaqueous	7	3	5	1	0.544659
					29.37619

Non-carcinogenic Human Health Risk

	Unlined Subaerial	Lined Subaerial	Unlined Subaqueous	Lined Subaqueous	Priorities
Unlined Subaerial	1	0.25	1	0.1666667	0.088039
Lined Subaerial	4	1	0.5	0.3333333	0.212508
Unlined Subaqueous	1	2	1	0.2	0.153005
Lined Subaqueous	6	3	5	1	0.546448
					27.45

Carcinogenic Human Health Risk

	Unlined Subaerial	Lined Subaerial	Unlined Subqueous	Lined Subqueous	Priorities
Unlined Subaerial	1	0.25	1	0.1666667	0.088039
Lined Subaerial	4	1	0.5	0.3333333	0.212508
Unlined Subqueous	1	2	1	0.2	0.153005
Lined Subaqueous	6	3	5	1	0.546448
					27.45

Analytical Hierarchy Process Alternative Matrix Tables (continued)

Ecological Footprint

	Unlined Subaerial	Lined Subaerial	Unlined Subaqueous	Lined Subaqueous	Priorities
Unlined Subaerial	1	0.333333	0.25	0.1428571	0.055428
Lined Subaerial	3	1	1	0.1666667	0.165902
Unlined Subaqueous	4	1	1	0.25	0.200688
Lined Subaqueous	7	6	4	1	0.577982

Note: ecological footprint includes impact on soil and water not air. 31.14286

Containment Effectiveness

	Unlined Subaerial	Lined Subaerial	Unlined Subaqueous	Lined Subaqueous	Priorities
Unlined Subaerial	1.000	0.143	1.000	0.143	0.066
Lined Subaerial	7.000	1.000	5.000	1.000	0.404
Unlined Subaqueous	1.000	0.200	1.000	0.143	0.068
Lined Subaqueous	7.000	1.000	7.000	1.000	0.462

34.629

Ecological Risk

	Unlined Subaerial	Lined Subaerial	Unlined Subaqueous	Lined Subaqueous	Priorities
Unlined Subaerial	1	0.25	0.5	0.1428571	0.062485
Lined Subaerial	4	1	1	0.2	0.204669
Unlined Subaqueous	2	1	1	0.2	0.138647
Lined Subaqueous	7	5	5	1	0.594199

30.29286

Construction Cost

	Unlined Subaerial	Lined Subaerial	Unlined Subaqueous	Lined Subaqueous	Priorities
Unlined Subaerial	1	6	2	8	0.532339
Lined Subaerial	0.166667	1	1	1	0.099161
Unlined Subaqueous	0.5	1	1	7	0.297484
Lined Subaqueous	0.125	1	0.14285714	1	0.071016

31.93452

Analytical Hierarchy Process Pairwise Matrix Tables

Pairwise Matrix for Cost

	Construction cost	Maintenance Cost	Priorities
Construction cost	1.000	0.200	0.167
Maintenance Cost	5.000	1.000	0.833

Pairwise Matrix for Human Health Risk

	Carcinogenic risk	Non-carcinogenic risk	Priorities
Carcinogenic risk	1	2.00	0.6667
Non-carcinogenic risk	0.5	1	0.3333

Analytical Hierarchy Process Decision Goal Matrix Table

Decision Goal Matrix

	Human Health Risk	Ecological Risk	Cost	Containment Effectiveness	Ecological Footprint	Priorities
Human Health Risk	1.000	2.000	3.000	2.000	2.000	0.347
Ecological Risk	0.500	1.000	2.000	1.000	2.000	0.225
Cost	0.333	0.500	1.000	0.500	0.500	0.098
Containment Effectiveness	0.500	1.000	0.500	1.000	2.000	0.173
Ecological Footprint	0.500	0.500	2.000	0.500	1.000	0.156

1.000